UNIVERSITY OF OKLAHOMA

GRADUATE COLLEGE

IN SITU TESTING AND ITS APPLICATION TO FOUNDATION ANALYSIS FOR FINE-GRAINED UNSATURATED SOILS

A DISSERTATION

SUBMITTED TO THE GRADUATE FACULTY

in partial fulfillment of the requirements for the

Degree of

DOCTOR OF PHILOSOPHY

By

RODNEY WOTHERSPOON COLLINS
Norman, Oklahoma
2016

IN SITU TESTING AND ITS APPLICATION TO FOUNDATION ANALYSIS FOR FINE-GRAINED UNSATURATED SOILS

A DISSERTATION APPROVED FOR THE
SCHOOL OF CIVIL ENGINEERING AND ENVIRONMENTAL SCIENCE

BY

_____
Dr. Gerald Miller, Chair

_____
Dr. Amy Cerato

_____
Dr. Andy Elwood Madden

_____
Dr. Tohren Kibbey

_____
Dr. Kanthasamy Muraleetharan

_____
Dr. Jeffery Volz

To my mother and father.

Acknowledgements

This work was made possible by Dr. Gerald Miller, my advisor. His guidance and support at the University of Oklahoma were essential. My mother and father provided unwavering support; without their love, I would not have been able to complete this work. My wife, Kylie, who has been with me nearly ten years has supported and loved me through this entire process. Kylie has given me two beautiful sons, Malcolm and Damien, and has sacrificed to make our lives wonderful. My siblings Kelly, Max, and Jackson make me laugh and are good friends. My close friends Frank Zarones, Loren Brown, and Kiley Molinari always pretend to be moderately interested in listening to what I am doing at work. Thank you all!

Thank you to my committee: Dr. Cerato, Dr. Elwood Madden, Dr. Volz, Dr. Muraleetharan, and Dr. Kibbey.

Thank you to the CEES staff: Mike Schmitz who constructed the MPMT and model footing bearing capacity test equipment, Ronald Conlon, Susan Williams, Molly Smith, Brenda Clouse, and Audre Carter.

Oklahoma Department of Transportation: Christopher Clarke, John Nicholson, and Stephen Bettis.

My friends and Colleagues: Wassim Tabet, Roy Doumet, Arash Hassanikah, Maryam Varsei, Bo Zhang, Hoda Soltani, Alison Quiroga, Tommy Bounds, Theresa Ngo, Shivani Rani, Luis Pena, Nathan Ferraro, and Yujei Wei.

Table of Contents

List of Tables

List of Figures

Abstract

The in situ test is an important part of a geotechnical engineer's arsenal. Currently, there are no established methods for interpreting results of in situ tests in unsaturated soils. The difficulty in interpreting in situ tests in unsaturated soil comes from the presence of suction, which is often unknown and directly influences a soil's stress state. Unsaturated soils are also subject to fluctuating soil moisture conditions and therefore, fluctuating suction and stress states. For such soils, it is important to establish a methodology to estimate the influence of variable moisture conditions on the interpreted results of in situ tests. This is particularly true when those in situ tests are used as a basis for analysis and design in geotechnical projects. The doctoral study outlined in this dissertation is an important step toward the development of a comprehensive methodology for interpreting in situ tests considering possible variations in soil suction resulting from changes in moisture content. In addition, this study goes one step further by including a laboratory scale investigation of foundation response to loading in unsaturated soil at different moisture conditions that has been also been tested using the pre-bored pressuremeter. The goal is to observe the influence of suction on the results of an in situ test and foundation performance, simultaneously. In this way, the methods of analysis developed for interpreting in situ tests in unsaturated soil can be calibrated and validated against observed foundation performance.

The primary objectives of the research work described in this dissertation include collection of data that describes the influence of matric suction on in situ test results including the pressuremeter (PMT), cone penetration test (CPT), and standard penetration test (SPT). In situ test and suction data was analyzed and recommendations

for interpreting results of aforementioned in situ tests when soil moisture conditions fluctuate were made. Finally, a method was developed through which bearing capacity and settlement of shallow foundations on unsaturated fine-grained soils can be predicted based on pressuremeter results. To achieve the objectives of this project the following tasks were completed: 1) a detailed literature search was performed to gather information regarding in situ tests in unsaturated soil, model bearing capacity tests on unsaturated soils, and predicting shallow foundation behavior in unsaturated soil with the pressuremeter. 2) Established two field test sites to perform field tests including the pressuremeter, cone penetration test, and standard penetration while monitoring weather conditions and soil volumetric moisture content. Performed in situ tests, collected soil samples, and observe field sites over a two-year period. 3) Performed soil tests to identify engineering properties of the soil for both field sites and developed soil water characteristic curves for soils involved in the research to establish the relationship between the soil moisture content and suction. 4) Conducted extensive analysis of the results of in situ tests to establish empirical relationships. 5) Conducted extensive theoretical analysis of the pressuremeter and CPT data using cavity expansion theory for unsaturated soils. 6) Constructed a testing chamber and load frame such that model bearing capacity tests on unsaturated soils could be performed. Constructed a miniature pressuremeter for testing soil in the chamber. 7) Performed pressuremeter and model bearing capacity tests on unsaturated soil and conducted extensive analysis of the data. The major contributions of this research include: 1) a unique and valuable dataset including the results of PMTs at two fine-grained soil sites, with accompanying measurements of soil moisture content determinations, total suction determinations, and

other supporting laboratory test data was developed. Similar datasets were developed for CPTs and SPTs. 2) Empirical relationships between matric suction and pressuremeter parameters including: limit pressure, pressuremeter modulus, and unload-reload modulus were developed for different soil types encountered at the test sites. In addition, relationships including the limited data that could be extracted from the literature, were developed, which expand the knowledge gained through the current study. 3) Empirical relationships between matric suction and CPT parameters including: tip resistance, and sleeve friction, were also developed for different soil types encountered at the test sites. Further empirical relationships between matric suction and standard penetration test N-value and $N_1(60)$ were also developed. 4) The use of unsaturated cylindrical cavity expansion theory for prediction of limit pressures under fluctuating soil moisture conditions was further investigated. This involved developing a theoretically based approach to estimating limit pressure as a function of changing suction. In a similar manner to the PMT, a method to apply unsaturated spherical cavity expansion theory for prediction of tip resistance under fluctuating soil moisture conditions was provided. 5) A unique and incredibly valuable dataset was obtained by conducting model scale footing tests and miniature pressuremeter tests in unsaturated soil prepared to different moisture conditions. The dataset includes load-displacement curves from five footing tests, pressuremeter test curves from all five test beds, water content and total suction data from test beds as well as other supporting laboratory data. Observations from this testing were extremely valuable in providing insight into the use of PMT for shallow foundation analysis in unsaturated soi

Chapter 1 Introduction

1.1 Overview

Unsaturated soils exist in a state between fully saturated and completely dry. These soils are found throughout the world and require special attention in geotechnical engineering projects. Most areas around the world are subject to seasonal wetting and drying that can cause soil moisture content to vary, sometimes over extreme ranges in moisture content. This can lead to soil being either saturated or unsaturated. Geotechnical engineering analyses typically apply to soils in a fully saturated condition using methods of analysis based on the effective stress concept. Effective stress is defined as the difference between total stress at a depth of interest and the pore water pressure at the same depth. It is a measure of the intergranular stress or stress carried by the soil skeleton. Geostatic total stress is easily calculated by simply knowing the unit weight or density of the material while hydrostatic pore water pressure can be found if the height of the water table is known.

The state of stress of unsaturated soils cannot be described using the traditional effective stress technique. This is because water in unsaturated soil does not fill all of the void space. In unsaturated soil, air is present in voids and the contractile skin, which is the air-water interface, should be accounted for to understand the full state of stress. Several different equations have been developed to describe the stress state of unsaturated soil; which equation is best is not fully agreed upon by researchers. One method developed by Bishop (1959) includes a soil parameter, χ, which accounts for the soils degree of saturation, and the soil's matric suction, ψ. Matric suction, otherwise known as capillary pressure, is the difference between the pore air and water pressure in

the soil at the time. The addition of a soil property to describe a stress state is contrary to traditional approaches to constitutive modeling. Experimental evidence suggests that for proper modeling of the state of stress in unsaturated soils, two stress state variables may be needed. Many researchers have adopted the two stress state variable approach in their attempts to model unsaturated soil behavior. Two stress state variables often adopted include: 1) net normal stress, which is the difference between total stress and pore air pressure, and 2) matric suction, which was described earlier. The two stress state variable approach was proposed by Fredlund and Morgenstern (1977). For studying in situ test results from unsaturated soils described in this dissertation, the net normal stress and matric suction were assumed the controlling stress state variables; however, different effective stress models were examined with regard to interpreting the test results.

Currently, there are no established methods for interpreting results of in situ tests in unsaturated soils. The difficulty in interpreting in situ tests in unsaturated soil comes from the presence of suction, which is often unknown and directly influences a soil's stress state. Unsaturated soils are also subject to fluctuating soil moisture conditions and therefore, fluctuating suction and stress states. For such soils, it is important to establish a methodology to estimate the influence of variable moisture conditions on the interpreted results of in situ tests. This is particularly true when those in situ tests are used as a basis for analysis and design in geotechnical projects. The doctoral study outlined in this dissertation is an important step toward the development of a comprehensive methodology for interpreting in situ tests considering possible variations in soil suction resulting from changes in moisture content. In addition, this

study goes one step further by including a laboratory scale investigation of foundation response to loading in unsaturated soil at different moisture conditions that has been also been tested using the pre-bored pressuremeter. The goal is to observe the influence of suction on the results of an in situ test and foundation performance, simultaneously. In this way, the methods of analysis developed for interpreting in situ tests in unsaturated soil can be calibrated and validated against observed foundation performance.

In situ testing is a valuable tool in a geotechnical engineer's arsenal. The main goal when performing a geotechnical investigation is to assess the engineering behavior and mechanical properties of a soil profile of interest. It is a challenging problem because most soil profiles are not observable without invasive testing and collection of samples for laboratory tests. The results of these tests can also be deceiving due to problems associated with disturbance. Soil, in situ, exists at a certain level of vertical and horizontal stresses, as well as, specific pore air and water pressures. These can be estimated and reproduced in a laboratory; however, the stress states imposed under laboratory conditions are often isotropic, and only approximate the conditions of the soil in a field setting. Furthermore, the laboratory samples suffer from the influence of disturbance and stress relief during the sampling and testing process. While in situ tests are not without issues associated with soil disturbance, they offer several advantages over laboratory testing including the fact that generally more tests can be conducted in less time, and encompass a much larger volume of the site soil profile. Furthermore, for some in situ tests, the soil response observed is directly related to the initial field stress conditions prior to testing. However, it is very important that engineers, who rely on in

situ test results for geotechnical analysis and design, fully appreciate the impact that variable moisture conditions can have on in situ test results in the unsaturated soil zone. This study examines the impact of varying suction relative to three invasive in situ tests, the pre-bored pressuremeter test (PMT), cone penetration test (CPT) and the standard penetration test (SPT).

The pressuremeter test (PMT) is the only in situ test that provides a stress-strain curve. It encompasses both the elastic and plastic behavior of soil. Thus, both elastic parameters and shear strength can be estimated from the results of a single test. The pressuremeter probe has a rubber or steel-sheathed membrane surrounding a hollow metal pipe. There is tubing running through the center of the metal pipe that runs to a control unit. Figure 1.1 shows a schematic of a pressuremeter test. The open borehole the pressuremeter is placed in is created with a hand auger or drilling rig, and care must be taken to ensure there is limited disturbance on the walls of the borehole. Once it reaches the test depth, it is held in place and the membrane is expanded while volume and pressure are recorded. Analysis of the results provides the pressure and volume change in the soil. There are several versions of the pressuremeter and most of the differences come from the manner in which the device is inserted into the ground. There are full-displacement pressuremeters with conical tips that are pushed to the desired depth, while others are low displacement self-drilling units. The pressuremeter that will be focused on for this research is the pre-bored pressuremeter test that involves lowering the pressuremeter in a pre-bored hole. With respect to the degree of installation disturbance of the soil surrounding the test probe, the pre-bored pressuremeter falls in between the full-displacement and self-boring devices. From here

on the pre-bored pressuremeter test will simply be referred to as the pressuremeter test or PMT.

Cone penetration testing (CPT) is popular throughout the world due to its ability to define soil types and soil profiles fast and simply. The cone penetration test consists of a cone instrumented with load cells to measure the resistance from the soil on the tip of the cone, as well as, the sleeve friction on the side of the cone that develops as the cone is pushed vertically into the ground. Figure 1.2 shows a schematic of a cone truck, pushing the cone into the ground and an example of CPT test results. As shown in Figure 1.2, a CPT test provides a continuous profile of tip resistance and sleeve friction with depth that can be used to determine soil type and estimate numerous soil properties. In saturated soil, pore water pressure (pwp) measurements associated with the piezocone penetrometer (PCPT), can be useful for classification, as well as, pore water dissipation testing to determine rate of consolidation information.

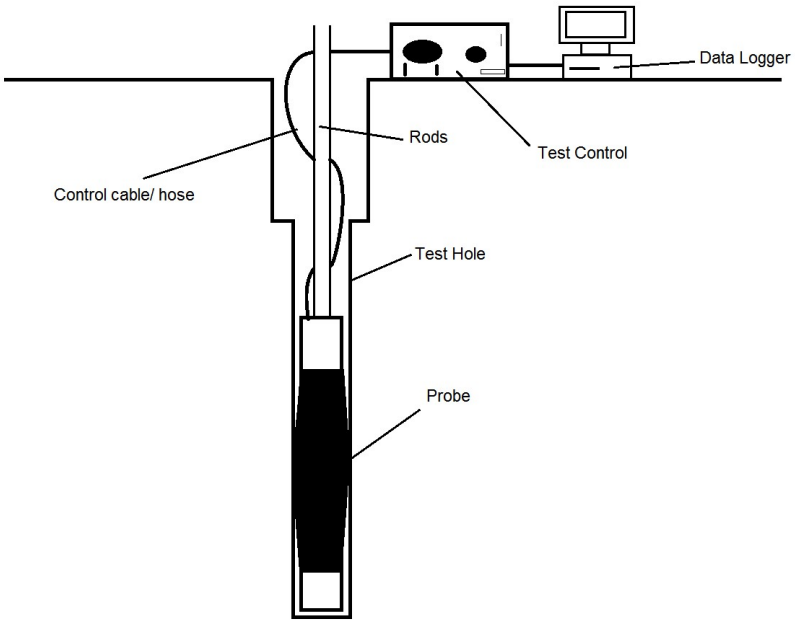

Figure 1.1: Pressuremeter set up

The standard penetration test (SPT) is the most common in situ test performed at a site of interest in a geotechnical investigation. The test is dynamic and consists of a split spoon sampler attached to drill rod stem that is driven by a hammer. The hammer hits an anvil on top of the drill rods that in turn drives the split spoon sampler into the ground. The number of blows per six inches of penetration are counted until a total of eighteen inches is obtained. The SPT "N" value is the number of blows obtained for the last 12 inches of penetration. There are a number of correlations between SPT test results and soil parameters. For example, these correlations include relative density (Kulhawy and Mayne, 1990) and shear strength (De Mello, 1971), as well as studies to assess seismic soil liquefaction potential (e.g. Cetin et al., 2004).

The current methods of interpretation for the PMT, CPT, and SPT rely on the assumptions that soil is either saturated or completely dry. Depending on geographic location, such conditions may exist at one time or another on a seasonal basis and in most cases considering a saturated condition provides a conservative design. The problem is that the in situ conditions on the day of testing may or may not represent a worst-case condition. Furthermore, in arid regions, some soils may never actually see saturated conditions so assuming a saturated soil condition in the analysis can lead to an overly conservative and costly design.

In addition, another problem comes with performing an in situ test in unsaturated soil. In places such as Oklahoma that are subjected to prolonged periods of drought, soil can become extremely stiff and strong. This is due to an increase in matric suction. If a period of wetting occurs that brings the soil out of drought conditions, the

soil becomes soft and weak. No method of in situ test interpretation can account for future changes in soil moisture conditions. Therefore, one goal of this research is to provide a method of interpretation for engineers so that in situ tests can be performed on any day with any soil moisture condition and interpreted in a manner that accounts for fluctuations in soil moisture. As part of the research to accomplish this goal, in situ tests were performed in two fine-grained soil deposits at instrumented test sites over a two-year period in order to observe the test response to changing moisture conditions.

There are relatively simple equations in existence that allow for determination of bearing capacity and settlement from pressuremeter parameters. The influence of changes in matric suction on bearing capacity and settlement predicted by the pressuremeter has not been explored for fine-grained soils. To gain some new perspective on the effects that varying moisture conditions have on pressuremeter predicted bearing capacity and settlement, some model footing bearing capacity tests were performed in an unsaturated soil profile in the laboratory. In addition, pressuremeter tests were performed in the model soil profile and then used to predict bearing capacity and settlement.

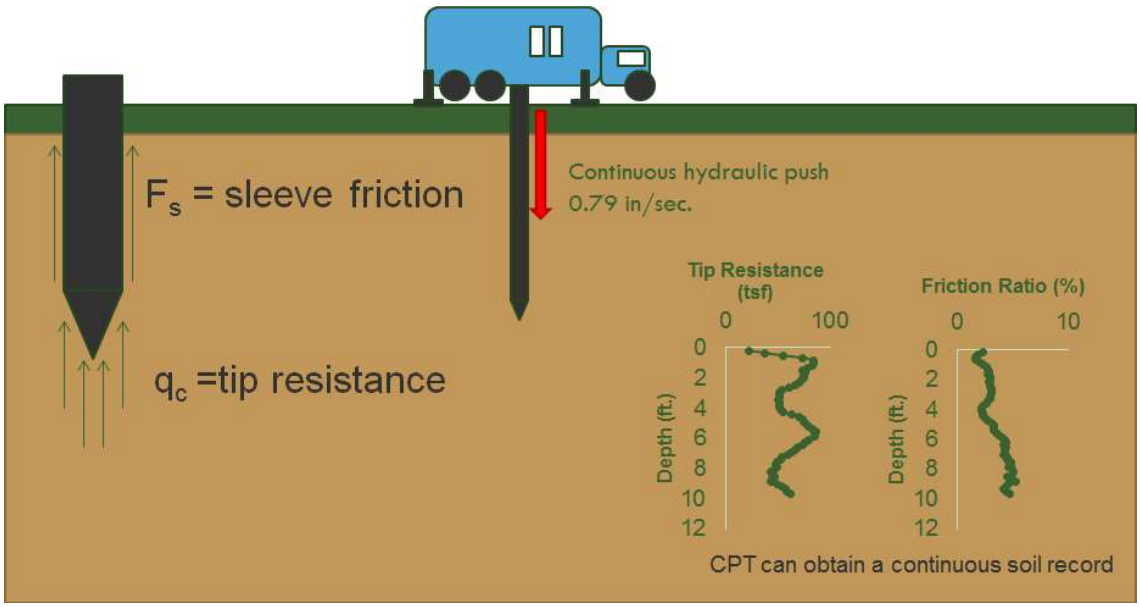

Figure 1.2: Cone Penetration Test (CPT) setup

1.2 Objectives and Tasks

The primary objectives of the research work described in this dissertation include: 1) Collect data that describes the influence of matric suction on in situ test results including the pressuremeter (PMT), cone penetration test (CPT), and standard penetration test (SPT). 2) Analyze trends observed in the in situ test and suction data and, establish recommendations for interpreting results of aforementioned in situ tests when soil moisture conditions fluctuate. 3) Develop a method through which bearing capacity and settlement of shallow foundations on unsaturated fine-grained soils can be predicted based on pressuremeter results.

In order to achieve the objectives of this project the following tasks were completed:

1) Performed a detailed literature search to gather information regarding in situ tests in unsaturated soil, model bearing capacity tests on unsaturated soils, and

predicting shallow foundation behavior in unsaturated soil with the pressuremeter.

2) Established two field sites with relatively uniform soil properties to perform field tests including the pressuremeter, cone penetration test, and standard penetration while monitoring weather conditions and soil volumetric moisture content. Perform in situ tests, collected soil samples, and observe field sites over a two-year period.
3) Performed soil tests to identify engineering properties of the soil for both field sites and developed soil water characteristic curves for soils involved in the research to establish the relationship between the soil moisture content and suction.
4) Conducted extensive analysis of the results of in situ tests to establish empirical relationships.
5) Conducted extensive theoretical analysis of the pressuremeter and CPT data using cavity expansion theory for unsaturated soils.
6) Constructed a testing chamber and load frame such that model bearing capacity tests on unsaturated soils could be performed. Constructed a miniature pressuremeter for testing soil in the chamber.
7) Performed pressuremeter and model bearing capacity tests on unsaturated soil and conducted extensive analysis of the data.

1.3 Organization of Dissertation

The dissertation presented herein was written so that information would flow in a logical arrangement. Chapter 2 provides the literature review, which is structured to

introduce each subject that is relevant to the development of this dissertation, provide further details regarding the state of knowledge for that subject, and provide limitations of the current state of knowledge. Chapter 3 provides a detailed discussion of the research methodology for the situ tests performed. Chapter 4 provides details regarding the model footing tests. Chapter 5 discusses the results obtained from in situ testing and model bearing capacity tests. Chapter 6 provides the conclusions and recommendations based on the results of this research.

Chapter 2 Literature Review

2.1 Organization of literature review

This literature review is divided into three main topical areas. The first deals with in situ testing. This includes relevant literature regarding the pressuremeter (PMT), cone penetration test (CPT), and standard penetration tests (SPT), as well as, literature describing their analysis in unsaturated soils. The second section examines cavity expansion theory that has been used to describe and interpret PMT and CPTs in unsaturated soil. The literature describing the use of cavity expansion theory to interpret in situ tests results from unsaturated soil was also included in this survey. The PMT and CPT are often used for foundation design. Therefore, the final section provides an outline of foundation analysis based on in situ test results. This is followed by discussion of literature regarding model-bearing capacity testing of unsaturated soils. Finally, the literature review concludes in a section that summarizes the main gaps in knowledge exposed by the literature review, and how the research described in this dissertation helps to fill the knowledge gaps with regard to in situ testing and foundation analysis for unsaturated soil conditions.

2.2 In Situ Tests

In situ testing in combination with a thorough laboratory investigation is a useful tool and vital part of any geotechnical investigation. The ultimate goal in any geotechnical investigation is to understand the soil in intricate detail including soil type, layering, plasticity, shear strength, and compressibility behavior. There are many approaches to obtain this type of information from a site of interest. The most common

method is to use a combination of field sampling with laboratory tests, and some in situ tests.

2.2.1 Pressuremeter Test (PMT)

The pressuremeter is a device that can be placed into soil to determine its mechanical properties. The pressuremeter consists of an aluminum or stainless steel body with a rubber membrane covering the central portion of the body. At the ends are collars that secure the rubber membrane in place. Fluid is pumped into the sealed annulus behind the rubber membrane, which results in expansion. The pressure used to pump the fluid into the probe is controlled by the user, so different pressure increments can be used to accommodate soils of varying stiffness. Probe pressure corrected for device effects is equal to the pressure felt by the soil. The volume of fluid injected into the probe is measured so that the corresponding soil displacements can be determined. This allows the user to make a determination of the stress-strain response of the soil around the pressuremeter.

There are several ways to insert the pressuremeter into the soil at the desired depth. The pre-bored borehole method is most popular; and was used in this research. This method consists of excavating a borehole, in this case with a hand auger, and inserting the pressuremeter into the hole. The borehole should be no greater than 1.2 times the diameter of the uninflated probe and no less than 1.03 times the diameter of the uninflated probe (Briaud 1992). This minimizes the inaccuracy during testing from overinflating the probe and helps to achieve proper placement.

The pressuremeter test (PMT) is based on theory in which the probe is modeled by the expansion of an infinitely long cylinder in an infinite soil mass. Results from a

PMT are presented in terms of corrected volume versus corrected pressure, as shown in Figure 2.1. These corrected values represent the actual change in volume of the soil and actual pressure applied to the soil surrounding the probe. Corrected volume represents the volume of liquid injected into the probe at a given pressure, corrected for the system compressibility. Corrected pressure represents the pressure measured above the ground surface, corrected for the resistance of the membrane surrounding the probe and includes the additional pressure that results from fluid head between the measuring point and the center depth of the probe. The pressuremeter expansion curve can be used to create an in situ stress-strain curve for the soil. The radial stress is obtained from the probe pressure while hoop strain is obtained from volume change measurements associated with an assumed expanding radial soil cavity. From the in situ stress-strain curve, or the corrected pressure-volume curve, several soil parameters can be determined.

As shown in Figure 3, there are three phases associated with the PMT expansion curve. In the first phase, the probe is expands to fill the borehole cavity and is assumed to reload the soil to the in situ state of stress. The second phase is the pseudo-elastic region of the expansion where the soil response is assumed primarily elastic. However, an unload-reload procedure is assumed to provide a truer estimate of the elastic response as the pseudo-linear initial loading behavior is believed to be influenced by soil disturbance. The third and final phase of the test begins with soil yielding and development of a failed plastic zone of soil around the expanding cavity. The transition points between these phases and soil response within Phases II and III are used to determine soil parameters of interest.

The first parameter is the at rest total earth pressure, P_{oh}, which can be estimated from the transition point between Phase I and II. The pressuremeter modulus, E_p, and unload-reload modulus, E_r, represent the Young's modulus of elasticity. These parameters are found by fitting a straight line to the initial linear portion in Phase II, and a secant line to the unload-reload portion in an unload reload loop, respectively. The yield pressure shown in Figure 3 represents the transition from elastic to plastic behavior while the limit pressure corresponds to the ultimate resistance when the plastic zone surrounding the probe is fully mobilized. Practically, the limit pressure is determined as the radial soil stress corresponding to a soil cavity that has been inflated to twice its initial volume. The limit pressure is usually not obtained during field measurements, and so it is found by extrapolating the pressure-volume response to estimate the pressure at two times the initial soil cavity volume.

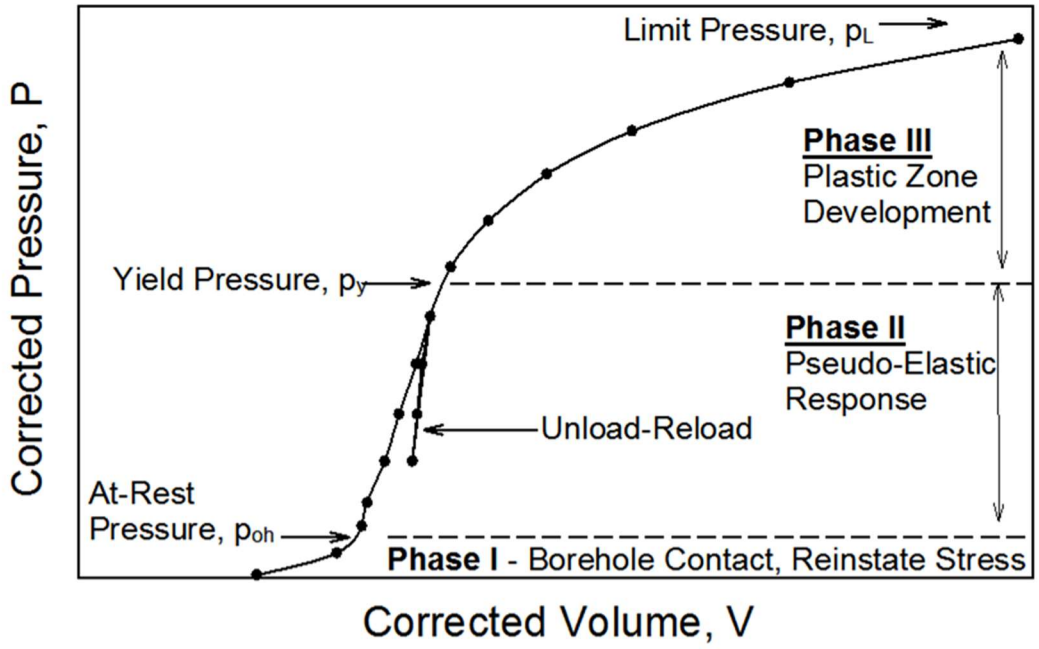

Figure 2.1: Pressuremeter curve showing different test phases

2.2.2 Pressuremeter Tests in Unsaturated Soil

The pressuremeter has been proven a useful and reliable tool for obtaining soil parameters in a geotechnical investigation. However, established methods of interpreting data from a pressuremeter such as those described by Briaud (1992), do not account for soil suction. The presence of suction has a direct influence on soil strength (Fredlund et al., 2012). Suction in unsaturated soils has been shown to have a major effect on parameters derived from the pressuremeter including the modulus and limit pressures (Miller and Muraleetharan 2000, Miller 2014, Miller and Tan 2008, etc.). In general, soils with low suction exhibit softer characteristics than soils with high suction. This means that if two PMT are performed at the same depth for the same site during the wet and the dry times of the year, the drier test will show a stronger soil deposit than the wetter test. This becomes troublesome because planning a soil investigation around the weather is not common practice and shallow foundations designed based on results of a particular pressuremeter test can end up being either under or over designed in the long term. Due to the complexity of the problem, there have been only limited studies completed to address the problem.

The first noted description regarding use of the pressuremeter in unsaturated soils is described by Schnaid et al. (1996). The authors recommend the use of the pressuremeter in unsaturated soil deposits to identify the influence of suction on soil strength. This was recommended due to the difficulty in performing suction controlled laboratory testing. The pressuremeter performed in situ in combination with saturated lab testing provided a complete soil property profile that could be used in design. This study did not attempt to create any framework for interpretation of the pressuremeter in

unsaturated soils; however, it did indicate early recognition of the importance of suction on the PMT test results.

The first demonstrated attempt at constructing a method of interpretation for the pressuremeter in unsaturated soil was presented in Miller and Muraleetharan (2000). The authors presented data from unsaturated silt tested during wet and dry periods. The site was instrumented with tensiometers in order to measure matric suction. The data showed increasing limit pressure for increasing matric suction. Modulus was unaffected by the changes in suction. Calibration chamber data was also presented that showed increasing limit pressure and modulus for increasing matric suction. Cavity expansion equations originally derived by Vesic (1972), and modified for unsaturated soils via Muraleetharan et al. (1998), were used to obtain expressions for ultimate cavity pressure, which is analogous to limit pressure in a pressuremeter test. The equations, which will be presented in detail in a later section, contain several soil parameters that can be readily estimated or determined by laboratory testing. However, the determination of two of the parameters is much more difficult; these parameters include the change in matric suction and volumetric strain in the plastic zone during expansion. Due to the difficulty in obtaining these, the authors developed a method to estimate these parameter based on their unsaturated PMT test results. They did this using an iterative approach whereby experimentally determined soil properties and pressuremeter test results were incorporated into the theoretical equations and then volumetric strains were changed iteratively until the resulting changes in degree of saturation and matric suction were consistent with experimentally determined soil-water characteristic behavior.

The method developed by Miller and Muraleetharan (2000) produced reasonably promising results; however, it has several facets that make it difficult to use in professional practice. Further, the method is somewhat cumbersome due to the large number of unknown variables in the cavity expansion equations.

Muraleetharan et al. (2003) performed numerical modeling of the PMT in unsaturated soil. The analysis compared PMT performed in a calibration chamber using a miniature pressuremeter to results of a numerical model. The numerical model made reasonable predictions of pressure-volume changes; however, the model overconsolidation ratio for the calibration chamber soil had to be increased by around three times the measured values, so that predictions matched measured PMT curves. The analysis did not model the stress release in the soil due to drilling of the borehole prior to pressuremeter insertion. The change in suction in the zone of influence during pressuremeter expansion was found to be quite small and nearly insignificant, which is a useful finding for simplifying cavity expansion models.

Pereira et al. (2003) developed a numerical model to predict pressuremeter behavior in unsaturated soil. The results of this modeling showed differences in the results between saturated and unsaturated soils during pressuremeter expansion. The influence of the suction on the pressuremeter data was reasonable; however, it was not compared to experimental results.

The work of Tan (2005) provided a framework to describe the behavior of the PMT in unsaturated soil. The author performed PMTs in a suction controlled calibration chamber, which allowed for control of initial mean effective stress, and suction. The results of this testing showed that increasing matric suction also increased limit pressure

and modulus of a pressuremeter test. The author used unsaturated cavity expansion equations to predict the influence of suction on pressuremeter results. The author developed a series of volumetric strain versus suction curves, which can be used in the simplified unsaturated cavity expansion equations to predict limit pressure. The analysis indicated that some of the back calculated volumetric strains for the soil in the test data showed compression because the magnitude of the result was positive. The amount of compression in the plastic zone decreased with increasing matric suction and limit pressure. Only one soil type was studied in this research so it is difficult to apply the results to other soil types. The nature of calibration chamber testing is that the user can control nearly all variables during testing; the method developed through this testing was not verified by any field-testing. Typical field-testing at shallow depths, similar to what was performed in this research would have lower initial mean effective stress compared to the calibration chamber.

Miller and Tan (2008) evaluated the at-rest lateral stress based on miniature pressuremeter tests in the calibration chamber. The interpreted at-rest lateral earth pressure was on average close to chamber confining pressure for the low confining pressure condition. As the confining pressure increased, the interpreted at-rest lateral earth pressure was around 80% of the applied chamber pressure. The matric suction and dry unit weight of the soil bed were found to have an influence on the interpreted at-rest coefficient of lateral earth pressure (K_0). The K_0 values decreased with increasing confining pressure, increased with increasing suction, and increased with increasing dry unit weight. The presence of unsaturated soil was again shown to have a profound impact on pressuremeter results.

Miller et al. (2012) described the influence of matric suction on pressuremeter modulus based on miniature pressuremeter tests in the calibration chamber. The results showed that increasing suction increased pressuremeter modulus and unload-reload modulus. The modulus obtained from a PMT relates the stress to strain behavior during expansion and is related to the soil's stiffness.

Zhang et al. (2013) provided a methodology for identifying soil parameters for use in the Barcelona Basic Model (BBM) based on inverse analysis of cavity pressure/strain curves from PMT in unsaturated soil. This work did not attempt to create a methodology for the interpretation of PMT in unsaturated soils. It does use unsaturated PMT data to obtain soil properties in soil profiles that are influenced by suction. This is another example of researchers using the pressuremeter to identify unsaturated soil properties. The authors also recommend significant laboratory testing so that the saturated soil conditions are well known. This is another example for the need of a method of interpretation of the pressuremeter in unsaturated soils that does not rely so heavily on other advanced laboratory testing methods.

Another attempt to find a method of interpretation for the pressuremeter in unsaturated soils is shown by Miller (2014). In this paper, the author uses the yield pressure, the point at which the soil behavior transitions from linear elastic to yielding, to create a prediction model for limit pressure in unsaturated soils. The author assumed the soil experienced elastic-perfectly plastic behavior and that the stress path of a soil element next to the pressuremeter was one of simple shear. Under these assumptions, the yield stress is equal to the radial stress, which is equal to the major principal stress at failure. Incorporating an unsaturated Mohr-Coulomb failure law, the relationship

between suction, yield stress and strength parameters can be established. For a given set of unsaturated strength parameters, the relationship between yield stress and suction can be determined. Further, the actual PMT limit pressure can be estimated using an assumed ratio of limit pressure to yield pressure. Test results from the calibration showed that the ratio of limit to yield pressure did not vary consistently or significantly with changes in suction. This method was used to make predictions for lab and field tests. The method did not work perfectly, but it provided reasonably close predictions with the assumptions made.

Elwood et al. (2015) examined PMT in compacted or heavily overconsolidated soils. Theses soils can have a degree of saturation that would qualify them as unsaturated soil, however, during pressuremeter expansion the soil may undergo volume changes which results in the compression of occluded air. This indicates the initial circumferential strains during pressuremeter expansion are a function of volumetric changes and not a result of borehole expansion alone. The authors developed a method to determine the applied radial total stress that results in saturation during a pressuremeter test.

2.2.3 Cone Penetration Test (CPT)

The cone penetration test (CPT) is one of the most useful in situ tests commonly used in geotechnical testing. Its usefulness comes from its ability to "rapidly" test to great depth and provide near continuous indications of soil stratigraphy. This makes it possible to know site stratigraphy in detail and obtain a basic knowledge of the soil properties at the site rather quickly. The drawbacks of the CPT are that one must have a fully functional truck and specialized equipment to perform the test, and thus it is

relatively expensive. In addition, the test does not allow for subsurface sampling and so must accompany standard field sampling methods. Field testing with an electric friction cone penetrometer involves pushing an instrumented probe into the ground at a standard rate of 2 cm/s (0.79 in./s), while simultaneously measuring the force exerted by the soil on the tip and on a separate friction sleeve just behind the tip. These forces are converted to the tip resistance and sleeve friction by dividing by the projected area of the tip and sleeve area, respectively.

One primary application of the cone penetration data is soil classification (e.g. Robertson et al., 1989) using tip resistance and friction ratio, where the friction ratio is sleeve friction divided by tip resistance. Here the tip resistance and friction ratio are normalized for overburden at the depth of interest. Together these two values can be used to determine the soil behavior type using an empirically derived method. Pore-water pressure measurements can be used to refine soil identification based on cone penetration results. There are many applications of the CPT in soil deposits around the world. There is however, very little information regarding the interpretation of cone penetration results in unsaturated soil deposits. The ease of use and quality of results produced in saturated soil profiles also makes it an ideal candidate for use in unsaturated deposits. The lack of a tangible method of interpretation in unsaturated deposits, however, hinders the proper interpretation of the cone test results. Further information about the current state of knowledge regarding this topic is subsequently presented.

2.2.4 Cone penetration testing in unsaturated soils

In general, cone penetration testing in unsaturated soils is not well explored in the literature. There are notable studies where researchers have explored the CPT in sand, such as Russell et al. (2010), Lehane et al. (2004), Pournaghiazar et al. (2013), and Yang and Russell (2015b). On the other hand, research on the CPT in unsaturated fine-grained soil is very limited (Tan 2005). The previously mentioned studies have taken steps towards development of a method to interpret the CPT in unsaturated soils; however, none of this work has moved far enough to be generally applicable in practice.

Most of the work surrounding the CPT in unsaturated soil deals with sand and comes from researchers in Australia. The work published by Lehane et al. (2004) documented the effects of performing a CPT at one site during a dry and wet time of year. The CPT profiles obtained from the test results showed different results that were attributed to differences in matric suction. During the dry season tip resistance and sleeve friction were higher than when measured during the wet season. The suction profiles were back calculated using a relationship between stiffness values (determined in the laboratory) and relative density (determined through correlation with tip resistance). This work was one of the first to look at different sets of data from the same site and attribute differences in test results to matric suction.

Russell et al. (2010) presented a method of interpretation for the CPT in unsaturated sands. The method is based upon the power law proportionalities between initial effective stress and cone penetration resistance. An equation was developed that allowed for suction to be back calculated based on tip resistance profiles.

Pournaghiazar et al. (2013) performed CPT in a calibration chamber containing unsaturated sands at different initial densities and confining stresses. The authors showed that suction has a significant influence on tip resistance, and increased the tip resistance above that of saturated samples in all cases. The authors used the power law relationship described by Russell et al. (2010) to find a relationship between net stress and tip resistance that includes the soil suction. The authors provide a theoretical example for a soil in which suction is not accounted for in cone penetration analysis in an unsaturated soil. The result is that by failing to account for matric suction in cone penetration analysis leads to an overestimation of relative density and friction angles using empirical correlations. This work provides a simple way to incorporate soil suction into the interpretation of CPT results and shows the impact that fluctuations in suction can have. The work is limited to clean sand however, which typically exhibits suction values much lower than would be encountered in clays and silts.

In Yang and Russell (2015b), the cone penetration test in unsaturated silty sands is examined. The calibration chamber used in Pournaghiazar et al. (2013) was again used this time in a mostly sand soil with 27% non-plastic fines. The authors found that using a constant Bishop's effective stress parameter multiplied by suction could simplify data interpretation. This is useful because changes in suction during cavity expansion have been noted to increase the complexity of the problem in pressuremeter applications (Miller and Muraleetharan 2000). The work also shows that initial hydraulic state (i.e. if the soil is in a state of wetting or drying) has a negligible influence on the tip resistance versus net confining stress relationship. A failure to account for the effects of suction resulted in overestimation of relative density and peak

friction angle using a semi-theoretical correlation. This is one of the first studies of cone penetration in unsaturated silty sands and provides a useful set of data that may have some applicability for similar soil types.

Relatively few studies evaluate the CPT on unsaturated fine-grained soils. Tan (2005), as previously described, worked with silt in a calibration chamber. The author used spherical cavity expansion equations to build a methodology for interpreting CPT in unsaturated silt. The increase of suction in the soil caused increasing tip resistance determined by miniature CPTs. The application of spherical cavity expansion equations revealed that soil in the plastic zone around the cone undergoes dilation during probe penetration, volumetric strain in the plastic zone decreased with increasing matric suction, and volumetric strain also decreased with increasing tip resistance. The prediction method developed by the author was used to interpret field data. The predictions made were reasonable based on the results of the field data.

The Tan (2005) study has, to date, been the most comprehensive study on unsaturated fine-grained soils. The findings from Tan's research and the findings from other researchers who have worked with sands are examined within the context of the current research presented in this dissertation.

2.2.5 The Standard Penetration Test (SPT) in unsaturated soil

The standard penetration test (SPT) is the most commonly used test in any geotechnical investigation. The results of the test includes the dynamic blow count necessary to drive a split-barrel sampler into the soil (N-Value). Many correlations are used in the design of shallow foundations based on the SPT N-value. These can be used to estimate density, stiffness, friction angle, and undrained shear strength. Empirical

correlations even exist to predict bearing capacity and settlement of foundations based on N-value. The samples that are collected during SPT can be used for soil index testing such as Atterberg limits and grain size distribution.

The popularity of the SPT in almost all applications would suggest that there are correlations that will allow the user to interpret results from unsaturated soil profiles; however, this is not the case. One study, where a reference to SPT in unsaturated soil was made was in Mohamed and Vanapalli (2015) who used a combination of SPT, and in situ plate load tests to establish a relationship between N-value and bearing capacity of unsaturated sands. The authors used SPT correlations to determine CPT tip resistance and then used a relationship to relate tip resistance to bearing capacity. The authors found good correlation between the predicted bearing capacity and measured bearing capacity. This method provides a simple way to predict the impact of suction on bearing capacity. However, the soil tested was poorly graded sand, so resulting correlations are unlikely to be appropriate for fine-grained soils.

2.2.6 Cavity Expansion Theory for Unsaturated Soils

Cavity expansion theory defines the expansion of a cylindrical or spherical cavity in an infinite soil mass. The importance of cavity expansion theory in geotechnical engineering comes from its connection with a number of geotechnical problems including bearing capacity of deep foundations, interpretation of pressuremeter tests, cratering by explosives, and breakout resistance of anchors (Vesic, 1972). The work of co) presented a general framework for cylindrical and spherical cavity expansion theory in an infinite soil mass. This work was then carried on by researchers who were able to

use cavity expansion theory to describe stress components of PMT and CPT (e.g. Yu 1990, Salgado et al. 1997, etc.)

Some caveats to the cavity expansion theory described by Vesic (1972) includes the assumptions that cavity expansion takes place in drained or undrained conditions. This means that only a single stress-state variable, the Terzaghi effective stress, is needed to describe the soils strength behavior. In soils that are not fully saturated a Bishop-type effective stress model or two stress-state variable approach is needed. Research described in this dissertation focuses on the two stress-state variables presented in Fredlund and Rahardjo (1993). These include the net normal stress, which is defined as the difference between total stress and pore air pressure (σ_n-u_a) and the matric suction, defined as the difference between the pore air and pore water pressure (u_a-u_w).

In order to use cylindrical and spherical cavity expansion equations in unsaturated soils the two stress-state variables must somehow be included in the general equations provided by Vesic (1972). To do this Muraleetharan et al. (1998) derived cylindrical and spherical cavity expansion equations for unsaturated soils incorporating the net normal stress and matric suction as well as associated elastic parameters and strength parameters associated with two stress-state variables. The equations were applied to pressuremeter analysis in Miller and Muraleetharan (2000) as previously mentioned. Further, Tan (2005) used the cylindrical and spherical cavity expansion equations described in Muraleetharan et al. (1998) to interpret results of CPTs and PMTs in a calibration chamber.

These equations were developed considering the equilibrium of stress conditions at the boundary of the elastic and plastic zones indicated by the arrow marked "R_p" shown in Figure 2.2. The inner portion of Figure 2.2 represents the expanding spherical or cylindrical cavity. The initial radius of the cavity is indicated as R_i, R_u represents the ultimate cavity radius and P_u represents the ultimate cavity pressure. The radius of the plastic zone is indicated by R_p and radial and circumferential stresses are shown as σ_r and σ_θ, respectively. The radial displacement is indicated as u_p. The radial stress at r = R_p is indicated as σ_P. The assumptions involved in the analysis and further assumptions employed by Tan (2005) were as follows:

- The soil beyond the plastic zone behaves as a linear elastic solid and soil within the zone behaves as a compressible plastic solid. This allows for determination of the relationship shown in Equation 2-1, which relates the radius of the plastic zone to the radius of the cavity. This is described in more detail in Tan (2005).

$$\frac{R_p}{R_u} = \sqrt{I'_{rr}} \qquad \text{(Eq. 2-1)}$$

- Young's Modulus was taken as the pressuremeter modulus, E_P.
- Poisson's ratio, ν, is known and is equal to 0.333.
- Gravimetric water content, *w,* and matric suction do not change during expansion. This was an assumption employed by Tan (2005) to simplify the analysis. It is also supported by Muraleetharan et al. (2003) where numerical modeling indicated matric suction did not change during PMT expansion.
- Pore air pressure, u_a, remains at atmospheric pressure (u_a=zero kPa gage pressure) during cavity expansion.

Employing these assumptions, reduced forms of cylindrical and spherical cavity expansion equations were presented as follows.

1) The reduced form of cylindrical cavity expansion equation for unsaturated soil is given as Equation 2-2,

$$P_u = F'_q p + F'_c c \quad \text{(Eq. 2-2)}$$

Where:

P_u = ultimate cavity pressure,

F'_q, F'_c = dimensionless cylindrical cavity expansion factors

p = mean net normal stress

c = effective cohesion

$$c = c' + (u_a - u_w) \tan(\phi^b) \quad \text{(Eq. 2-3)}$$

c' = cohesion

u_w = pore water pressure

u_a = pore air pressure

ϕ^b = angle of internal friction with respect to matric suction variation

$$F'_q = (1 + \sin\phi') I'_{rr}{}^{\sin\phi'/(1+\sin\ '')} \quad \text{(Eq. 2-4)}$$

ϕ' = angle of internal friction,

I'_{rr} = reduced rigidity index,

$$I'_{rr} = \frac{1+\varepsilon_v}{\frac{f_2}{I'_r}+\varepsilon_v} \quad \text{(Eq. 2-5)}$$

$$f_2 = \cos\phi' \quad \text{(Eq. 2-6)}$$

$$F'_c = (F'_q - 1)\cot\phi' \quad \text{(Eq. 2-7)}$$

$$I'_r = \frac{E}{2(1+\nu)[p\tan\phi' + c]} \quad \text{(Eq. 2-8)}$$

I'_r = rigidity index and,

ε_v = volumetric strain in the plastic zone.

2) The reduced form of spherical cavity expansion equation in unsaturated soil is given by Equation 2-9,

$$P_u = F'_q p + F'_c c \quad \text{(Eq. 2-9)}$$

Where parameters are the same as for Equation 2-2, except:

F'_q, F'_c = dimensionless spherical cavity expansion factors,

$$F'_q = \frac{3(1+sin\phi')}{3-sin\phi'} I'_{rr}{}^{4sin\phi'/3(1+sin\phi')} \quad \text{(Eq. 2-10)}$$

$$F'_c = (F'_q - 1)\cot\phi' \quad \text{(Eq. 2-11)}$$

$$I'_{rr} = \frac{1+\varepsilon_v}{\frac{f_1}{I'_r}+\varepsilon_v} \quad \text{(Eq. 2-12)}$$

$$f_1 = \frac{3cos\phi'}{3-sin\phi'} \quad \text{(Eq. 2-13)}$$

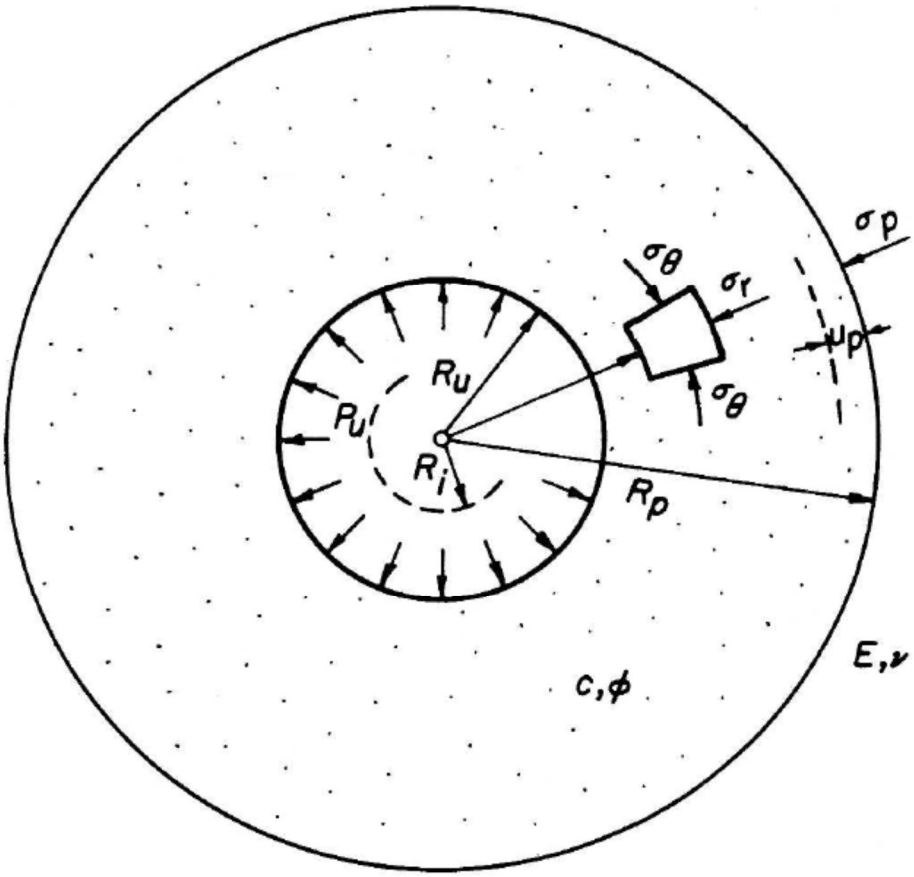

Figure 2.2: Expansion of cavity (Vesic, 1976)

The appeal in using the above equations to interpret pressuremeter and cone penetration data is that nearly all of the parameters can be determined through laboratory and field-testing. The lone parameter that cannot be determined through testing is the volumetric strain in the plastic zone, ε_v. The results obtained by Tan (2005) from calibration chamber testing using miniature pressuremeter and cone penetration tests produced enough data such that ε_v could be back calculated. The volumetric strain was found to correlate with ultimate cavity pressure, which is analogous to limit pressure and tip resistance. Thus, Tan (2005) computed volumetric strain for different cavity pressure ranges and soil suction ranges. With estimates of the

volumetric strain, it is possible to predict changes in cavity pressure due to changes in matric suction if the elastic parameters and shear strength parameters can be estimated for the soil. The method developed by Tan (2005) was investigated relative to the field data collected in this dissertation.

The effects of hydraulic hysteresis in cavity expansion behavior were evaluated by Yang and Russell (2015a&b). They developed a numerical model to simulate cavity expansion in an unsaturated silty sand. The investigation focused on the soil's initial location on its soil-water characteristic curve (SWCC). The authors found that starting location on the SWCC was significant to the cavity wall pressure developed via their numerical model. The authors used three soil moisture conditions in their model and evaluated the effect of each on the result. These included constant suction, constant moisture content, and constant contribution of suction to the effective stress meaning that as cavity expansion progressed the Bishop effective stress parameter multiplied by suction, χs, remained constant. The constant contribution, of the suction to effective stress was found to provide the best approximation of the other two conditions simplifying in situ test analysis. This partly justifies the assumption made by Tan (2005) that suction is constant during cavity expansion, which results in the reduced cavity expansion equations.

2.2.7 Use of in situ tests for foundation analysis

In situ testing is often a key component of foundation design. The key aspects of a foundation design include analysis of bearing capacity and settlement. Many in situ tests are capable of providing direct inference of properties used to calculate bearing capacity and settlement potential. Most geotechnical investigations involve the SPT.

Ideally the SPT should be used to collect samples and identify soil layers for further investigation as necessary; however, in many investigations it is the only in situ test conducted and N-values become the basis for foundation analysis. The prevalent use of the SPT has led to the development of many correlations that can be used to predict shear strength, friction angle, and density, as well as, provide direct estimates of bearing capacity and settlement. Correlations that exist for clays, however, are not recommended to obtain shear strength (Reese et al. 2006).

The CPT allows for simple determination of bearing capacity by using one of the several available correlations. Lunne et al. (1997) lists several correlations for cohesionless soils based on tip resistance multiplied by some empirical factor related to the shape of the foundation, the soil overburden pressure, or a combination of the two. In fine-grained soils, correlations based on tip resistance are used to determine undrained shear strength for bearing capacity determination. The undrained shear strength is calculated according to the following equation,

$$s_u = \frac{(q_c - \sigma_{vo})}{N_k} \quad \text{(Eq. 2-14)}$$

Where:

s_u = undrained shear strength,

q_c = tip resistance,

σ_{vo} = vertical overburden stress, and

N_k = empirical cone factor which is about equal to 17 for many soils.

The undrained shear strength is used to determine bearing capacity according to the following equation,

$$q_{ult} = N_c s_u + \sigma_z \quad \text{(Eq. 2-15)}$$

Where:

q_{ult} = ultimate bearing capacity,

N_c = Terzaghi bearing capacity factor, 5.7 for a friction angle of zero, and

σ_z = total overburden pressure acting at the base of the foundation.

The results of pressuremeter testing are straightforward to apply to foundation engineering. To determine bearing capacity there is a simple equation presented by Briaud (1992) as,

$$q_L = kP_{Le}^* + q_o \quad \text{(Eq. 2-16)}$$

Where:

q_L= ultimate bearing capacity,

k = pressuremeter bearing capacity factor, 0.8-1.2 for clay, 0.8-1.5 for silt, and 0.8-2 for sand,

$$P_{Le}^* = \sqrt[n]{P_{L1}^* P_{L2}^* \dots P_{Ln}^*} \quad \text{(Eq. 2-17)}$$

P_{Le}^*= equivalent net limit pressure determined from PMT tests with 1.5B of the bearing level,

$$P_{Ln}^* = P_L - P_{OH} \quad \text{(Eq. 2-18)}$$

P_{Ln}^*= net limit pressure from test n equal to the limit pressure minus at-rest horizontal earth pressure, and

P_{OH}= at rest horizontal earth pressure.

One equation for settlement from Janbu et al. (1956) is as follows,

$$s = \mu_0 \mu_1 (1 - \nu^2) q \frac{B}{E_p} \quad \text{(Eq. 2-19)}$$

Where:

s = settlement,

μ_0 = correction factor which account for depth of embedment,

μ_1= correction factor which accounts for depth to a rigid stratum,

ν = Poisson's ratio,

q = bearing pressure,

B = foundation width, and

E_p = pressuremeter modulus.

2.2.8 In situ testing applied to foundation analysis for unsaturated soils

The equations described in the previous section allow for determination of bearing capacity and or settlement based results from a single in situ test. This shows the practicality of performing in situ tests even if it is only part of a larger investigation. However, there has been very little research involving the use of in situ tests for foundation design is in the area of unsaturated soils. This represents a significant gap in available knowledge in light of the fact that nearly all shallow foundations are constructed on unsaturated soils. As mentioned previously, some limited work was recently published by Mohamed and Vanapalli (2015) that describes using a correlation to relate the SPT N-value to cone penetration tip resistance, which is then corrected for suction using an empirical correlation before determining bearing capacity. The study was performed in sand. The research described in this dissertation begins to fill the knowledge gap by addressing the use of in situ tests in fine-grained soils for foundation analysis.

2.3 Model bearing capacity testing in unsaturated soil

The challenge of working with soil is that site-to-site the characteristics of the material can change. This challenge has led to the development of site-specific solutions

to understand the fundamental characteristics of the material that will be relied upon. One site-specific solution that has developed over time is the plate load test. This test essentially aims to mimic the behavior of a shallow foundation on soil loaded to an ultimate failure state to obtain specific solutions to bearing capacity and settlement problems. There are countless examples of researchers using model footings in a laboratory or field setting to collect bearing capacity and settlement data (e.g. Cerato and Lutenegger 2007, Zhu et al. 2001, Skempton 1951, Anderson et al. 2007, etc.). This research has led to many developments on how to perform these tests on all types of soils. The research regarding the use of these tests in unsaturated soil is much more limited.

The work of Costa et al. (2003) details some model bearing capacity tests performed on a lateritic clayey sand layer. The authors performed ten plate load tests using a circular plate 0.8 meters in diameter and 25 mm thick. Two distinct loading procedures were used, the first being a slow maintained load, the other a quick maintained load. A settlement criterion was established to determine when subsequent incremental loads should be applied during testing. The settlement criteria used for the slow maintained load was presented as follows,

$$s_t - s_{t/2} \leq 0.05(s_t - s_{ti}) \quad \text{(Eq. 2-20)}$$

Where:

s_t= settlement recorded at time t,

$s_{t/2}$= settlement recorded at time t/2, and

s_{ti}= initial settlement at t=zero.

For the quick maintained load, each increment was held constant for 15 minutes and readings were taken at 0, 1, 2, 3, 6, 9, 12, and 15 minutes. In five of the ten tests, the test pit was inundated with water. In the other five tests, the in situ moisture content was maintained. In order to obtain different soil suctions, tests were performed at various times of the year. Suction was monitored using tensiometers installed next to the pit at depths of 100, 300, 600, and 800 mm. The authors did not see a clear failure pattern in the test results. Most soils tested exhibited punching failure and strain hardening. Therefore, the failure criteria were set by the authors to be the yield stress. The results showed that the plate-load test results were heavily influenced by increasing matric suction. A nonlinear relationship was developed for the ultimate stress at failure, σ_f, which corresponds to the onset of permanent soil deformation and is as follows:

$$\sigma_f = 48.1 + 6.2(u_a - u_w)^{0.70} \quad \text{(Eq. 2-21)}$$

The rate of settlement showed a non-linear decreasing response with increasing soil suction. For an applied stress level, settlement rate increases with decreasing soil suction. The influence of suction was more significant for comparatively high-applied stress levels and for comparatively low suction values.

Xu (2004) performed plate load tests on an unsaturated expansive soil. A square plate 30 x 30 cm was used in the testing. A load-controlled test was used where each load was applied until the settlement reached less than 0.01 mm per hour. Tests were performed in situ on Handan and Ningxia soils, which are locally expansive clays. The clays were tested in a saturated and unsaturated condition. The results of the testing showed that samples with lower moisture content (higher suctions) had larger bearing capacity. The unsaturated soils studied had relatively high degree of saturation (greater

than 80%). The authors related bearing capacity to swelling pressure because it is typically easier to measure in a laboratory than unsaturated strength parameters and matric suction. The predictions of bearing capacity based on swell pressure are quite good.

Rojas et al. (2007) performed five plate load tests on an unsaturated lean clay deposit, and two in a saturated condition. Five different matric suction values were used in the tests, which were verified using tensiometers inserted at depths of 10, 30, 60, and 90 cm around each test pit. For each load increment, the load was held until the maximum deformation of 0.03 mm/min was obtained for three consecutive readings. Tests were stopped when either the maximum capacity of the hydraulic jack used to apply the load was reached, or the plate reached 10% settlement. The authors found an increasing nonlinear trend between matric suction and bearing capacity.

Vanapalli and Mohamed (2007) proposed a technique to predict the bearing capacity of an unsaturated poorly graded sand using saturated shear strength parameters, c' and,ϕ'. The authors performed bearing capacity tests using a model footing in a laboratory. The tank, which contained the soil, had an adjustable water table, which was used to achieve a desired matric suction. The matric suction was measured using commercially available tensiometers. The authors noticed an increase in bearing capacity based on an increase in matric suction. An equation was developed for bearing capacity based on the Terzaghi's (1943) bearing capacity equation. The new equation included effective cohesion, which was presented as Eq. 2-3. The influence of suction on shear strength as described by the friction angle with respect to matric

suction,ϕ^b is difficult to determine experimentally, so a relationship between the effective friction angle and degree of saturation was used instead, as follows,

$$\tan \phi^b = S^k \tan \phi' \quad \text{(Eq. 2-22)}$$

Where,

S = degree of saturation, and

k = fitting parameter.

This equation is then used to define bearing capacity for unsaturated soils as follows:

$$q_u = [c' = (u_a - u_w)S^{\psi} \tan \phi'] N_c \xi_c + 0.5 \gamma B N_\gamma \xi_\gamma \quad \text{(Eq. 2-23)}$$

Where,

$\psi =$ Bearing capacity fitting parameter, and

N_c, N_γ = Terzaghi (1943) bearing capacity factors for cohesion and unit weight,

ξ_c, ξ_γ = Vesic (1973) shape factors for cohesion and unit weight,

γ = unit weight,

B = footing width.

To make full use of the equation provided by Vanapalli and Mohamed (2007) it is necessary to have information about the soil's shear strength parameters, including cohesion, and friction angle, as well as, the soil water retention curve data. The authors plotted measured bearing capacity versus matric suction and back calculated the fitting parameter, ψ. This, together with data from literature was used to find a relationship between plasticity index and the fitting parameter that can be obtained through the following equation,

$$\psi = 1 + 0.34PI - 0.0031PI^2 \quad \text{(Eq. 2-24)}$$

Where:

PI = plasticity index.

The bearing capacity of unsaturated sands was further evaluated by Li (2008) who performed model bearing capacity tests on three sands under saturated and unsaturated conditions. The results showed that bearing capacity of fine-grained sand increased as matric suction increased, and for coarse-grained sand decreased with increasing matric suction. The explanation for the decrease in bearing capacity in the coarse-grained sand was attributed to the sensitivity of the soil to compaction energy. However, this is interpreted, as the void ratio was higher as suction increased which caused a decrease in bearing capacity. The author had difficulty installing tensiometers so suction was estimated by using the distance to the water table from the soil surface.

Oh and Vanapalli (2013) evaluated the modified effective stress approach (MESA) presented in Vanapalli and Mohamed (2007) for application to footings in fine-grained soils. The modified effective stress approach essentially replaces the cohesion parameter in Terzaghi's bearing capacity formula with parameters that account for the impact of matric suction. An example of the MESA is shown in Equation 2-23. The authors identified some limitations in using the MESA and sought to overcome these by using a modified total stress approach (MTSA). The modified total stress approach (MTSA) essentially reduces the Terzaghi bearing capacity equation to only the first parameter and now the "c" parameter is equal to the undrained shear strength. The authors' previous research indicates the main failure mechanism in bearing capacity tests of unsaturated fine-grained soils is punching shear. The authors assumed that the compressibility characteristics of the soil below the footing dominates the

bearing capacity of unsaturated fine-grained soil. The constant water content triaxial test is the most reasonable test to simulate loading and drainage for unsaturated fine-grained soils; however, these tests are time consuming and require specialized equipment. For these reasons, the authors used unconfined compression testing to estimate bearing capacity of unsaturated fine-grained soils. To evaluate the validity of the MTSA and MESA an experimental program using a 50 x 50 mm model footing on fine-grained soils for five matric suction profiles was conducted. A low PI (PI=15) soil was used in the study. The results of the testing showed that the MTSA could be used to predict bearing capacity behavior of fine-grained soils based on UC tests. The bearing capacity factor, N_c, was back calculated based on the results of the bearing capacity testing. The MTSA was then tested using data from Consoli et al. (1998) who conducted in situ plate load tests in an unsaturated low PI (PI=20) deposit. The results showed good agreement when compared to Consoli et al. (1998); however, the UC test used to make the calculation must come from a depth that represents the average suction for the site.

The modulus of elasticity is important for the computation of settlement in soil. Oh et al. (2009) presented work that resulted in a method to predict the variation of modulus of elasticity with respect to matric suction for sandy soils based on the soil water characteristic curve (SWCC) and saturated modulus of elasticity. The authors presented results of model footing tests for three separate sands, using two different footing sizes. Tests were completed at matric suctions ranging from 0-0.87 psi. Modulus of elasticity was calculated from the linear portion of the stress versus settlement relationship of the bearing capacity tests. A model to predict the unsaturated modulus of elasticity was developed that makes use of the modulus of elasticity for

saturated conditions, the current matric suction, atmospheric pressure, degree of saturation, and two fitting parameters, α, and β. The parameters α, and β control the nonlinear variation of modulus of elasticity. The authors found that the model provided a good fit to measured modulus values. Fitting parameters of $\alpha = 2.5$, and $\beta = 1$ provide reasonable estimation of modulus for unsaturated sandy soil. The authors suggested that α between 1.5 and 2 provides conservative elastic settlements in engineering practice. The authors also looked at the effects of desaturation on the elastic modulus and found that it is at a peak value near the air entry point on the soil water characteristic curve.

2.4 Summary of Knowledge Gaps and Contribution of Current Research

The literature review reveals that while there have been significant advancements in knowledge, there is very little real data that reveals the influence of variable saturation on results of in situ tests or foundation performance. Most experimental work on foundation performance focused on sandy soils and there appears to be a lack of studies involving nearly simultaneous foundation testing and in situ testing in the same soils under variable saturation. Research conducted and described in this dissertation contributes to the knowledge base in several ways as follows:

1. Created valuable data set, which included pressuremeter, cone penetration, and standard penetration tests at two fine-grained sites under variable saturation.
2. Created valuable data set, which included miniature pressuremeter and model footing, tests on a clayey soil under variable saturation in the laboratory.
3. Developed an empirical and analytical method of analysis for interpreting in situ tests in unsaturated soils.

4. Developed methods for foundation analysis using PMT under variable saturation.

Chapter 3 Experimental Testing: In Situ

3.1 Overview

In situ tests, including cone, pressuremeter, and standard penetration, were performed at two field sites over the course of two years. During each site visit, detailed test and site data were collected and analyzed. At each of the two sites, a weather station was installed to track weather information at the site, as well as volumetric soil moisture data from sensors located at 1ft, 3ft, and 6ft below the ground surface. Index property testing was performed on soil samples from the site to identify basic soil parameters such as particle size, plasticity index, and specific gravity. Strength testing was performed with constant water content triaxial tests for soil depth of 3ft, 6ft, and 9ft from each of the field sites. From each site visit soil, samples were collected for suction and moisture content determination. Details on the methods used to perform tests are provided in this section.

3.2 Test Sites

Two sites were chosen for this research. These sites will be referred to as the North Base and Goldsby sites. Both sites were located a short driving distance from the University of Oklahoma campus, which made them ideal candidates for testing. The North Base site is located west of the Max Westheimer Airport in Norman, OK (latitude: 35°14'6.58"N, longitude: 97°27'46.39"W). The soil profile at the site contains low and high plasticity soil with soil plasticity greater near the surface. A water table was found to fluctuate between depths of 8 to 9 feet. The majority of material found at

North Base is considered fine-grained; however, there were some rock inclusions found near bedrock. The Goldsby site is located near Goldsby, OK approximately 5 miles south of the University of Oklahoma (latitude: 35° 9'20.61"N, longitude: 97°28'40.04"W). The soil profile contains low plasticity clay for at least ten feet, which was the depth of interest for this investigation. There was no bedrock or a water table encountered during the research at Goldsby. The city of Norman and surrounding areas are shown in Figure 3.1. Indicated on the figure are the North Base site, and the Goldsby site.

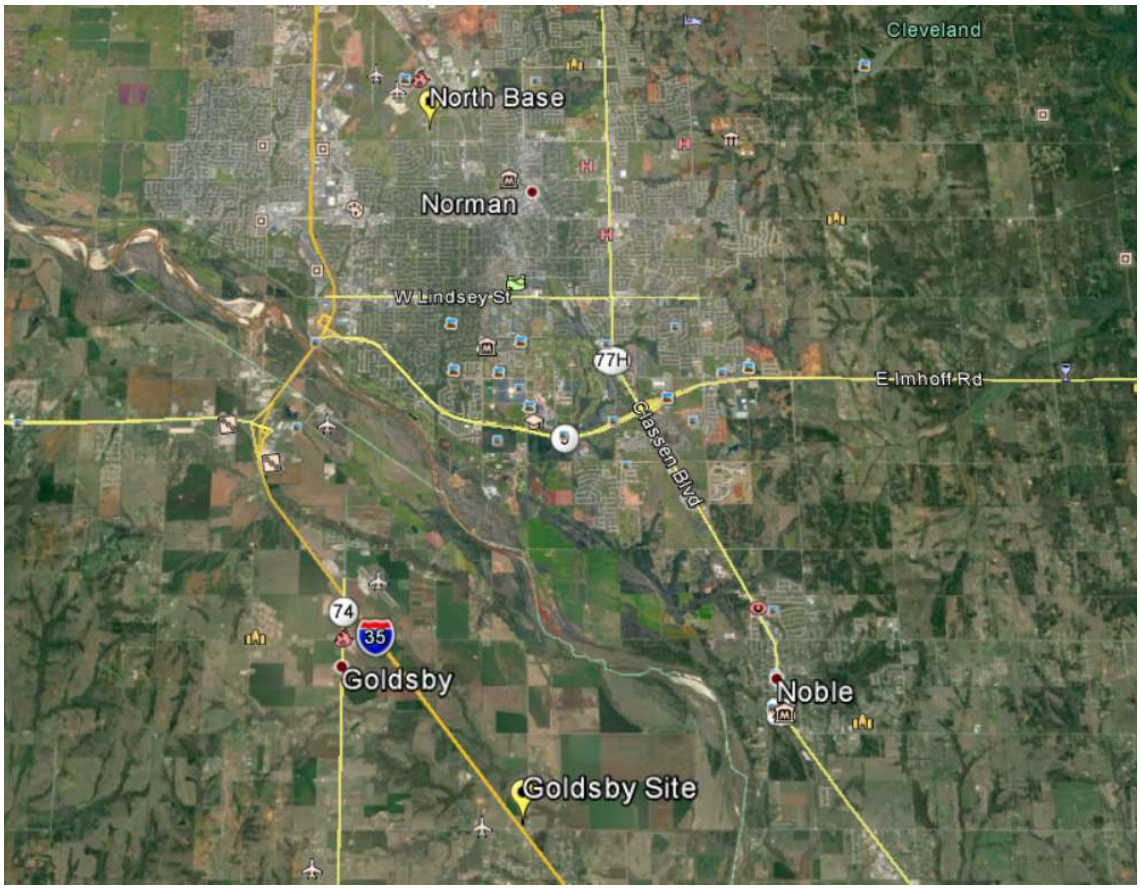

Figure 3.1: City of Norman with Goldsby and North Base research sites highlighted with yellow indicators

3.3 Site Instrumentation

The initial fieldwork started at the Goldsby site in June 2012, at which time the weather station was installed and data collection was initiated. The weather station was manufactured by Campbell Scientific Instruments. It included sensors that quantify rainfall, air temperature, relative humidity, wind speed, wind direction, solar radiation, and volumetric water content at three depths in the soil profile.

A similar weather station was installed at the North Base site in August 2012 at which time data collection began. A photograph of the weather station installed at North Base is shown in Figure 3.2. Also shown in the picture is the Oklahoma Department of Transportation (ODOT) Cone Penetration Test (CPT) truck on one of their site visits. The weather station details are shown in Figure 3.3; this includes the component parts connected with model numbers. The range of measurement of the sensors is also provided in Figure 3.3.

Figure 3.2: Weather station installed at North Base test site, Oklahoma Department of Transportation truck in background performing CPT.

Figure 3.3: Components of Campbell Scientific weather station including range of measurements (Doumet, 2015)

3.4 In Situ Site Characterization

The site visits were a key aspect of this research. Tests were performed on roughly 100-ft.-by-100-ft. plots. Each site visit would typically consist of a sampling phase followed by testing. Tests were performed as often as possible. Typical PMT tests were performed either monthly or bi-monthly depending on equipment availability.

CPT and SPT was performed as often as the Oklahoma Department of Transportation (ODOT) was available. Test locations were mapped so that multiple tests would not be performed at the same location. Maps of each sites with test locations are presented in later sections. This was done in unison for pressuremeter testing. When the Oklahoma Department of Transportation (ODOT) was on site the sampling was done using split barrel tube sampling during Standard Penetration Testing (SPT). The sampling during pressuremeter testing (PMT) was performed using a 3-inch diameter hand auger. At the North Base (NB) site, bedrock was found at around 9 feet on average and the water table rose throughout the first year of testing. Thus, sampling was limited to depth of 7.5 feet at North Base. At Goldsby (GB) and sampling was conducted in the upper 9.5 feet of the soil profile. The sampling procedure for both sites proceeded as follows: at each six inch interval a sample was taken from the hand auger for moisture content determination, these were placed in sample tins and sealed with electrical tape to prevent any premature evaporation. In the intermediate depths between the six inch intervals material was collected in sandwich bags for use in grain size analysis, plasticity indices, and specific gravity determination. This process was repeated until the termination depth was reached. In the case of pressuremeter testing the sampling was placed on hold near test depths of 3ft, 6ft (5ft for NB), and 9ft (7ft for NB) so that probe could be inserted and a test could be administered. After completion of the test, sampling continued as previously described. The samples were then transported to the laboratory where soil index property testing, moisture content determinations, and suction measurements were made. Results of these tests will be provided in more detail in further sections.

Additional in situ samples were collected using Shelby tubes. The Shelby tubes were pushed into the ground using an ODOT drilling truck. Shelby tube samples were then sealed on top and bottom using a combination of rubber caps and duct tape. Samples were brought to the laboratory as quickly as possible for extrusion. Once extruded, samples were measured and weighed, then sealed in plastic wrap and stored in a moisture room until they were required for testing.

3.5 Laboratory Testing Methods

3.5.1 Basic soil properties

Laboratory testing was conducted to determine basic physical and index properties. Grain-size distribution and liquid and plastic limit tests were conducted in general accordance with ASTM standards (D422, D4318) on samples obtained at depths encompassing the locations of in situ tests (0 to 10 ft.). Results of these tests were used to classify the soils at each test site. Specific gravity was determined on selected samples in accordance with ASTM Standard D854.

In addition, Cation Exchange Capacity (CEC) was determined for selected samples by a commercial laboratory, Agsource, in Lincoln Nebraska. The summation of cations method was used to determine the amount of exchangeable cations. This method involves measuring the amounts of available calcium, magnesium, potassium, and sodium; the method used by Agsource is described in detail in Brown and Warncke (1988).

3.5.2 Soil Water Characteristic Curve (SWCC) test

The WP4 dewpoint potentiameter, manufactured by Decagon, was the primary method for the determination of the SWCC for Goldsby and North Base. The WP4

measures total water potential (total suction) using the chilled mirror method to determine the relative humidity of the air above a sample in a closed chamber. The relative humidity above the sample is assumed to be at equilibrium with the air in the sample. At temperature equilibrium, relative humidity is directly related to water potential. Total suctions in the range of approximately 1 to 300 MPa (145 to 65,265 psi) can be determined using this method, as indicated by Decagon.

The material collected in the moisture tins at the field location was brought to the laboratory and immediately subjected to a suction measurement. The WP4 device comes with small stainless steel cups that are filled, by hand, half way with a representative sample. The cups filled with soil are placed inside the WP4 chamber and a suction measurement is made. Figure 3.4 shows the Decagon dewpoint potentiameter with stainless steel sample cups half filled with soil. The remaining material in the moisture tin is weighed and placed in an oven for moisture content determination in accordance with ASTM D2216.

Figure 3.4: Decagon dewpoint potentiameter and soil sample cups

3.5.3 Determination of shear strength

The soil samples collected in Shelby tubes were used to determine shear strength characteristics of the soil at the in situ test sites. The samples extruded from the Shelby tubes were tested in a conventional triaxial compression device. After extrusion from the Shelby tubes, samples at depths of interest were trimmed and placed in the rubber membranes inside of a triaxial cell. A multi-stage isotropically consolidated undrained compression test (CIUC) with pore water pressure measurement was used to obtain shearing characteristics. Undrained triaxial testing coupled with pore water pressure

measurement was desired so that drained and undrained shearing information could be obtained according to ASTM D4767.

Table 3.1 presents the site name, borehole number, sample depth, cell pressure, and backpressure used for each triaxial test. The effective stress range was varied. Backpressure saturation was used to reach close to 100% saturation.

3.6 In Situ Testing Methods

The in situ tests used in this research included the pressuremeter test (PMT), cone penetration test (CPT), and standard penetration test (SPT). The PMT was performed by the author and an assistant. The CPT and SPT were performed with cooperation of the Oklahoma Department of Transportation (ODOT).

3.6.1 Pressuremeter tests (PMT)

The pressuremeter probe used in all tests was a Roctest Texam pressuremeter with a rubber membrane shown in Figure 3.5. This probe has an expandable portion measuring 14.25 inches long and approximately 2.75 inches in diameter. The rubber membrane was used as opposed to a steel-sheathed "Chinese lantern" style membrane because the soils tested were relatively soft, so a flexible membrane provided better contact and more uniform cavity expansion. Stress-controlled tests were conducted in accordance with ASTM D4719-09 procedure A, whereby expansion pressure is increased incrementally while monitoring volume injected into the probe during a 60-second interval for each pressure increment. Regulated nitrogen was used to force fluid into the pressuremeter probe while injected volume was monitored using a sight glass on the fluid standpipe.

The PMT probe was placed in the borehole such that the center of the inflatable portion of the probe was placed at the depth of interest. Relatively small pressure increments were used in an attempt to produce well-defined expansion curves and in most cases; an unload-reload sequence was used. To capture an unload-reload loop the soil was loaded until it showed slight yield behavior. At this point, the pressure was decreased and the soil was allowed to rebound for five minutes prior to reloading. When reloading commenced, the probe inflation continued until the injected volume reached the safe limit. The probe was then deflated and retracted from the borehole. A summary of PMT tests conducted during this study is provided in Table 3.2. Table 3.2 includes test dates, test depths, measured suction and water contents obtained for each test depth.

3.6.2 Cone penetration testing (CPT)

The Oklahoma Department of Transportation (ODOT) performed cone penetration tests at both Goldsby and North Base. Three test soundings were obtained per site visit. The cone was pushed to a depth of approximately 10 feet for each sounding. Thirty-nine cone soundings were conducted over the course of this research, as summarized in Table 3.3.

The CPT was run in general accordance with ASTM standard D5778-12, with a penetration rate of approximately 0.73 in./sec (2cm/sec) using a standard cone with a 60-degree apex conical point having a projected tip area of 1.55in^2, and a friction sleeve just behind the cone with an area of 23.3 in^2. Electronic signals from the tip and sleeve load cells were collected with a data acquisition system and used to compute tip resistance and skin friction.

3.6.3 Standard penetration testing (SPT)

Standard penetration testing (SPT) was performed by the Oklahoma Department of Transportation (ODOT). An automatic hammer was used to drive the split spoon sampler into the ground. One test was performed per test date in general accordance with ASTM D1586-11.

Table 3.1: Summary of multi stage triaxial compression tests conditions for Goldsby and North Base.

Site	Sample Date	Sample Depth (in.)	Back pressure (psi)	Cell pressure (psi)		
				Stage 1	Stage 2	Stage 3
Goldsby	12/8/2014	30-37.5	61	64	68	76
	5/10/2013	71-81	50	52	57	79
North Base	9/3/2013	48-54	50	53	57	65
	7/31/2014	70-77	105.6	116.9	127.6	150.6

Figure 3.5: Roctest Texam NX long probe pressuremeter used for all PMT.

Table 3.2: Summary of PMTs from Goldsby and North Base

	Test Date	Tested Depth (ft.)					
		3		5		7	
		Suction (psi)	Water Content	Suction (psi)	Water Content	Suction (psi)	Water Content
North Base	2/1/2013	463.4	14.8	95.7	17.2	-	
	3/11/2013	302.4	14.5	72.5	16.2	-	
	4/12/2013	359.7	14.7	117.5	13.8	45	19.5
	4/30/2013	378.1	15.8	168.2	16.1	59.5	18.2
	10/11/2013	427.9	16.2	103	21	84.1	21
	1/7/2014	224.8	23.5	121.8	19.5	113.1	26.1
	3/31/2014	223.4	21.6	71.1	22.9	-	
	7/25/2014	91.4	20.6	46.4	20.8	7.25	20.3
	8/22/2014	245.1	20	100.1	20.4	53.7	22.6
	10/31/2014*	226.3 269.8	18 19	110.2 76.9	18.5 17.8	76.9 15.9	19.2 19.9
Goldsby	2/1/2013	306.5	13.5	73.5	15.6	89.9	17.8
	3/13/2013	310.4	10.6	103.7	12.2	46.4	16.9
	4/15/2013	62.4	20.4	53.7	14.3	46.4	18.1
	5/2/2013	81.2	20.3	90.4	13.8	74.9	17.2
	6/10/2013	87	21.4	130.5	12.7	87	17.1
	10/16/2013	124.7	13.5	63.8	18.5	72.5	20.3
	1/8/2014	81.2	19.2	85.6	17.6	110.2	21.8
	3/31/2014	46.4	18.8	34.8	21.2	8.7	20.5
	7/23/2014	103	15.1	85.6	16.2	66.7	18.1
	8/22/2014	174	13.7	92.8	14.8	81.2	17.2
	10/17/2014*	195.8, 339.4	10.5, 9.8	84.1, 89.9	15.1, 13.8	78.3, 68.2	18.0, 17.6
* two tests performed on this date							

Table 3.3: Summary of CPT from Goldsby and North Base

	Test Date	Number of Soundings	Average Site Moisture Content
North Base	2/1/2013	3	16.6
	5/6/2013	3	20.5
	9/3/2013	3	17.7
	11/21/2013	3	20.2
	2/18/2014	3	22.6
	9/10/2014	3	18.9
	12/30/2014	3	20.4
Total North Base Soundings		21	
Goldsby	2/1/2013	3	15.1
	5/6/2013	3	16.7
	7/29/2013	3	16.8
	11/21/2013	3	16.8
	2/18/2014	3	18.5
	9/10/2014	3	13.9
Total Goldsby Soundings		18	

Chapter 4 Experimental Methods: Model Footing Bearing Capacity Testing

4.1 Overview

Model footing (4-in. diameter) bearing capacity tests and miniature pressuremeter tests were performed in an unsaturated low plasticity clay in a testing chamber prepared at five different moisture contents. Three miniature pressuremeter tests were performed prior to the bearing capacity test at locations surrounding the footing. The tests were performed at a distance of 6 inches from the outside diameter of the footing. This distance was assumed to be far enough from the footing that any disturbance from the excavation would be minimal to the bearing capacity test. The holes were backfilled after completion of the MPMT. It was thought that the model footing test would influence the MPMT more than the MPMT would influence the footing test. A hydraulic pump was used to apply pressure to a hydraulic jack that transferred axial load to the footing. A load cell placed between the hydraulic jack and the bearing plate was used to measure force applied. Two diametrically opposed dial indicators were used to measure settlement. At the end of each test, post-mortem sampling was performed on the soil bed to determine density, moisture content, and total suction. This chapter describes details of the methods used to perform model bearing capacity and miniature pressuremeter tests.

4.2 Bearing Capacity Test Apparatus

The apparatus for testing was constructed using a structural steel tank mounted to a steel base plate. Four threaded rods were used to mount a reaction frame that was

constructed from two steel channel sections welded together. A schematic of the test apparatus is shown in Figure 4.1. The baseplate used was 38 inches in diameter with 2.5-inch thickness. Sitting on top of the baseplate is the structural steel tank. This tank had an inner diameter of 29 inches, 20 inches in height, and 1-inch wall thickness, which was selected based on the largest size chamber shell available in the laboratory. There was a two-inch flange mounted on the outer rim the top and bottom of the tank with boltholes for connecting the reaction frame and baseplate.

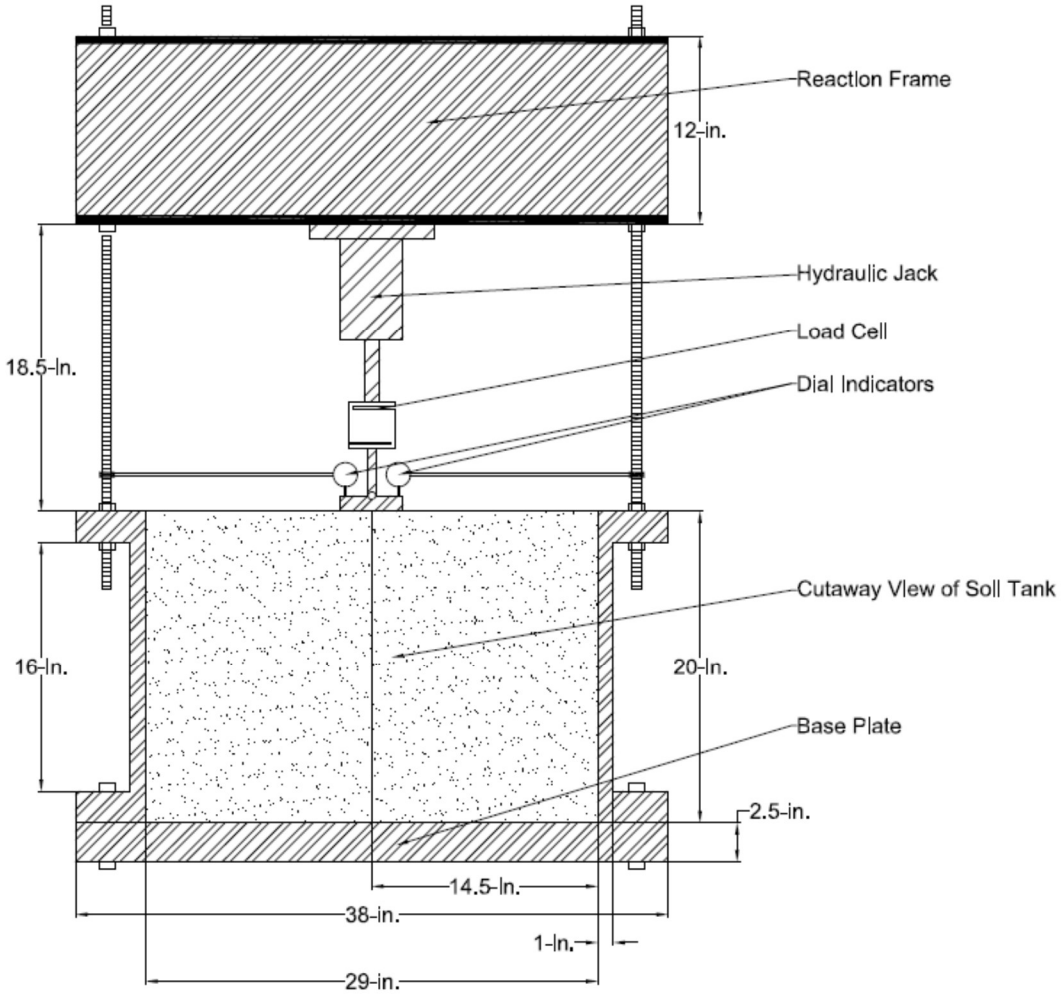

Figure 4.1: Model bearing capacity test assembly

Four ¾-inch all-thread rods were used to connect the reaction frame to the soil tank. Nuts and washers were used to secure the rods to the tank and the reaction frame to the rods. The reaction frame was sized such that deflection during loading was assumed negligible. A ten-ton hydraulic jack was mounted to the base of the reaction frame. A 10-kip load cell was secured to the hydraulic jack using threaded rod. A ball joint was used to connect the threaded rod at the base of the load cell to the bearing plate. The ball joint was used as a moment break to ensure that only concentric axial load reached the footing. Two dial indicators with 0-1 inch range of measurement were mounted to the side of the testing tank using magnets, and positioned to measure vertical displacement of the bearing plate.

4.3 Soil Properties

A low plasticity clay soil was desirable for this research to ensure that the effects of suction did not make the sample overly strong and for workability during sample preparation. The soil chosen for this research was collected near Chickasha, Oklahoma. It comes from the McClain Series soil, which is primarily a thick layer of silty-clay material (Esmaili, 2014). The soil was collected along U.S. Route 62. It is referenced by Esmaili (2014) as cs2780 (cross-section 2780). The basic soil properties for the McClain clay are presented in Table 4.1, which come from tests performed by Esmaili (2014). The Atterberg limits, grain size distribution, maximum dry unit weight and optimum moisture content were determined in accordance with ASTM D4318, D422, and D698, respectively. The soil was classified using the USCS as low plasticity clay, CL.

Table 4.1: McClain clay soil properties (after Esmaili, 2014)

McClain Clay	
Liquid Limit	39%
Plastic Limit	22%
Plasticity Index	17%
% Passing #200	95.2%
Optimum Moisture Content	18%
Maximum Dry Unit Weight	119.7pcf
Friction angle	34.2°
Cohesion	3.0 psi

4.4 Sample Preparation

The McClain clay used in this study had been stockpiled from a previous study that had made use of the soil (Esmaili, 2014). The soil was brought into the laboratory and spread on a concrete floor with a fan circulating dry air over the sample to allow it to come to air-dry conditions. The soil was turned with a shovel to ensure that the soil was uniformly dry. Once this state was reached, the soil was processed through a #4 sieve. The soil was then sealed in 5-gallon buckets until mixing.

The aim of this research was to measure the influence of matric suction on the bearing capacity characteristics of low plasticity clay and develop a method of prediction of bearing capacity using the pressuremeter. To do this several moisture contents were targeted in a range of 10% to 17%, which produced a range of suctions consistent with that expected under field conditions. A density equal to 90% of maximum dry unit weight (119.7 pcf) was selected as the target. The target dry unit

weight was 107.7 pcf and used for all tests performed while target moisture contents were varied. Target moisture contents, suctions determined using the WP4, and dry densities for the five test beds are presented in Table 4.2. The average suctions, and moisture contents shown are based on post mortem sampling of the test bed in one-inch increments for the full 19 in. depth of the test bed. The dry density is based on the amount of soil put into the test tank and the moisture content of the material. The variations in dry density relative to the target are attributed to some difficulty during compaction.

To prepare for each test, the hygroscopic moisture content of the dry soil was determined. From this, the amount of water and dry soil that would be necessary to achieve the target moisture content and dry unit weight was calculated for each test. First, an empty mixing tub was placed on the scale and its mass was determined. Then around 45-50 lbs. of dry soil depending, on the sample being prepared, was put into the mixing tub. Water was then "rained" over the soil using a watering can. Once the correct amount of water was added to the soil, the soil and water were mixed by hand until they were observed to be homogenous. After this point was reached, the mixture was transferred to a five-gallon bucket and sealed with a lid overnight.

The soil was compacted into the tank in seven layers. The buckets were prepared such that three buckets would contain the correct amount of soil to fill each layer; thus, a total of 21 buckets of soil were prepared for each test. Once the soil was placed into the test tank, it was spread so that it was level. Compaction was performed using a tamper. Horizontal lines were marked inside of the tank to ensure the proper layer height. Once the proper height of each soil layer was achieved, the top of the layer was

scarified and the next layer was added. This process was repeated until the soil reached the top of the tank. Excess soil was then trimmed from the top, collected and weighed so that dry density of the material in the tank could be determined. Soil near the surface of the tank was difficult to compact because there was no lateral confinement above the rim of the tank, which is believed to contribute to the inconsistency in the dry density of the tests performed. After leveling the surface of the soil in the tank, it was covered with thick plastic sheeting to prevent any moisture loss. The sample was allowed to sit for 24 hours prior to testing.

4.5 Miniature Pressuremeter Testing (MPMT)

The work of Tan (2005) involved the successful use of a miniature pressuremeter (MPMT) in calibration chamber testing of silt. This success and the size of the test bed used in this research made a miniature pressuremeter a good choice. The miniature pressuremeter works the same as a traditional pressuremeter; however, the scale of the equipment is smaller. Water is injected into an expandable rubber membrane while pressure and volume are maintained until the safe limit of the rubber membrane is reached. The MPMT used for this research was constructed at the University of Oklahoma with an aluminum body. It is pictured with the membrane attached in Figure 4.2 in its uninflated form. The expandable portion of the pressuremeter measures 6.26 inches in length and has a diameter of 0.75 inches. This provides a length to diameter ratio of 8.3, which exceeds the recommended value of 6.5 needed to simulate plane strain cylindrical cavity expansion (Briaud 1992, Tan 2005). The MPMT was conducted in three locations around the model footing. The tests were

conducted in a zone of soil roughly located between the stress bulb created by the model footing and the walls of the container.

Rubber surgical tubing was used for the MPMT membrane. This was obtained from Kent Elastomer in a size of ½ in. inner diameter (I.D.), and 1/16 in. wall thickness (W.T.). Originally, a ½ in. I.D., 1/32 in. W.T was used; however, this size was discontinued so the slightly thicker tubing was used. The first three test beds were tested using the thinner wall thickness surgical tubing for a membrane. The latter tests were performed using the thicker tubing. Typical corrections for a pressuremeter test include a correction for membrane resistance and system compressibility during testing. These corrections were determined for each membrane. The results of the compressibility testing for both the thinner wall thickness tubing and the thicker tubing are shown in Figure 4.3. The pressure loss in the system for both the thinner tubing and the thicker tubing curves are shown in Figure 4.4. The results of pressuremeter tests were corrected based on these figures.

Table 4.2: Average suctions, moisture content, and dry density for model footing bearing capacity tests

Date of Test	Average Suction (psi)	Average Moisture Content (%)	Dry Density (lb./ft^3)
2/29/2016	84.9	17.0	104.8
3/14/2016	115.6	12.7	102.2
3/28/2016	190.8	9.6	105.3
5/5/2016	94.6	13.9	110.1
5/27/2016	200.0	10.5	100.1

Figure 4.2: Miniature pressuremeter shown in uninflated condition

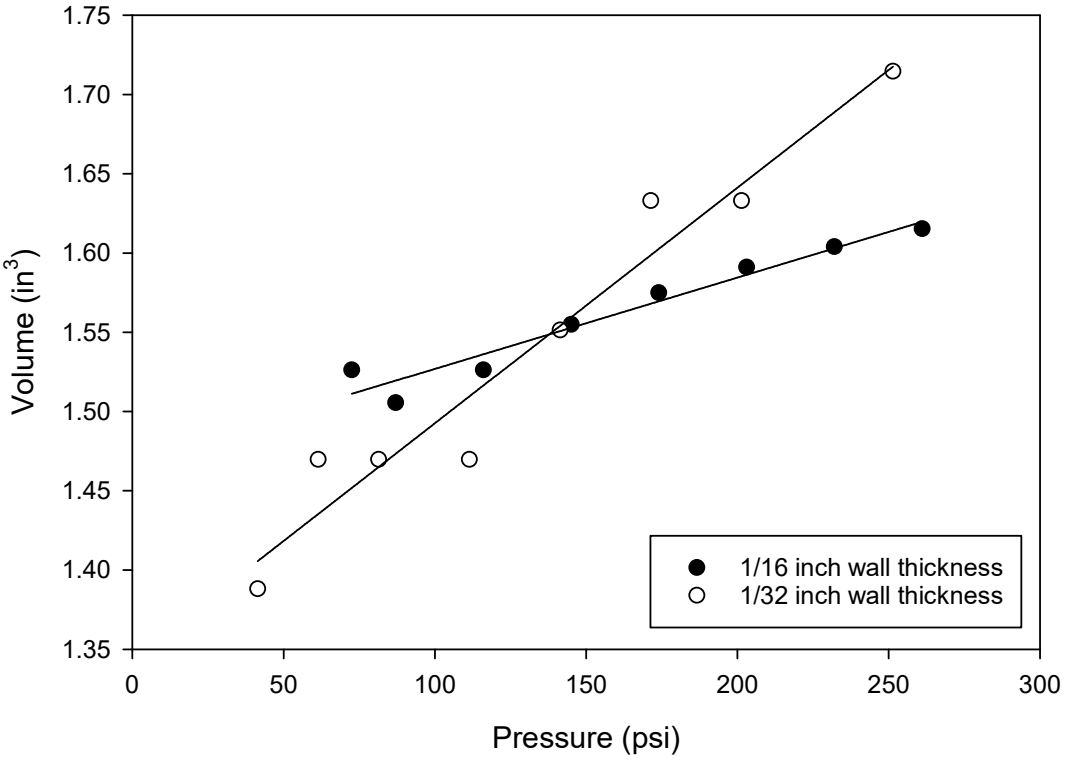

Figure 4.3: PMT system compressibility curves for using different membranes

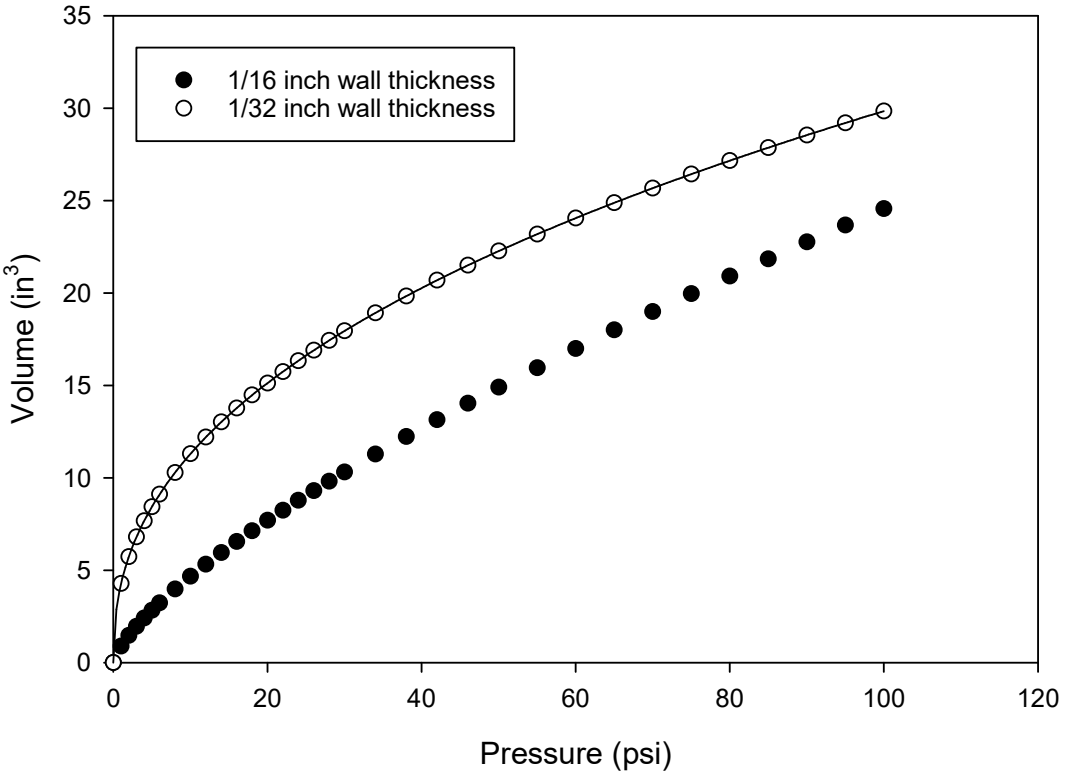

Figure 4.4: Membrane pressure loss for miniature pressuremeter membranes

Initially, MPMT tests were performed using nitrogen gas attached to a standpipe of fluid equipped with a sight glass to measure volume change. It was noted that the resolution of the sight glass was not sufficiently accurate to observe small changes in volume required to inflate the MPMT. The only tests performed using this method were the first two tests on the first test date. Subsequent testing was performed using a GDS Standard Pressure Controller V2. This device is shown in Figure 4.5.

It is essential to have proper borehole size when performing a pressuremeter test (Briaud, 1992). A proper borehole should be no greater than 1.2 times the diameter of the uninflated probe and no less than 1.03 times the diameter of the uninflated probe (Briaud, 1992). The borehole was created using a 0.75-inch diameter wood bit on a

battery operated hand drill. This meets the limit set by Briaud (1992) for an acceptable borehole. After completion of the MPMT, the borehole was filled with leftover material that had been trimmed from the top of the sample and tamped into place.

4.6 Model Bearing Capacity Test Methodology

Once the MPMTs were performed, the upper frame was put into place and the 4-inch diameter footing was set on the center of the soil bed. Dial indicators were placed diametrically opposed on the footing and the load cell was turned on. Model footing tests were performed immediately after completion of the MPMT. All tests were load-controlled. Small loading increments were used initially to seat the plate and account for any slop in the testing apparatus. Settlements were measured at 0, 0.5, 1, 2, 4, 8, and 16 minutes, or until the movement between readings was less than 0.005 inches. Loading of the plate continued to the recommended settlement, which was 10% of the footing width (0.4 inches). The first test performed was stopped prematurely; however, all subsequent tests were carried to at least 0.4 inches of settlement. The load was maintained for each increment with an accuracy of ± 10 lbs.

After the completion of a bearing capacity test, moisture content and suction samples were collected. An excavation was made under the center of the footing .A hand auger was used to make a borehole in the soil. Soil was collected in moisture tins at one-inch increments and sealed. Small soil samples were taken from moisture tins and total suction was measured using the WP4. The remaining sample was dried in an oven and moisture content was determined. The soil that remained in the test tank after testing was removed and moved to another room to dry for use in subsequent tests.

Figure 4.5: Pressure controller and miniature pressuremeter used in model footing tests

Chapter 5 Results and Discussion: Laboratory and Field Testing

5.1 Field Instrumentation

Monitoring of weather data at the Northbase site lasted from August 24, 2012 to October 20, 2014. The following data were collected: average daily air temperature, wind speed, maximum daily relative humidity, maximum and minimum air temperature, total daily solar radiation, precipitation, and average daily soil volumetric moisture content and temperature at depths of 1, 3, and 6 feet. For the monitored dates, the average daily temperature ranged from 105°F to 5°F at North Base. For this research, the most important information obtained from the weather stations includes the rainfall information and the soil volumetric water content. Therefore, this information will be highlighted; further information is presented in Doumet (2015).

The average daily temperature, rainfall, and volumetric water contents at depths of 1 ft., 3 ft., and 6 ft. for North Base are shown in Figure 5.1. From this figure, it is noticeable that after rainfall there are peaks in volumetric moisture content. These peaks are staggered with depth. The smallest overall change in volumetric moisture content is at the lowest depth, which is logical as it takes more time for water to permeate through fine-grained soil. There are several areas on the volumetric moisture content graphs where there are no values viewable, which is due to readings exceeding the devices range of measurement. It is also noticeable from the graphs that the volumetric water contents of the soil around February 2013 are relatively low, which is consistent with high soil strength determined by in situ testing.

The temperature, rainfall data, and volumetric moisture contents at 1ft, 3ft, and 6ft for the Goldsby site are presented in Figure 5.2. The main noticeable difference

between the North Base and Goldsby volumetric moisture content data is that there are sharper differences in peaks. This is attributed to the higher permeability of the Goldsby soil compared to the North Base soil, which has on average higher plasticity and greater fines content. There is a delay period between the rainfall and the moisture content increase, which is due to the low permeability of the fine-grained soil. On average, the variations in moisture content at the Goldsby Site are greater than at the North Base Site.

Total monthly rainfall for the months prior to the start of the in situ testing regime left most of Oklahoma in drought conditions. In situ testing at North Base started in February of 2012. The total monthly rainfall in inches for both test sites, which were only 5.5 miles apart, is shown in Figures 5.1 and 5.2. Prior to February there was meager rainfall amounts; however, by the end of August nearly the entire state of Oklahoma was out of drought conditions after record rainfall.

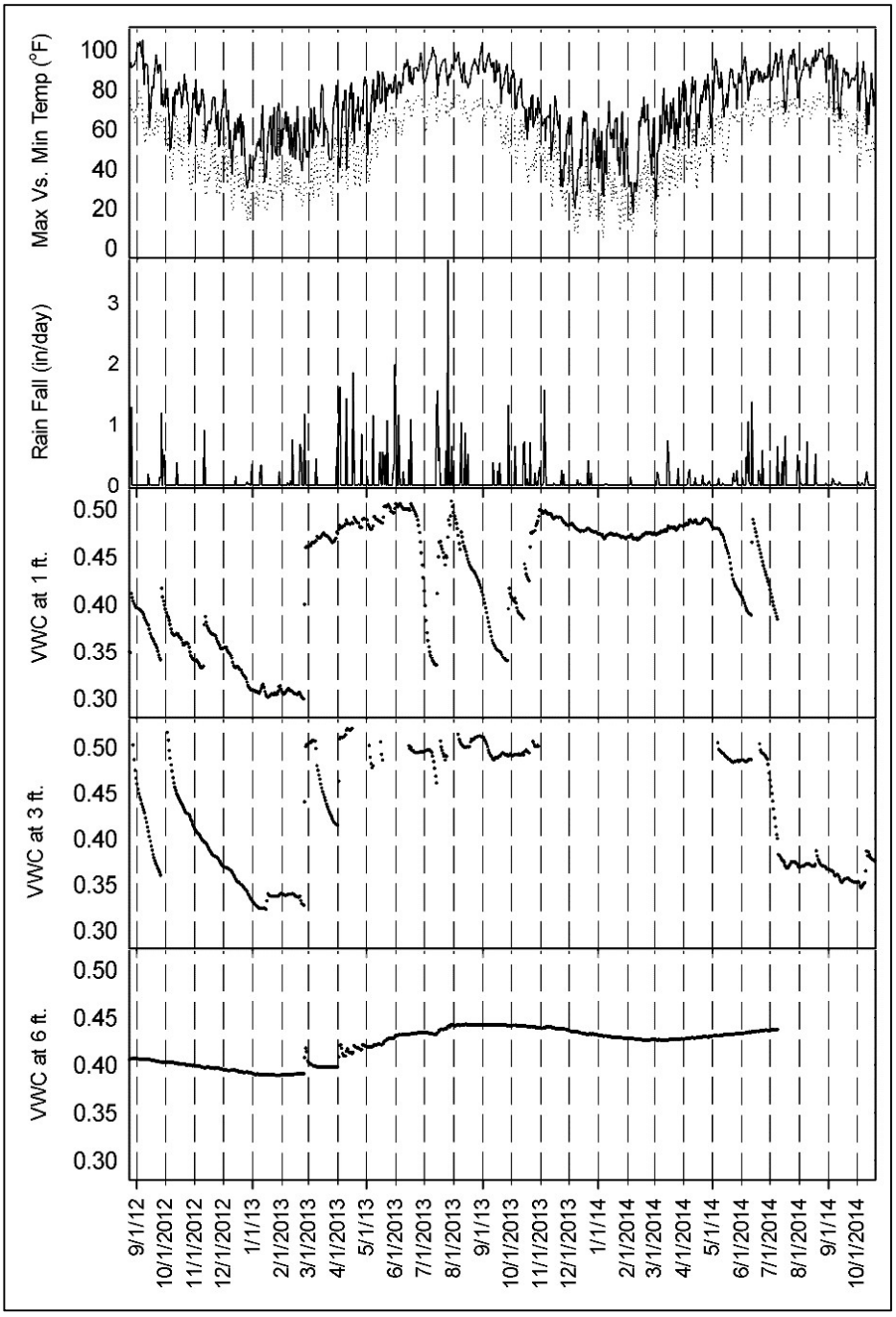

Figure 5.1: Maximum and minimum daily temperature, total rainfall, and volumetric moisture content at North Base.

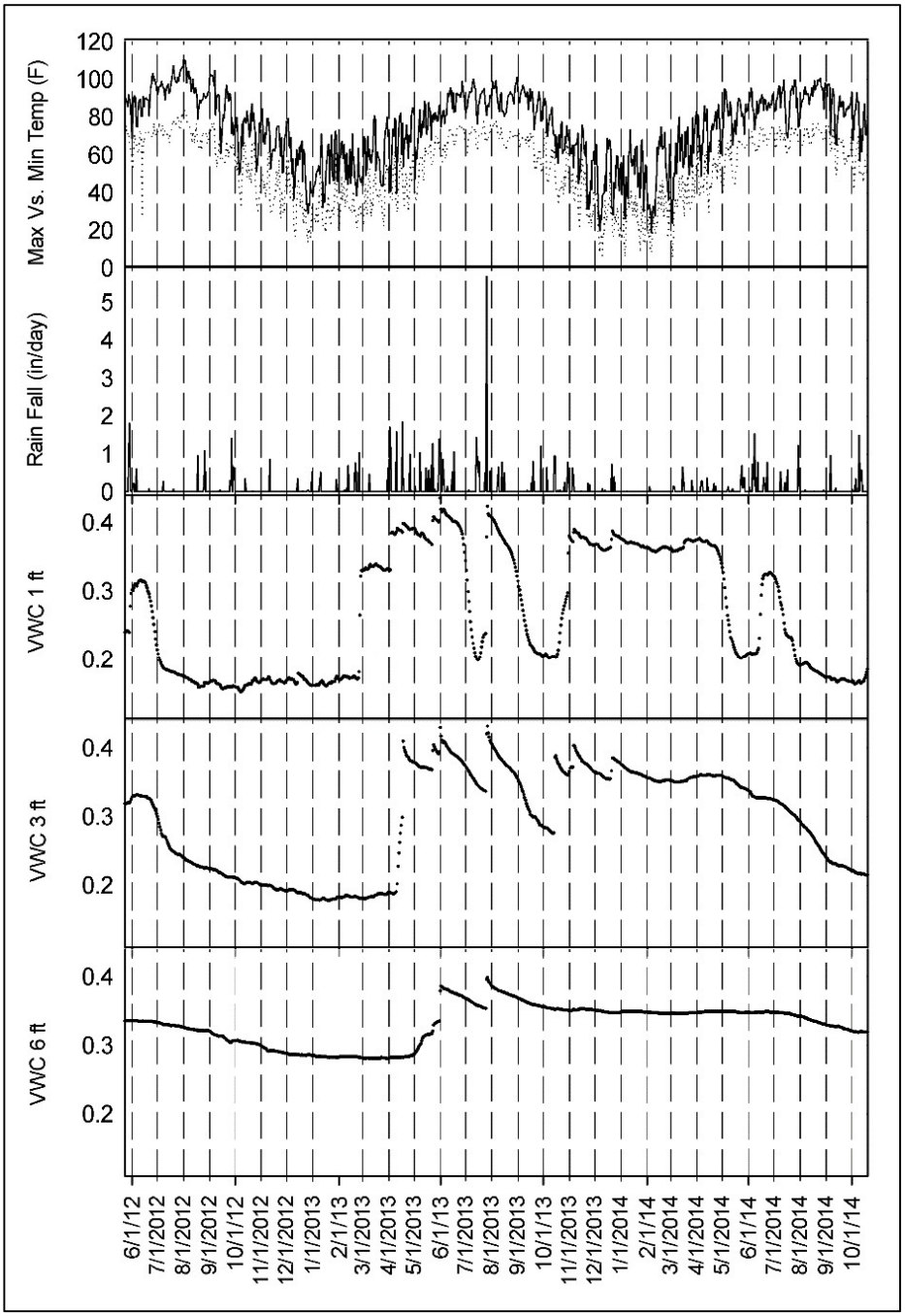

Figure 5.2: Maximum and minimum daily temperature, total rainfall, and volumetric water content at the Goldsby site.

5.2 Test Site Soil Characteristics

Particle size distribution was the first test performed on soil returned from each test site. The majority of material from each site was fine-grained. To determine the fine-grained particle size distribution, two tests were performed. First, one sample from each foot of depth was wet washed through a No. 200 sieve to determine fines percentage. Second, for selected depths a hydrometer analysis was used to determine actual particle size distribution of the fines. Atterberg limits were then determined for each foot of soil at both sites. The results of these tests were used to classify the material at the sites and create profile graphs.

The soil profile for Goldsby is shown in Figure 5.3. Above 5 feet, over 90% of material passed through a No. 200 sieve. Below this depth, there was more sand present in the soil. The percent of fines for all tests is 75% or above which indicates a mostly fine-grained soil profile. The plasticity indices through ten feet of depth are relatively low with an average PI of 11. There is an increase in plasticity around four feet where the PI reaches 14; however, it returns to near the average value below this depth.

The soil profile for North Base is shown in Figure 5.4. The majority of material from North Base passed through a No. 200 sieve, which classifies it as fine-grained. The average percent of material passing the No. 200 sieve is around 85%. The Atterberg limits at North Base revealed two distinct soil layers. With the exception of the first foot of soil at North Base, the PI in the top five feet of soil is above 40. Below five feet, the average PI drops to around 14.

Other visual/manual tests were performed to characterize the soil at both sites including the dry strength test and acid reaction tests. It was noted that soil from both

sites have high dry strength and Goldsby soil reacted to HCl, which indicates the presence of calcium carbonate. The only significant reaction to HCl at North Base was on samples collected at a depth of ten feet, where the weathered rock layer was encountered. The specific gravities for North Base and Goldsby are presented in Table 5.2. Specific gravity was measured for three depths at each site. For both sites, shallow depths had lower specific gravity. Soils at both sites had specific gravities consistent with clay, silt and sandy soils.

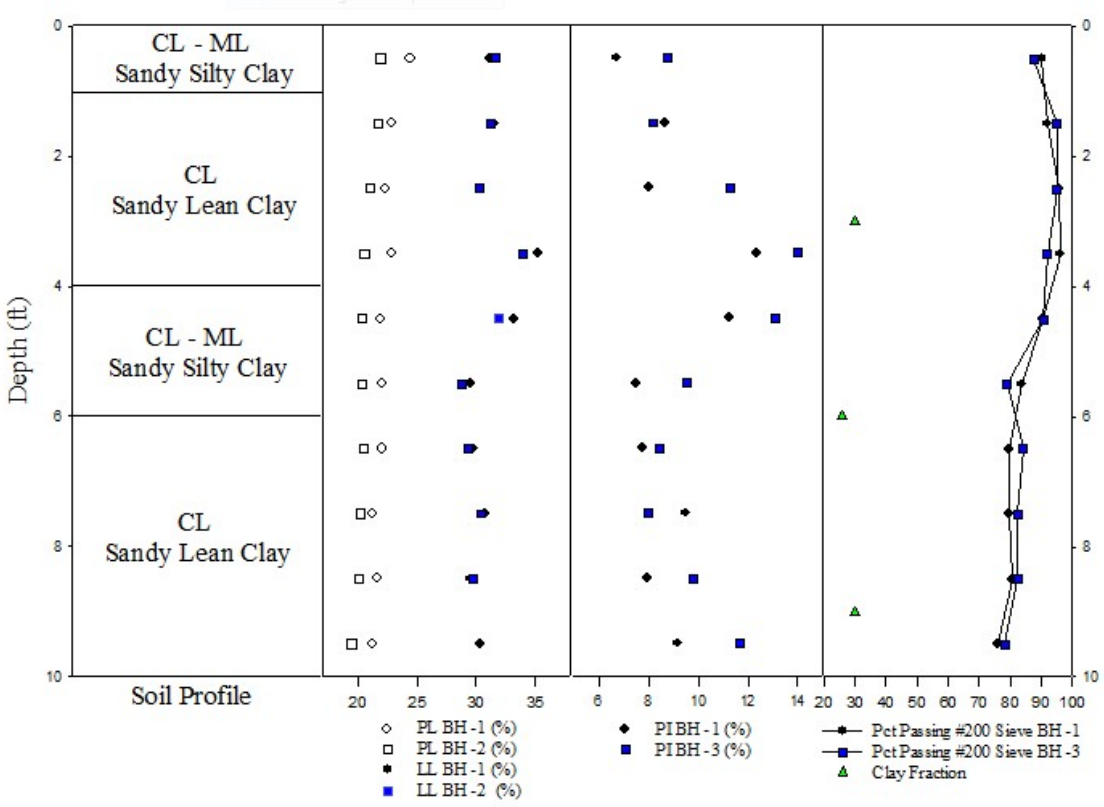

Figure 5.3: Goldsby site profile including Atterberg limits and percent of material passing a No. 200 sieve.

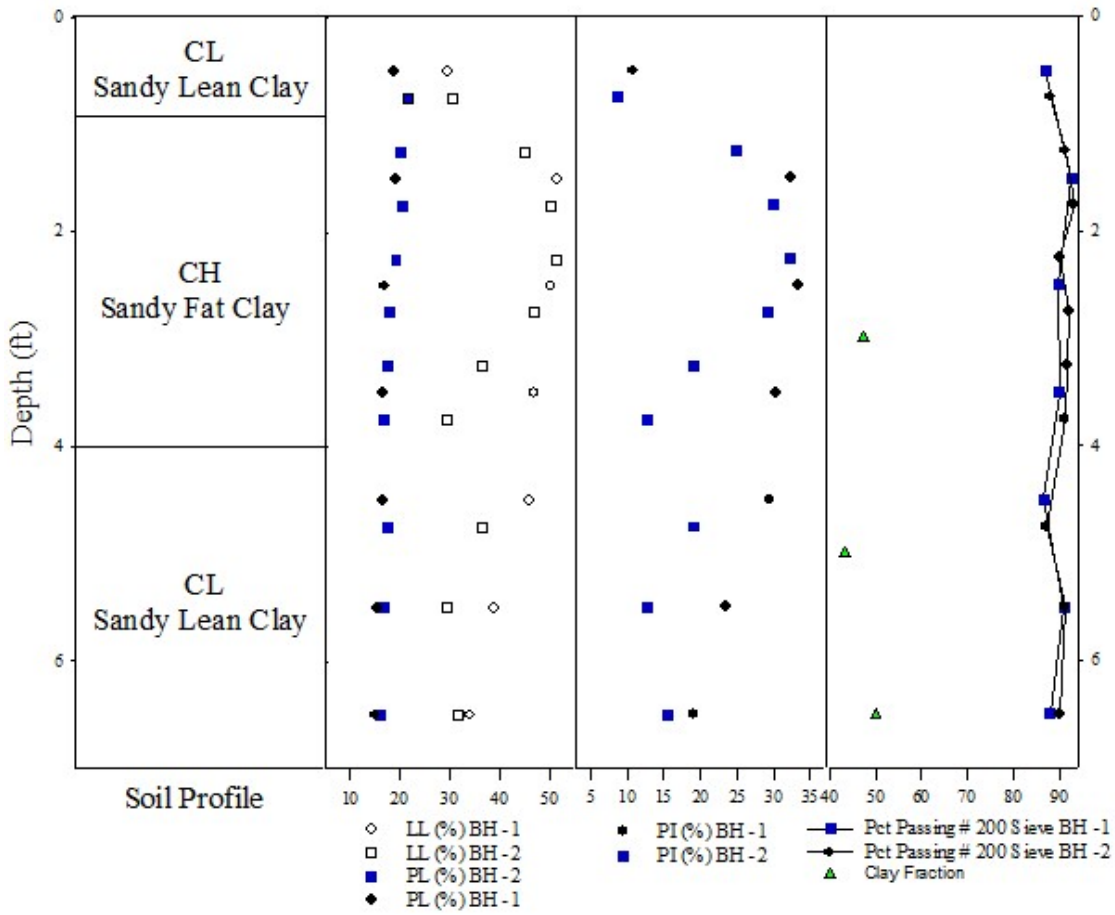

Figure 5.4: North Base site profile including Atterberg limits and percent of material passing a No. 200 sieve.

Cation exchange capacity (CEC) was measured for both sites for all depths. Cation exchange capacity is typically measured in milliequivalents per 100g of soil (meq/100g). A higher CEC corresponds to a higher ability for the soil to hold exchangeable cations. This becomes a measure of a soils attraction to water which results in greater shrink/swell characteristics and soil plasticity. Soils with high CEC typically exhibit behavior that makes construction with them more challenging. They may be useful in situations where absorption of water is a desirable feature such as liners in landfills. The results of CEC testing are shown in Table 5.2. Generally, Goldsby soils show lower CEC than North Base. The CEC for Goldsby is lower for the

top four feet of soil and then increases for depths of 5 to 8 feet followed by a decrease at 9 feet. North Base soil shows especially high CEC at 3 feet and then decreases with increased depth.

The location of tests for North Base and Goldsby are shown in Figures 5.5 and 5.6 for Goldsby and North Base, respectively. Seen in the figures are the location of CPT, PMT, and SPT. The test locations were selected such that the same location was not selected twice.

Table 5.1: Specific gravity and cation exchange capacity for North Base and Goldsby

Depth (ft.)	Goldsby		North Base	
	CEC (meq/100g)	G_S	CEC (meq/100g)	G_S
1	11			
2	11.9		20.6	
3	10.7	2.66	38.2	2.66
4	13.3		29.7	
5	19.4		21.6	
6	21.6	2.79	18.1	2.75
7	20.3		15.3	
8	16.9			
9	12.1	2.69		2.74

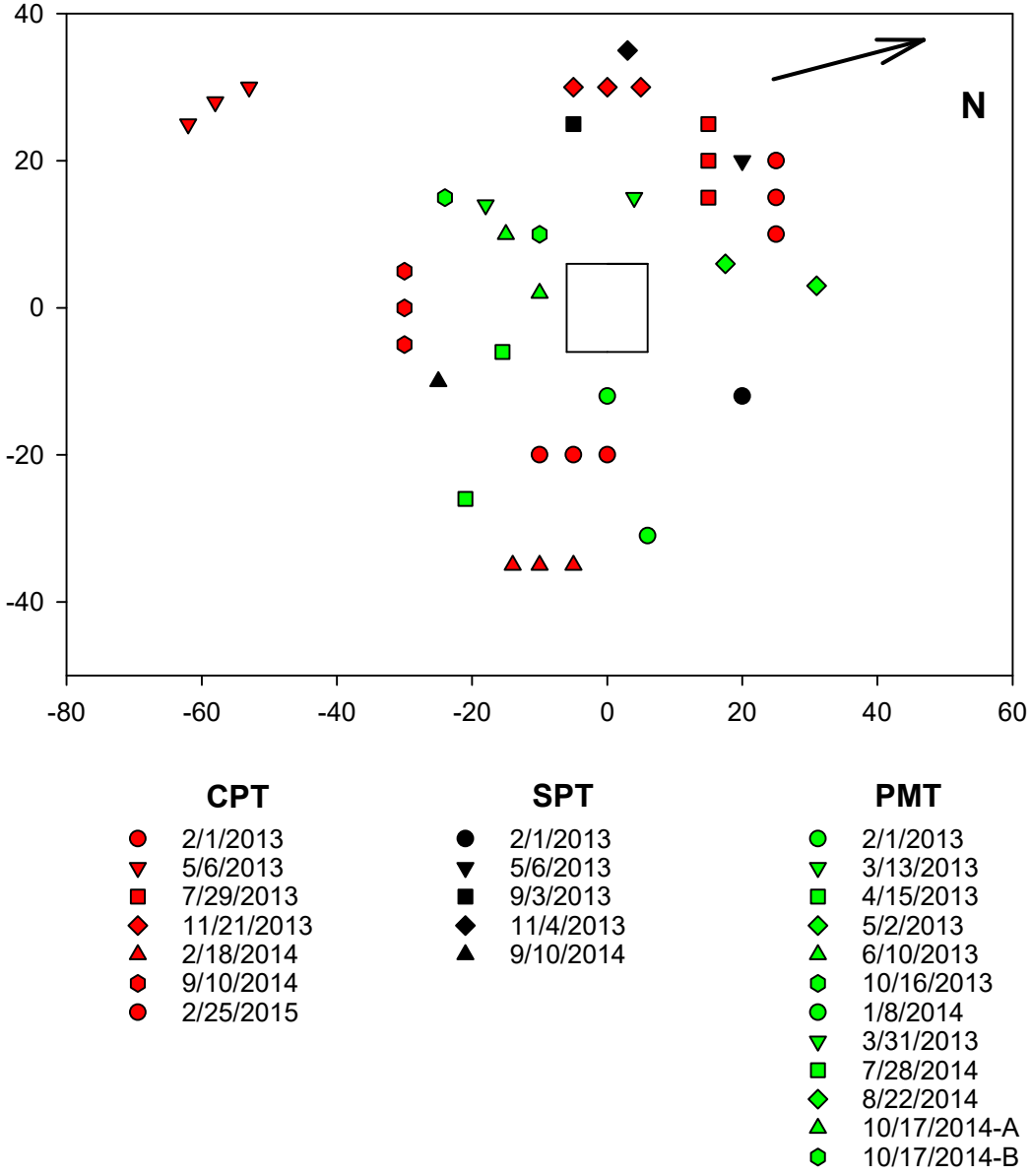

Figure 5.5: Goldsby site map and test locations

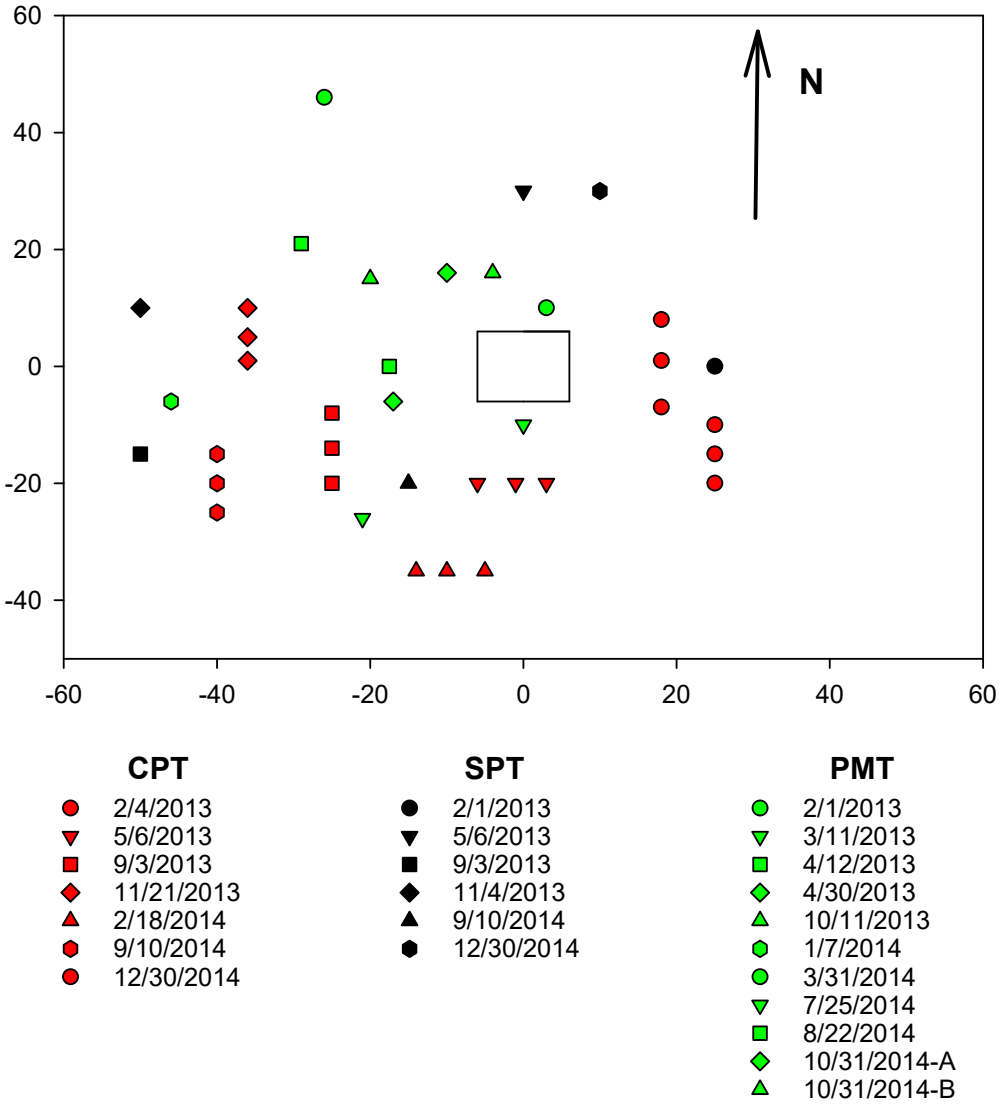

Figure 5.6: North Base site map and test locations

5.3 Soil Water Characteristic Curve (SWCC) testing

The soil water characteristic curve (SWCC) is an essential relationship necessary to relate soil moisture content or degree of saturation to soil suction. The SWCC for this work was determined using four methods. These methods are as follows:

1. Make total suction and moisture content measurements in the laboratory from multiple samples collected in the field. Use this relationship to represent the SWCC for the field sites.
2. Create total suction SWCCs for field sites at depths corresponding to PMT measurements in the laboratory by measuring total suction on a single sample while drying and wetting.
3. Perform the pressure plate test on selected samples to obtain direct measurements of matric suction and water content for both field sites.
4. Determine the SWCC in the form of gravimetric water content versus matric suction using methods provided by Zapata et al. (2000).

The Decagon WP4 was used to complete total suction measurements. It was initially assumed that the osmotic suction, which is one of the components of the total suction, would be minimal. This would allow total suction measurements to represent matric suction (u_a-u_w) measurements. There were some initial clues that the total suction may not be accurately representing the matric suction, particularly for high water contents. The first of the clues came from preliminary review of pressuremeter data. Limit pressure data showed comparatively large changes in suction had little to no effect on limit pressure as shown in Figure 5.7 for the data between 50 and 100 psi. Review of limit pressure versus water content data from the same depth and site showed relatively strong correlation as shown in Figure 5.8.

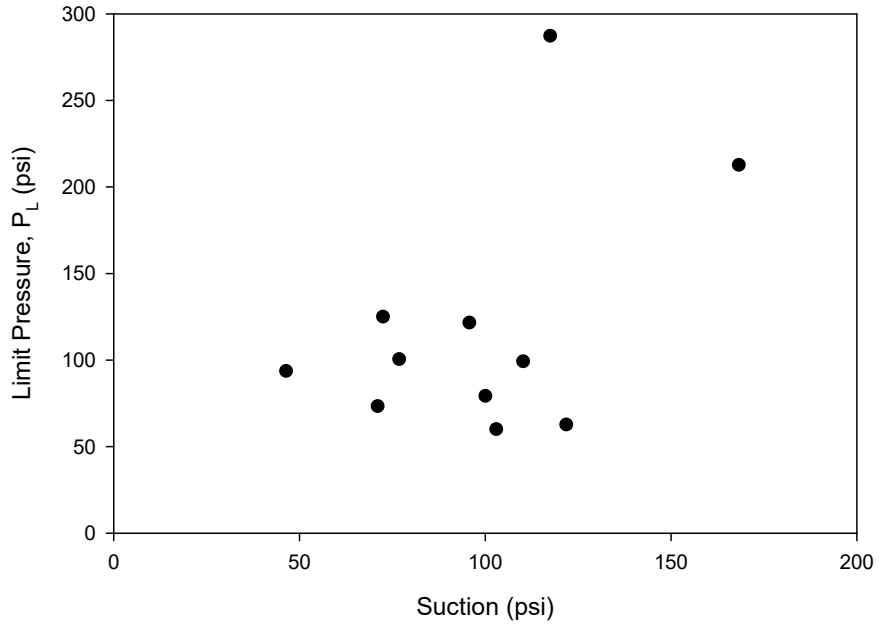

Figure 5.7: Total suction versus limit pressure from North Base at five feet with little changes in limit pressure for large changes in suction

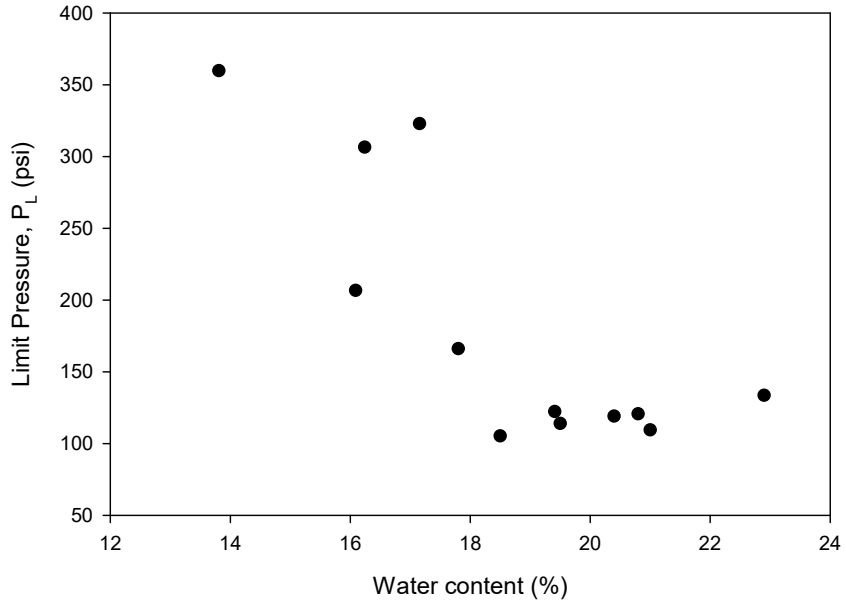

Figure 5.8: Water content versus limit pressure from North Base at five feet

Soil samples were collected for each field visit. These samples typically correspond to the depth of interest for PMT (i.e. 3 ft., 6 ft., and 9 ft. for Goldsby) or

CPT (i.e. every foot). These samples are retrieved either during SPT or with a hand auger. Samples are immediately placed in moisture tins, sealed, and brought to the laboratory. In the laboratory, the moisture tins are opened, and a small part of the sample is removed and placed in a WP4 soil cup and the total suction is measured. The remainder is used to determine moisture content. The relationship between total suction and moisture content was plotted for both field sites. Figure 5.9 shows the total suction versus moisture content data points for Goldsby (green stars).

A SWCC was created based on total suction measurements for depths corresponding to PMTs. The samples used in these tests were collected using a thin-walled tube sampler (Shelby tube). The minimally disturbed samples were brought to the laboratory and extruded. Samples from representative depths (i.e. 3 ft., 6 ft., and 9 ft. for Goldsby) were carefully trimmed to fit into oedometer rings. Filter paper was then placed over the top and bottom of the oedometer ring, followed by porous stones. Some weights were placed on the samples in an attempt to minimize swelling. The samples were then inundated with water and allowed to imbibe water for 48 hours. After this, the samples were trimmed further to fit into WP4 sample cups. The total suction, mass, and volume of the sample was determined. Then each sample dried while periodic total suction and mass measurements were made. The total suction versus water content was plotted. It is displayed in Figure 5.9 for Goldsby (black and white circles and triangle). It is clear that there is discrepancy between measured total suctions from discrete in situ test measurements and SWCCs determined from individual samples in the laboratory. This is likely because field measurements represent individual samples obtained on different dates and subject to natural variability with

respect to density, sample disturbance, and drying and wetting paths. On the other hand, laboratory SWCCs were obtained from dying a single sample from an initially saturated state.

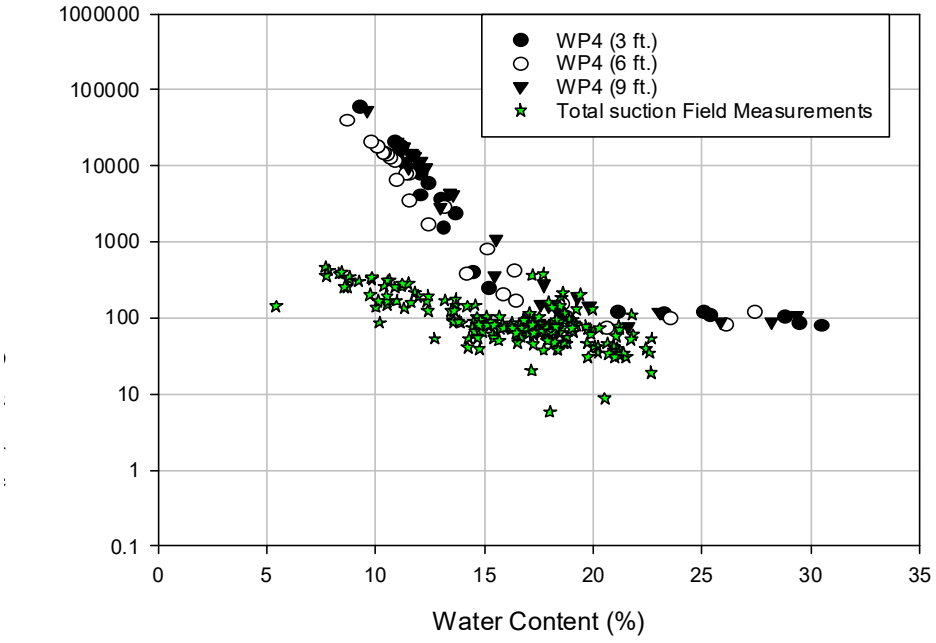

Figure 5.9: Field total suction measurements and total suction SWCC measured using WP4

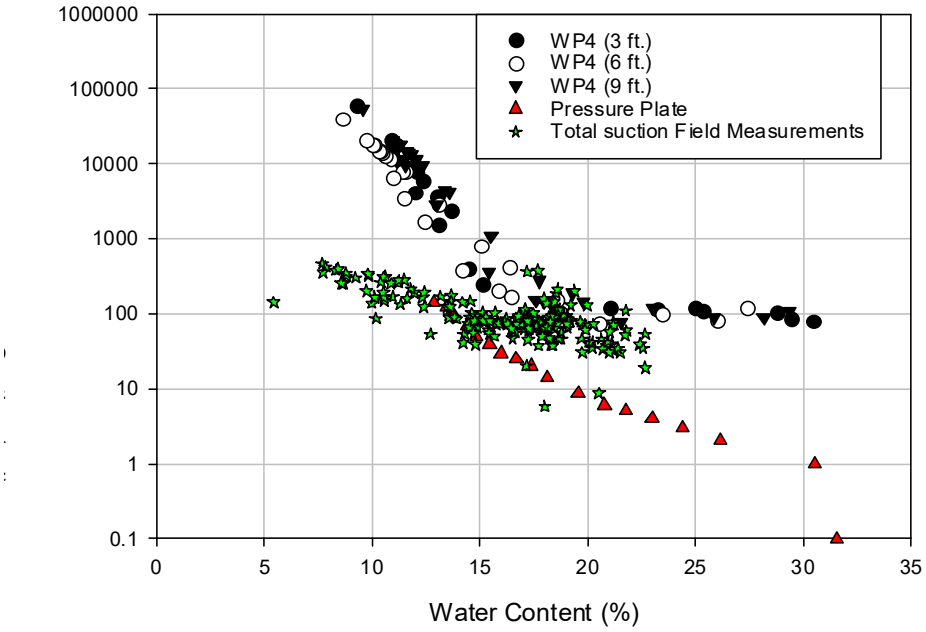

Figure 5.10: Addition of pressure plate data to soil moisture/ total suction measurements using WP4

Pressure plate measurements of matric suction were made from samples obtained from a Shelby tube sample collected in the field. The sample came from a depth of 3 ft. from Goldsby and 4 ft. from North Base. There were no adequate samples available from North Base at 3 ft., which corresponds to a PMT depth, so the next closest depth, 4 feet, was used; it was assumed that the soil from these depths was similar. The Shelby tube sample was trimmed to fit into thin rubber rings and filter paper was placed on the bottom of the sample. These samples were then saturated. After saturation was reached, the pressure plate test was completed by incrementally increasing the matric suction. The pressure plate data is shown as red triangles in Figure 5.10.

Once pressure plate data was added, there was still considerable discrepancy in the data. The first discrepancy appears to come from osmotic suction, which is the difference between total suction and matric suction. The osmotic suction can be seen clearly in Figure 5.10 as the difference between the red pressure-plate data points and the green stars, which represent field data, or the black and white circles and triangles, which represent laboratory total suction SWCC. The second discrepancy is related to the saturated water content and the related suction measurement.

Wet soils collected from the field and appearing to be near saturation had moisture contents near 24%. Furthermore, analysis of Shelby tube samples from Goldsby also indicated saturated water contents should be about 23% to 24%; this analysis does not account for volume change due to swelling upon imbibition of water. However, both the pressure plate data and the total suction SWCC data show saturated water contents near 31%, which is most likely the result of saturation of WP4 and pressure plate samples that allows for nearly unrestrained swelling in the lab. This results in higher gravimetric water contents at saturation than observed for field samples. In addition, volume increases in lab samples may result from sample disturbance and stress unloading. Therefore, an estimated saturated water content of 23% is reasonable to represent the field SWCC given that the range of overburden pressures at depths of interest would somewhat restrain volume change during complete saturation.

Finally, the Zapata et al. (2000) method was used to determine the SWCC representing gravimetric water content versus matric suction. This procedure relies the plasticity index and percentage of soil passing a #200 sieve for a site of interest. From

this, the matric suction can be estimated for a given water content using modified parameters from the Fredlund and Xing (1994) SWCC curve fitting technique. The result is shown in Figure 5.11, which includes the previously mentioned suction and moisture content measurements. In general, the Zapata et al. (2000) matric suction predictions appear closer to the measured field total suction values at low water contents where the difference between total suction and matric suction is less distinguishable. At higher water contents, the difference between total and matric suction is obvious because osmotic suction dominates the total suction measurement. The final predicted SWCC representing matric suction based on Zapata et al. (2000) is shown as the dashed line in Figure 5.11. This curve was ultimately used to determine matric suction for field samples based on the measured gravimetric soil moisture content. Since matric suction, and not osmotic suction, controls the mechanical behavior of the soil, particularly at high water contents, the Zapata et al. (2000) curve was used to estimate field matric suction. Further, this curve was selected over the pressure plate SWCC since it corresponds to the estimated field saturated water content. Finally, it generally agrees with pressure plate data at lower water contents. A similar procedure was followed in order to obtain matric suction SWCC for North Base.

As mentioned and shown in Figure 5.4 there are two distinct soil layers at North Base. Therefore, two SWCC plots were made for North Base representing the upper CH layer, and lower CL layer. The in situ total suction and water content data showed different suction ranges depending on whether it was collected above or below four feet from North Base. This behavior suggests that using two SWCC to describe the North Base soil profile is logical. The pressure plate SWCC was obtained from soil collected

from 4 feet, which corresponds, to the upper layer at North Base. The estimated matric suction values for this layer, Layer 1, fall in the same range as the measured matric suctions. The suction versus moisture content plot for North Base is shown in Figure 5.12. For fitting the SWCC, the saturated water content in the field was estimated to be close to 28% based on experimental observations, in a manner similar to Goldsby. These included observations indicating the influence of matric suction was negligible at water contents above approximately 28%, and calculations of saturated water content from Shelby tube samples.

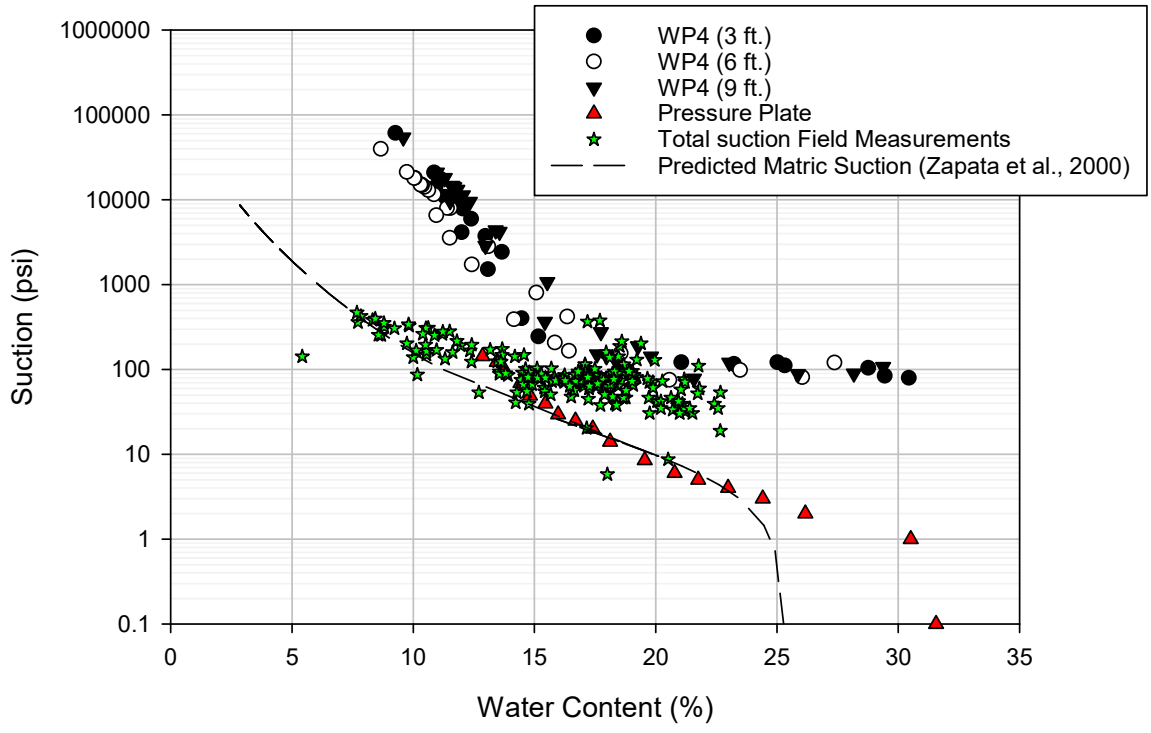

Figure 5.11: Full SWCC for Goldsby

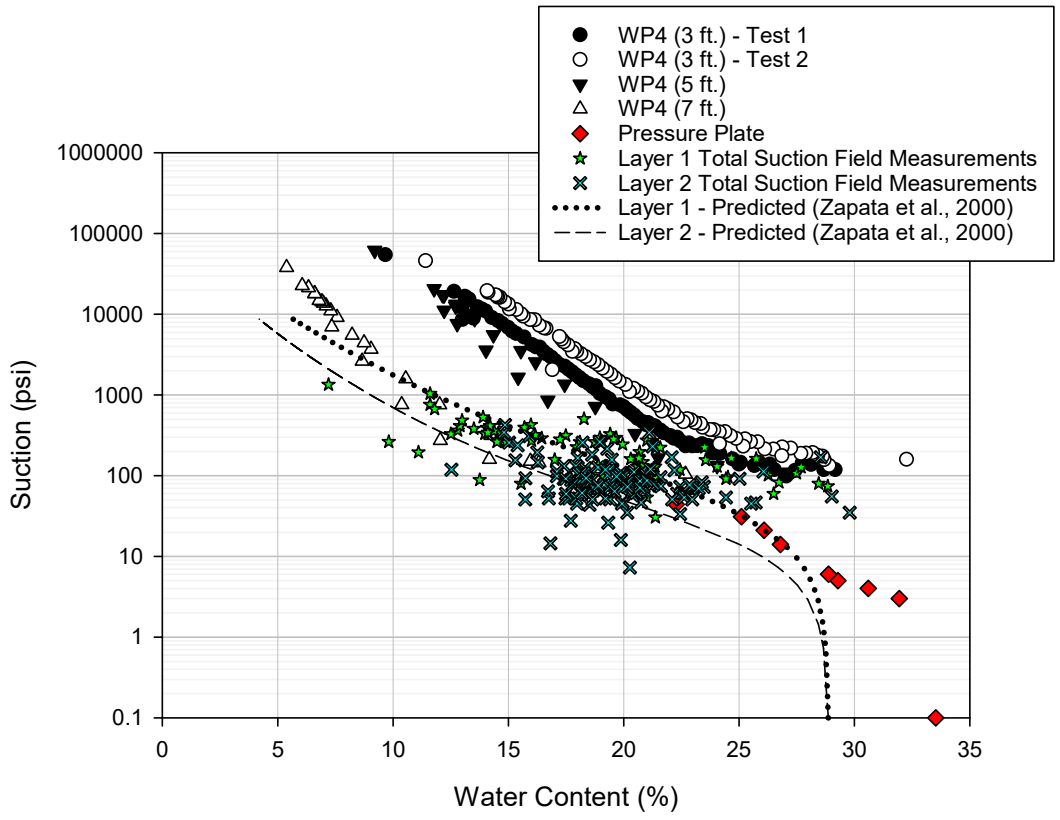

Figure 5.12: SWCC for North Base

5.4 Isotropically consolidated undrained compression (CIUC) triaxial test results

Isotropically consolidated undrained compression (CIUC) triaxial tests were performed for Goldsby and North Base soils at depths of interest at each test site. A summary of triaxial results is presented in Table 5.4. The test results show that both sites have soil with increasing friction angles with greater depths. On the other hand, effective stress cohesion intercepts tend to decrease with depth. These observations are consistent with a soil profile that is more overconsolidated near the ground surface and less so with depth. In this case, apparent overconsolidation of the soil profile is influenced by weathering, which are greatest in the near surface soils. Failure envelopes for the data shown in Table 5.4.

Table 5.2: Summary of triaxial results for North Base and Goldsby

	Goldsby			North Base		
Depth (ft.)	**3**	**6**	**9**	**3**	**5**	**7**
Moisture Content (%)	19.1	24.2	18.3	20.2	23.9	15.6
Wet Unit Weight (pcf)	122.7	134.7	111.3	121.8	124.6	136.3
Dry Unit Weight (pcf)	103.0	108.5	94.1	101.3	100.6	117.9
c' (psi)	2.5	2.0	-	10.0	1.0	-
ϕ' (°)	25.4	31.0	-	26.0	31.0	-

5.5 Pressuremeter (PMT) results

5.5.1 Overview

This section will present the results of pressuremeter tests (PMT) at the Goldsby and North Base sites. First, an overview of the results from both sites is presented followed by a comparison of pressuremeter test parameters to the in situ moisture condition/suction measurements. Later in Chapter 7, relevant trends in this data are used to formulate empirical prediction methods for the PMT parameters based on the moisture/suction conditions. Further, in Chapter 7, the application of the cylindrical cavity expansion theory for unsaturated soils is examined as a means of providing a theoretically based prediction method.

5.5.2 Testing locations for North Base and Goldsby

The testing locations were mapped to ensure there was no location that was tested more than once during the project period, and to make sure the locations were within reasonable proximity to each other. The test site maps show a small rectangular box indicating the location of the weather station. Around the weather station are test points indicated by different markers that correspond to the test dates in the legend. The test site maps for PMT are shown in Figures 5.13 and 5.14 for Goldsby, and North Base, respectively. The weather station for both sites is centered at (zero, 0) and each side of the box is twelve feet in length. An arrow indicates the North direction and all distances are shown in feet.

The location of PMTs performed at Goldsby are shown in Figure 5.13. The tests were performed on all sides of the weather station, as the soil surface was relatively uniform and free of any natural slopes or big differences in surface vegetation. The North Base PMT locations are shown in Figure 5.14. Tests at North Base were mostly confined to the northwest corner of the research site. A natural drainage channel ran east to west just south of the weather station. Due to the channel, there was a slight slope to the drainage channel on the southern side of the site. Tests were then performed on the northwest corner of the site, as it was most level.

5.5.3 Influence of soil suction on PMT results

Soil suction was observed to have a significant impact on the results of pressuremeter tests. The PMT stress-strain curves determined from each pressuremeter test are presented for both test sites in Appendix A.1 (Figures A.1-A.25). Differences in the shape and behavior of some of these stress-strain curves is evident for different test

depths at different dates when moisture conditions were different. These differences in the stress-strain behavior result in differences in the interpreted limit pressure (P_L), pressuremeter modulus (E_P), and unload-reload modulus (E_R). These are important parameters used in geotechnical analyses based on pressuremeter testing.

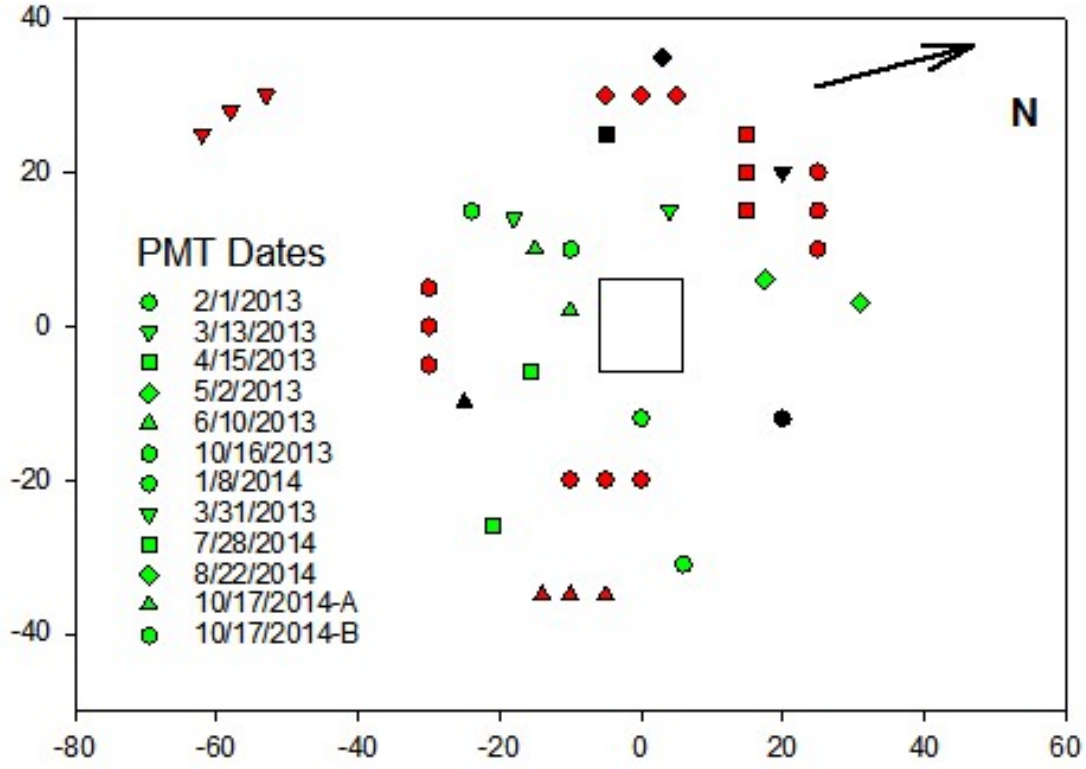

Figure 5.13: Goldsby PMT location map.

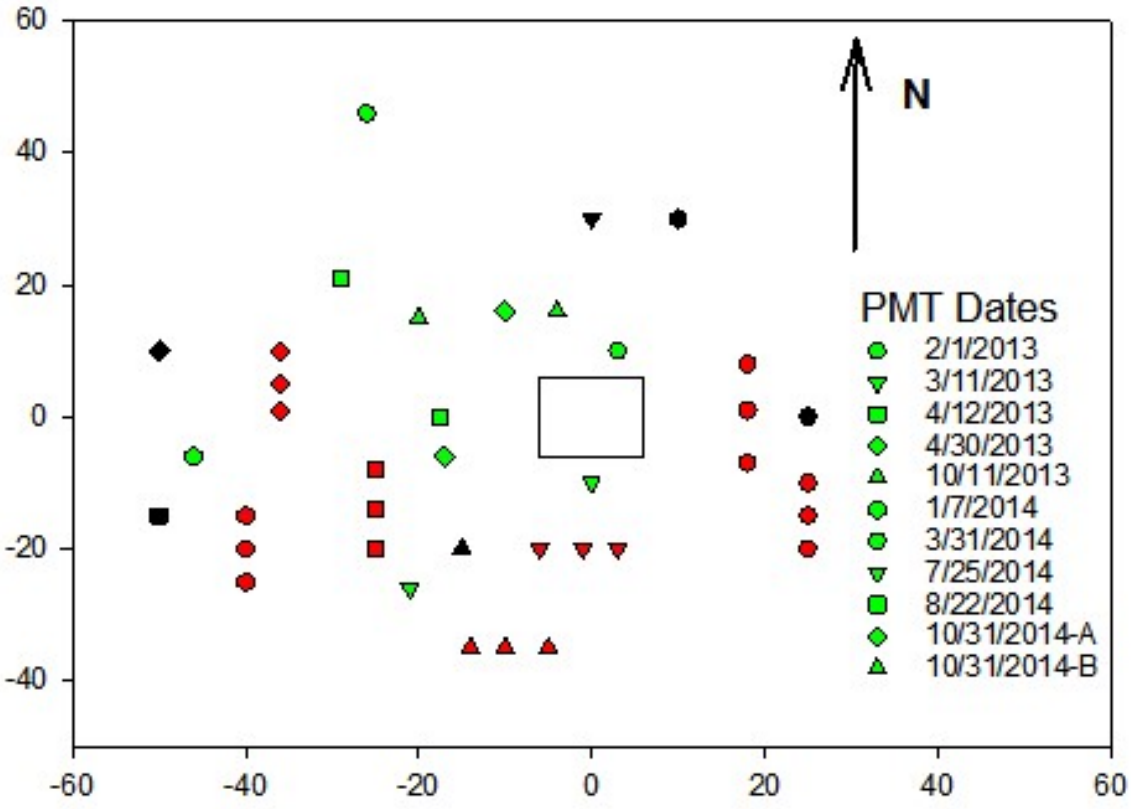

Figure 5.14: North Base PMT location map.

The results of PMT at both test sites for all test depths were interpreted to determine the limit pressure (P_L), pressuremeter modulus (E_P), unload-reload modulus (E_R), the in situ horizontal stress (P_O), and the coefficient of lateral earth pressure at rest (K_0). The date the test was performed, the soil moisture condition, and total suction were determined as described previously. In addition, the corrected pressure-volume curves were used to determine in situ soil stress-strain curves (Briaud 1992) for each test depth.

An example of the influence of changing soil moisture conditions on corrected pressure volume curves for Goldsby is presented in Figure 5.15. The data shown in Figure 5.15 represent one year of pressuremeter tests conducted at Goldsby at the 3-foot

test depth. There are significant differences in the test data for this date. The tests conducted in February and March show steep slopes in the linear portion of the curve, which indicates a comparatively stiffer material. The peaks reached for these data are higher, which also indicates strong material compared to tests conducted at other dates. The water contents measured directly relate to the test data in that water contents measured in February and March are much lower than those measured through the spring and summer are. This behavior is similar for both sites and all test dates.

One goal of the research plan was to use sites that had semi-uniform soil profiles to minimize differences from site variability. However, this was much easier in theory than practice. It was found that at both sites, the test results could be quite variable on any given date, because of natural site variability. This is demonstrated in Figure 5.16, which shows soil moisture content and pressuremeter results based on two tests conducted in adjacent boreholes at Goldsby on 10/17/2014. The main variation in the data is seen at 3 and 6 feet, which are depths more likely to be influenced by seasonal wetting and drying. The curves shown have corresponding limit pressures of 132 psi for Test 1 and 262 psi for Test 2 at 3-feet, and limit pressures of 117 psi for and 172 psi for tests at 6-feet. These differences are significant for pressuremeter tests performed on the same day, and in what was thought to be the same soil. Some of the variation seen in Figure 5.16 may be caused by the differences in moisture content between the two tests. While not all of the scatter observed in the in situ test data presented in this dissertation can be attributed to site variation, it does seem to play an important part. In general, however, correlations between matric suction and in situ test parameters are strong enough to suggest matric suction has a large and noticeable effect on soil strength.

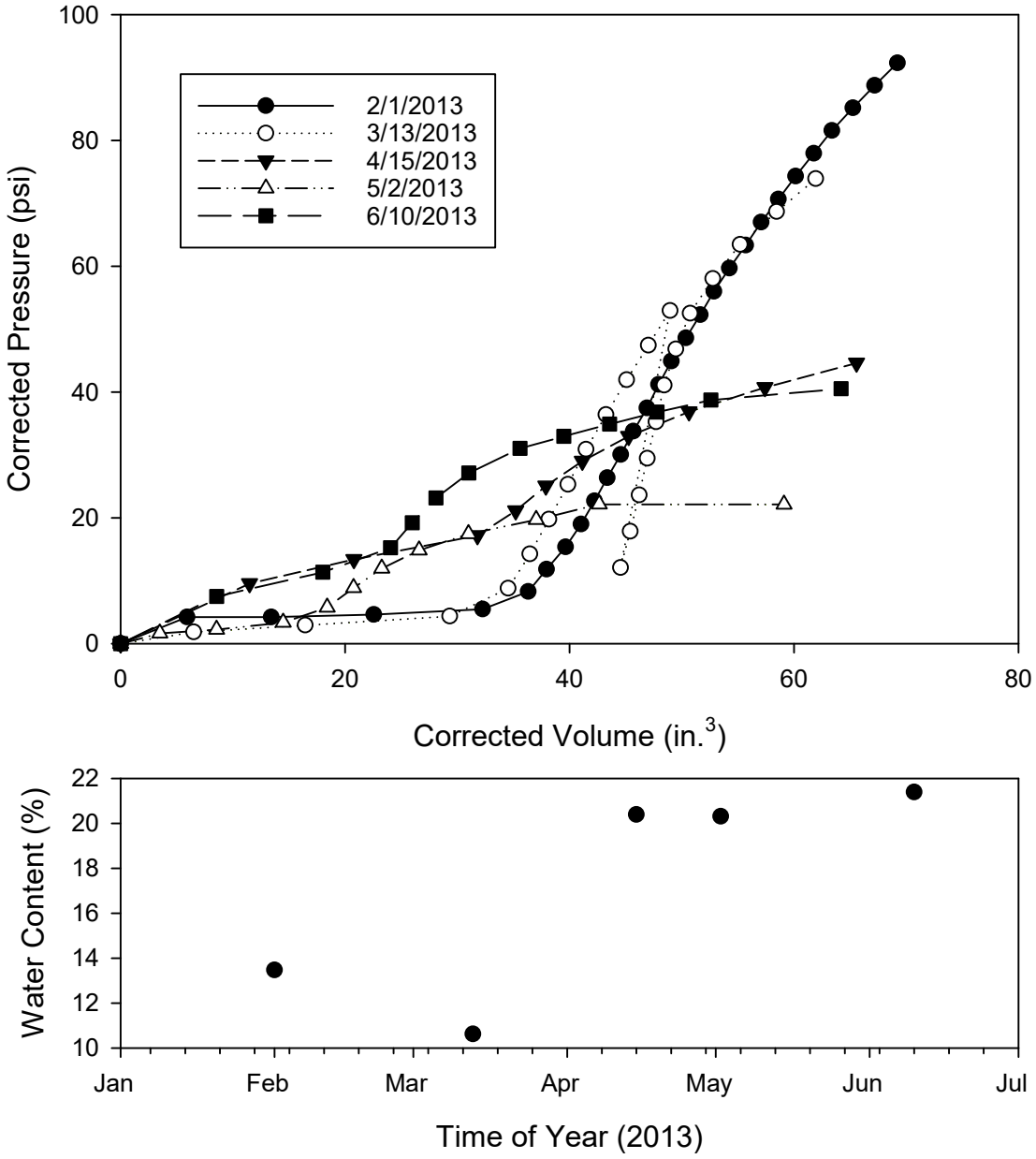

Figure 5.15: PMT pressure-volume curves and water content data for Goldsby at 3 feet obtained in 2013

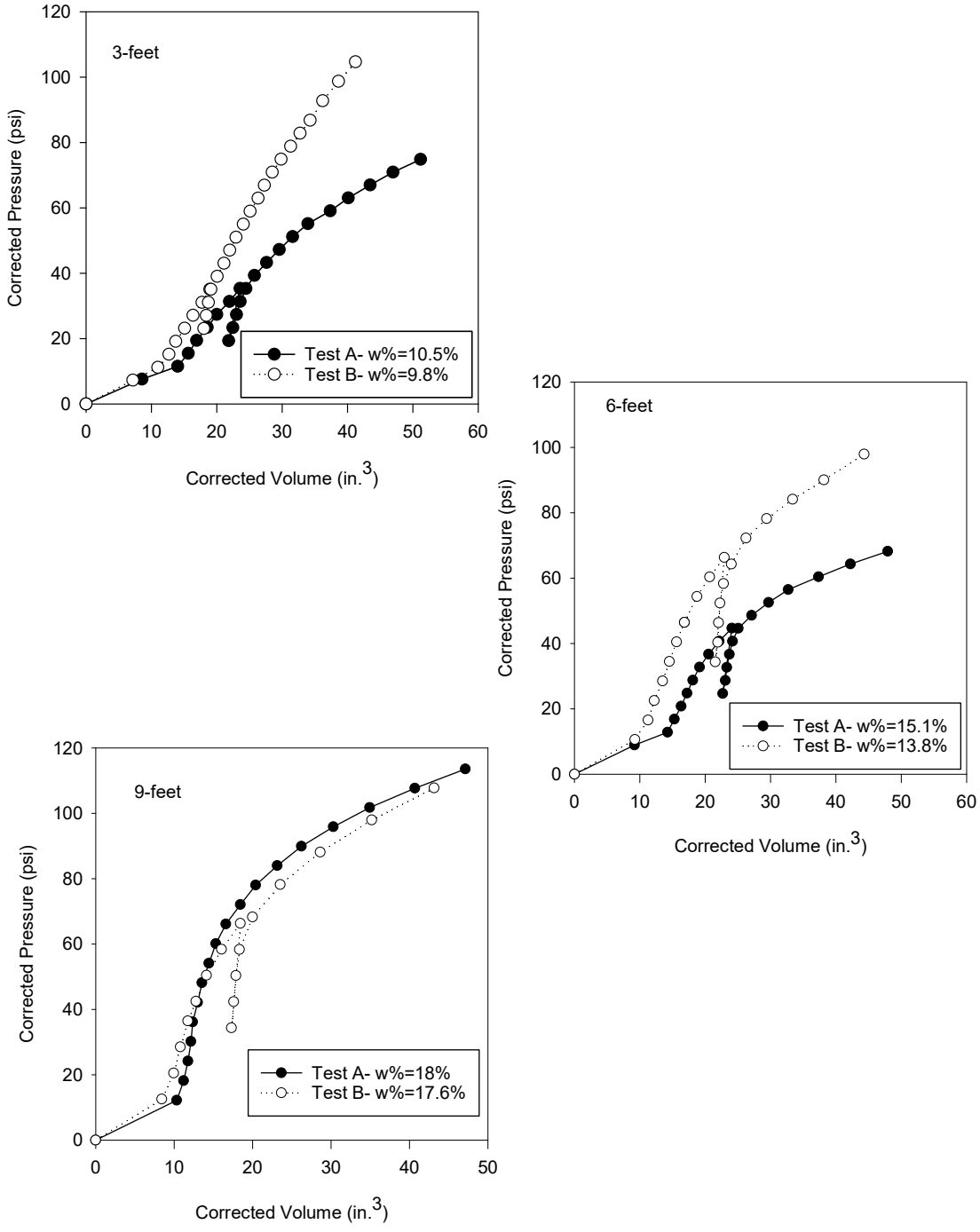

Figure 5.16: Comparison of pressure-volume curves from two PMTs performed at Goldsby on 10/17/2014

Limit pressure obtained from a PMT provides an indication of the soil's ultimate strength. As previously mentioned this value can be used to calculate shear strength parameters and bearing capacity. Figure 5.17 presents the limit pressure against matric suction determined for Goldsby for all test depths. Limit pressure versus matric suction was fitted with a power function best-fit curve. A power function reasonably represents the theoretical behavior in that a measurable minimum limit pressure should exist at zero suction and a maximum threshold matric suction should exist above which no further increases in limit pressure occur. The goodness of fit for the correlation between limit pressure and matric suction decreases with depth as reflected by the r^2 value. Nevertheless, with the exception of an outlier or two, the trend in the data is obvious and as expected. Note also that the range of suction measurement also decreases with depth because of the fact that seasonal variations in moisture content diminish with depth. At Goldsby, minimal variations in soil moisture content were observed below 5 feet, and this is reflected in the matric suction determinations.

The pressuremeter modulus relates the stress and strain experienced by the soil and is related to soil stiffness. Pressuremeter modulus values versus matric suction are shown in Figure 5.18. There does not seem to be a strong correlation between soil suction and pressuremeter modulus. It appears, for most of the range of measured matric suction values, the pressuremeter modulus was less sensitive to suction as compared to the limit pressure.

Unload-reload modulus is calculated in a similar manner to pressuremeter modulus except that unload-reload modulus is determined after an initial loading and unloading of the soil, prior to any significant plastic deformation. The purpose of

conducting an unload-reload sequence during the PMT is to eliminate the influence of soil disturbance that may affect the initial loading and determination of E_P. The unload-reload modulus values for PMTs performed at Goldsby versus matric suction are shown in Figure 5.19. Similar to E_P there seems to be minimal correlation between unload-reload modulus and matric suction.

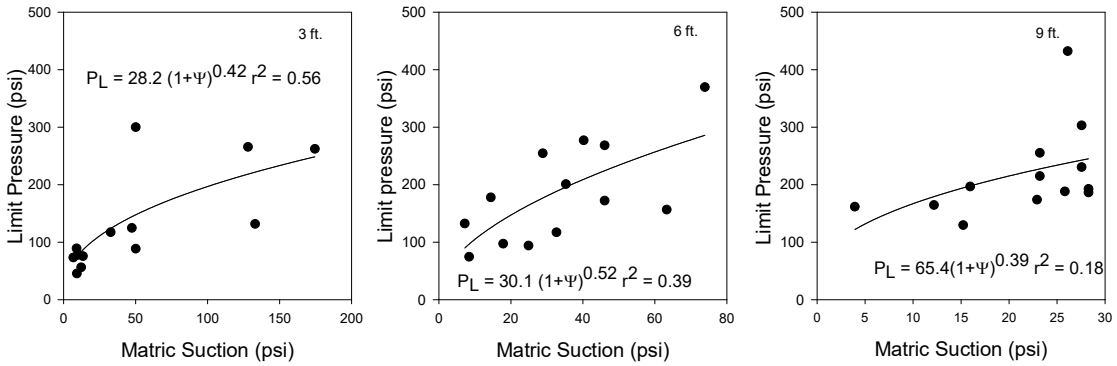

Figure 5.17: Limit pressure versus matric suction for Goldsby (3-ft., 6-ft., and 9-ft.)

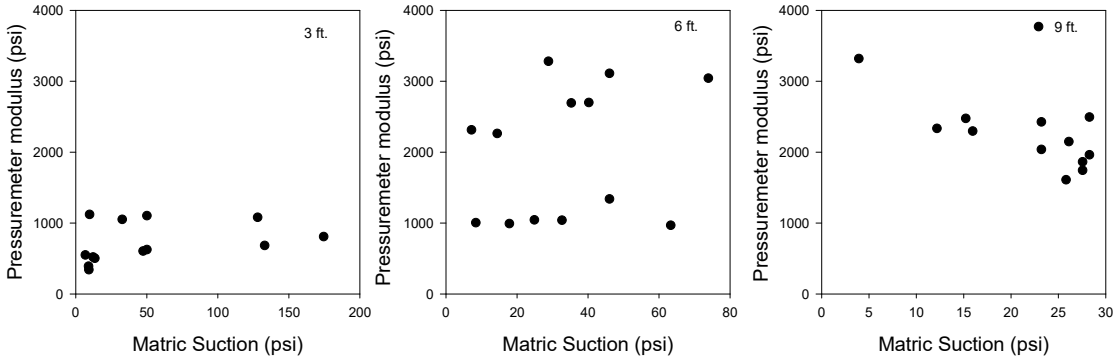

Figure 5.18: Pressuremeter modulus versus matric suction for Goldsby (3-ft., 6-ft., and 9-ft.)

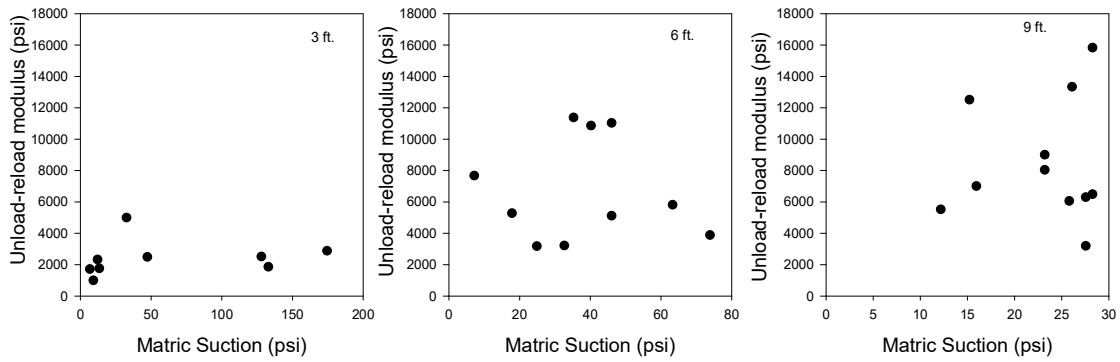

Figure 5.19: Unload-reload modulus versus matric suction for Goldsby (3-ft., 6-ft., and 9-ft.)

The in situ horizontal stress (P_{0H}), and the coefficient of lateral earth pressure at rest was determined from each PMT test. The in situ horizontal stress can be determined in a straightforward manner by evaluating the corrected pressure-volume curve. A straight line is extended through the initial portion of the curve prior to contact with the borehole wall and another straight line is drawn through the linear pseudo-elastic portion of the loading curve. The intersection of these two lines is considered an approximation of the in situ horizontal stress prior to loading. The result of this analysis is presented in Figure 5.20. The results show a small positive correlation between matric suction and in situ horizontal stress at three feet. This relationship seems logical because as suction increases, one would expect an increase in stiffness of the soil upon reloading. For increased depth the positive correlation is not as apparent, which could be due to the low suction range, variation in site stratigraphy, and other experimental variations.

The determination of the in situ horizontal stress allows the at-rest horizontal earth coefficient (K_0) to be determined. Unlike saturated soils, for unsaturated soils K_0 is determined as the ratio of total horizontal to total vertical stress, rather than a ratio of

effective stresses. The vertical stress can be simply determined by using the total unit weight of the soil multiplied by depth. The K_0 is then determined by dividing the horizontal stress determined by the PMT, P_{0H}, by the vertical stress. The results of these calculations are shown in Figure 5.21. There appears to be very little to no correlation between matric suction and K_0; however, when the results from all tests depths are plotted together there appears to be positive correlation. Natural soil variability could provide some explanation to the observed scatter noted. This includes variations in the soil constituents, density, and stress history. Test method accuracy and experimental methods may also be a contributing factor to PMT scatter at Goldsby. Further, the influence of disturbance is likely to be much more significant at the beginning of the test when the accuracy of the pressure and volume measurements are the lowest because the measured values are small. Furthermore, at small strains the importance of suction is less profound compared to larger strains that mobilize the shear strength of the soil.

It is noted in Figure 5.21 that K_0 values are in range of less than one to about 14. Values much greater than 3 seems excessively large considering that passive earth pressure coefficients generally do not exceed 10. There does appear to be some correlation between matric suction and K_0. The relationship is shown in Figure 5.22, which includes K_0 data from all depths. This result indicates that there may be an unforeseen impact of matric suction on the at-rest earth pressure obtained from pressuremeter tests.

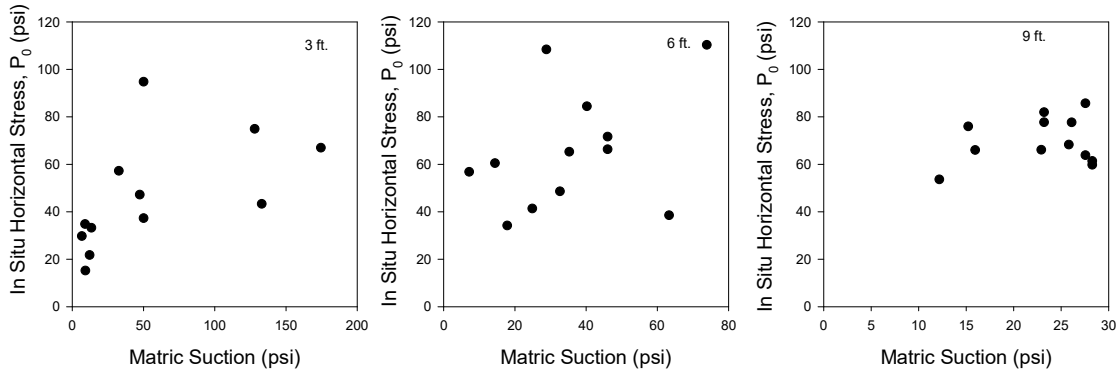

Figure 5.20: In situ horizontal stress versus matric suction for Goldsby at all depths (3-ft., 6-ft., and 9-ft.)

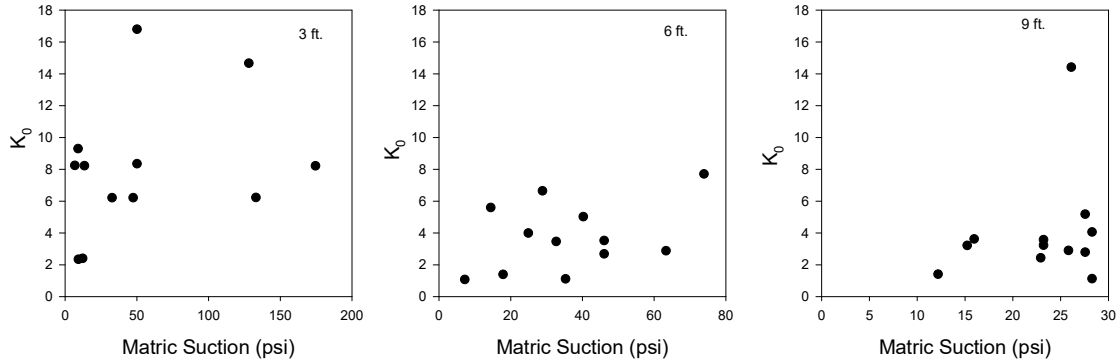

Figure 5.21: At rest earth coefficient versus matric suction for Goldsby for all depths (3-ft., 6-ft., and 9-ft.)

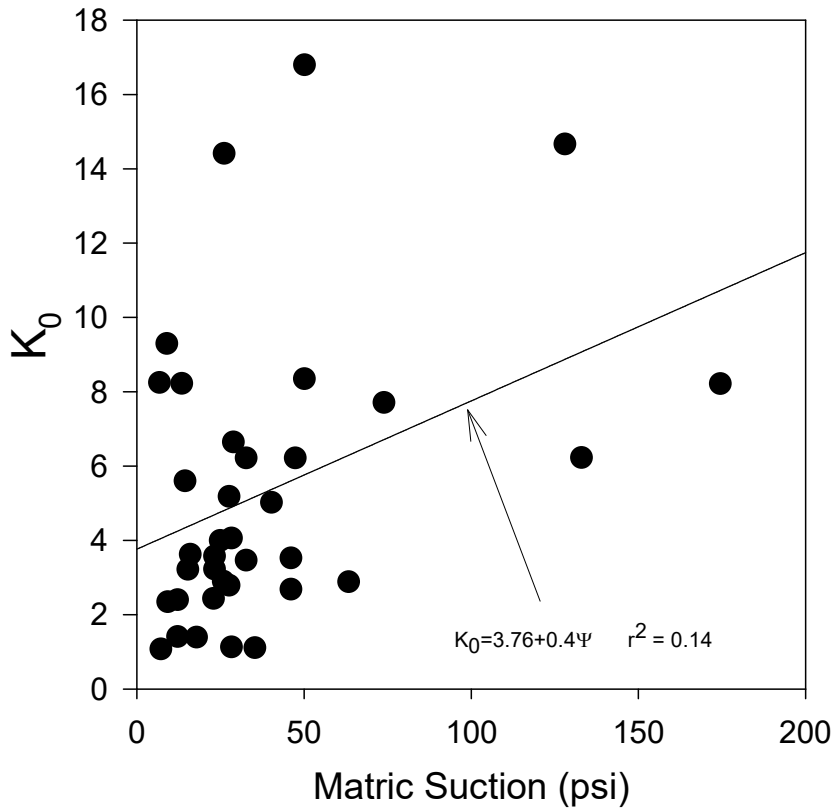

Figure 5.22: At-rest earth pressure versus matric suction determined from pressuremeter tests at Goldsby for all depths (3-ft., 6-ft., and 9-ft.)

The PMT data from North Base was examined in a similar manner to the Goldsby data. The limit pressure versus matric suction data for North Base for all depths are shown in Figure 5.23. There is strong positive correlation between matric suction and limit pressure at three and five-feet. The correlation decreases at seven feet; however, at this depth soil was consistently soft due to the rising water table at the site. This resulted in low matric suction values and relatively low limit pressures. By looking at the graphs in Figure 5.23, it appears matric suction has little effect on limit pressure until it increases above 80 psi.

The pressuremeter modulus at North Base was examined at all depths tests were performed. The results showed some positive correlation between matric suction and

pressuremeter modulus at three and five feet. The data is presented in Figure 5.24. The data at three and five feet was fitted with a power function in similar fashion to the pressuremeter data. The modulus correlation at North Base is in stark contrast to Goldsby, which showed no strong correlation at any depth. The difference seems to be a result of the increased matric suctions observed at North Base. Limit pressure data at North Base showed a threshold matric suction below which there was a minimal effect on strength. There appears to be similar phenomena for modulus. Again, this may be due to an error in the model SWCC used to determine matric suction.

The unload-reload modulus at North Base showed positive correlation with matric suction as shown in Figure 5.25. This again is in contrast to the behavior observed at Goldsby and is likely the result of the higher suction range encountered at North Base. At all depths, there is improvement in correlation between unload-reload modulus and pressuremeter modulus. This is likely because the soil at North Base is sensitive to borehole disturbance. The unload-reload loop corrects for any disturbances in the borehole. This improvement in correlation from pressuremeter modulus to unload-reload modulus was not seen at Goldsby, which may indicate the soil there is less sensitive to borehole disturbance comparatively.

The in situ horizontal stress (P_o) and at-rest earth pressure (K_0) were determined from tests data. The result is presented in Figures 5.26and 5.27. For both sets of data, there is some correlation with matric suction if data from all depths are plotted together. This is similar to what was found at the Goldsby site. The at-rest earth pressure coefficients for all tests at North Base versus matric suction is presented in Figure 5.28. The results show strong correlation between matric suction and at-rest earth pressure.

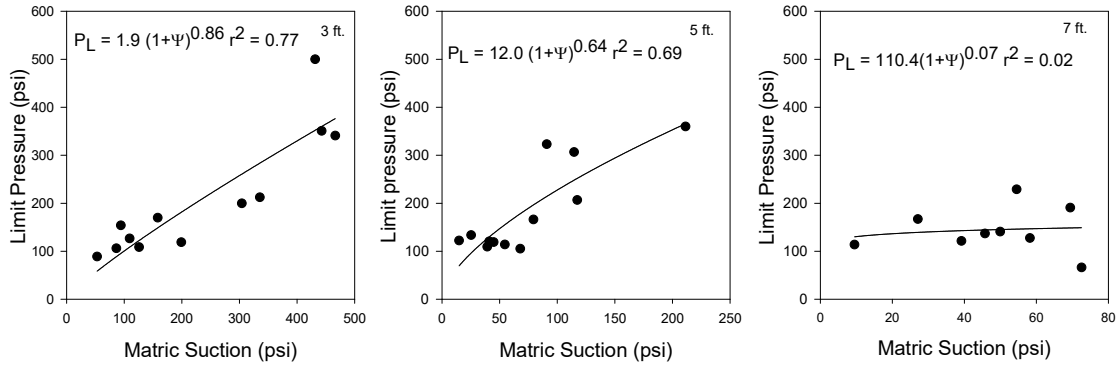

Figure 5.23: Limit pressure versus matric suction for North Base (3-ft., 5-ft., and 7-ft.)

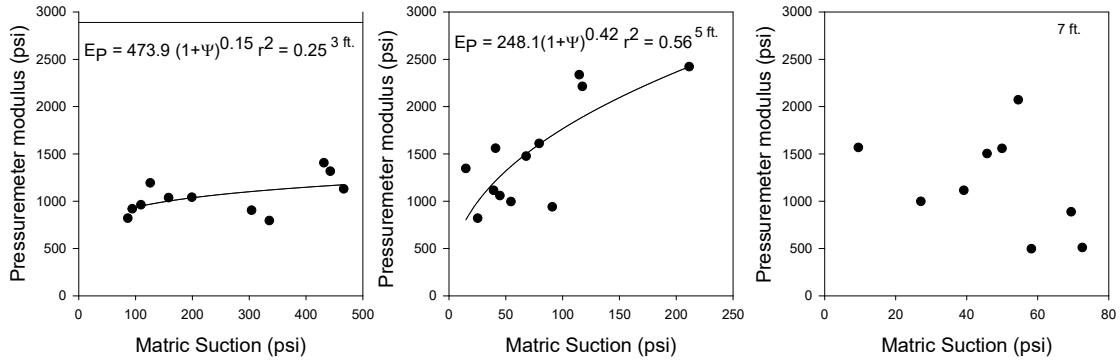

Figure 5.24: Pressuremeter modulus versus matric suction for North Base (3-ft., 5-ft., and 7-ft.)

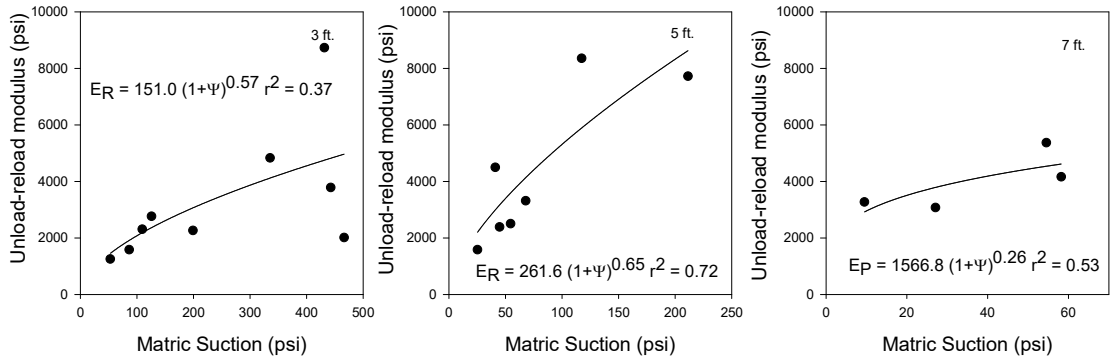

Figure 5.25: Unload-reload modulus versus matric suction for North Base (3-ft., 5-ft., and 7-ft.)

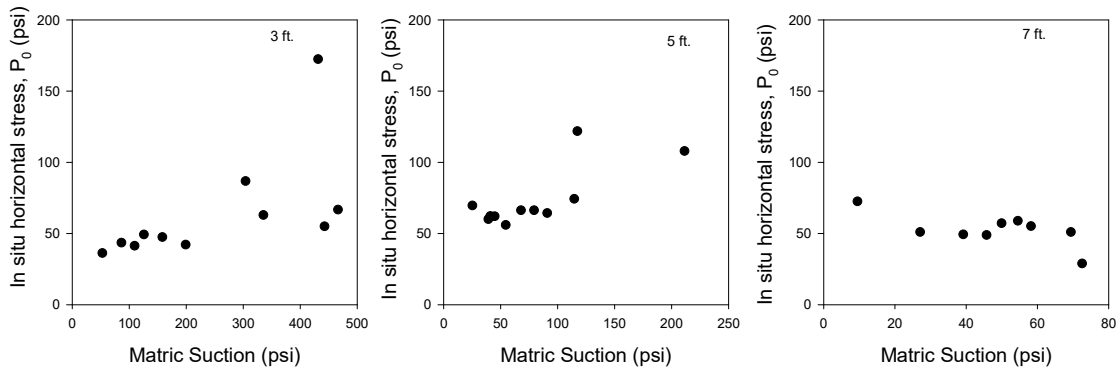

Figure 5.26: In situ horizontal stress versus matric suction for North Base (3-ft., 5-ft., and 7-ft.)

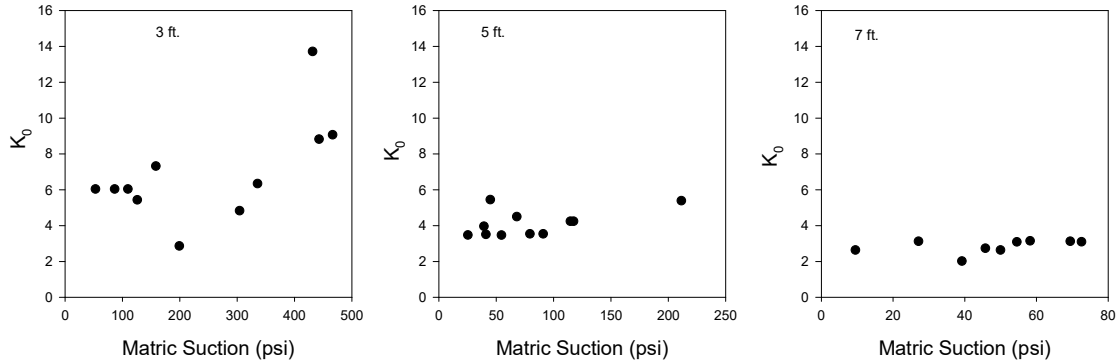

Figure 5.27: At rest horizontal earth pressure coefficient for North Base (3-ft., 5-ft., and 7-ft.)

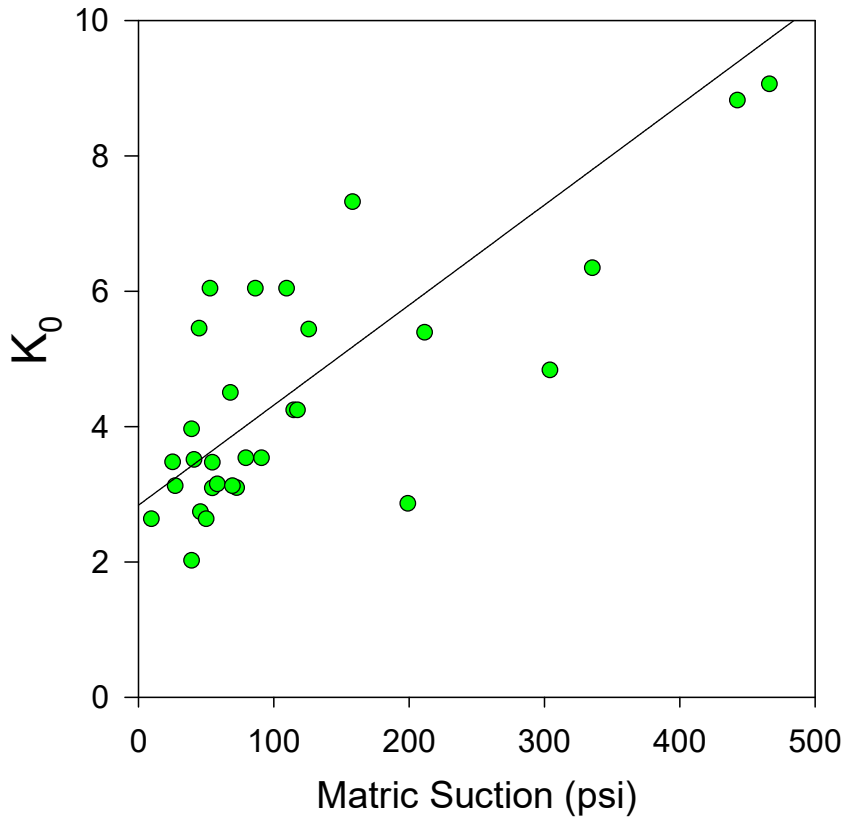

Figure 5.28: At-rest earth pressure coefficient versus matric suction determined from pressuremeter tests at North Base for all depths (3-ft., 5-ft., and 7-ft.)

5.6 Cone penetration test (CPT) results

5.6.1 Location of CPT tests at North Base and Goldsby

The map of cone penetration test locations at North Base is presented in Figure 5.29. The weather station is centered on the figure with the arrow directed towards North. The CPTs conducted at North Base were limited to the south of the weather station due to a water pipe running east to west on the north end of the test site. Three tests were performed per test date. Distances are shown in feet. The map of CPTs performed at Goldsby is shown in Figure 5.30.

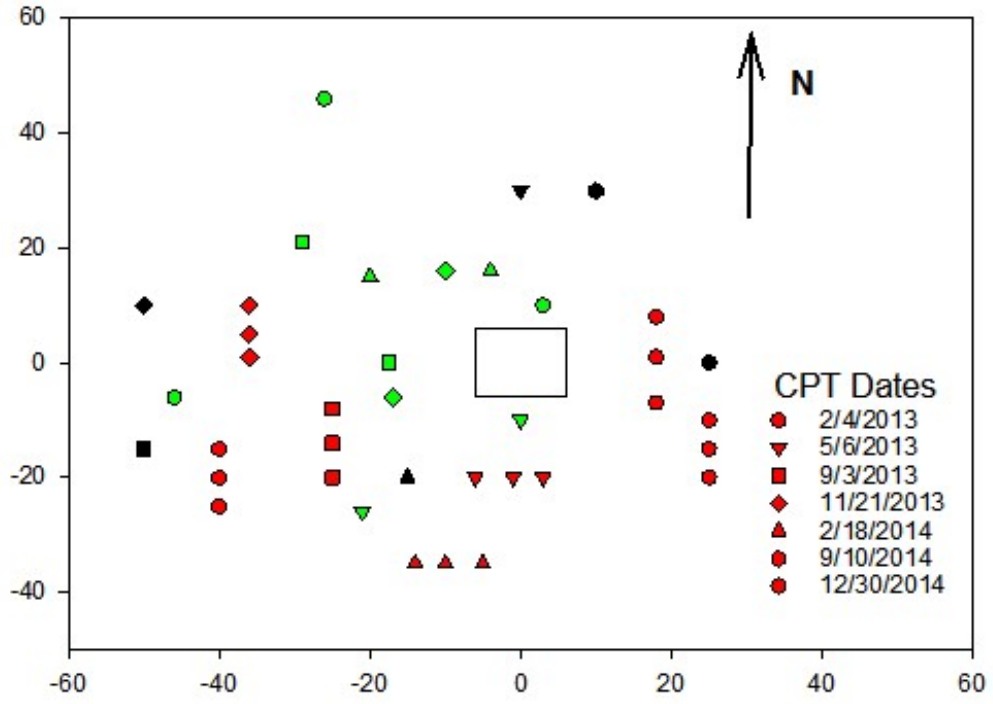

Figure 5.29: North Base CPT Location map

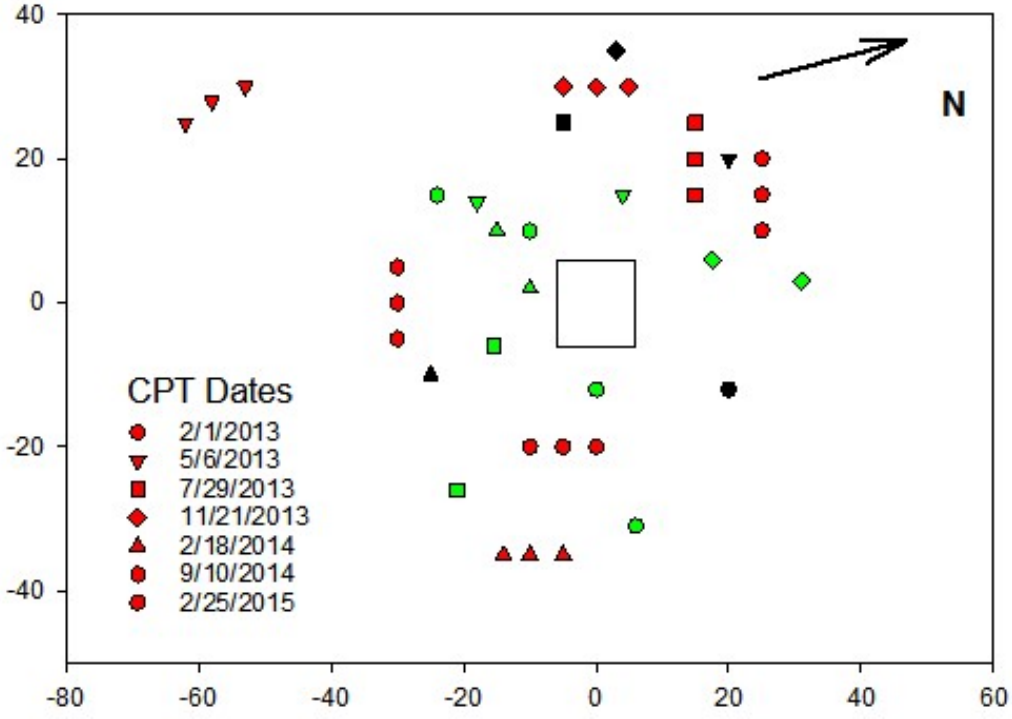

Figure 5.30: Goldsby CPT Location Map

5.6.2 Cone Penetration Test (CPT) results

The influence of matric suction at North Base was investigated by comparing three cone penetration tests conducted on a particular day. The tip resistance, sleeve friction, normalized tip resistance, and normalized friction ratio were compared to matric suction, which was determined from samples collected at the date of testing, and the SWCC constructed using Zapata et al. (2000). A figure was constructed for each date that presents moisture content (w %), matric suction (Ψ), tip resistance (q_t), sleeve friction (F_s), normalized cone resistance (Q_T), and normalized sleeve friction (F_R). The Figures for Goldsby and North Base are presented in the Appendix Figures A.26-A.39. To illustrate the effects of matric suction on tip resistance some selected test data will be used.

The best way to illustrate the influence of matric suction on CPT results is to select two days with different soil moisture conditions and compare the measured data. Figure 5.31 presents the results of CPT performed on 7/29/2013 and 9/10/2014. The moisture content, matric suction, tip resistance, and sleeve friction profiles from the tests are presented in the figures. Looking at moisture content above a depth of 5-feet, the water content on 7/29/2013 was comparatively drier than the test conducted on 9/10/2014, and thus these will be referred to as “dry” and “wet” tests, respectively. The tip resistance values measured during the “dry” test are on average 60 psi higher than the values measured during the “wet” test above a depth of 6 feet. For the same depths, the sleeve friction data show a similar pattern with a difference of 1.0 tsf between “wet” and “dry” days. Below a depth of 6 feet, the tip resistance and sleeve friction data for the two dates are more similar. This is consistent with the observation that moisture

contents change relatively little below a depth of 5 feet. However, on average the dry test date shows higher tip resistance and sleeve friction below 5 feet. This may be attributed to the fact that soil below 5 feet is actually undergone a small amount of drying that could result in suction increase due to the hysteresis effect. Use of a single SWCC to estimate matric suction for both dates would not capture this effect. The data shown in Figure 5.31 shows some scatter between tests; however, trends are relatively consistent for both sites.

The CPT from North Base on two different dates is shown in Figure 5.32. The results are comparable to Goldsby where on the "dry" date the tip resistance is higher and the sleeve friction is lower compared to the "wet date". The hysteresis observed at Goldsby is not noticeable in the North Base data. This may be attributed to them being on the wetting curve of the SWCC so the fluctuations observed at Goldsby in data that were nearly a year apart are not noticeable.

The CPT data can be broken down further to better illustrate the effect of matric suction on tip resistance, and sleeve friction. The tip resistance (q_t) and sleeve friction (f_s) determined from each of three tests for each test date were averaged and the result plotted versus matric suction. Results for North Base are presented in Figure 5.33. Tip resistance, and sleeve friction are shown on each y-axis. The test results indicate a strong positive correlation between matric suction, and average values of tip resistance and sleeve friction. A power function was used to provide best-fit curves for test depths with strong correlation. The functions and r^2 for each curve are presented in each corresponding figure.

The average tip resistance and sleeve friction versus matric suction plot for Goldsby can be found in Figure 5.34. The tip resistance shows some correlation with matric suction at most depths. There is a lack of correlation at three feet using all data; however, there is one point, which appears to be an outlier, and removal of this point would result in improved correlation at this depth. Sleeve friction does not seem to correlate well for Goldsby compared to North Base. This material is lower in plasticity than North Base, which may be a contributing factor as to why this behavior is observed.

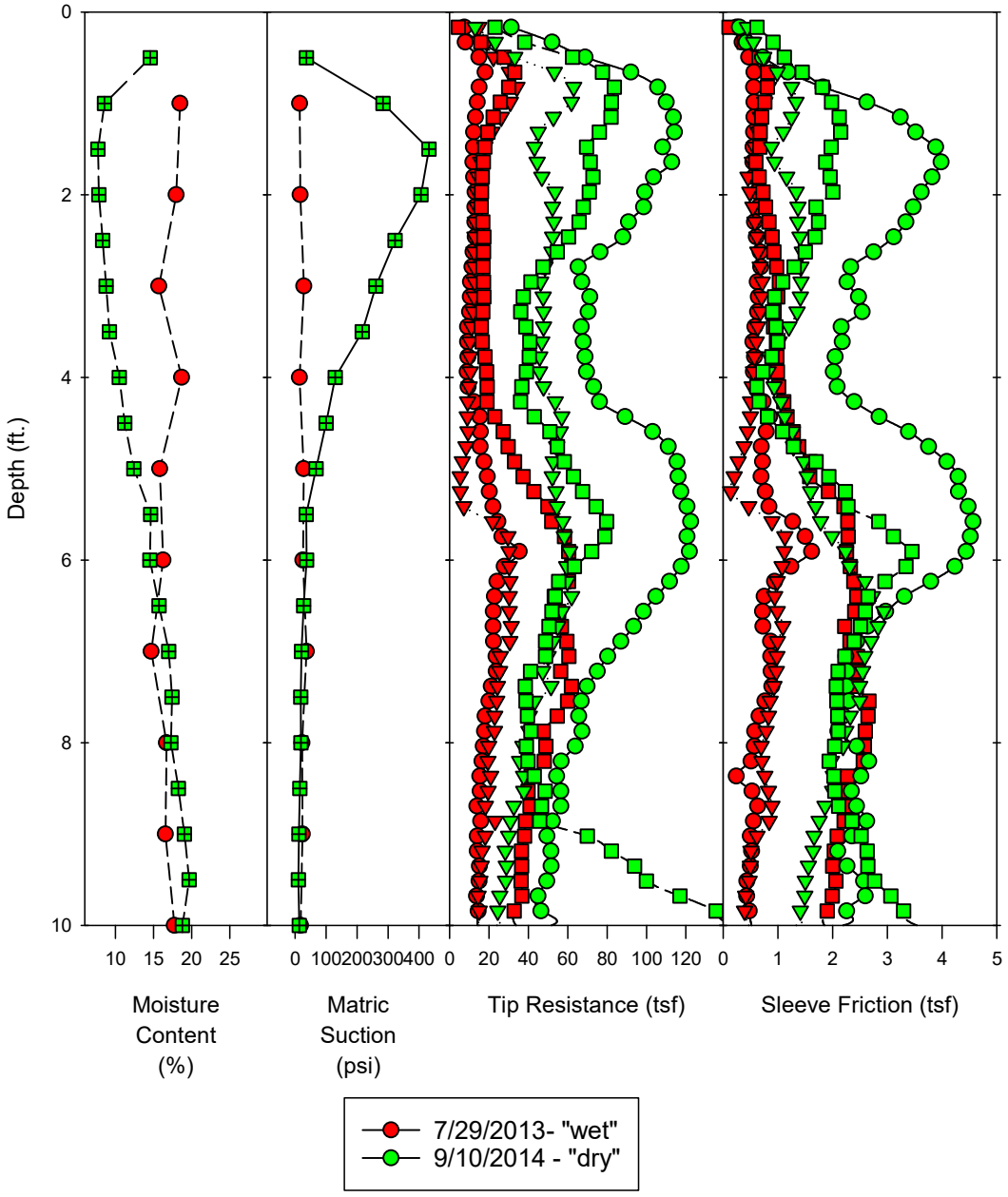

Figure 5.31: CPT from "wet" and "dry" test dates for Goldsby

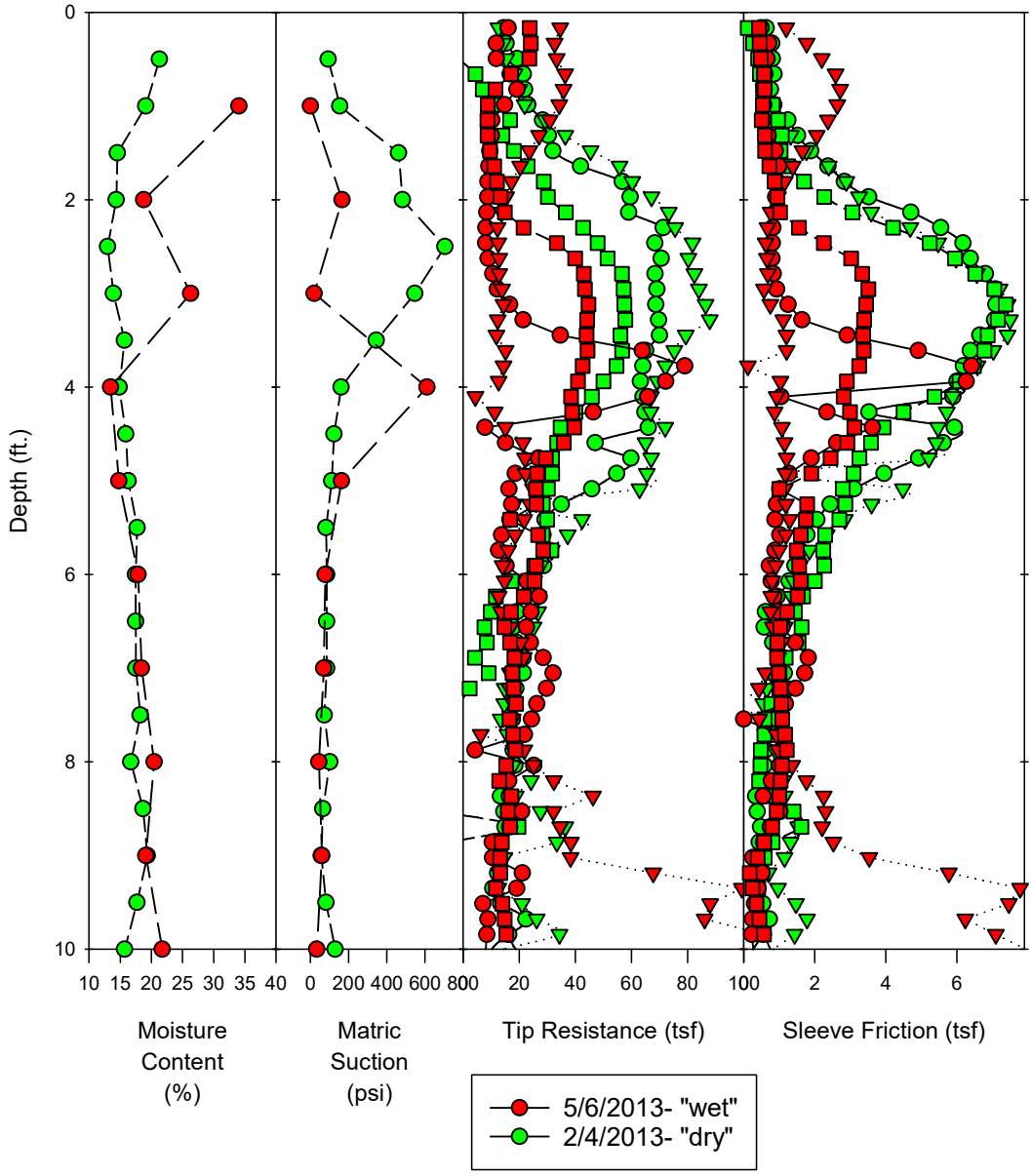

Figure 5.32: CPT from "wet" and "dry" test dates for North Base

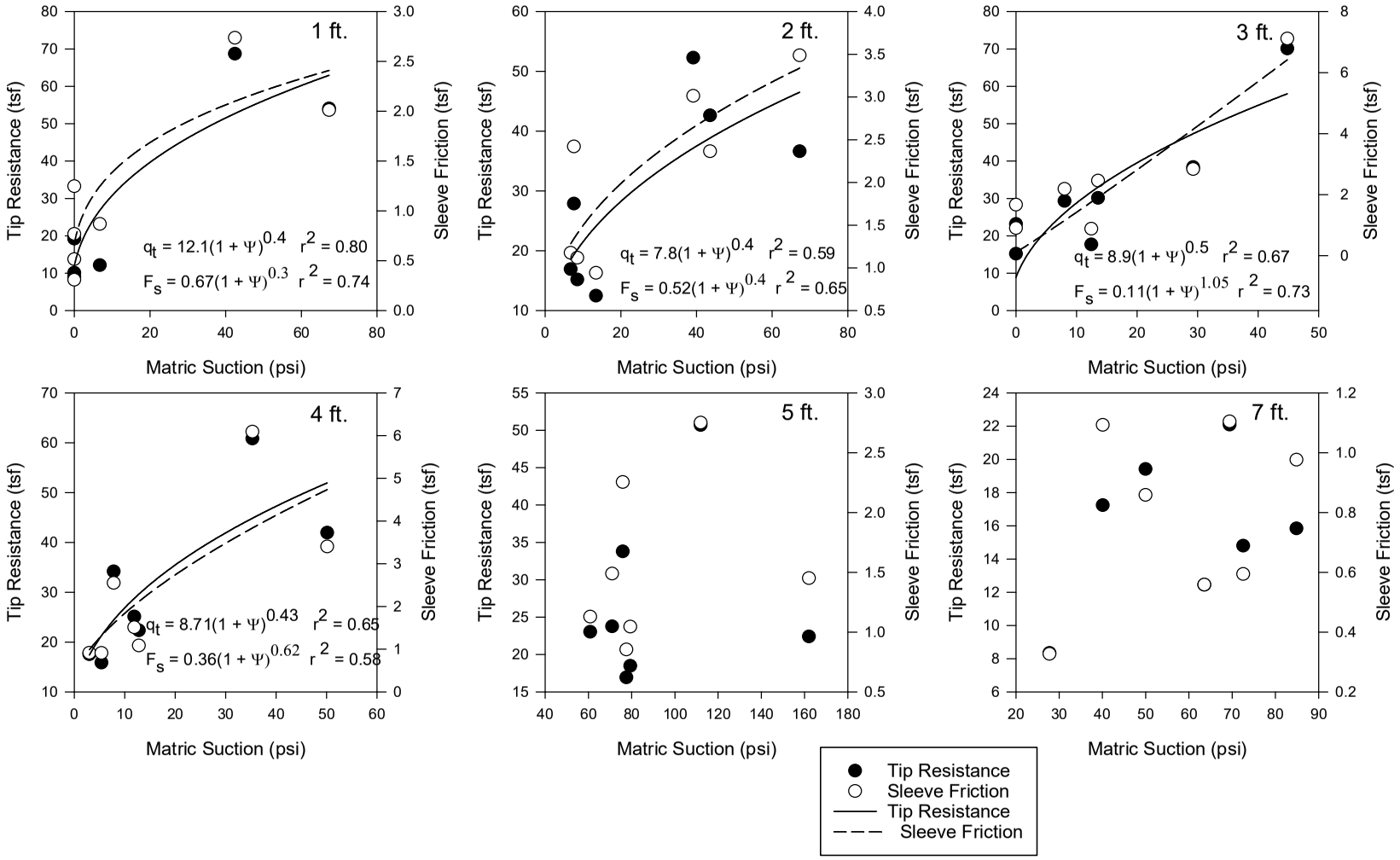

Figure 5.33: CPT parameters from North Base versus matric suction

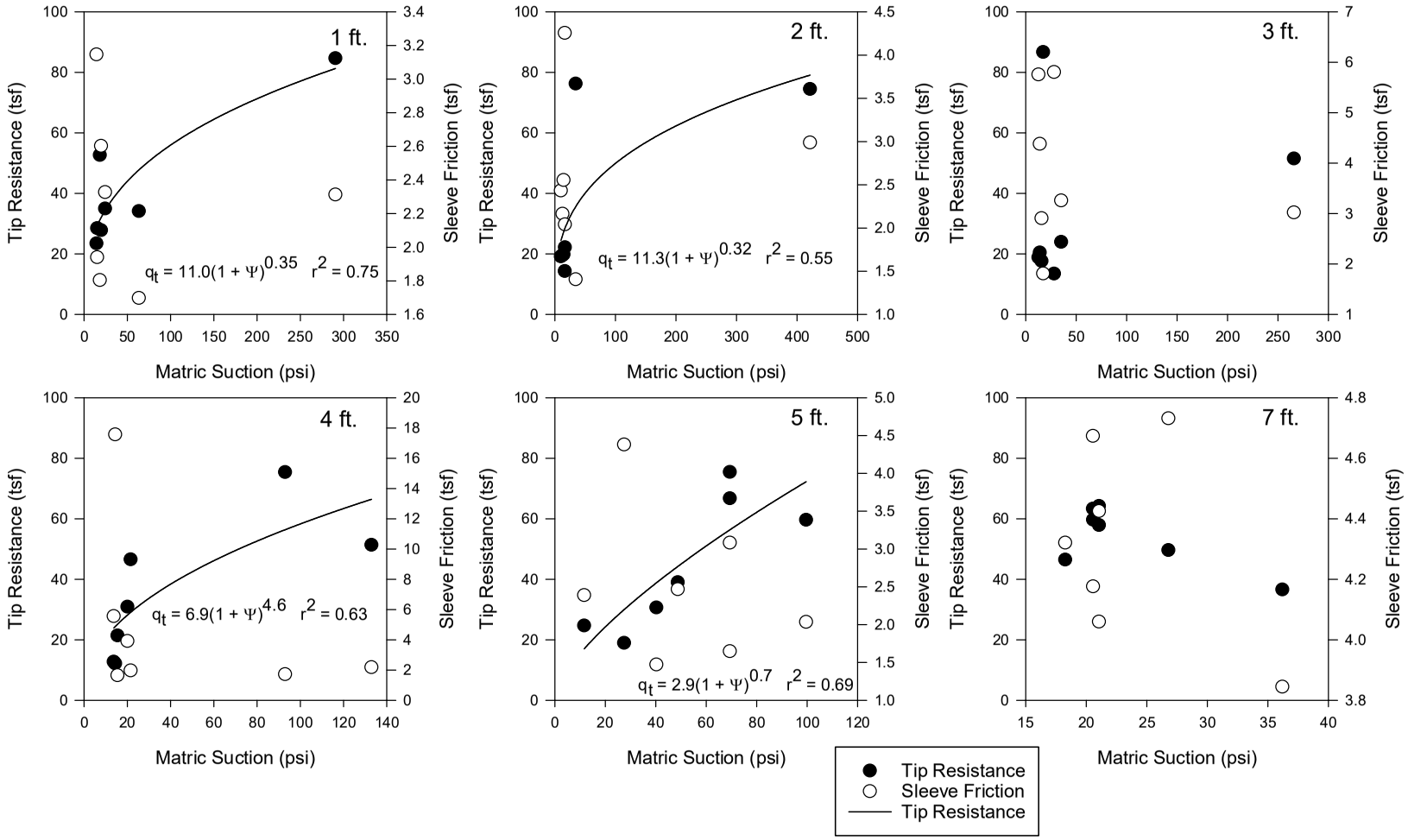

Figure 5.34: CPT parameters versus matric suction for Goldsby

5.7 Standard penetration testing (SPT) results

5.7.1 Location of SPT tests at North Base and Goldsby

The map of SPT locations at North Base is presented in Figure 5.36. The map of Goldsby SPT locations is presented in Figure 5.35. The arrow on each map is directed in the North direction. Distances are shown in feet.

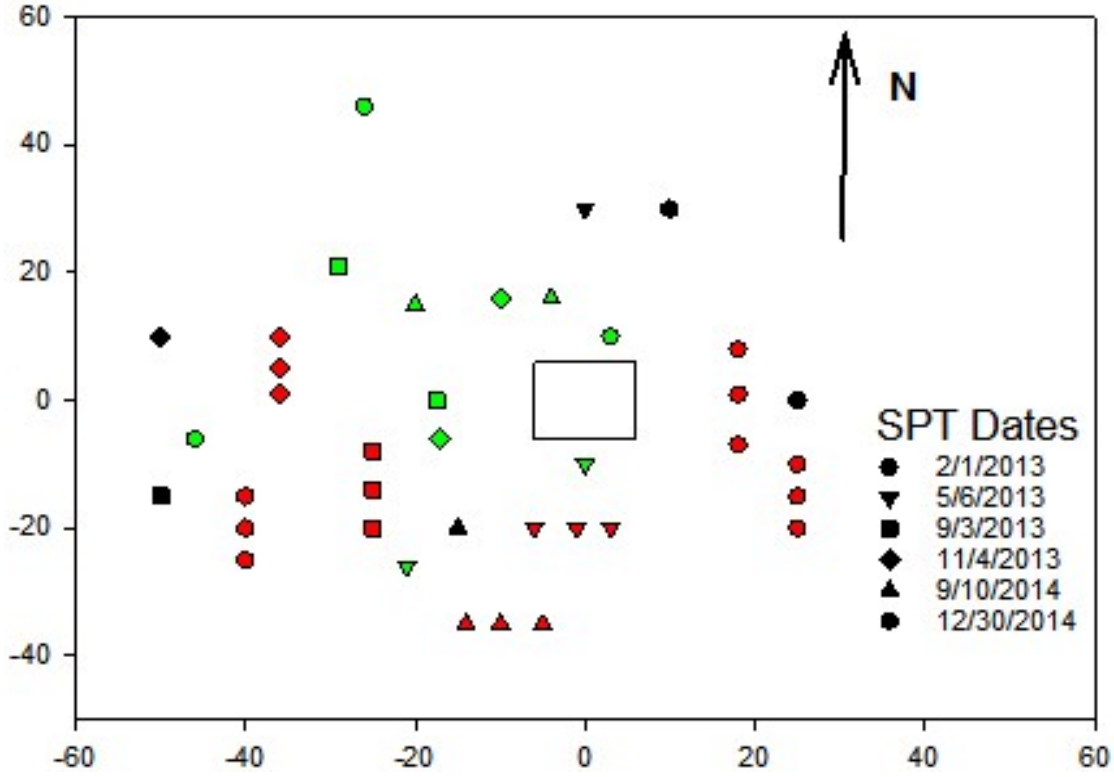

Figure 5.35: North Base SPT location map

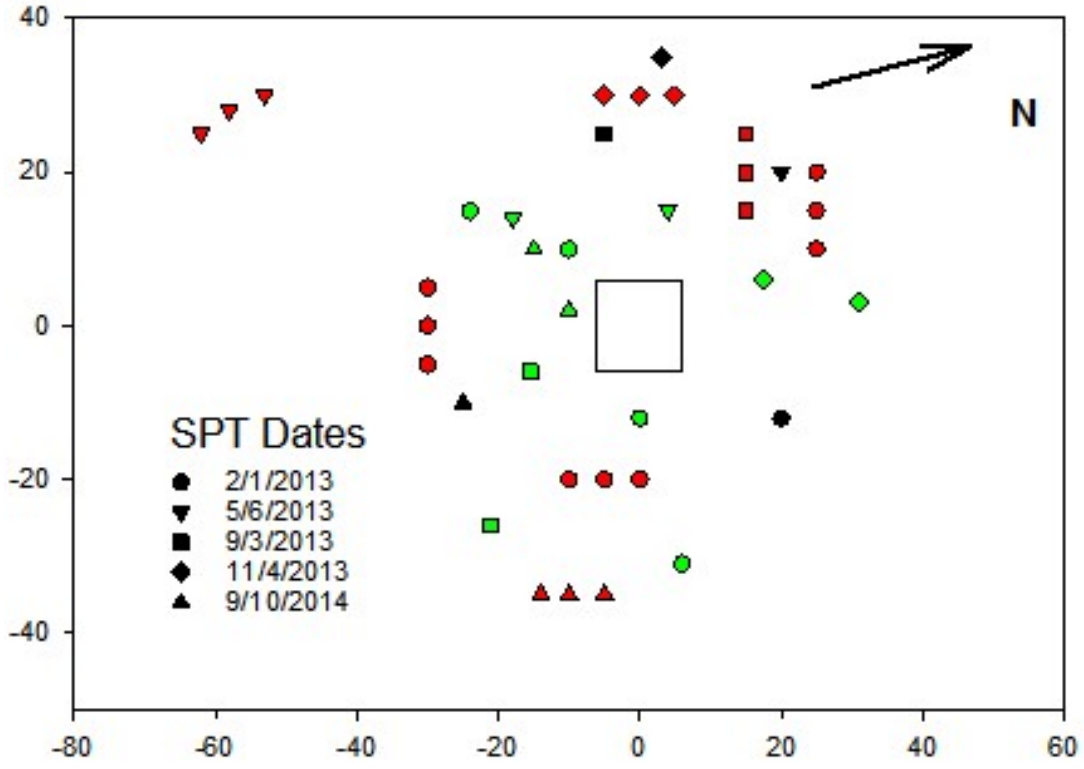

Figure 5.36: Goldsby SPT location map

5.7.2 Influence of soil suction on SPT results

The SPT conducted at North Base indicates that soil suction has a direct impact on the measured N-value. North Base SPT versus depth and soil suction is presented in Figure 5.37. The N-value seems to increase for soils with increased soil suction and decrease with a decrease in suction. The tests conducted in February, and May 2013, show the largest N-Values especially below 2 feet depth. The suction values also are shown to be highest for these for these dates.

Goldsby SPT results are presented in Figure 5.38. This figure shows a similar trend to what is observed for the SPT at North Base, as well as, the CPT results from both sites. SPT N-value shows some increase with an increase in soil suction; however, the strength of the correlation is low. The test results from Goldsby show the

phenomena better than the results obtained from North Base. The tests conducted in February 2013 and September 2014 both show larger N-values and larger soil suction. Other tests presented show lower N-values and lower soil suction measurements.

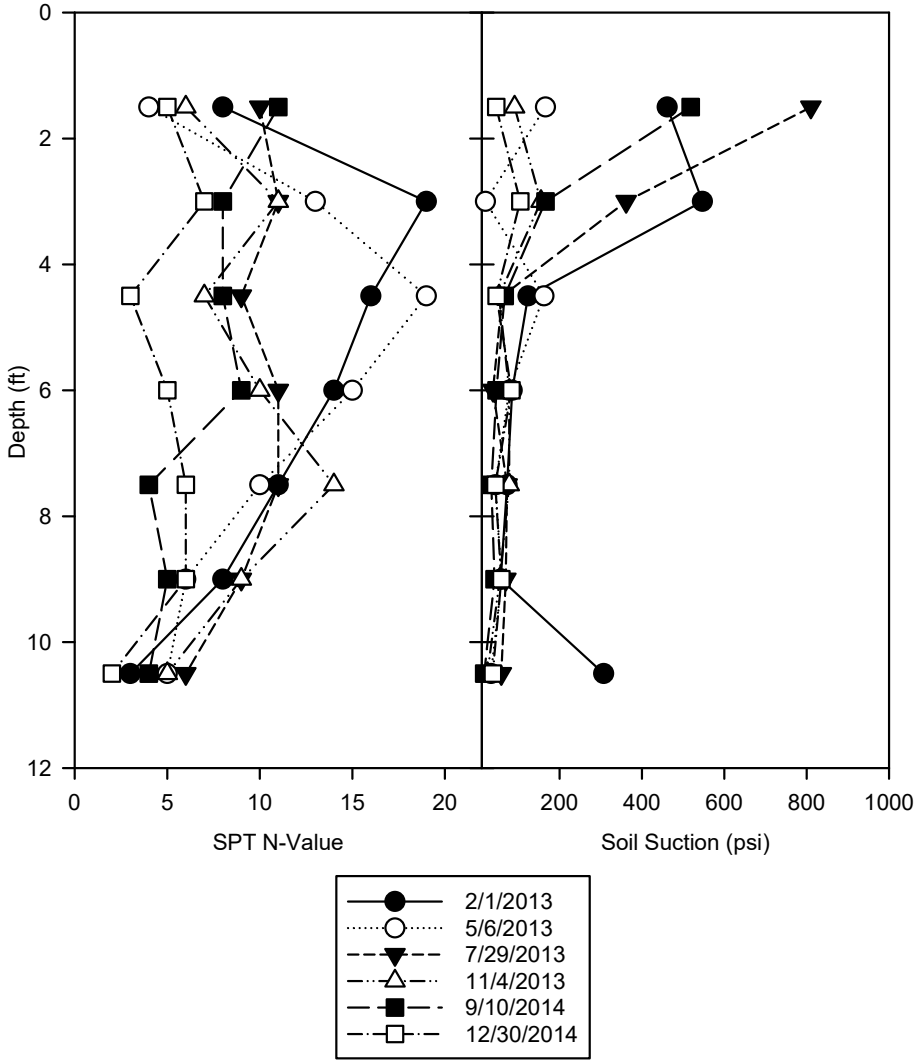

Figure 5.37: SPT N-value and matric suction versus depth for North Base

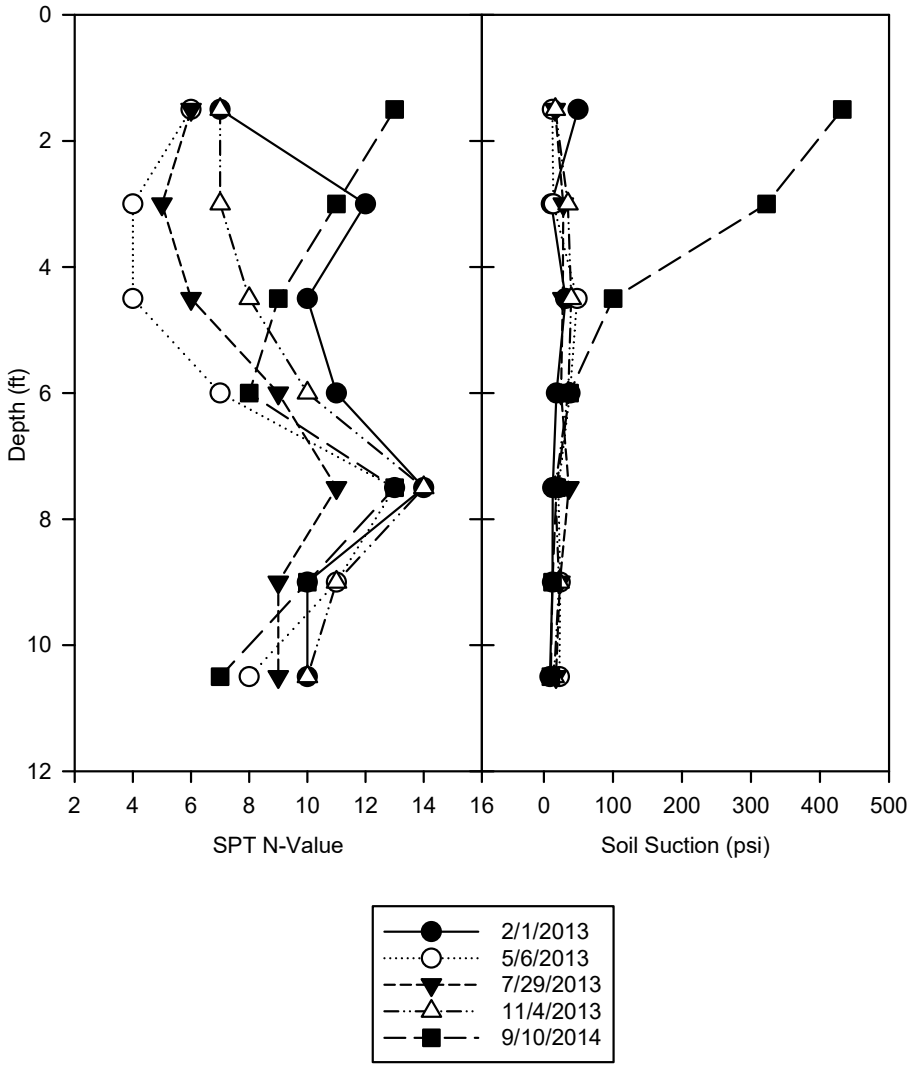

Figure 5.38: SPT N-value and matric suction versus depth for Goldsby

Chapter 6 Results and Discussion: Model Bearing Capacity Testing

6.1 Overview

A total of five load-controlled model footing bearing capacity tests were performed with in parallel with miniature pressuremeter testing. An unsaturated low plasticity clay was used and water content and matric suction were varied in each test. The same dry density was targeted for each test. The bearing capacity and settlement equations from Briaud (1992), which are described in detail in Chapter 2, were used to build a baseline prediction model for changes in matric suction and its predicting the effect of changes in matric suction on predicting bearing capacity and settlement.

6.2 Determination of matric suction

The matric suction for the McClain soil used in model footing bearing capacity tests was estimated in similar fashion to how matric suction was estimated for North Base and Goldsby. First, total suction soil water characteristic curves were completed on representative soil from two compacted samples. The compacted samples were prepared at the upper and lower end of water contents used in the model footing tests. These samples had dry densities equal to 107.7 lb. /ft^3, which was the target dry density for all model-footing tests. The water content during compaction was 17%, and 10.5%, which includes the upper most and second lowest water contents used in model footing tests. After compaction the samples were saturated which increased the initial water content to 22.6% and 20.9%, respectively. From each compacted specimen, two samples were trimmed and placed and WP4 cups for total suction measurements. Mass

measurements were made on the samples as water evaporated in combination with total suction measurements. These total suction soil water characteristic curves are shown in Figure 6.1, and labeled WP4 1-4. The data from the higher water content compaction points are labelled WP4 1-2, while the lower water content compaction points are labelled WP4 3-4.

A total suction soil water characteristic curve was made for the McClain soil by Esmaili (2014). The results of this test are also included in Figure 6.1. No details are given about the initial water content or density. The results fall slightly below the range of the total suction measurements made with the WP4 for the previously mentioned density and water contents.

Also included in Figure 6.1 is the total suction measurements made on samples collected during model footing tests. These are shown by their test dates and in general fall in a lower range than their WP4 total suction SWCC measurements. This phenomenon was also seen in field data compared to WP4 SWCC measurements described in Section 5.3. This is likely the result of the significant differences in drying and wetting paths that SWCC samples followed (compacted, wetted to saturation, then dried) compared to footing test soil that was mixed with water and compacted to a target moisture content that changed very little thereafter.

The percent of McClain soil passing a #200 sieve (92.5%) and the plasticity index (17%) was used to construct the SWCC based on matric suction following the method of Zapata et al. (2000). This SWCC is presented as the matric suction line in Figure 6.1. The curve is lower than the measured total suctions at high moisture contents due to the osmotic suction. At higher moisture contents, the test data

corresponds well with the estimated matric suction. The matric suction curve is parallel to total suction measurements made with the WP4. The water content of test samples will be used along with this SWCC to determine matric suction in subsequent analyses.

6.3 Model footing tests

Five model-footing tests were performed. The target water content was varied and the target dry density was held constant. The samples were compacted by hand using a tamping mass, which may account for the variation in density between tests. A table of the test dry density, average water content, average matric suction, and bearing capacities used in this study is presented in Table 6.1. Water content profiles for each test bed were determined from samples taken after completion of the bearing capacity and MPMT. A hand auger was used to extract the soil from the test bed and soil from each inch was obtained for moisture content determination. The full water content and matric suction profiles for all test beds are presented in Figure 6.2. There was some variability in the moisture content measurement with depth. This can be attributed to accuracy of the scale and variable humidity air temperature in the laboratory, and grain-size distribution, which can lead to lead to different degrees of moisture loss during preparation of the test bed. The matric suction versus depth profiles were determined using the measured moisture contents and the soil water characteristic curve (SWCC) shown in Figure 6.1.

Load settlement curves are presented for the model bearing capacity tests in Figure 6.3. The bearing capacity was determined in two ways. The first method is simply taking the measured bearing pressure at a settlement equal to 10% of the footing

width, which for this research was 0.4 inches the load settlement curve with bearing capacities determined for 10% B are shown in Figure 6.3. The other method is described by Oh and Vanapalli (2013), which is determined by fitting tangent curves to the initial straight-line portion of the load settlement curve and the straight-line portion obtained after yielding. The intersection of these points determines the bearing capacity. It is referred to herein as the graphical method.

The settlement shown is the average displacement of the two dial indicators placed on the footing that were diametrically opposed and equidistant from the center. In all but the first test, loading continued until the cumulative settlement reached 10% of the footing width, or 0.4 inches. The lone exception was the first test completed with soil having an average matric suction of 30.1 psi. This test was stopped early because of concerns with the loading equipment, which were addressed after completion. For subsequent tests, all footing settlements exceeded 0.4 inches. The bearing capacity was taken as the load at 0.4 inches of settlement. For the first test where 0.4 inches was not reached, the load-settlement curve was extrapolated to 0.4 inches.

Table 6.1: Summary of average moisture content and matric suction of model bearing capacity tests

Test Date	Moisture content (%)	Matric suction (psi)	Dry Density (pcf)	Bearing Pressure 10% strain (psi)	Bearing Pressure Graphical (psi)
2/29/2016	17.0	30.1	104.83	90.5	55
3/14/2016	12.7	103.8	102.17	180.0	187
3/28/2016	9.6	298.2	105.3	150.0	200
5/5/2016	13.9	72.6	110.12	147.0	128
5/27/2016	10.5	215.9	100.14	134.0	130

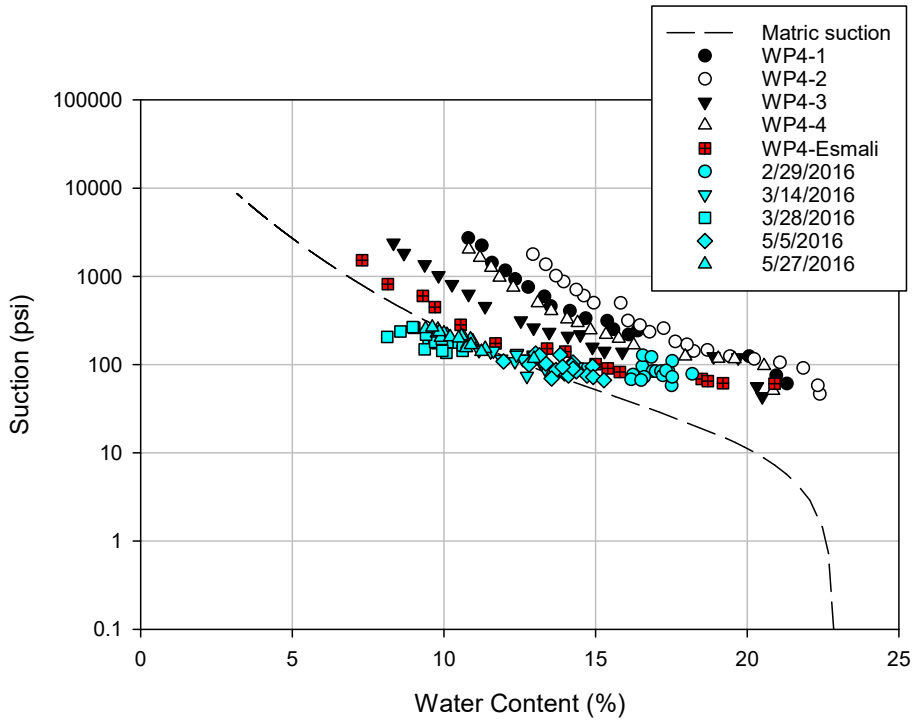

Figure 6.1: Estimated Soil Water Characteristic Curve (SWCC) and measured total suction data for McClain Soil

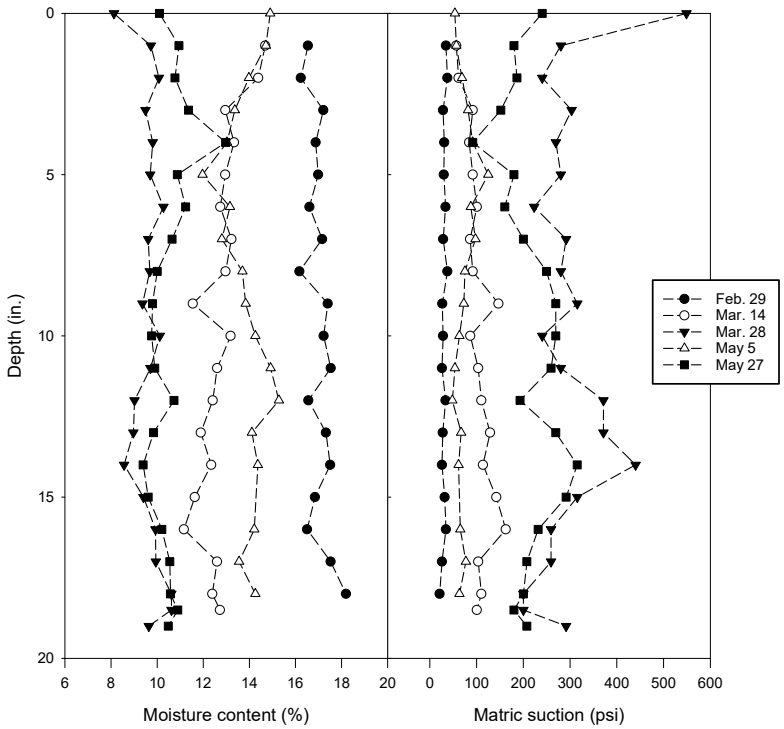

Figure 6.2 Water content and matric suction profiles for model footing tests

The measured bearing capacity versus average limit pressure is shown in Figure 6.4 along with the limit pressure versus matric suction. It can be seen that there is a strong relationship between limit pressure and bearing capacity. The ultimate bearing capacities determined using the 10% method show incredibly strong correlation with limit pressure. The result indicates that the 10%B method for determination of bearing capacity is more consistent; thus, reported bearing capacities determined using this method are analyzed in subsequent sections.

The comparison of ultimate bearing pressure and limit pressure in Figure 6.4 makes it clear that the limit pressure and bearing capacity are responding to the different soil conditions and changing suction in a similar, consistent, and predictable manner. This is an extremely important observation as it verifies that the changes in the pressuremeter limit pressure due to variable soil conditions in unsaturated soil are adequately reflecting and generally proportional to the changes observed in bearing capacity of a footing loaded on the same soil. Thus, the pressuremeter should be a reliable tool for predicting bearing capacity of shallow foundations on unsaturated soils. Further, if one can predict the changes in PMT limit pressure due to changes in unsaturated soil conditions, using methods described in this dissertation for example, and then it should be possible to predict changes in bearing capacity under similar changes in soil conditions.

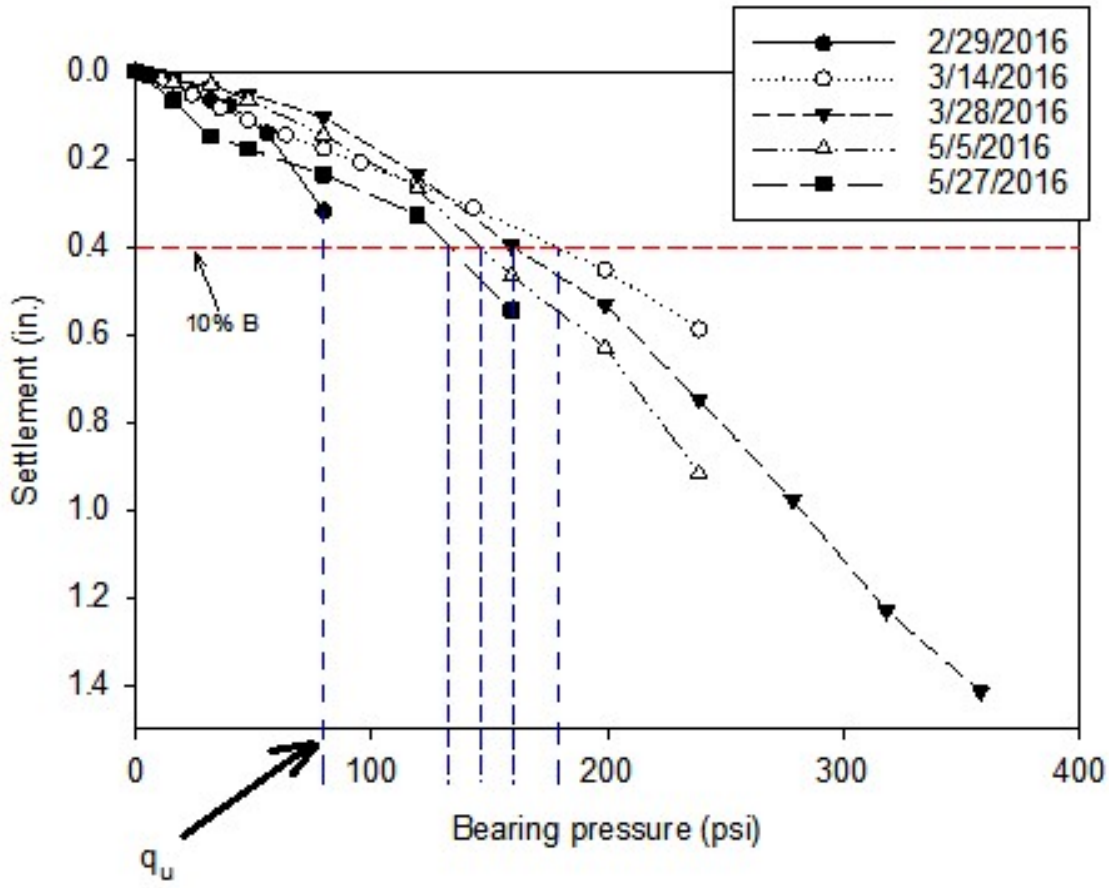

Figure 6.3: Load settlement curves for model footing tests with bearing capacity determined using the 10% method

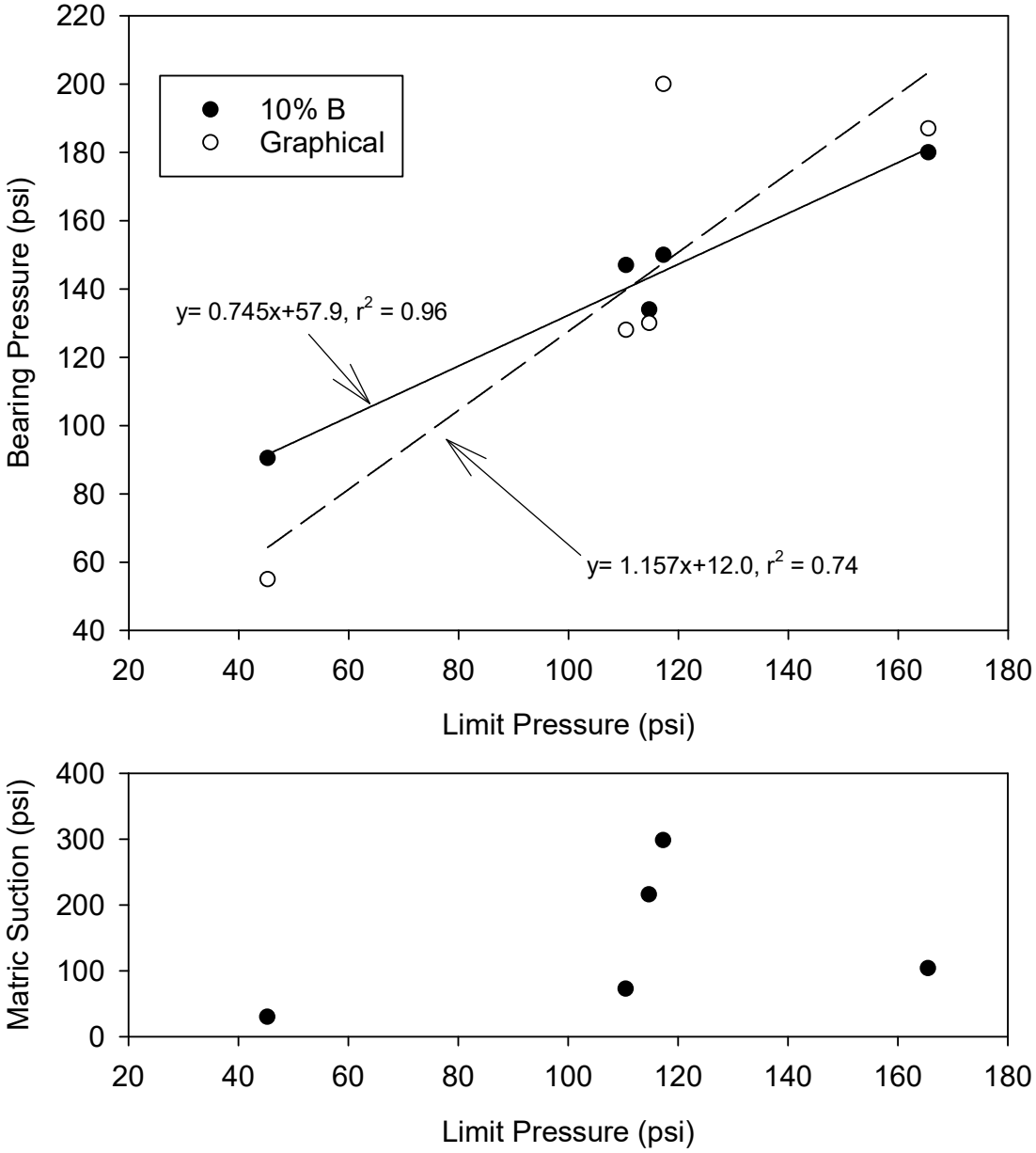

Figure 6.4: Comparison of 10%B and graphical method for determination of ultimate bearing capacity and limit pressure versus matric suction for same data points

6.4 Miniature pressuremeter tests

As described in detail in Chapter 4 (Section 4.3), MPMT were conducted at locations around and outside of the circumference of the bearing plate prior to initiating

the load test. Three pressuremeter tests were taken per bearing capacity test. The average limit pressure, pressuremeter modulus, and unload-reload modulus are reported for each test in Table 6.2. Figure 6.5 presents limit pressure (Figure 6.5a), pressuremeter modulus (Figure 6.5b), unload-reload modulus (Figure 6.5c) and dry density (Figure 6.5d) versus matric suction. The general trend in all pressuremeter parameters indicates that a peak in limit pressure and moduli occurs at an average matric suction of 100 psi, followed by a drop in these parameters at increased suctions. It was expected that the pressuremeter parameters would continue to increase at increased suctions as were observed from the field tests in presented in Chapter 5. There are several possible competing factors that may play a role in the observed behavior and that may provide a partial explanation for why PMT parameters decreased above a matric suction of 100 psi. These factors include the variation in dry density, the influence of matric suction, and variations in the soil fabric between test beds.

The dry density can have a strong influence on PMT results. Soil with lower dry density has more void space than a soil with high dry density, reducing shear strength and increasing compressibility. However, looking at Figure 6.5 there seems to be no correlation between dry density and PMT parameters, which indicates that while dry density may be one factor controlling pressuremeter parameters, it is not the only factor.

The tests conducted at the three lowest matric suction values range in dry density from 102 pcf to 110 pcf. Matric suction for these tests increases from 30 psi to nearly 100 psi. There is an increase in pressuremeter parameters for all three of these tests even though dry density fluctuates. Matric suction has potential to cause an increase in mechanical soil properties so this could be a potential explanation for the

increase in pressuremeter parameters. However, the trend of increasing PMT parameters with increasing matric suction does not hold for the two highest matric suctions. This does not mean that matric suction is not playing at important role in the increase in PMT parameters from 30 psi to 100 psi.

Matric suction is literally the difference between pore air and pore water pressure. As matric suction increases, there is an increase in the tensile force between soil particles which results in increased strength. There is a threshold matric suction where the area of the water between contact points of soil particles becomes so small that it no longer has much of an effect on soil strength. Above this matric, suction there would be little to no noticeable increase in soil strength from increased matric suction. This could partly explain the drop in PMT parameters for tests above 100 psi.

Another possible explanation for the variation in PMT parameters at various matric suction is the difference in the soil fabric between tests. Each matric suction shown in Figure 6.5 comes from variation in the moisture content during test bed preparation. This means that each new test bed had a different initial soil structure depending on the initial water content. Drier soil exhibits a clod structure with considerable dual porosity, having macropores between clods and micropores within clods. Suction has a much different effect on such soils compared to soils compacted at higher water contents with more of a uniform porosity. These soil structural differences in the test beds certainly affect the pressuremeter results and may provide a partial explanation for the variation in results.

Table 6.2: Miniature pressuremeter parameters for all test dates

	Test #	P_L (psi)	E_p (psi)	E_r (psi)
2/29/2016	1	42.8	331.9	663.9
	2	49.6	377.7	-
	3	43.3	692.7	-
	Avg.	45.2	467.5	663.9
3/14/2016	1	156.1	4907.0	23494.7
	2	174.9	5913.1	34091.8
	Avg.	165.5	5410.0	28793.2
3/28/2016	1	134.3	-	-
	2	130.5	2234.2	2366.6
	3	87.0	3655.7	10436.5
	Avg.	117.3	5579.8	10913.3
5/5/2016	1	114.9	1356.4	3152.3
	2	102.5	1349.2	3058.9
	3	114.1	1608.1	3717.9
	Avg.	110.5	1437.9	3309.7
5/27/2016	1	117.0	2446.3	3623.8
	2	120.5	2690.9	4052.0
	3	106.7	2517.8	4268.9
	Avg.	114.7	2551.7	3981.6

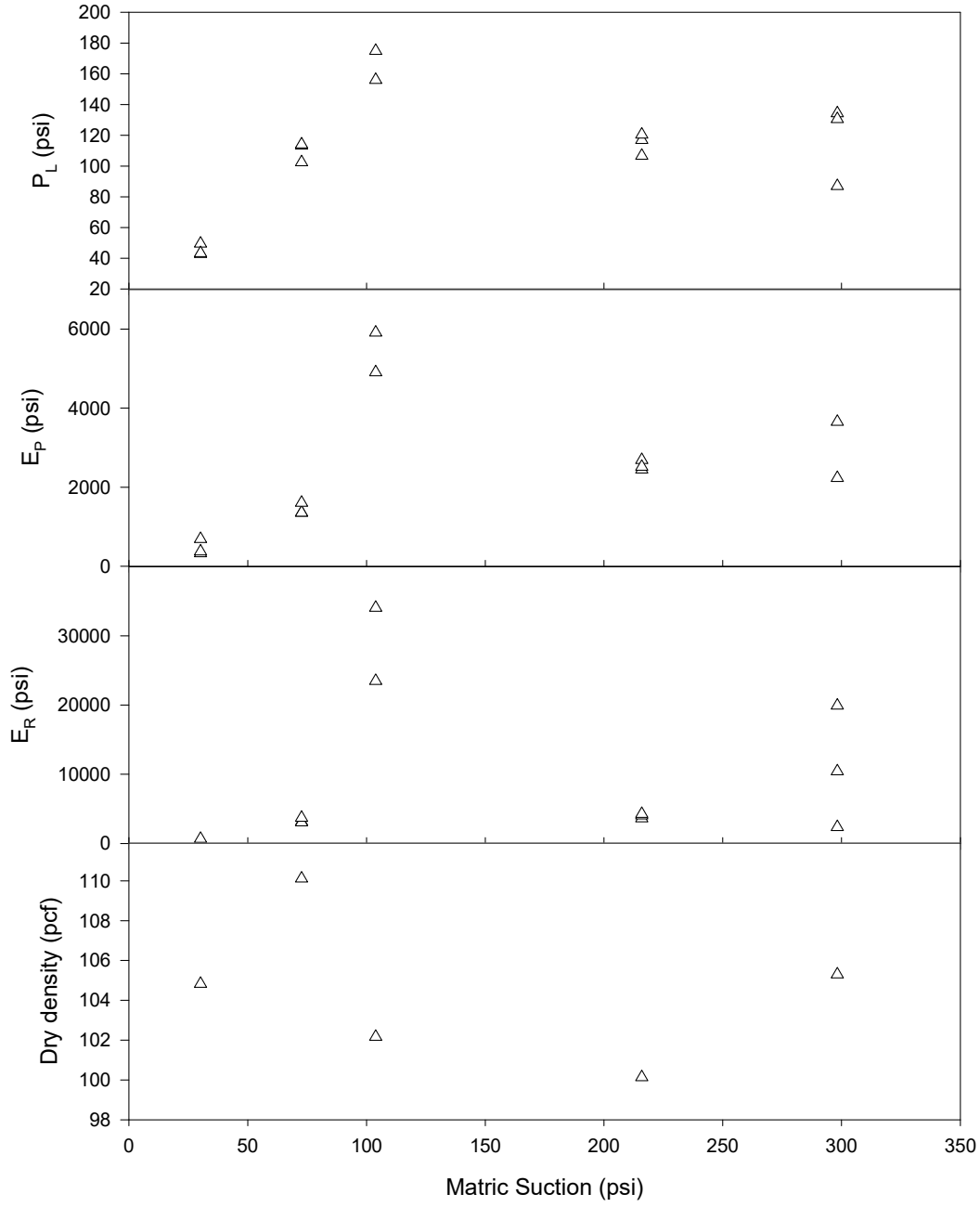

Figure 6.5: Limit pressure (a), pressuremeter modulus (b), unload-reload modulus (c), and dry density (d) versus matric suction

The corrected pressure versus corrected volume curves obtained during PMT are presented in the Appendix (Figures A.40-A.44). Pressuremeter curves shown in the Figures indicate that relatively consistent limit pressure and modulus values were

obtained in each test bed. There is some variation in the tests conducted on 3/28/16, which was due to some issues with the PMT membrane; this membrane material was replaced for subsequent tests.

6.5 Prediction of bearing capacity and settlement based on PMT

Briaud (1992) presents a method to predict the bearing capacity of a shallow foundation based on the pressuremeter limit pressure. The Equation presented in Chapter 2 as Equation 2-16 can be used to predict bearing capacity if three factors are known. These factors are: 1) a bearing capacity factor, which is empirically estimated to be 0.8 for the McClain clay used in this study. 2) P_{Le}^{*} (Eq. 2-17), the equivalent net limit pressure, which will be based on the three PMTs performed per test bed. 3) q_o, which is the overburden pressure at the depth of embedment (zero for all tests).

The bearing pressure is determined from PMT data by simply multiplying the equivalent net limit pressure by a factor of k. The parameter k, which is the bearing capacity parameter, comes from the relationship between the horizontal and vertical stress. This value is typically 0.8 for all soils (Briaud, 1992) when there is zero depth of embedment. The bearing capacity calculations using k=0.8 are plotted in Figure 6.6. It is clear that k=0.8 does not provide a good match for the experimentally measured bearing capacity. Some possible reasons for this includes: a scale effect due to the fact that these measurements were made using a model footing, or these soils are unsaturated and k is a empirically derived parameter that may not apply to all soils and soil conditions. In the following sections, a theoretically based approach to determine k was explored for unsaturated soils.

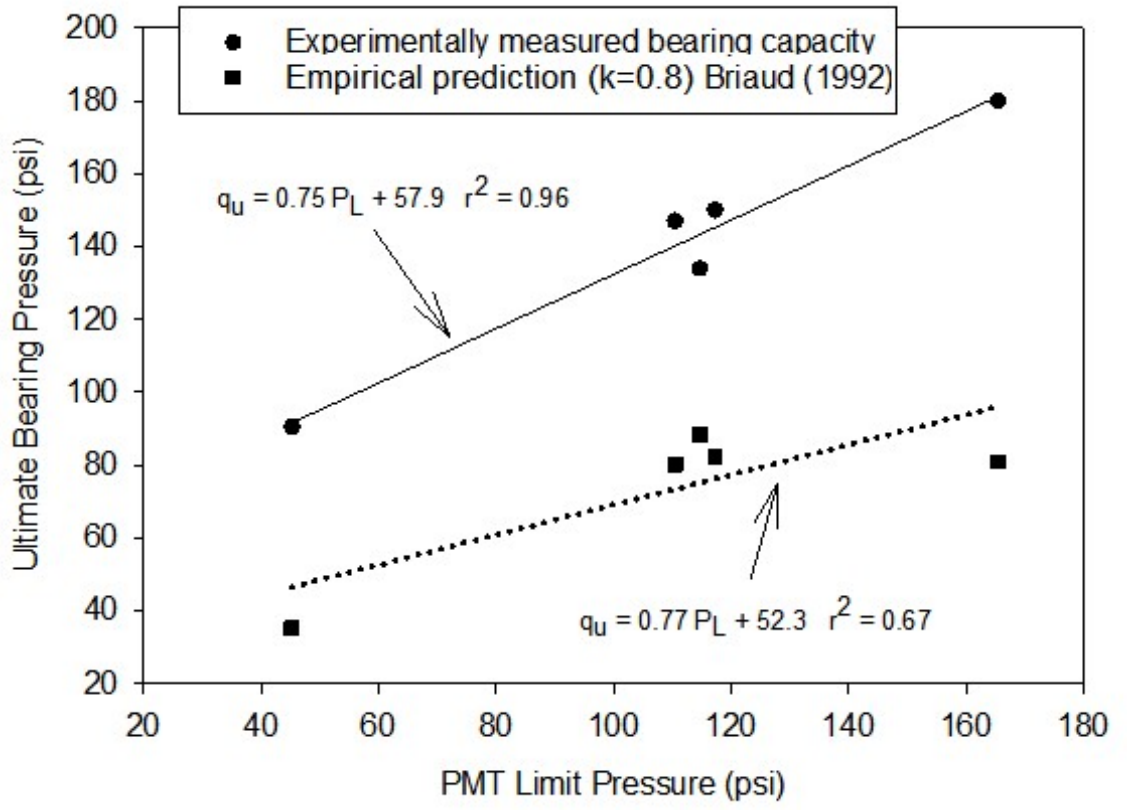

Figure 6.6: Limit pressure versus measured and predicted bearing capacity

In Briaud's (1992) discussion of the bearing capacity factor (k), it is described as the ratio ($k=q_u/q_{uh}$) of the total vertical resistance (i.e. ultimate bearing capacity, q_u) to the ultimate horizontal resistance component (q_{uh}), which contributes to the ultimate bearing capacity. The idea is that the limit pressure is equal to the horizontal component of resistance ($P_L=q_{uh}$), which contributes to ultimate bearing capacity of vertically loaded footings. Thus, multiplying the limit pressure of the soil by the bearing capacity factor described above provides an estimate of ultimate bearing capacity of vertically loaded footings.

To emphasize this point, a simple derivation of the bearing capacity factor based on theoretical considerations is provided in Briaud (1992) for undrained loading of clay.

Figure 6.7 shows the total and vertical resistance to loading and its relation to the k-factor for saturated undrained loading as described in Briaud (1992). The basic idea is that the ultimate bearing capacity can be broken up into vertical and horizontal components ($q_u=q_{uv}+q_{uh}$) and the goal is to develop theoretical expressions for q_u and q_{uh} in order to calculate $k=q_u/q_{uh}$, as described above. In the simplified analysis presented by Briaud, the ultimate bearing capacity for a circular footing at the ground surface is about six times the undrained shear strength ($q_u=6s_u$). The vertical contribution (q_{uv}) to this is assumed to come from the soil beneath the footing with the surrounding soil removed, or in another words it is equal to the unconfined compression strength ($q_{uv}=2s_u$). The difference between the total ultimate resistance (q_u) and vertical component (q_{uv}) gives the horizontal contribution to the bearing capacity (q_{uh}), which is 4Su. The bearing capacity factor as defined above is given as, $k=q_u/q_{uh}= 6S_u/4S_u$, which is equal to 1.5.

The Briaud (1992) discussion of the k-factor can be further refined to determine a bearing capacity factor for unsaturated soils. The first step is to modify the ultimate bearing capacity equation for use with unsaturated soils by considering a c-ϕ soil with cohesion, c, modified to account for soil suction. The Terzaghi bearing capacity equation for general shear failure for a circular footing of diameter B is,

$$q_u = 1.3cN_c + 0.3\gamma BN_\gamma + \gamma DN_q \qquad \text{(Eq. 6-1)}$$

Where:

N_c, N_γ N_q = Terzaghi bearing capacity factors,

γ = soil total unit weight,

B = footing width,

D = depth of embedment and,

c=cohesion component of shear strength.

The cohesion component of shear strength can be modified to account for suction using Equation 6-2 or some other appropriate representation of the suction contribution.

$$c = c' + (u_a - u_w) \tan(\phi^b), \quad \text{(Eq. 6-2)}$$

Assuming the suction is constant during loading, the vertical component of resistance (q_{uv}) can be derived, similar to Briaud's approach, by considering only the soil beneath the footing with surrounding soil removed. The unconfined loading of this soil is simulated by drained triaxial compression loading from zero initial net-normal stress. The major principal stress at failure is equal to the vertical component of ultimate bearing capacity (q_{uv}), which for unconfined loading is equal to the deviator stress at failure since the minor principal stress is equal to zero ($q_{uv}=q_f=(\sigma_v-\sigma_h)/2$). The Mohr-Coulomb failure envelope and stress path for drained triaxial compression of an unsaturated soil are shown in Figure 6.8 in the p-q-r space; where: $p = (\sigma_v+\sigma_h+2u_a)/2$, $q = (\sigma_v-\sigma_h)/2$, $r = u_a-u_w$, σ_v = vertical total stress, and σ_h = horizontal total stress. In this analysis, pore air pressure is assumed to be zero ($u_a=0$) and matric suction (u_a-u_w) is constant for drained loading. From the geometry of the problem and analyzing the stresses at failure the equation for the major principal stress at failure equal to the vertical component of ultimate bearing capacity (q_{uv}) is given as,

$$q_{uv} = \frac{2(c' + (u_a - u_w)\, tan(\phi^b)) \cos \phi'}{(1 - \sin(\phi'))}$$

(Eq. 6-3)

To obtain the total horizontal component of ultimate bearing capacity (q_{uh}), the vertical component (q_{uv}, Eq. 6-3) can be subtracted from the total resistance (q_u, Eq. 6-1). The total resistance can now be divided by the horizontal resistance to obtain the theoretical bearing capacity, k, for unsaturated soils. The bearing capacity factor can be determined for different soils and the effects of matric suction can be observed. The bearing capacity factor was determined for three cases: first, friction angle with respect to matric suction was assumed equal to zero ($\phi' = 0$); second high cohesion and low friction angle was considered; third, was high friction angle with low cohesion. Density was assumed equal for all conditions. Matric suction was varied from zero to 1,000 psi and results shown in Figure 6.9 indicate that matric suction has no impact on bearing capacity factor. This seems logical given that Equations 6.1 and 6.3 depend on the shear strength, which includes the contribution from suction, and both are based on the assumption that shear strength is isotropic.

The bearing capacity factor, k, back calculated from model footing bearing capacity and miniature pressuremeter tests was close to 1.5. The closest derived bearing capacity in the previous analysis comes from the undrained condition and is equal to 1.37. While these theoretically derived k values are somewhat reasonable, there are several reasons they may not match the empirically derived k values. Of particular importance is that modeling the vertical component of ultimate bearing capacity using an unconfined compression analogy does not properly model the kinematics or stress paths of soil elements beneath a footing.

In an attempt to capture the actual soil mechanics involved in this problem, another approach to derive the bearing capacity factor k was investigated. The essential

elements of this approach, and differences and similarities to the previous approach are summarized as follows:

1) As with the previous approach, bearing capacity factor, k, is defined as the ratio of the ultimate bearing capacity to PMT limit pressure, $k=q_u/P_L$.
2) Similarly, ultimate bearing capacity, q_u, is calculated using Equation 6-1.
3) Unlike the previous approach, theoretical limit pressure, P_L, is calculated using cylindrical cavity expansion equations for unsaturated soil presented in Section 2.2.6 of this dissertation. The theoretically derived ultimate cavity pressure is assumed to be equal to the PMT limit pressure ($P_u = P_L$). While more complicated than the previous approach, this theory better models the actual kinematics and evolution of stresses and strains during a PMT.
4) Unlike the previous approach, an attempt was made to capture the non-linear behavior of the limit pressure versus matric suction and bearing capacity versus matric suction relationships observed in the experimental data (Figure 6.5). This was accomplished by incorporating a non-linear model for the variation in shear strength as it relates to matric suction. The model used incorporates the influence of effective degree of saturation on the contribution of suction to the effective stress state of the soil (Alonso et al. 2009). The non-linear shear strength is embodied in the cohesion, c, which is used in equations describing the ultimate bearing capacity of footings and those describing the ultimate cylindrical cavity pressure.

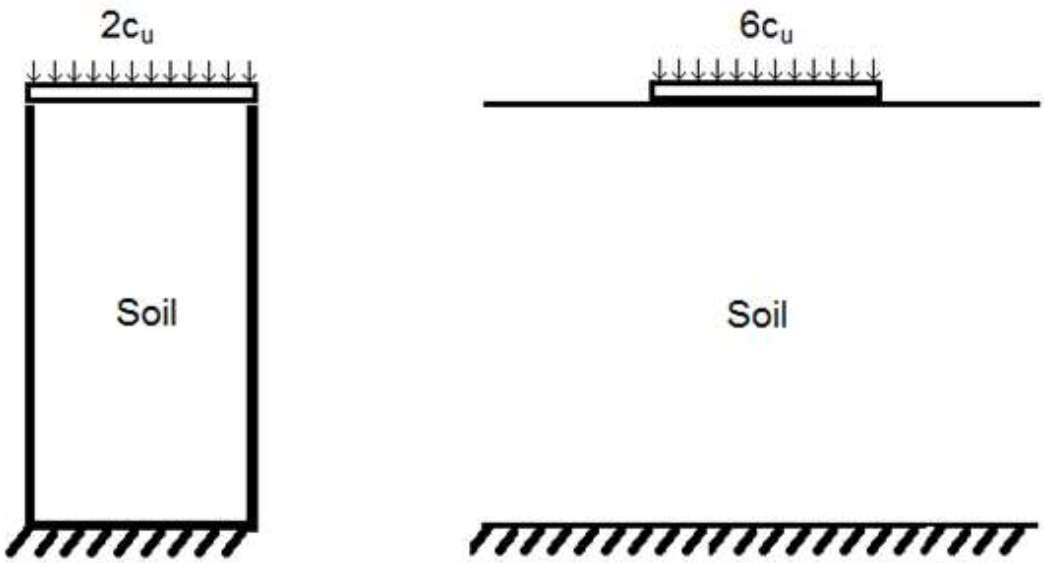

Bearing Capacity of Plate = $6c_u$

Bearing Capacity Due to Vertical Resistance only = $2c_u$

Bearing Capacity Due to Lateral Resistance only = $4c_u$

Where c_u = Undrained Shear Strength

$$q = k P_{Le}$$

$$6c_u = k 4c_u \longrightarrow k = 1.5$$

Figure 6.7: Bearing capacity factor relating horizontal loading to total resistance (after Briaud 1992)

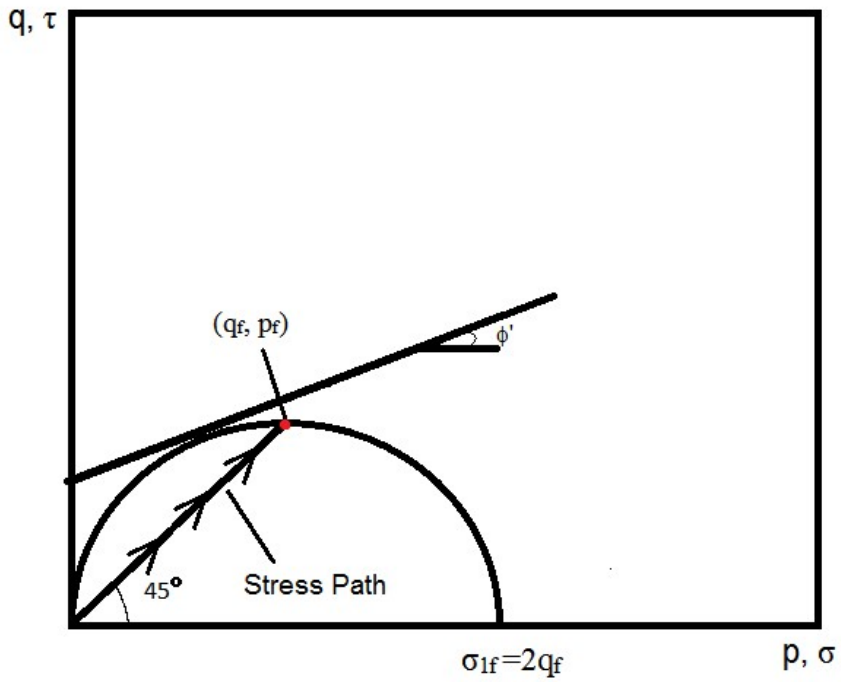

Figure 6.8: Mohr-Coulomb failure envelope and stress path for unconfined compression

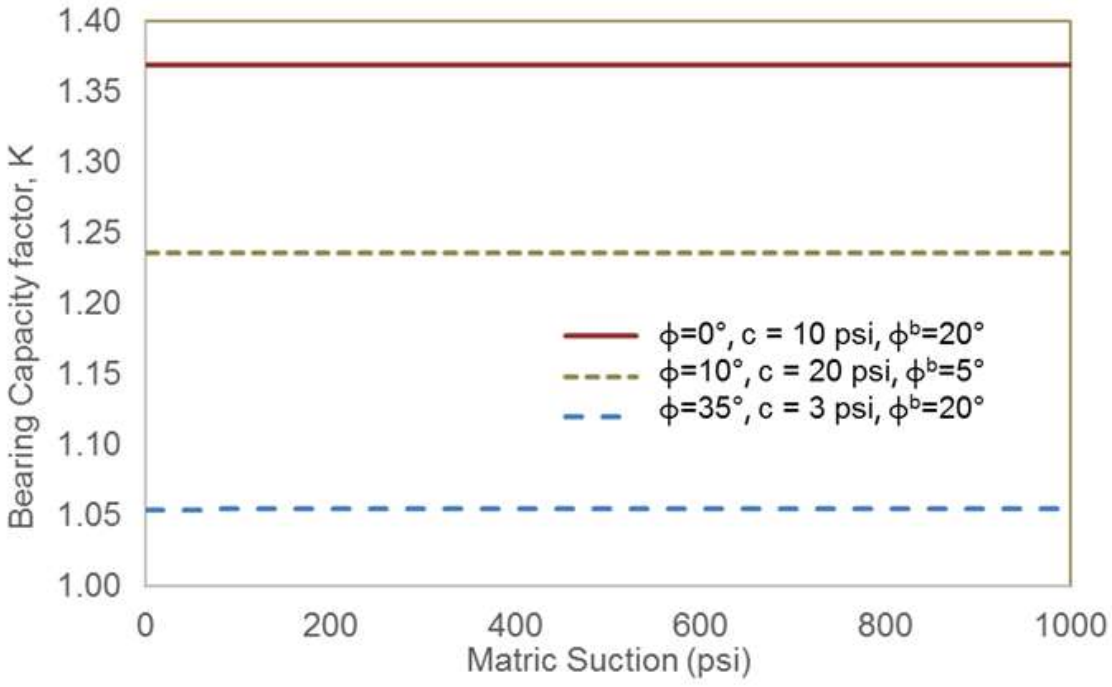

Figure 6.9: The effect of varied matric suction on bearing capacity

Using the model of Alonso et al. (2009) gives the cohesive contribution to strength as,

$$c = c' + S^{\alpha}(u_a - u_w)\sin(\phi') \quad \text{(Eq. 6-4)}$$

Where:

S^{α} = effective degree of saturation,

S = degree of saturation, and

α = material parameter.

The bearing capacity factor, k, for unsaturated soils using cavity expansion was determined as follows:

1. The ultimate bearing capacity determined from model footing test was used to back-calculate parameters needed in the ultimate bearing capacity equation (Eq. 6-1).
2. McClain soil properties including measured friction angle, total density, estimated matric suction, and footing dimensions were used in the back calculation. The cohesion was assumed equal to zero.
3. Terzaghi bearing capacity factors used to calculate ultimate bearing capacity are shown in Table 6.3.
4. The effective cohesion (Eq. 6-4) was used to back-calculate ultimate bearing capacity.
5. The material parameter in equation 6-4 is dependent on soil type. For this analysis, it was adjusted until measured results fit predicted results.
6. Once the ultimate bearing capacity matched the measured value then ultimate cavity pressure was determined.

7. Volumetric strain in the plastic zone was unknown, so it was back calculated based on measured limit pressures prior to model footing tests.
8. The unsaturated bearing capacity factor was then determined by dividing the ultimate bearing capacity factor by the ultimate cavity pressure. It was also determined based on Briaud's (1992) simplified method however; Eq. 6-4 was used as the cohesion parameter.

The result of this analysis is shown in Table 6.4. The pressuremeter bearing capacity determined using Briaud's (1992) simplified analysis is also included in the upper half of Table 6.4. All bearing capacity factors determined through this method are on average 1.06. The bottom half of Table 6.4 shows the parameters used to determine ultimate cavity pressure (P_u) using cylindrical cavity expansion. The unload-reload modulus from the miniature pressuremeter tests was used for modulus. The determination of the pressuremeter bearing capacity factor using cylindrical cavity expansion seems to show closer agreement with the model footing tests than other methods. The average k, determined using cavity expansion is 1.37, which compared to the value Briaud (1992) recommends (0.8) is much more reasonable. One possible explanation for the continued deviation of the measured to predict values may come from the type of failure experienced in model footing tests. In all footing tests performed, punching failure was observed for each test. The ultimate bearing capacity equation may not accurately the ultimate resistance to loading for the footing tests due to the mode of failure.

Table 6.3: Terzaghi bearing capacity factors

N_c	N_q	$K_{p\gamma}$	N_γ
52.6	36.5	76.0	0.0

Table 6.4: Bearing capacity factors determined from model footing tests

S%	α	γ_t (psf)	u_a-u_w (psi)	k (simplified)
0.68	6.55	122.7	30.1	1.07
0.44	3.72	115.2	103.8	1.04
0.54	6.93	115.5	298.2	1.08
0.77	11.47	125.4	72.6	1.05
0.56	7.11	110.6	215.9	1.08
E_r (psi)	P_u (psi)	ε_v		k (cav. Expansion)
663.9	45.2	-0.004447		2.00
28793.4	165.5	-0.000101		1.09
10913.3	117.3	-0.000298		1.28
3309.7	110.5	-0.001381		1.33
3981.6	114.7	-0.001066		1.17

6.6 Prediction of settlement based on PMT

The settlement of a shallow footing can be predicted based on pressuremeter results. Two methods make direct use of the pressuremeter modulus to predict settlement. The first was mentioned in Section 2 and shown as equation 2-20 from Janbu et al. (1956). The settlement prediction equation has two correction factors, μ_0, μ_1, which account for depth of embedment and depth to a rigid stratum, respectively. There is no depth of embedment in this study, so μ_0 is equal to 1.0. The correction factor for depth to a rigid stratum, μ_1, is equal to 0.58, which is based on the footing shape (circular), footing width (4 inches), and depth to the bottom of the test tank (19.25 inches). Poisson's ratio, ν, was assumed equal to 0.333. The bearing pressures in the elastic range can be used to predict settlement and compared to actual settlement to get

an idea of the effectiveness of settlement prediction. Pressuremeter modulus and unload-reload modulus will each be used to make predictions.

The second method to predict settlement based on the pressuremeter results comes from Baguelin et al. (1978). This method splits the settlement into two components. The first is settlement associated with deviatoric loading. The second component is from spherical loading. The settlement equation from Baguelin et al. (1978) includes the deviatoric and spherical components of settlement and is as follows:

$$s = \frac{qB}{9E_p}(2\lambda_d{}^{\alpha} + \alpha\lambda_c) \qquad \text{(Eq. 6-5)}$$

Where,

E_p = pressuremeter modulus within the zone of influence

q = footing net bearing pressure,

B = footing diameter,

α= rheological factor,

λ_d = shape factor for deviatoric term, and

λ_c = shape factor for spherical term.

The parameters α, λ_d, and λ_c can be obtained from Baguelin et al. (1978) and for this research are shown in Table 6.5. The test conducted at 30.1-psi matric suction uses and α equal to 2/3, all others use 1.0. The α parameter is based on the ratio of pressuremeter modulus to limit pressure further values for different soil types and ratio ranges are shown in Baguelin et al. (1978). The settlement was determined using pressuremeter modulus and unload-reload modulus. Baguelin et al. (1978) indicates that use of Equation 6-5 for footings with no depth of embedment will over predict settlements by 20%. Nevertheless, settlements were predicted for the five model footing

tests. The measured versus predicted settlements for the model footing tests using the pressuremeter modulus (similar results are obtained using unload-reload modulus) and the method presented by Baguelin et al. (1978) are shown in Figure 6.10. Perfect agreement between measured and predicted results would show 1:1 agreement. For the lowest suction test, the predicted settlements are about 20% higher than measured settlements, which generally agrees with expectations reported in Baguelin et al. (1978). All other test results were under predicted using this method. The Janbu et al. (1956) method was also used to predict settlement, and the results are shown in Figure 6.11. Similar observations are made for the Janbu (1956) method, with some results over predicted while others are under predicted.

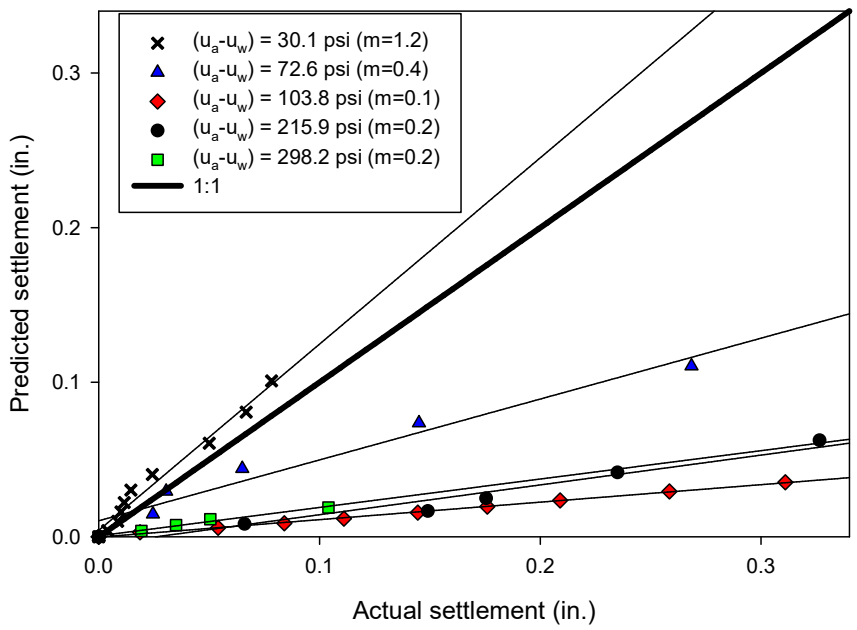

Figure 6.10: Measured versus predicted settlement for model footing tests using Baguelin et al. (1978) method

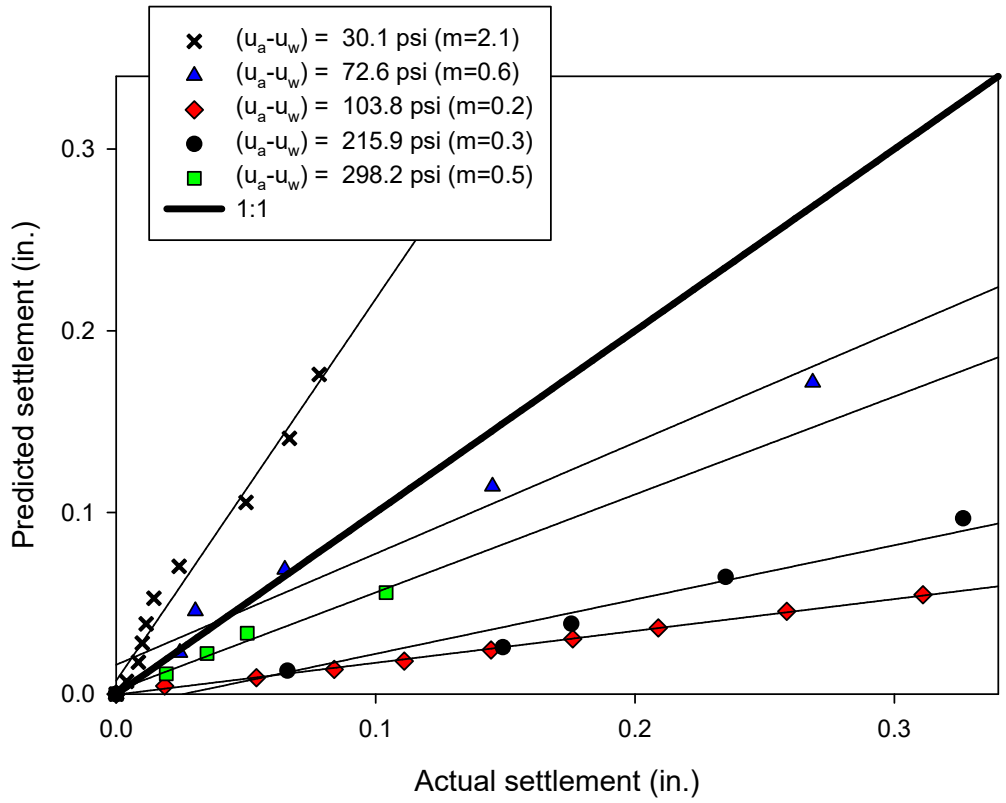

Figure 6.11: Measured versus predicted settlement for model footing tests using Janbu et al. (1956) method

Table 6.5: Parameters needed for settlement determination based on spherical and deviatoric components using Baguelin et al. (1978)

α	λ_c	λ_d
1 (2/3 for 30.1 psi matric suction)	1.0	1.0

The parameters in both the Janbu et al. (1956) equation and the Baguelin et al. (1978) methods leave little room for adjustment. This indicates that the pressuremeter modulus is not adequately representing the stiffness of the soil. The unload-reload modulus is usually more adequate at representing the stiffness, however, based on this analysis there is no improvement. The suction may be playing a role in how the equations predict settlement. The trend for both methods show that at the suction near

saturation is more compared to increased suction. Suction has shown to increase soil stiffness which is likely the reason the equations over predict settlement. A possible solution to this based on this test data is to plot the slope of the measured versus predicted settlement ($S_{p/m}$) curves versus matric suction which is shown in Figure 6.12. For this example, the Janbu et al. (1956) settlement predictions will be used.

A possible solution to address the disparity between predicted and measured settlements is to use an empirical correction factor that is a function of the matric suction. Thus, the Janbu Equation 2-20, for example, would become,

$$s = CF * \mu_0 \mu_1 (1 - \nu^2) q \frac{B}{E_p} \quad \text{(Eq. 6-6)}$$

Where: *CF* = empirical correction factor that depends on suction and the rest of the terms are as defined for Equation 2-20.

The empirical correction factor is obtained by plotting the slope of the measured versus predicted settlement ($S_{p/m}$) curves versus matric suction, as shown in Figure 6.12 for the Janbu et al. (1956) settlement predictions. Then the correction factor is simply, $CF = 1/S_{p/m}$.

The predicted settlements using Equation 6-6 shown in Figure 6.13 are much closer to the measured values, as expected. This method provides a similar result using the Baguelin et al. (1978) settlement prediction method. It is clear that further study of settlement prediction based on pressuremeter modulus is required. The empirical approach used to enhance the traditional settlement equations is limited to the specific soil used in this study. The correction factor is dependent on the relationship between the slopes of the measured versus predicted settlement relationship. For this particular study low matric suction caused an over prediction of settlement, while high suction

caused under prediction. If this behavior holds for other unsaturated soil types, then a similar exponential decay equation can be used to correct settlement data. More tests on different soil types are required to obtain the viability of an empirical correction factor. Other characteristics such as density, void ratio, and differences in soil skeleton between tests is unaccounted for by the correction factor and they may play a significant role in predicting settlement based on pressuremeter modulus.

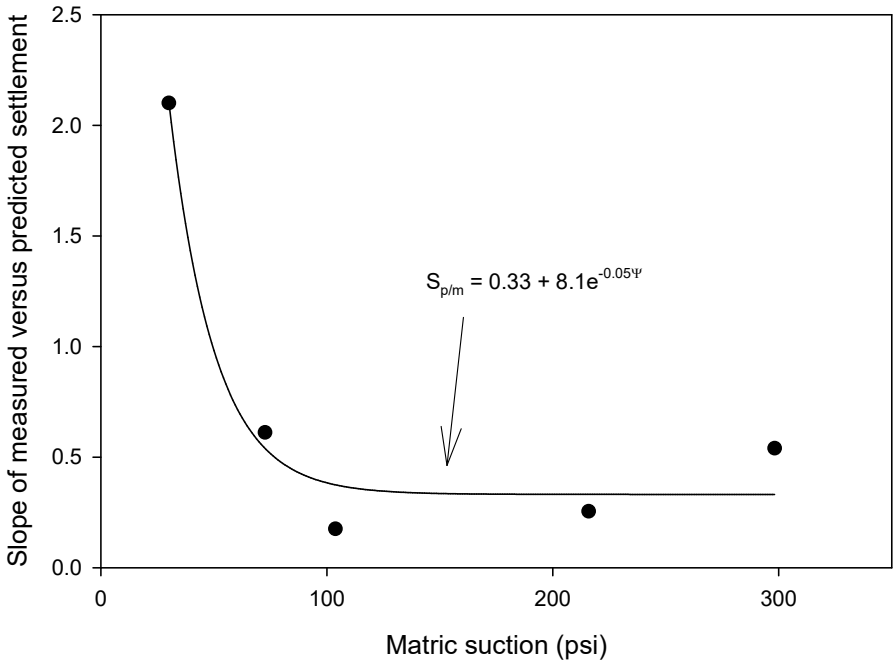

Figure 6.12: Slope of measured versus predicted settlement based on Janbu et al. (1956) versus matric suction

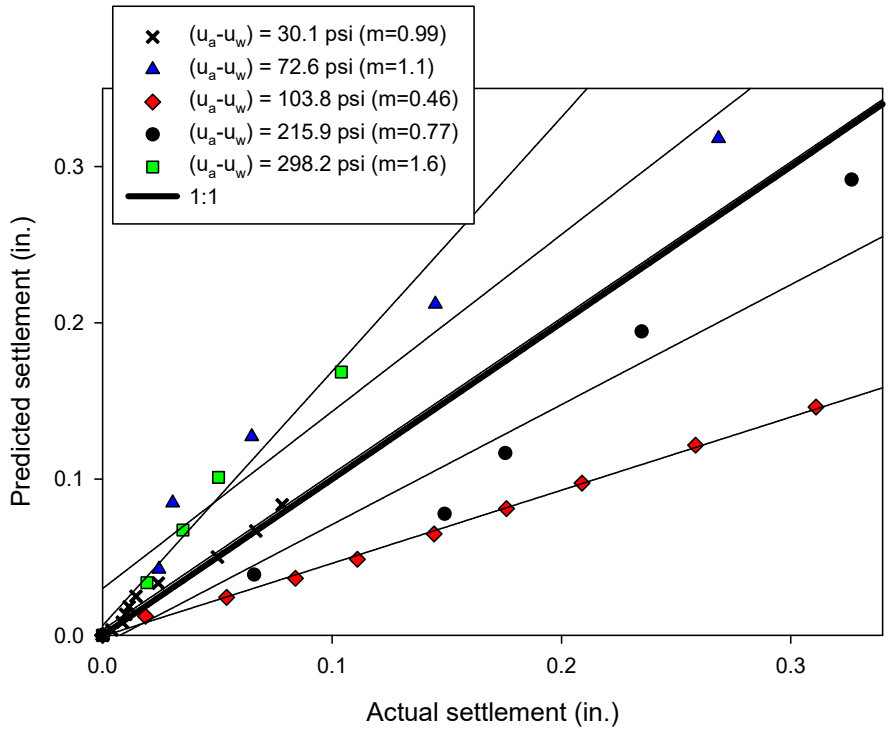

Figure 6.13: Settlements predicted using Janbu et al. (1956) divided by slope of measured versus predicted values

Chapter 7 Prediction methods for in situ tests in unsaturated soil

7.1 Introduction

The in situ testing at Goldsby and North Base has provided a substantial data set of test results at various soil moisture conditions. These data were collected to create and implement a method for interpretation of PMT, CPT, and SPT in fluctuating soil moisture conditions. There have been historical attempts to develop methods to interpret the PMT and CPT (Miller and Muraleetharan 2000, Cudmani and Osinov 2001, Pereira et al. 2003, Lehane et al. 2004, Tan 2005, Russell and Khalili 2006, Russell et al. 2010, Miller 2014) however, there are no standard recommendations for practice. Many of the historical methods have shown promise; some are specialized for particular soil types, while others are overly cumbersome in terms of their application to practice. Included in this dissertation are some of the complex theoretical approaches as well as simple empirical approaches to interpretation. The spherical and cylindrical cavity expansion methods described by Muraleetharan et al. (2000) are applied to create a method of interpretation, while empirical relationships are provided to complement the theoretical application and provide soil specific recommendations.

The three primary goals for the development of the method of interpretation are as follows:

1) The method should allow an engineer to predict how much change will occur in a given in situ test parameter in a given soil type if the suction changes a specified amount from some initial value corresponding to the date of testing. In other words, the question “How much will the limit pressure change if the suction decreases by 20 psi from the date of testing?” for example, can be

answered. The PMT parameters addressed in this dissertation include the limit pressure, pressuremeter modulus, and unload-reload modulus. The CPT parameters included tip resistance. The SPT parameter included the N-value.

2) The second goal for developing interpretation methods was to include as many soil types as possible by utilizing to the extent possible, results from other published studies. Data from in situ testing in unsaturated soil, along with matric suction measurements, are scarce in the literature.
3) Finally, based on model footing tests and miniature pressuremeter testing a method was constructed to predict bearing capacity, and settlement in unsaturated soils using PMT parameters. The goal of the method is to use the existing bearing capacity, and settlement equations described in Briaud (1992) to account for matric suction, and therefore predict changes in settlement and bearing capacity when soils moisture and matric suction changes at a site.

7.2 Empirical approach for predicting the influence of matric suction on PMT parameters

The results of pressuremeter testing at North Base and Goldsby has revealed that there is strong and undeniable relationship between pressuremeter parameters and matric suction. These relationships could be used to provide users a guide to predict changes in pressuremeter parameters with a change in matric suction. As mentioned in Section 5.3 there are two distinct soil layers at North Base. The Goldsby soil profile does not show significant variation. Therefore, for interpretation purposes the upper layer at North Base was separated from the lower layer. This allows for interpretation of three distinct soil types. The upper layer at North Base has an average plasticity index

(PI) of 30, which classifies as CH. The lower layer has an average PI of 20, which classifies it as CL. Goldsby on average has a plasticity index of 10, which also classifies it as CL. The different soil types are categorized as three zones: North Base upper layer (Zone 1), North Base lower layer (Zone 2), and finally Goldsby (Zone 3).

Limit pressure was normalized for the three soil zones and plotted versus suction. The results are presented in Figure 7.1. For all three-soil zones, there is strong correlation between the normalized limit pressure and suction. The data for each soil type was fitted with a linear function because it provides the best fit. Linear functions are not completely representative of actual soil conditions because they show increase in limit pressure with increasing matric suction without bound. It is more likely that the limit pressure will reach an uppermost value then stabilize. The coefficient of determination for the soil from North Base (Zone 1 & Zone 2) is greater than for the Goldsby (Zone 3) data. There are several explanations for the decrease in correlation in the Zone 3 data. The Zone 3 data accounts for all soil depths, whereas Zone 1 only accounts for data collected at three-feet, while Zone 2 contains data from five and seven-feet. Pressuremeter tests from field data shown in Chapter 5 showed a decrease in correlation between limit pressure and matric suction below the active zone. This was likely due to lack of fluctuation in soil moisture, which means that the variation in data below the active layer is likely the result of numerous factors including matric suction, site variability, borehole disturbance, etc.

The curves presented in Figure 7.1 can be used to make predictions of limit pressure as long as the soil type is similar. The soil water characteristic curve for the soil should be available otherwise it is difficult to know how a change in water content

corresponds to a change in matric suction. It is assumed that PMT performed in similar soils will behave in a similar manner. To best illustrate the impact in a decrease in matric suction consider the following example. A PMT is conducted in a low plasticity clay (PI≈20) in relatively dry conditions and it is desired to find how much the limit pressure will decrease if there is a prolonged wetting period. The initial PMT is conducted at a matric suction of 120 psi at a depth of seven-feet. The measured limit pressure on this date is 310 psi. If the matric suction drops to 25 psi then the change in limit pressure can be determined using the equation shown for Zone 2 in Figure 7.1. First, the initial pressuremeter reading should be normalized based on the sites overburden at the depth of the test. For this example, assume the soil has a total unit weight of 105 pcf. This will give a normalized limit pressure value of 60.7. Now, the equation shown in Figure 7.2 ($P_L/\sigma_v = 13.3 + 0.37\Psi$) for Zone 2 can be utilized to determine the new limit pressure, which is 115.1 psi, at the desired matric suction, 25 psi.

Other parameters can be determined in similar fashion. Figure 7.2 presents the normalized pressuremeter modulus versus suction for the three soil zones. The degree of correlation between normalized modulus and suction is much weaker compared to limit pressure, especially for Zone 3. The unload-reload moduli for the three soil zones are presented in Figure 7.3. There is a better degree of correlation for Zones 1&2 compared to the pressuremeter modulus; however, for Zone 3 there is very little correlation. The limited correlation for Zone 3 may suggest that the modulus of elasticity in low plasticity clays minimally affected by fluctuations in soil moisture and suction for the range of values observed. Thus, a user of these empirical relationships

may assume that the modulus will fluctuate minimally and use their measured value for all calculations. In this case, it would be more conservative to use the pressuremeter modulus and not the unload-reload modulus.

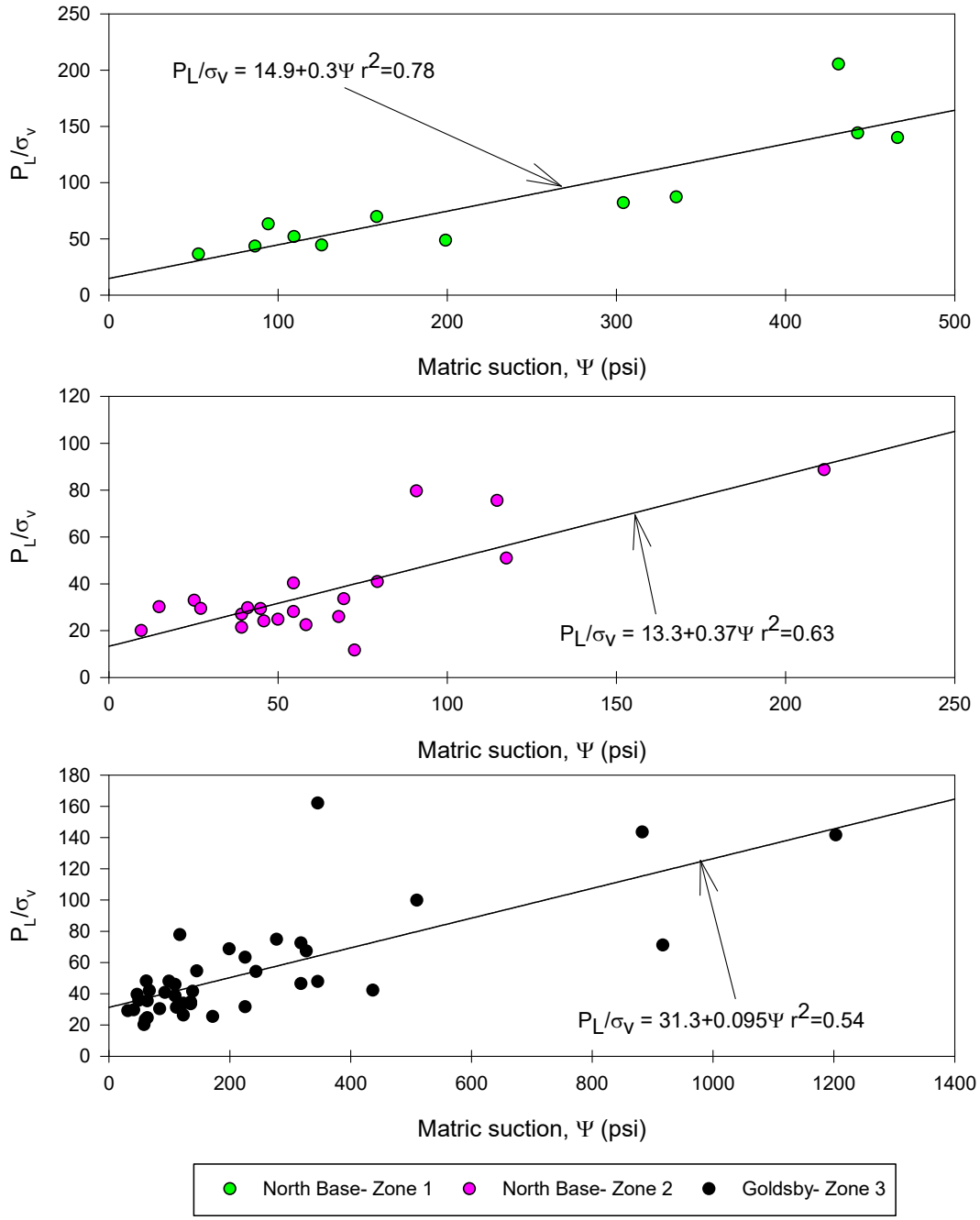

Figure 7.1: Normalized limit pressure versus suction for three soil types

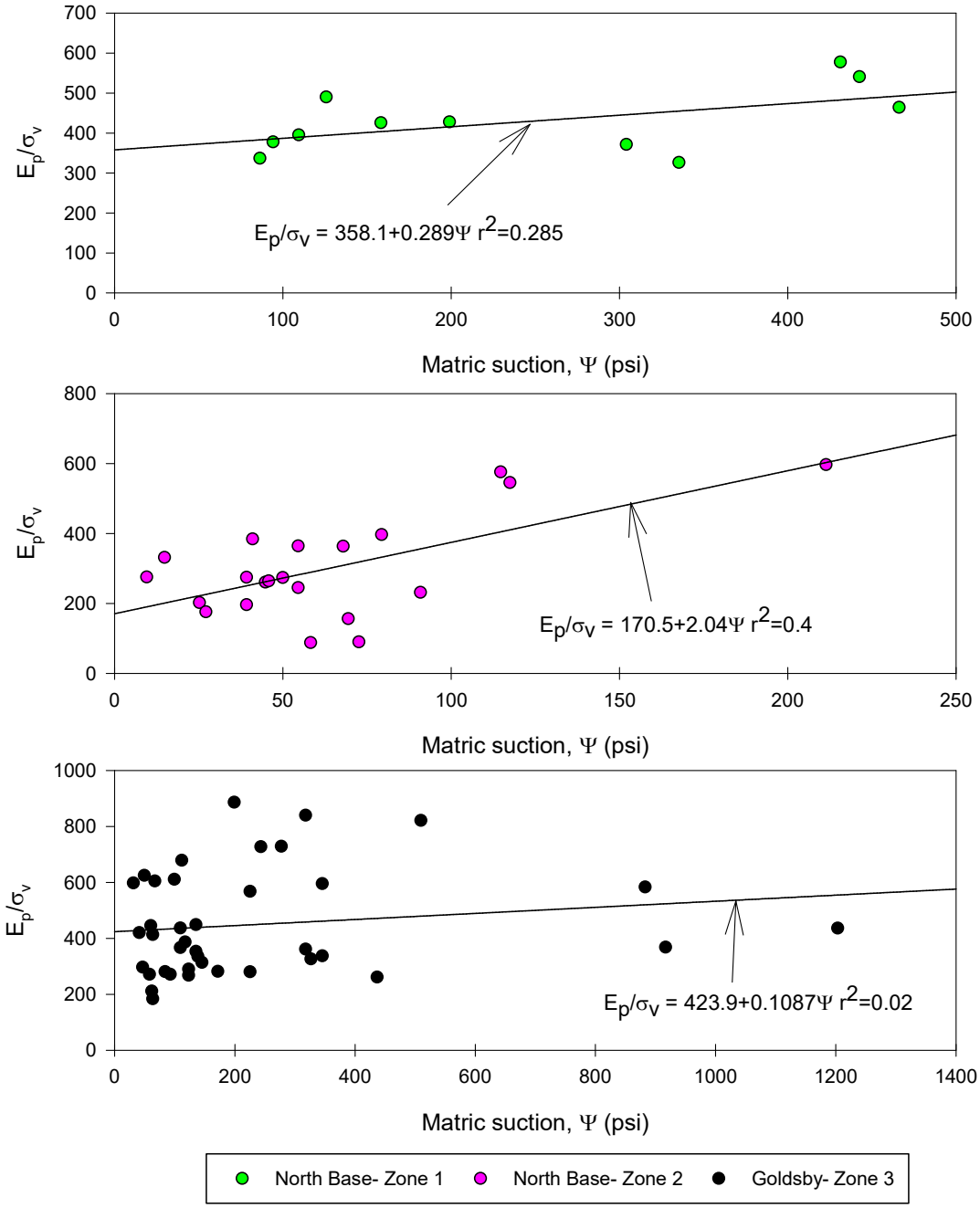

Figure 7.2: Normalized PMT modulus versus matric suction for three soil types

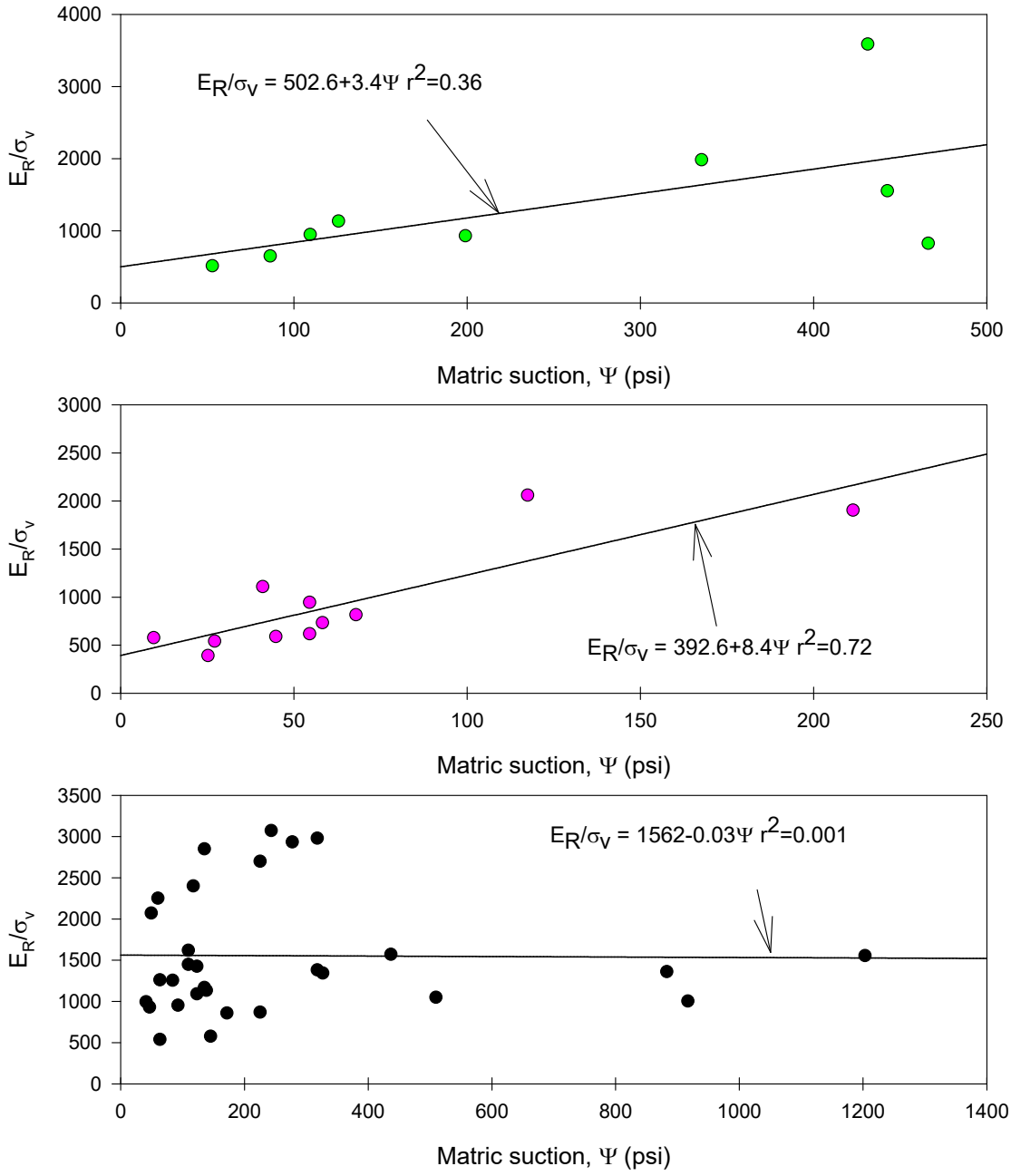

Figure 7.3: Normalized unload-reload modulus versus normalized suction for three soil types

The existing data regarding the effects of matric suction on pressuremeter parameters presented in Figures 7.1-7.3 are extremely limited. The only other data that relates matric suction to pressuremeter parameters comes from Tan (2005). There are

problems comparing the normalized field data presented in the previous figures because the tests performed in Tan (2005) were conducted in a calibration chamber at higher net normal stress than the comparative field stress. This causes some inconsistency when normalizing the PMT parameters. The measured limit pressure and matric suctions from Zones 1-3 and Tan's limit pressure data are plotted in Figure 7.4. The results show a clear separation in the range of limit pressure data depending on soil type. The pressuremeter modulus and unload-reload modulus for all test data is presented in Figure 7.5 &7.6. These figures show no correlation between matric suction and modulus.

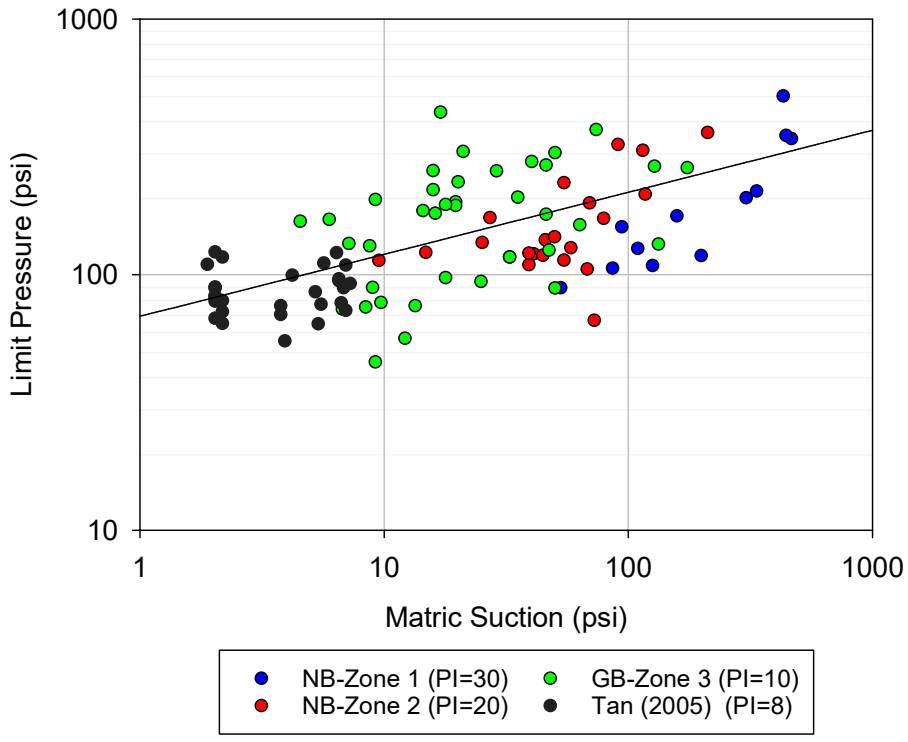

Figure 7.4: Limit pressure versus matric suction from field test and Tan (2005) calibration chamber data

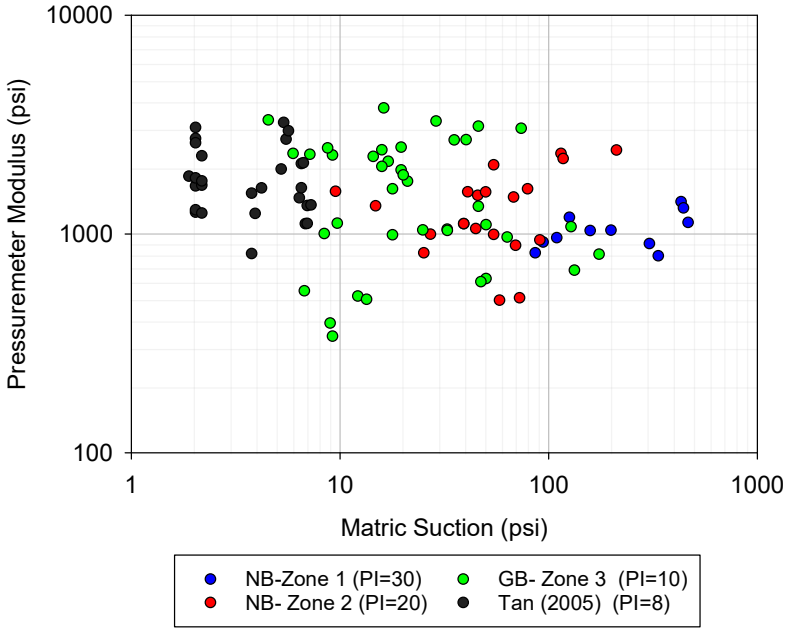

Figure 7.5: Pressuremeter modulus versus matric suction from field test and Tan (2005) calibration chamber data

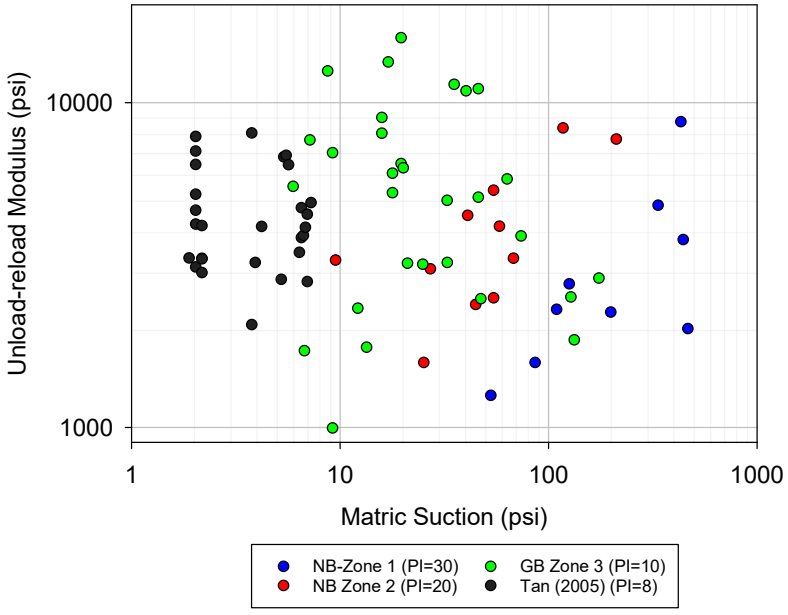

Figure 7.6: Unload-reload modulus versus matric suction from field test and Tan (2005) calibration chamber data

7.3 Application of unsaturated cylindrical cavity expansion theory to pressuremeter test results

The cylindrical cavity expansion equations (Eq. 2-2 – Eq. 2-8) for unsaturated soils were applied to the results of field tests at Goldsby and North Base. If several assumptions about the equations are made, the only missing parameter needed to solve the equation is the volumetric strain in the plastic zone. The assumptions made are as follows:

1. The soil beyond the plastic zone behaves as a linear elastic solid and soil within the zone behaves as a compressible plastic solid. This allows for the relationship shown in Equation 2-1, which relates the radius of the plastic zone to the radius of the cavity. This is described in more detail in Tan (2005).

$$\frac{R_p}{R_u} = \sqrt{I'_{rr}} \qquad \text{(Eq. 2-1)}$$

2. Young's Modulus, was taken as the pressuremeter modulus, E_P,
3. Ultimate cavity pressure, p_u, was assumed to be equal to limit pressure, P_L,
4. Poisson's ratio, ν, is known and is equal to 0.333,
5. Gravimetric water content, *w,* and matric suction do not change during expansion, and
6. Pore air pressure, u_a, remains at atmospheric pressure (u_a=zero kPa gage pressure) during cavity expansion.

Based on the assumptions volumetric strain was calculated using the results of field data. Shear strength parameters including cohesion, and friction angle were obtained from triaxial data (Table 5.4). The friction angle with respect to matric suction,

ϕ^b, was assumed equal to 20° for all calculation. The mean net normal stress, p, was based on the overburden at the depth of the test.

Volumetric strain in the plastic zone versus matric suction plots were prepared for each soil zone. The equations for normalized limit pressure, and pressuremeter modulus shown in Figures 7.1 & 7.2 were used to create the generalized curves shown in Figures 7.7-7.9. The parameters such as mean net normal stress, friction angle, cohesion etc. used to calculate the curves are presented as average of each soil zone. This means that for Zone 1 (shown in Figure 7.7), which consists entirely of data from North Base at one foot, the net normal stress, friction angle and cohesion all come from this depth. However, for the Zone 3 data (shown in Figure 7.9), which is made up of all test data from Goldsby, an average friction angle, cohesion, and net normal stress were used to determine the curve shown. A similar procedure was used to determine the Zone 2 curve shown in Figure 7.8. The average parameters used to determine the volumetric strain in the plastic zone curves are included in the Figures. The volumetric strain figures all show significant scatter from measured test results in comparison to the average curves for each soil zone. The parameters used to calculate the general curve for each soil zone is presented within the figures.

The volumetric strain figures all show significant scatter from measured test results in comparison to the average curves for each soil zone. There are several possible explanations for this behavior. The field site is assumed homogenous and the same at each test location, however this cannot be predicted exactly, so small changes in the variability of the site may be having a large impact on the test results, which leads to a larger impact on the back calculation of volumetric strain. The assumptions made at

the start to simplify analysis may be contributing to the lack of correlation in the results. For example, one of the key assumptions made to simplify the equations is that matric suction does not change during pressuremeter expansion. While this is a reasonable assumption and has been shown to be near correct in a numerical approximation by Muraleetharan et al. (2003), there may be some change in matric suction that is unaccounted for in the analysis.

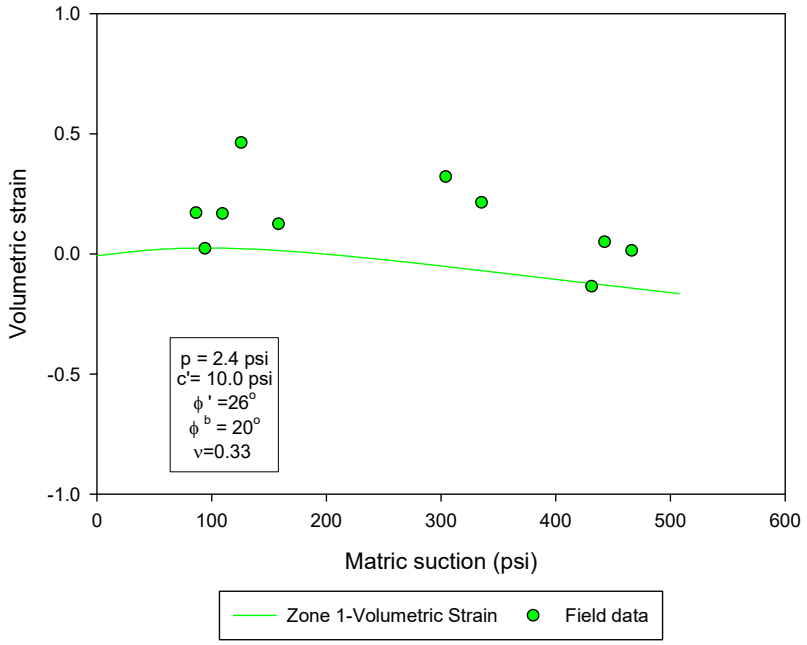

Figure 7.7: Back calculated volumetric strain from field test and general behavior for Zone 1

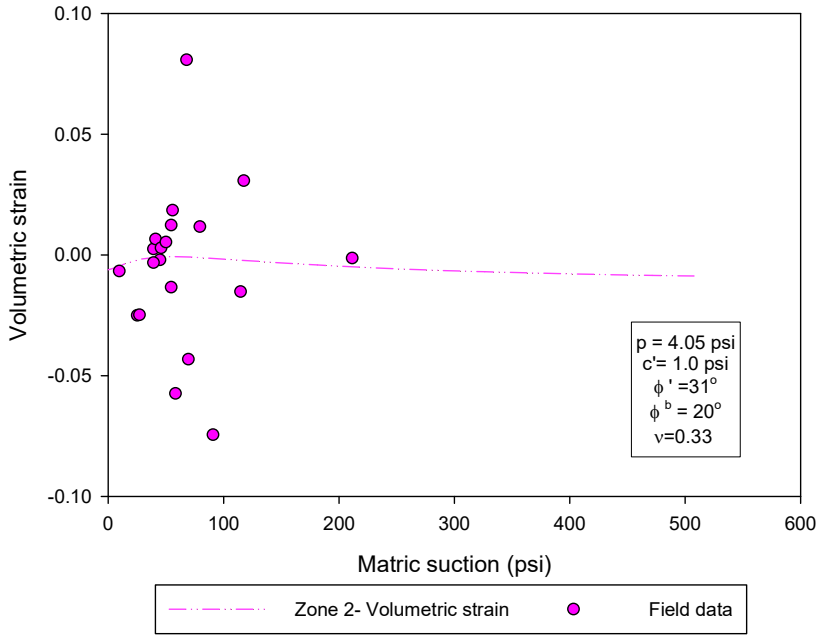

Figure 7.8: Back calculated volumetric strain from field test and general behavior for Zone 2

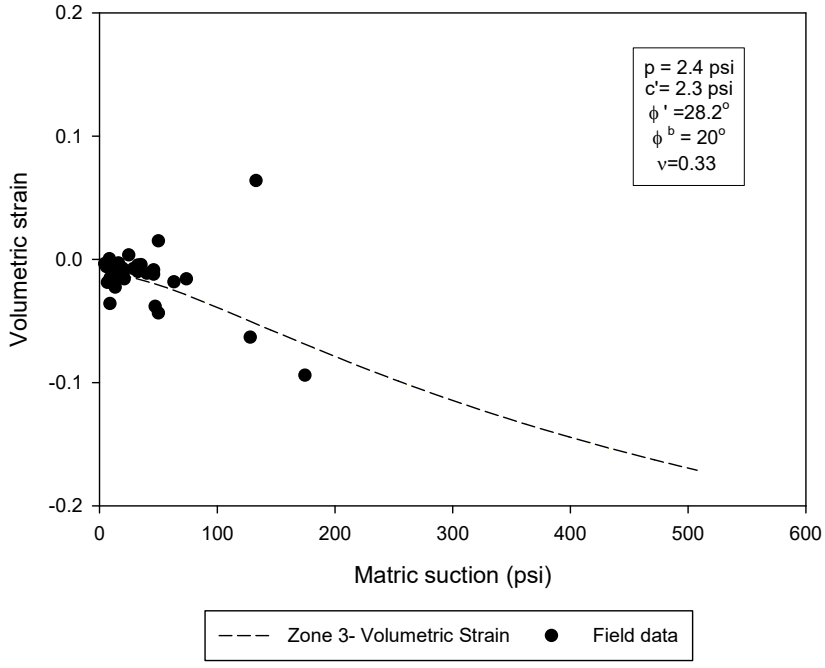

Figure 7.9: Back calculated volumetric strain from field test and general behavior for Zone 3

The volumetric strain in the plastic zone curves (Figures 7.10-7.12) can be used to make predictions about how a change in matric suction will change limit pressure. Based on the change in volumetric strain a new limit pressure can be determined. For example, the volumetric strain in the plastic zone can be back calculated from any pressuremeter test as long as some basic soil data is known. Based on this back calculated volumetric strain and soil type, the user can compare their volumetric strain to the average volumetric strain curve. Now, if the user wants to determine the effect of a change in matric suction on limit pressure they can find the change in volumetric strain for the corresponding change in matric suction and then calculate a new limit pressure based on the new volumetric strain.

Matric suction can be normalized to account for variations from soil type, however there are no published studies regarding the normalization of matric suction. Therefore, a new method to normalize matric suction is proposed such that soils of various matric suction ranges can be compared. An example of how to normalize matric suction using the suggested method is presented below. Consider the SWCC for Goldsby shown in Figure 7.10. The linear portion of the SWCC is overlain with a red line. The range of matric suction through this linear portion is indicated by two arrows separated by 54 psi. This linear portion can be found on most soil water characteristic curves, which makes it useful for normalization of any soil type. The measured matric suctions can be divided by the linear suction range in order to obtain a normalized matric suction (Ψ_N).

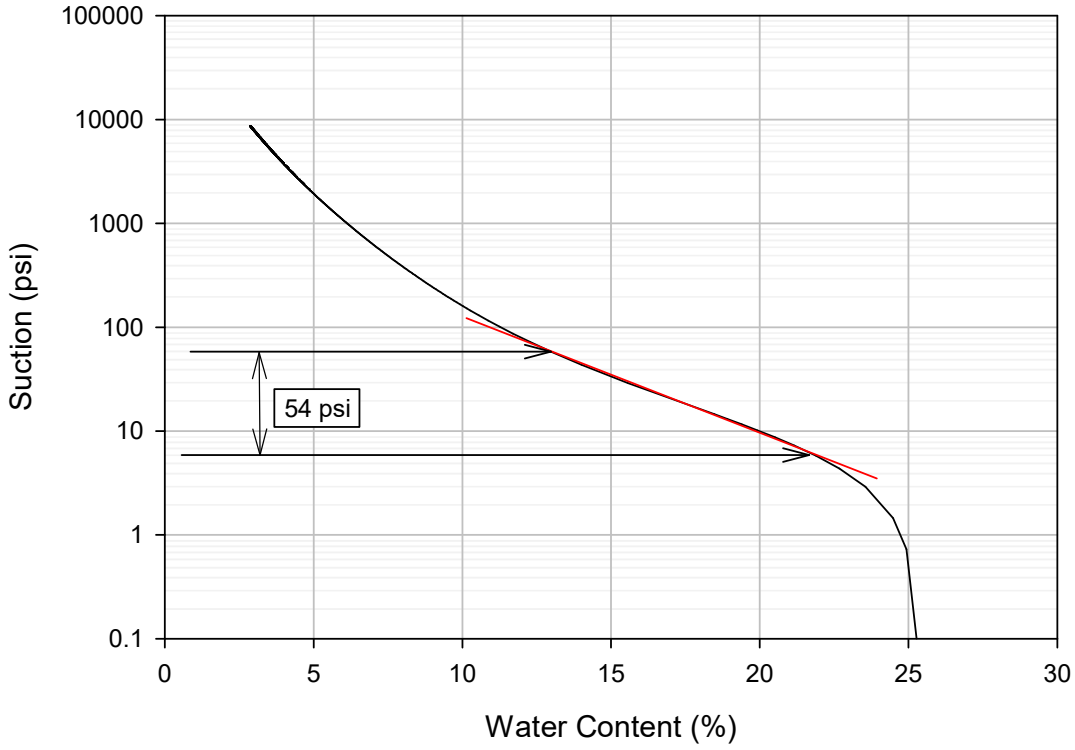

Figure 7.10: Determination of normalized matric suction range

The volumetric strain versus normalized suction for all soil zones is presented in Figure 7.14. This figure is useful in establishing how changes in matric suction will affect volumetric strain and therefore limit pressure. There are clear differences in the behavior of the volumetric strain depending on soil type and matric suction. The traditional geotechnical sign convention is used, which designates positive volumetric strain an indication of compression, and negative an indicator of dilation. The volumetric strain in Zone 1 starts negative and exhibits increasing volumetric compression to about 4%, followed by dilation as normalized suction increases. In Zone 2, the trend is similar but the magnitude of the change volumetric strain is much

smaller. The soil in Zone 3 shows greater dilation as normalized matric suction increases.

An example of how to calculate a change in limit pressure based on the volumetric strain is as follows. Consider the field data and SWCC from Miller and Muraleetharan (2000) shown in Figure 7.15 (a) which is normalized by overburden (5.7 psi). The field data comes from the Goldsby site; however, it was collected 15 years prior to the tests conducted in this study. It was not included in the database of test results used to create the prediction method. There is no other examples of field pressuremeter tests with matric suction measurements, therefore the data presented in Miller and Muraleetharan (2000) is the only "outside" data that can be used for predictions. The soil properties described for the soil are listed in Table 7.2. The prediction scenario involves a situation where only one PMT test is performed at a matric suction of 8 psi, and it is desired to predict the limit pressure of a test conducted at a lower matric suction of 4 psi. The following steps are used to estimate the limit pressure at the lower suction.

1. Determine the volumetric strain at the initial matric suction using the soil properties listed in Table 7.1 and the measured limit pressure and PMT modulus.

$$\varepsilon_{vo} = 7.092 \times 10^{-3} \text{ for } P_L = 436 \text{ psi, at } \Psi = 8.1 \text{ psi}$$

2. The soil tested in Miller and Muraleetharan (2000) most closely resembles the Zone 3 soil. It is assumed that similar soils will behave in a similar manner during pressuremeter expansion and that the volumetric strain matric suction relationship can be used to predict changes in limit pressure for changes in

matric suction. The mean net normal stress for the Zone 3 soil shown in Figure 7.14 is based on an average from all field data points. The curve shown in Figure 7.14 can be determined using the mean net normal stress of the field data to provide a closer approximation of the volumetric strain in the plastic zone as long as it falls within a reasonable proximity to the values found at Goldsby.

3. The suction should be normalized according to Figure 7.15 (b), and used with the curve from Zone 3. This gives an initial normalized suction for the field test data of: Ψ_N = 8.1 psi / 7.3 psi = 1.1. At this normalized suction, the volumetric strain for Zone 3 is $\varepsilon_{v1} = -1.9824 \times 10^{-2}$.
4. The normalized suction of interest is 4 psi, which gives a normalized suction: Ψ_N = 4.1 psi / 7.3 psi = 0.56. At this normalized matric, suction the volumetric strain in the plastic zone for zone 3 is $\varepsilon_{v2} = -1.2896 \times 10^{-2}$.
5. The change in volumetric strain from Zone 3 is $\Delta\varepsilon_v = \varepsilon v2 - \varepsilon_{v1} = -1.2896 \times 10^{-2} - -1.9824 \times 10^{-2} + = 6.928 \times 10^{-3}$.
6. The initial calculated volumetric strain was $\varepsilon_{vo} = 7.092 \times 10^{-3}$, addition of the change in volumetric strain in the plastic strain, $\Delta\varepsilon_v = 6.928 \times 10^{-3}$, gives the volumetric strain for the matric suction of interest:

$$\varepsilon_{vf} = \varepsilon_{vo} + \Delta\varepsilon_v = 7.092 \times 10^{-3} + 6.928 \times 10^{-3} = 1.402 \times 10^{-2}.$$

7. The new volumetric strain ε_{vf} can be used to calculate a new limit pressure, which gives: $P_{L\ predicted}$ = 47.6 psi. It was assumed that the pressuremeter modulus remained the same, which is a reasonable assumption for lean clay based on the Goldsby pressuremeter data. This can be compared to the actual

value from field-testing: $P_{L\ actual} = 49.3$ psi. This gives an overall agreement of 96.5%.

Figure 7.16 provides the referenced data points and the Zone 3 curve used to predict the change in limit pressure for a change in matric suction. The procedure used works well for the available field data. There is a lack of field data with corresponding matric suction measurements so it is not possible at this time to use this prediction method on data from different soil types. The agreement between the measured and predicted results indicates the method that has promise, and should be investigated further.

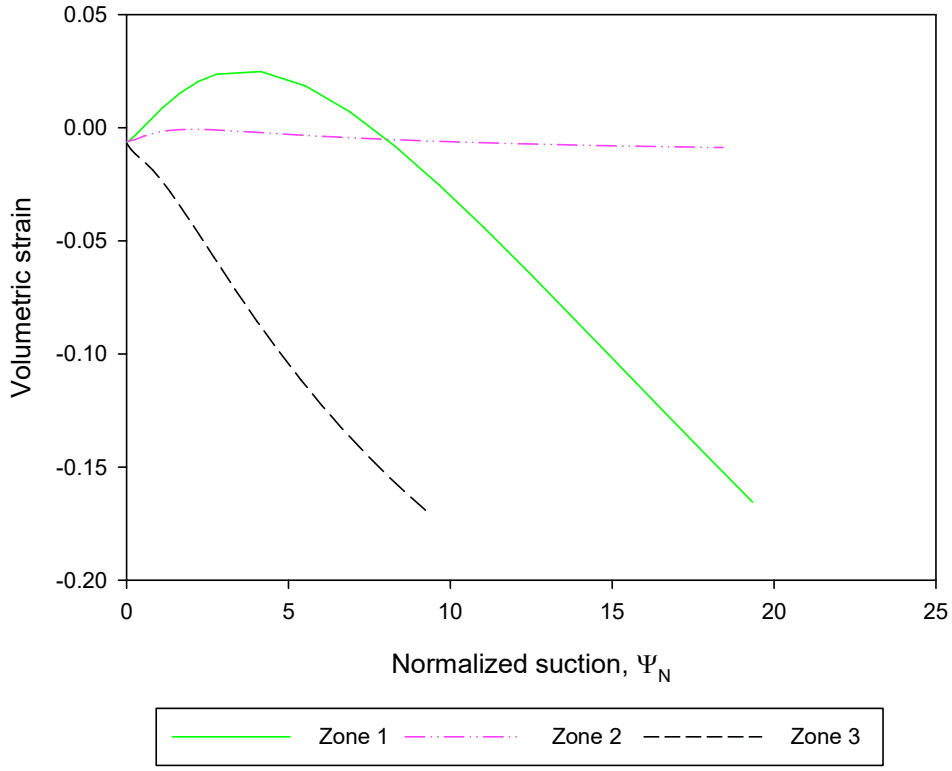

Figure 7.11: Volumetric strain versus normalized suction

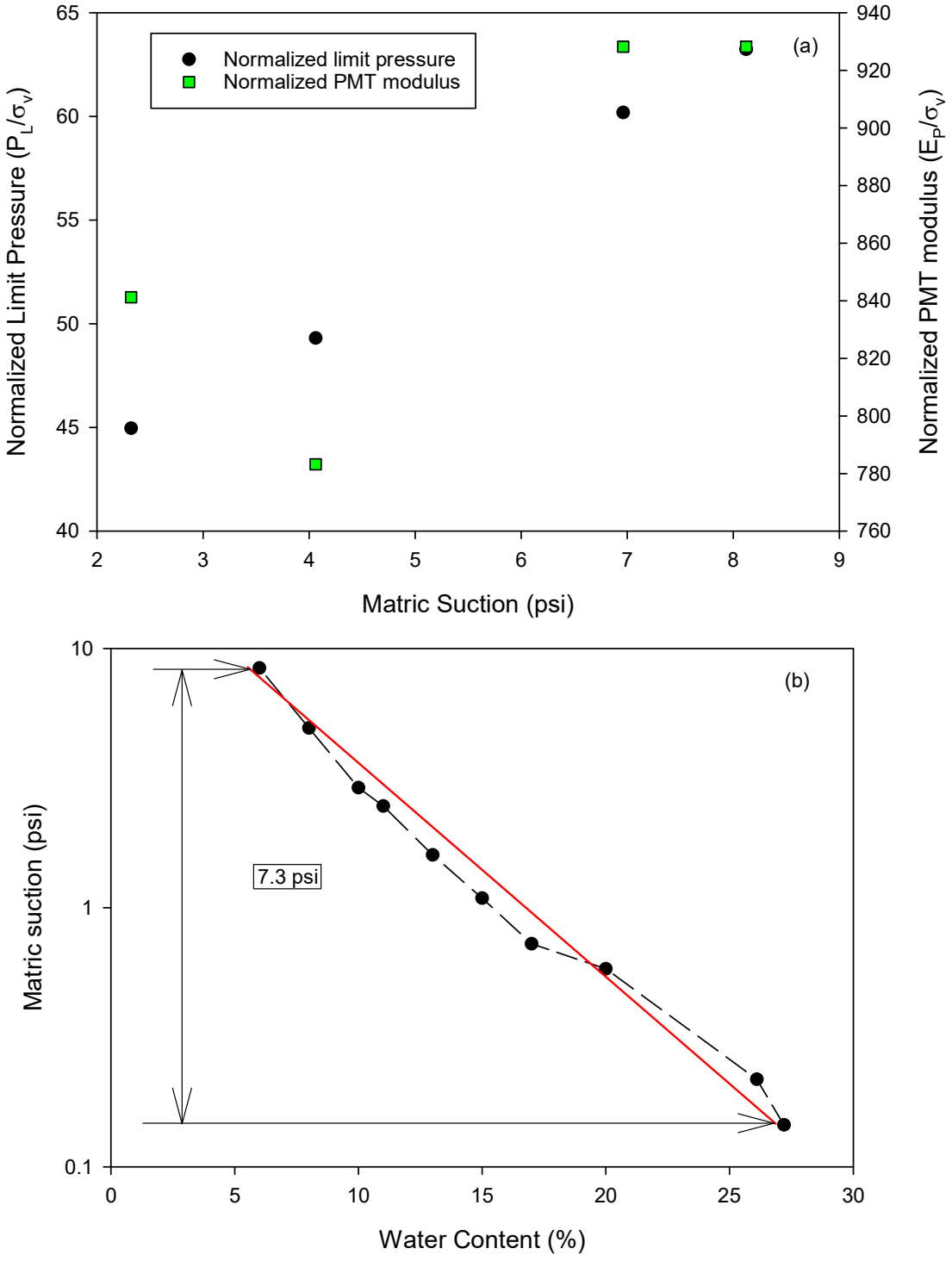

Figure 7.12: Limit pressure and PMT modulus versus suction and SWCC for field data from Miller and Muraleetharan (2000)

Table 7.1: Parameters from field-testing in Miller and Muraleetharan (2000)

ϕ	31°
ϕ^b	27.5°
c' (psi)	0.73
v	0.333
p (psi)	2.9

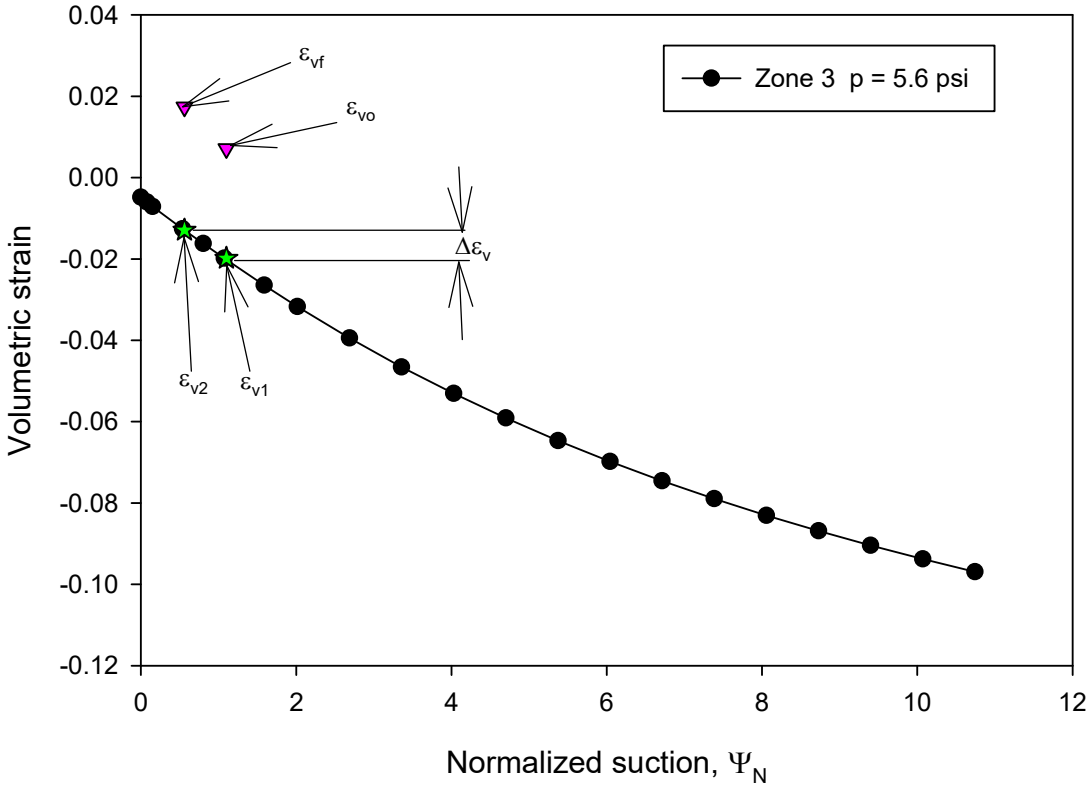

Figure 7.13: Zone 3 volumetric strain versus normalized suction plot used to predict effect of a decrease in matric suction on limit pressure results

7.4 Empirical approach for predicting the influence of matric suction on CPT parameters

The CPT data from field-testing showed positive correlation between tip resistance, and sleeve friction with matric suction. The correlations appeared to be soil type dependent as North Base data exhibited stronger correlations, while correlations

for Goldsby were comparatively weak. In Chapter 5 only a small collection of the average soil data was considered in order to get a general understanding of the effect of matric suction on CPT parameters. In general, these trends showed that increased matric suction results in increased tip resistance. The trends observed in Chapter 5 can be taken a step further by including all CPT Field data where matric suction measurements were made and by including CPT data from the literature. The additional field and historical data provides some clear relationships that can be useful for CPT analysis in unsaturated soil.

The tip resistance was normalized to account for the influence of overburden pressure on the results. This allows for a presentation of all CPT data on a similar scale with differences now coming from soil type and various states of density, which was not considered in the analysis, but likely provides a substantial contribution to observed variations in CPT behavior. Figure 7.7 presents normalized tip resistance versus matric suction for Goldsby, North Base, and data in the literature from Lehane et al. (2004), Tan (2005), and Yang and Russell (2015b). Several unique relationships can be observed from the data. The first is that soil type has a strong influence on the normalized tip resistance. This is similar to cone penetration in traditional saturated conditions, as different soil types will fall into different ranges of behavior. It is seen in Figure 7.7 that normalized tip resistance generally tends to increase with matric suction with the possible exception of nonplastic uniform sand. There is some overlap in the data that comes from variability in the soil profiles at the field sites and similarities between the soils at both sites. The fine grained soils with high PI tend to reach higher values of matric suction, which is why clay soil types tend to shift right on Figure 7.7.

The sandy soil types tend to have higher tip resistance at lower matric suction comparatively to the other soil types. In dense sands, the interparticle contact stress dominates resistance to loading, which is why changes in matric suction only have a minimal effect on the normalized tip resistance. There is significant scatter is normalized tip resistance for the silty sand from calibration chamber testing in Yang and Russell (2015b). The scatter could come from several factors that include sample preparation, and competition between matric suction and density controlling test behavior. There does appear to be an increasing trend for normalized tip resistance with increasing matric suction.

The friction ratio is also useful for CPT analysis for determining soil type. There is limited data, in the literature, regarding, the friction ratio and how it is affected by matric suction. The only published study, other than this dissertation, where friction ratio measurements are presented with subsequent matric suction measurements is Lehane et al. (2004). The results are presented with the results from field-testing in Figure 7.8. There appears to be a strong dependence on soil type and matric suction range on friction ratio. Figure 7.8 shows the friction ratio range increasing with increasing plasticity and matric suction. There are several outliers especially from the North Base and Goldsby field data, however the majority falls in a similar range.

The current methods of soil type identification using CPT database on Roberson and Campanella (1983) has difficulty accounting for unsaturated soil. Table 7.1 shows CPT data from different dates at Goldsby. The fluctuations in soil moisture content causes the soil type predictions to fluctuate for the same material. The normalized tip resistance and friction ratio plots in Figure 7.7 and Figure 7.8 show clear delineations in

soil type as a function of matric suction. These should be used in combination with Robertson and Campanella (1983) to improve soil type predictions using CPT data.

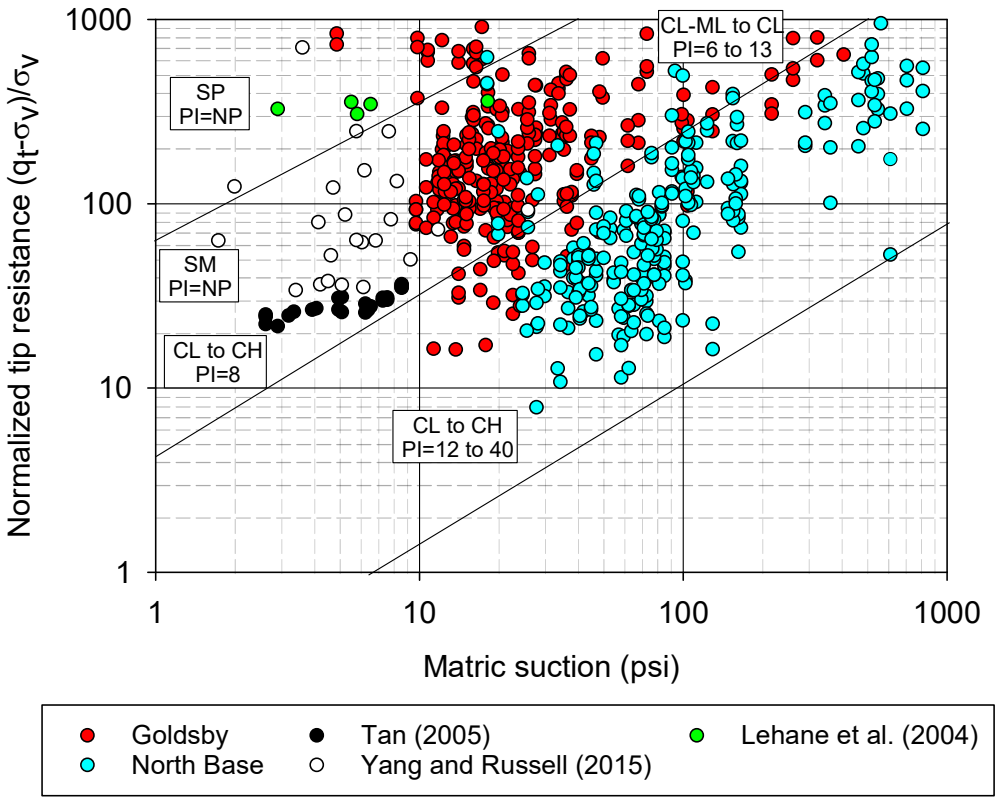

Figure 7.14: Normalized tip resistance versus matric suction for all test data

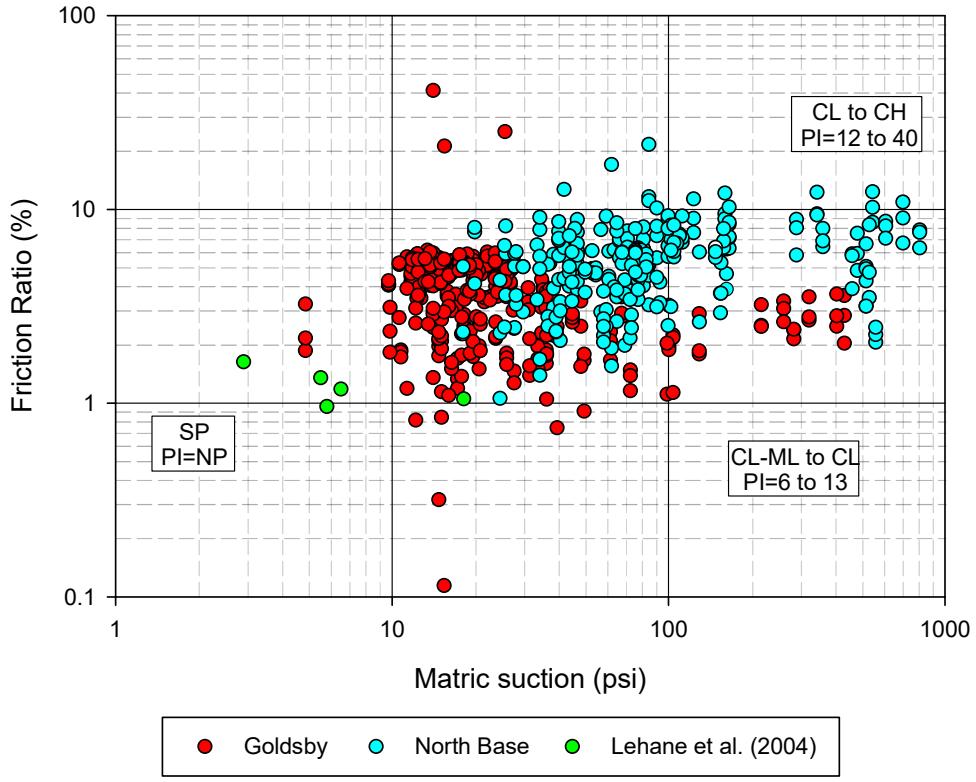

Figure 7.15: Friction ratio versus matric suction for all test data

Table 7.2: Soil type identification at Goldsby using Robertson and Campanella (1983)

Depth (ft.)	Date	w (%)	Tip (tsf)	FR (%)	Soil Type
1.5	2/1/2013	14.9	53	1.6	Silty Sand to Sandy Silt
	5/6/2013	19.1	24.2	1.9	Partially Drained Sandy Silt to Clayey Silt
	7/29/2013	18	14.5	3.8	Silty Clay to Clay
3	2/1/2013	11.2	76.3	1.8	Silty Sand to Sandy Silt
	5/6/2013	18.6	24.2	4.4	Silty Clay to Clay
	7/29/2013	15.7	12.7	5.8	Clay
4.5	2/1/2013	12.4	65.2	1.6	Silty Sand to Sandy Silt
	5/6/2013	13.6	38.1	2.5	Partially Drained Sandy Silt to Clayey Silt
	7/29/2013	15.8	18.5	4.4	Clay

7.5 Application of unsaturated spherical cavity expansion theory to cone penetration test results

Just as cylindrical cavity expansion has shown to be a useful tool in the interpretation of unsaturated pressuremeter testing the spherical version of the equations are useful for CPT interpretation in unsaturated soils. A methodology similar to that applied in the interpretation of PMT in unsaturated soil was applied to CPT. The tip resistance in this analysis is analogous to the ultimate cavity pressure in spherical cavity expansion analysis. The soil zones developed for North Base and Goldsby were also used in this analysis to include a range of soil types. The assumptions used in section 7.4 for cylindrical cavity expansion were also used in spherical cavity expansion. Some main differences are as follows:

1. The elastic modulus in cylindrical cavity expansion was assumed equal to the pressuremeter modulus. In spherical cavity expansion, the elastic modulus was also assumed to equal pressuremeter modulus from similar dates and depths.
2. Parameters including cohesion, c, and friction angle, φ were assumed constant for various layers and depths for ease of analysis and presentation. For example, in volumetric strain curves for each soil zone the data is made of tests from different depths, which would have different mean net normal stress, p, and potentially different soil parameters. These were assumed constant; however, these parameters can be adjusted by the user to account for any specific area of interest in a particular soil profile.

The soil at North base was divided into an upper zone, above 4 feet, of high plasticity (PI = 30) material and classified as Zone 1. The soil below 4 feet at North Base is lower plasticity material than Zone 1 (PI = 20), and is classified as Zone 2. The soil at Goldsby is relatively uniform, and is all low plasticity material (PI = 10), this is classified as Zone 3. Tip resistances collected from each soil zone were normalized by overburden pressure. For each test date three tests were performed. The results of these three tests were averaged for each date and plotted with their corresponding matric suction from the day of the test. The result of this is presented in Figure 7.17. It shows normalized tip resistance versus matric suction. The data shows relatively low r^2 values however, there does appear to be a strong and undeniable positive correlation between increasing matric suction and normalized tip resistance.

Volumetric strain in the plastic zone during spherical cavity expansion was back calculated from CPT results. The soil parameters for each depth and zone were used to make the calculation. A general curve for volumetric strain versus matric suction was constructed using the linear relationship between normalized tip resistance and matric suction. This eliminates a majority of the scatter in the results and provides curves that can be used to make predictions for similar soils. The result of this back calculation and refinement of the volumetric strain curves is presented in Figures 7.18-7.20.

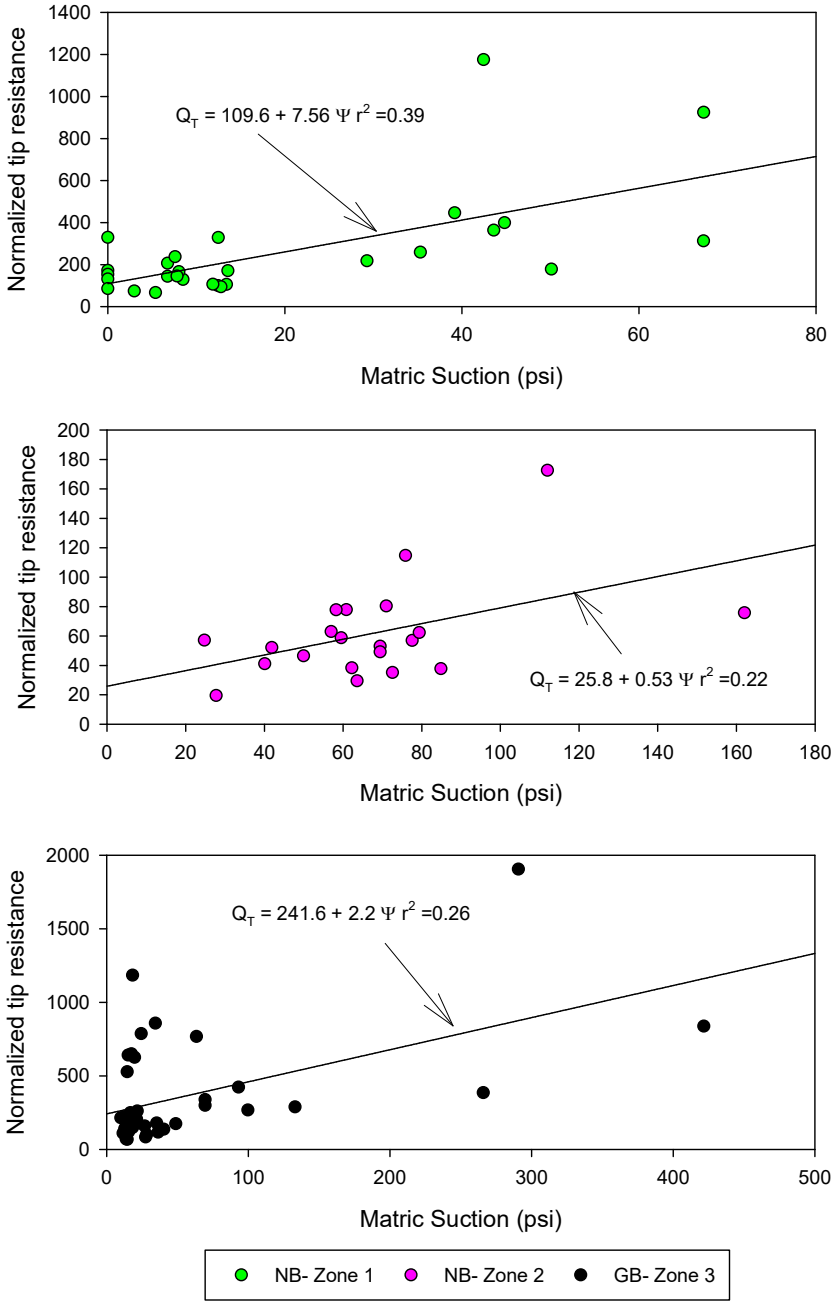

Figure 7.16: Normalized cone penetration parameters versus matric suction used in spherical cavity expansion analysis

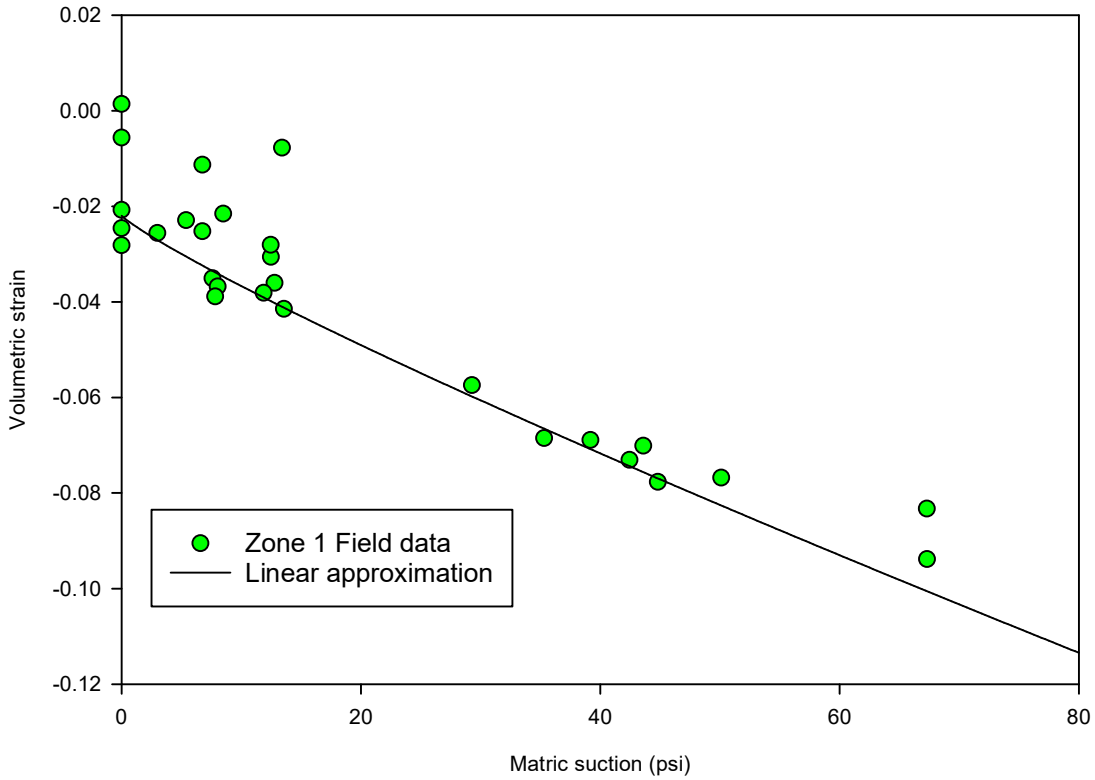

Figure 7.17: Volumetric strain in the plastic zone versus matric suction for Zone 1

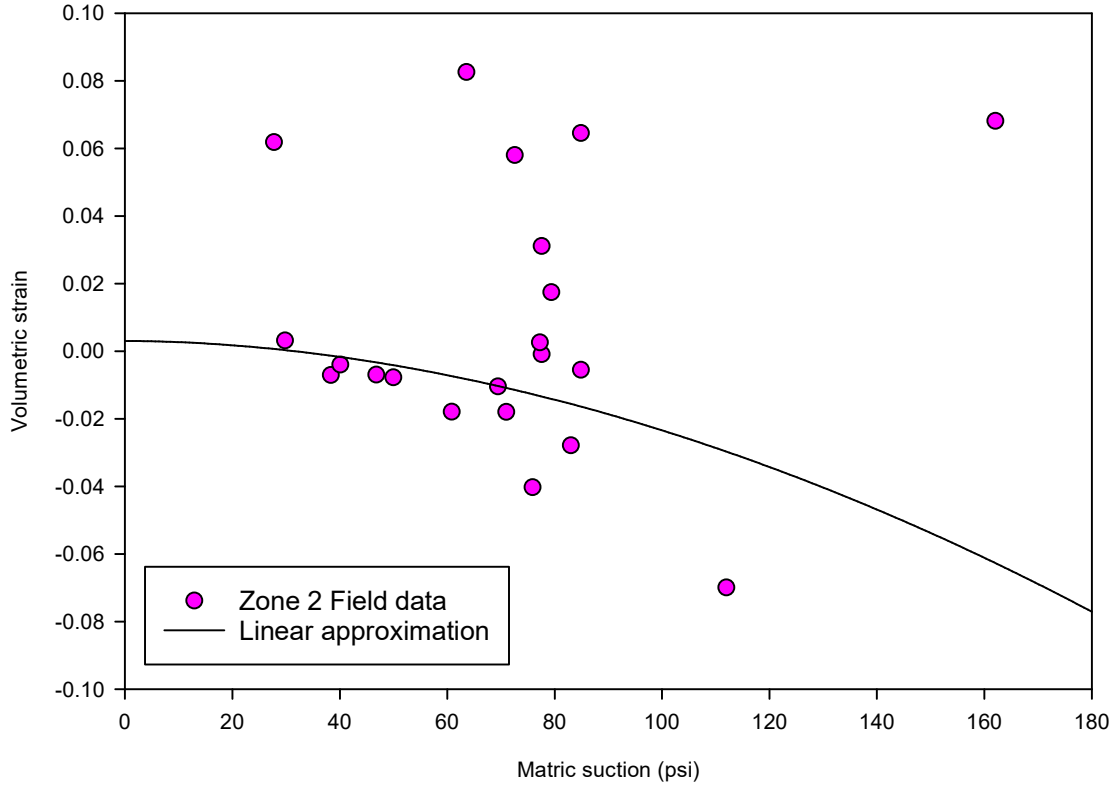

Figure 7.18: Volumetric strain in the plastic zone versus matric suction for Zone 2

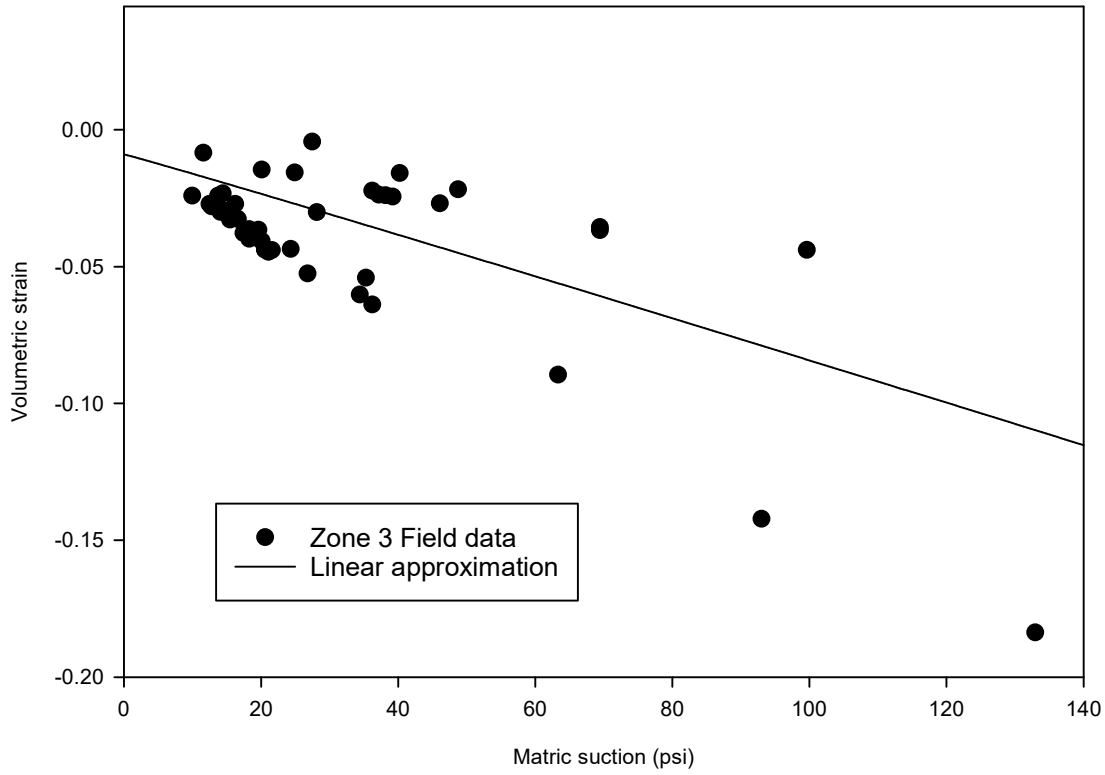

Figure 7.19: Volumetric strain in the plastic zone versus matric suction for Zone 2

The matric suction can be normalized as described in Section 7.4. This allows for comparative analysis of different soil types. The volumetric strain versus normalized suction plots for all three soil zones are presented in Figure 7.21. The method outlined in Section 7.4 for using a known limit pressure to determine how a change in matric suction would affect the results can be followed in a similar manner with the spherical cavity expansion equations. Figure 7.21 Soil from Zone 1 has a high range of matric suction therefore the linear portion of the SWCC stretches for a longer distance, which leads to a smaller range of normalized matric suction values in Figure 7.20. The soil from Zone 2 is lower in plasticity and has a smaller matric suction range than Zone 1, which results in a slightly larger zone of variation in volumetric strain. Soil Zone 3 has

the smallest range of matric suctions and therefore has the largest normalized suction range.

7.6 Empirical approach for predicting the influence of matric suction on SPT parameters

Standard penetration test interpretation in unsaturated soils can be extremely useful due to the widespread use of the test for geotechnical investigations. In Figure 7.9 the N-values, corrected for overburden pressure, obtained at the North Base and Goldsby site are plotted against the matric suction obtained at specific test depths on corresponding test dates. The $N_1(60)$ which is a standardization for the N-value based on the overburden and a hammer efficiency of 60% was used to normalize SPT values. The lower graph in Figure 7.9 shows the uncorrected N-value plotted against suction for comparison.

It can be seen from Figure 7.9 that by accounting for overburden pressure, an obvious trend results in the corrected N-Value versus suction results. While the degree of correlation is not terribly strong, as indicated by r^2, there is a noticeable increase in corrected N-value as suction increases, as expected. The scatter observed is likely due to natural variations in soil type, density, stress history, etc. that was also observed to affect the normalized CPT tip resistance. Figure 7.9 can be used to provide a rough quantitative indication of expected changes in corrected N-values due to suction changes. As with other correlations, care must be used in this application due to the limited number of sites investigated.

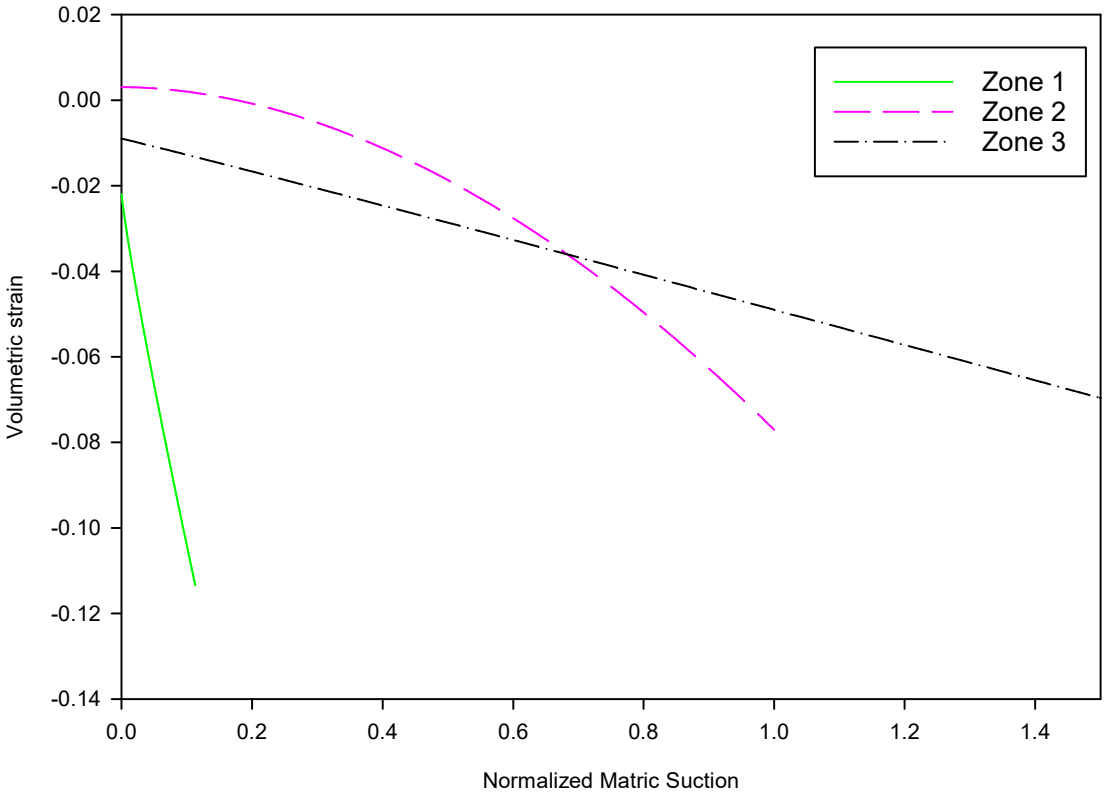

Figure 7.20: Volumetric strain versus normalized matric suction for all soil zones

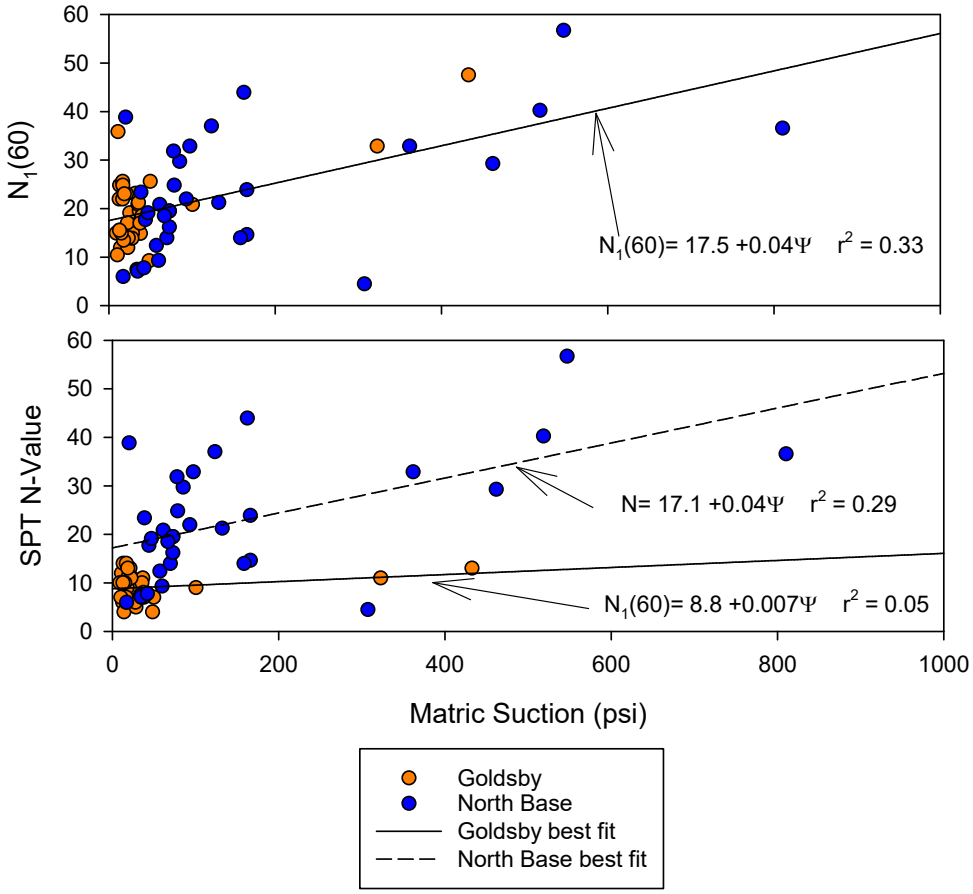

Figure 7.21: SPT N-value and $N_1(60)$ from North Base and Goldsby versus matric suction

Chapter 8 Conclusions and Recommendations

8.1 Major contributions of the research

This study involved monitoring soil moisture content and conducting in situ tests over about a two-year period at two test sites underlain by fine-grained soils. The in situ tests performed included the pressuremeter test (PMT), cone penetration test (CPT), and standard penetration test (SPT). The results of these tests were analyzed to identify relationships between matric suction and in situ test parameters. Unsaturated cavity expansion analysis was used to analyze the results in order to use volumetric strain in the plastic zone to predict how changes in matric suction will affect in situ test results.

The PMT is a useful tool for predicting bearing capacity and settlement of shallow foundations. Model footing and MPMTs tests were also performed on a fine-grained soil at variable degrees of saturation. The current methods of analysis for prediction of bearing capacity and settlement based on pressuremeter analysis are evaluated and suggestions for modifications were made for applications to unsaturated soils.

The following are considered the major contributions of this research:

1. A unique and valuable dataset including the results of PMTs at two fine-grained soil sites, with accompanying measurements of soil moisture content determinations, total suction determinations, and other supporting laboratory test data was developed. Similar datasets were developed for CPTs and SPTs. These rich data sets provide a basis for researchers to develop and validate constitutive,

analytical and numerical models to advance techniques for in situ characterization of unsaturated soils.

2. Empirical relationships between matric suction and pressuremeter parameters including: limit pressure, pressuremeter modulus, and unload-reload modulus were developed for different soil types encountered at the test sites. In addition, relationships including the limited data that could be extracted from the literature, were developed, which expanded the knowledge gained through the current study. While empirical relationships have limitations, especially in light of the limited amount of data available for unsaturated soils, they are important to give engineers some insight into the problem of characterizing sites with variable saturation. For example, through the proposed relationships, an engineer can see how variations in matric suction can produce a change in limit pressure as well as get an idea of the potential magnitude of that change. This is especially important considering that subsurface exploration and in situ testing often takes place during hot dry months and periods of drought, during which soil strengths and stiffness are highest.
3. Empirical relationships between matric suction and CPT parameters including: tip resistance, and sleeve friction, were also developed for different soil types encountered at the test sites. Further empirical relationships between matric suction and standard penetration test N-value and $N_1(60)$ were also developed. As mentioned above, such relationships are non-existent and while they must be used with caution in recognition of their inherent uncertainty, they are incredibly

valuable to provide engineers with some insight into how changes in saturation may influence in situ test results used for geotechnical analysis and design.

4. The use of unsaturated cylindrical cavity expansion theory for prediction of limit pressures under fluctuating soil moisture conditions was further investigated. This involved developing a theoretically based approach to estimating limit pressure as a function of changing suction. This method builds on earlier work by Tan (2005) and, while still considered preliminary due to limited validation, it provides another tool for engineers to address in situ test results in unsaturated soils.
5. In a similar manner to the PMT, a method to apply unsaturated spherical cavity expansion theory for prediction of tip resistance under fluctuating soil moisture conditions was provided, again following on the work of Tan (2005).
6. A unique and incredibly valuable dataset was obtained by conducting model scale footing tests and miniature pressuremeter tests in unsaturated soil prepared to different moisture conditions. The dataset includes load-displacement curves from five footing tests, pressuremeter test curves from all five test beds, water content and total suction data from test beds as well as other supporting laboratory data. Observations from this testing were extremely valuable in providing insight into the use of PMT for shallow foundation analysis in unsaturated soil. As a result, recommendations for the use of the PMT in unsaturated soil were developed in this dissertation. Further, the data will be valuable for use by other researchers working in the field; footing data from

unsaturated soils is incredibly scarce and data with additional in situ tests are virtually non-existent.

8.2 Conclusions based on pressuremeter testing in unsaturated fine-grained soils

1. The total suction measurement is significantly affected by the osmotic suction component using the WP4 device. It was expected that total suction would be nearly equal to matric suction; however, the difference was observed to be large and significant. The matric suction was estimated and results were compared to pressure plate, and total suction measurements. The resulting matric suction estimation based on Zapata et al. (2000) appeared to be an accurate representation.
2. At the two fine-grained soil sites examined in this research, fluctuations in soil moisture conditions caused variation in pressuremeter results. Pressuremeter parameters including: limit pressure (P_L), pressuremeter modulus (E_P), and unload-reload modulus (E_R), all showed sensitivity to changes soil moisture fluctuation.
3. The limit pressure (P_L) at North Base and Goldsby showed positive correlation with matric suction. In general, it was observed that as matric suction increased, limit pressure also increased.
4. The pressuremeter and unload-reload moduli showed positive correlation at North Base with matric suction. At Goldsby, there was little observed correlation between matric suction and moduli. This may indicate that the pressuremeter results in unsaturated fine-grained soils are sensitive to soil type.

However, it was observed that the relationships between suction and moduli at both sites involved considerably more scatter. This is likely because moduli are based on small volume change measurements and therefore more sensitive to borehole disturbance, soil non-uniformities, and test accuracy.

5. The at-rest earth pressure coefficient measured from the pressuremeter at both sites is much higher than what is typically found for similar soils. There does appear to be some correlation between matric suction and at-rest earth pressure and matric suction at both field sites. The observed trend was that as matric suction increased the at-rest earth pressure coefficient increased.

8.3 Conclusions based on cone penetration testing in unsaturated fine-grained soils

1. Soil moisture fluctuation has a direct impact on CPT results at two fine-grained soil field sites. The tip resistance was shown to increase with increasing matric suction at both field sites.
2. The skin friction increased with increasing matric suction at one site, but showed little correlation at the other. The site with strong correlation between matric suction and skin friction had higher plasticity index.
3. The Robertson and Campanella (1983) method for prediction of soil type based on CPT results is impacted by unsaturated soil conditions. CPT data from the same depth with different soil moisture conditions results in different soil type estimation based on Robertson and Campanella (1983). The normalized tip resistance and friction ratio versus matric suction show clear delineation of soil type. This can be used in combination with Robertson and Campanella (1983) to

provide a range of soil types for a particular result with various soil moisture conditions.

8.4 Conclusions based on model footing and miniature pressuremeter testing

1. The degree of saturation of the soil test bed played a direct role in the ultimate bearing capacity of the model footing. Test beds with high degree of saturation showed lower bearing capacities. It was observed that as degree of saturation decreased, ultimate bearing capacity increased.
2. Miniature pressuremeter tests showed increasing limit pressure with increasing matric suction. The pressuremeter modulus and unload-reload modulus showed a small tendency to increase with increasing matric suction; however, there is significant scatter in the data.
3. The prediction method for ultimate bearing capacity based on measured limit pressure described by Briaud (1992) was evaluated. The recommended bearing capacity factor, k=0.8 (Briaud 1992), under predicts ultimate bearing capacity. An adjustment of the bearing capacity factor to k=1.5, provides predictions comparable to measured results.
4. The bearing capacity factor was derived for unsaturated soils based on a simplified analysis from Briaud (1992). Three soil conditions were considered: 1) zero friction angle, 2) high cohesion, low friction angle and 3) low cohesion, high friction angle. The analysis indicates changes in matric suction have no effect on bearing capacity factor because the increase in matric suction is isotropic.

5. Settlement was predicted using the equations from Baguelin et al. (1978) and Janbu et al. (1956). The predictions show that at low matric suction, the equations over predict settlement. At higher matric suction values, the equations under predict settlement. A correction factor was created based on the slope of the measured versus predicted settlement. The settlement equations were divided by the correction factor to provide a closer estimate of measured settlement.

8.5 Conclusions based on application of unsaturated cavity expansion results

1. A method was established to normalize matric suction. This method is based on measuring the linear portion of the soil water characteristic curve. Subsequent matric suction values are divided by this linear portion to provide a normalized matric suction value.
2. The two field sites were divided into three general categories based on similar soil conditions. North Base was divided into two categories based on distinctly different soil conditions between an upper and lower layer. Volumetric strain in the plastic zone was determined based on the relationship between limit pressure and matric suction. It was observed that volumetric strain in the plastic zone decreased with increasing normalized suction.
3. Volumetric strain in the plastic zone for tip resistance decreased with increasing normalized matric suction.
4. A method was created to predict changes in limit pressure for a given pressuremeter result. The method uses volumetric strain in the plastic zone as a function of matric suction. The limit pressure was estimated to be 96% of the measured value based on test data from the same site.

5. A method was created to predict changes in tip resistance for a given cone penetration test result. The method uses volumetric strain in the plastic zone as a function of matric suction.

8.6 Recommendations for future research

1. Pressuremeter, cone penetration, standard penetration testing on other soil types with matric suction measurements to continue to build the database of results. This will also be useful for prediction of tip resistance and limit pressures using the methods described in Chapter 7.
2. Pressure plate testing and tensiometers should be employed for all future testing to ensure accurate measurement of matric suction.
3. Further tests involving the prediction of ultimate bearing capacity of shallow foundations using the pressuremeter should be performed on a variety of soil types.
4. The bearing capacity factor for predicting ultimate bearing capacity on unsaturated soil should be investigated further.
5. The settlement predictions made with pressuremeter parameters should be evaluated on other unsaturated soil types. The trends observed to create the correction factor for settlement prediction should be evaluated on other soil types.
6. The at-rest earth pressure predictions with a pressuremeter should be more thoroughly investigated because test data showed it to be much higher than typical values in the literature.

Bibliography

Alonso, E. E., Pereira, J. M., Vaunat, J., & Olivella, S. (2010). A microstructurally based effective stress for unsaturated soils. Géotechnique, 60(12), 913-925.

Anderson, J. B., Townsend, F. C., and Rahelison, L., (2007), "Load testing and settlement prediction of shallow foundation", Journal of Geotechnical and Geoenvironmental Engineering, 133: 1494-1502.

ASTM D1586-11, Standard Test Method for Standard Penetration Test (SPT) and Split-Barrel Sampling of Soils, ASTM International, West Conshohocken, PA, 2011, www.astm.org

ASTM D2216-10, Standard Test Methods for Laboratory Determination of Water (Moisture) Content of Soil and Rock by Mass, ASTM International, West Conshohocken, PA, 2010, www.astm.org

ASTM D422-63(2007)e2, Standard Test Method for Particle-Size Analysis of Soils (Withdrawn 2016), ASTM International, West Conshohocken, PA, 2007, www.astm.org

ASTM D4318-10e1, Standard Test Methods for Liquid Limit, Plastic Limit, and Plasticity Index of Soils, ASTM International, West Conshohocken, PA, 2010, www.astm.org

ASTM D4318-10e1, Standard Test Methods for Liquid Limit, Plastic Limit, and Plasticity Index of Soils, ASTM International, West Conshohocken, PA, 2010, www.astm.org

ASTM D4719-07, Standard Test Methods for Prebored Pressuremeter Testing in Soils (Withdrawn 2016), ASTM International, West Conshohocken, PA, 2007, www.astm.org

ASTM D4767-11, Standard Test Method for Consolidated Undrained Triaxial Compression Test for Cohesive Soils, ASTM International, West Conshohocken, PA, 2011, www.astm.org

ASTM D5778-12, Standard Test Method for Electronic Friction Cone and Piezocone Penetration Testing of Soils , ASTM International, West Conshohocken, PA, 2012, www.astm.org

ASTM D698-12e2, Standard Test Methods for Laboratory Compaction Characteristics of Soil Using Standard Effort (12 400 ft-lbf/ft3 (600 kN-m/m3)), ASTM International, West Conshohocken, PA, 2012, www.astm.org

ASTM D854-14, Standard Test Methods for Specific Gravity of Soil Solids by Water Pycnometer, ASTM International, West Conshohocken, PA, 2014, www.astm.org

Baguelin, F. (1978). The pressuremeter and foundation engineering. Trans Tech public.

Bishop, A. W. (1959), The principle of effective stress, Teknisk Ukeblad, 106(39), 859–863.

Briaud, J.L. (1992), "The Pressuremeter," A.A. Balkema, Rotterdam, Netherlands.

Brown, J. R., & Warncke, D. (1988). Recommended cation tests and measures of cation exchange capacity. Recommended chemical soil test procedures for the North Central Region. Bull, 499, 15-16.

Cerato, A. B., and Lutenegger, A. J., (2007), "Scale effects of shallow foundation bearing capacity on granular material", Journal of Geotechnical and Geoenvironmental Engineering, 133: 1192-1202.

Cetin et al. (2004) Standard Penetration Test-Based Probabilistic and Deterministic Assessment of Seismic soil Liquefaction Potential, Journal of Geotechnical and Geoenvironmental Engineering.

Consoli, N. C., Prietto, P. D., & Ulbrich, L. A. (1998). Influence of fiber and cement addition on behavior of sandy soil. Journal of Geotechnical and Geoenvironmental Engineering, 124(12), 1211-1214.

Costa, Y., Cintra, J., and Zornberg, J. G., (2003) "Influence of matric suction on the results of plate load tests performed on a a lateritic soil deposit", Geotechnical Testing Journal, Vol. 26, No. 2

Cudmani, R., & Osinov, V. A. (2001). The cavity expansion problem for the interpretation of cone penetration and pressuremeter tests. Canadian Geotechnical Journal, 38(3), 622-638.

De Mello, V.F.B. (1971) The standard penetration test. Proc. 4th Pan American Conf. Soil Mechs. Found. Eng., San Juan Puerto Rico, ASCE, v. 1, pp. 1-86.

Doumet, R., (2015), "Prediction of soil moisture content due to changes in weather conditions", Thesis, University of Oklahoma, 2015.

Elwood, D., Derek Martin, C., Fredlund, D., and Ward Wilson, G. (2015). "Volumetric Changes and Point of Saturation around a Pressuremeter Probe Used in Unsaturated Soils." J. Geotech. Geoenviron. Eng., Volume 141, Issue 11 (November 2015).

Esmaili, D., (2014), “A study on unsaturated soil-geotextile interface strength using multi-scale laboratory tests”, Dissertation, University of Oklahoma, 2014.

Fredlund D.G., Rahardjo H., 1993, Soil Mechanics for Unsaturated Soils, John Wiley & Sons, 1993.

Fredlund D.G., Rahardjo H., and Fredlund, M. D., 2012, Unsaturated Soil Mechanics in Engineering Practice, Wiley-Interscience; 1 edition (July 24, 2012).

Fredlund, D. G., & Xing, A. (1994). Equations for the soil-water characteristic curve. Canadian geotechnical journal, 31(4), 521-532.

Fredlund, D. G., and Xing (1994): "Equations for the Soil-Water Characteristic Curve." Canadian Geotechnical Journal.

Fredlund, D.G. and Morgenstern, N.R. (1977), “Stress state variables for unsaturated soils”, J. Geotech. Eng. - ASCE, 103, 447-466.

Janbu, N., Bjerrum, L., and Kjaernsli, B., (1956), “Stabilitetsberegning for fyllinger skjaeringer og naturlige skraniger”, Norwegian Geotechnical Publication No. 16, Oslo, Norway.

Kulhawy, F.H. and Mayne, P.W. 1990. Estimating Soil Properties for Foundation Design. EPRI Report EL- 6800, Electric Power Research Institute, Palo Alto: 306 p. www.epri.com

Lehane et al. 2004, Sesonal Dependence of In Situ Test Parameters in Sand Above the Water Table, Geotechnique,54, No. 3, 215-218.

Li, X., (2008), “Laboratory studies on the bearing capacity of unsaturated sands”, Thesis, University of Ottawa, Canada.

Lunne, T., Robertson, P.K. and Powell, J.J.M. (1997), “Cone Penetration Testing in Geotechnical Practice”, Blackie Academic/Routledge Publishing, New York.

Miller, G.A. and Muraleetharan, K.K. (1998), “In Situ Testing in Unsaturated Soil,” Proc. of UnSat’98, 2nd International Conference on Unsaturated Soils, Beijing, China, Aug. 27-30.

Miller, G.A. and Muraleetharan, K.K. (2000), “Interpretation of Pressuremeter Tests in Unsaturated Soil,” Geotechnical Special Publication No. 99, Geo-Institute of ASCE, pp. 40-53.

Miller, G.A. and Tan, N.K. (2008), “At-rest lateral stress from pressuremeter tests in an unsaturated soil calibration chamber,” Proc. of the 3rd International Conference on Site Characterization, Taipei, Taiwan, April 2008, Taylor and Francis Group, p. 621-626.

Miller, G.A., (2014) Use of the Yield Pressure to Interpret Pressuremeter Results in Unsaturated soil, Unsaturated soils: Research & Applications, Sydney, 2012.

Miller, G.A., Muraleetharan, K.K., Tan, N.K. and Lauder, D.A. (2002) "A Calibration Chamber for Unsaturated Soil," Proc. of UNSAT 2002, 3rd International Conference on Unsaturated Soils, Recife, Brazil, March 10-14, A.A. Balkema, Lisse, Netherlands, Vol. 2, pp. 453-457.

Mohamed, F., and Vanapalli, S., (2015), "Bearing capacity of shallow foundations I n saturated and unsaturated sands from SPT-CPT correlations", International Journal of Geotechnical Engineering, 22 Oct. 2014.

Muraleetharan, K. K., Yang, Y., Salehipour, S. A., and Dhavala, M .D. 1998, "Cavity expansion theories for unsaturated soils", Technical report, School of Civil Engineering and Environmental Science, University of Oklahoma, Norman, 1998.

Muraleetharan, K.K., Ravichandran, N., Miller, G.A. and Tan, N.K. (2003) "Fully Coupled Analyses of Pressuremeter Tests in Unsaturated Soils," Proc. 2nd UNSAT-Asia 2003, Unsaturated Soils – Geotechnical and Geoenvironmental Issues, Osaka, Japan, Published by Organizing Committee of UNSAT-ASIA 2003, pp. 313-318.

Oh, W. T., Vanapalli, S. K., & Puppala, A. J. (2009). Semi-empirical model for the prediction of modulus of elasticity for unsaturated soils. Canadian Geotechnical Journal, 46(8), 903-914.

Pereira et al. 2003, Numerical Modeling of Unsaturated Soils in a Pressuremeter Test, 16th ASCE Engineering Mechanics Conference, July 16-18, 2003, University of Washington, Seattle.

Pournaghiazar, M., Russell, A., R., Khalili, N., (2013), "The cone penetration test in unsaturated sands", Geotechnique 63, No. 14, 1209-1220.

Reese, L. C., Isenhower, W. M., and Wand, S. T. (2006), "Analysis and designing of shallow and deep foundations, Wiley, New York.

Robertson, P. K., & Campanella, R. G. (1983). Interpretation of cone penetration tests. Part I: Sand. Canadian geotechnical journal, 20(4), 718-733.

Robertson, P. K., (1989), "Soil classification using the cone penetration test", Canadian Geotechnical Journal, Vol. 27, 1990.

Rojas, J. C., Salinas, L. M., and Sejas, C., (2007), "Plate-load tests on an unsaturated lean clay" in book: Experimental Unsaturated Soil Mechanics, pp. 445-452, January 2007.

Russell, A. R., Pournaghiazar, M., & Khalili, N. (2010). Interpreting CPT results in unsaturated sands. In 2nd International Symposium on Cone Penetration Testing, Huntington Beach, CA, USA.

Russell, A. R., & Khalili, N. (2006). On the problem of cavity expansion in unsaturated soils. Computational mechanics, 37(4), 311-330.

Pournaghiazar, M., Russell, A. R., & Khalili, N. (2011). Development of a new calibration chamber for conducting cone penetration tests in unsaturated soils. Canadian Geotechnical Journal, 48(2), 314-321.

Salgado, R., Mitchell, J., K., & Jamiolkowski, M., (1997), "Cavity expansion and penetration resistance in sand", Journal of Geotechnical and Geoevnironmental Engineering, 123(4): 344-354, April 1997.

Schnaid, F., Sills, G. C., Consoli, N. C., (1996) Pressuremeter test in unsaturated soils. In: Craig (ed) Advances in site investigation practice. Thomas Telford, London, Sect 4b, pp 586–595.

Skempton, A. W. (1951). The bearing capacity of clays.

Tan, N. (2005) Pressuremeter and Cone Penetrometer Testing in a Calibration Chamber with Unsaturated Minco Silt, Thesis, University of Oklahoma, May 2005

Tan, N., Miller, G.A., and Muraleetharan, K.K. (2003) "Preliminary Laboratory Calibration of Cone Penetration in Unsaturated Silt," Proc. Soil-Rock America 2003, 12th Pan-American Conference on Soil Mechanics and Geotechnical Engineering/39th U.S. Rock Mechanics Symposium, Cambridge, Mass., June 22-26, VGE, Essen, Germany, pp. 391-396.

Tan, N.K. and Miller, G.A. (2005), "Pressuremeter Testing in a Calibration Chamber with Unsaturated Minco Silt," Proc. 16th International Conference on Soil Mechanics and Geotechnical Engineering, Osaka, Japan, Sept. 12-16, 2005.

Terzaghi, K. (1943). Theoretical soil mechanics. Wiley, New York.

Vanapalli SK and Oh WT (2010): "A Model for Predicting the Modulus of Elasticity of Unsaturated Soils Using the Soil-Water Characteristic Curve." International Journal of Geotechnical Engineering, USA.

Vanapalli, S. K., & Mohamed, F. M. (2007). Bearing capacity of model footings in unsaturated soils. In Experimental unsaturated soil mechanics (pp. 483-493). Springer Berlin Heidelberg.

Vesic, A. S. (1973). Analysis of ultimate loads of shallow foundations: Closure of discussion of original paper J. Soil Mech. Found. Div. Jan. 1973. 1F, 6R. J. GEOTECH. ENGNG. DIV. V100, N. GT8, 1974, P949–951. In International Journal of Rock Mechanics and Mining Sciences & Geomechanics Abstracts (Vol. 11, No. 11, p. A230). Pergamon.

Vesic, A.S. (1972). "Expansion of Cavities in Infinite Soil Mass." Journal of the Soil Mechanics and Foundation Division, ASCE, 98(3), 265-290.

Xu, Y., (2004), "Bearing capacity of unsaturated expansive soils", Geotechnical and Geological Engineering, 22: 611-625, 2004.

Yang, H., and Russell, A., R., (2015a), "Cavity expansion in unsaturated soils exhibiting hydraulic hysteresis considering three drainage conditions", International Journal for Numerical and Analytical Methods in Geomechanics,, February 2015.

Yang, H., and Russell, A., R., (2015b), "The cone penetration test in unsaturated silty sands", Canadian Geotechnical Journal, July 2015.

Yu, H., S., (1990), "Cavity expansion theory and its application to the analysis of pressuremeters", Thesis, University of Oxford.

Zapata, C. E., Houston, W. N., Houston, S. L., & Walsh, K. D. (2000). Soil-water characteristic curve variability. GEOTECH SPEC PUBL, (99), 84-124.

Zhang, Y., Gallipoli, D., and Augarde, C., (2013). "Parameter identification for elasto-plastic modelling of unsaturated soils from pressuremeters tests by parallel modified particle swarm optimization." Computers and Geotechnics 48 (2013) 293-303.

Zhu, F., Clark, J., and Phillips, R., (2001), "Scale effect of strip and circular footings resting on dense sand", Journal of Geotechnical and Geoenvironmental Engineering, 127: 613-621.

Appendix

The corrected pressure and volume curves for Goldsby and North Base are shown in Figure A.1-A.25. It is important to note that the first tests completed in February and March of 2013 at North Base, were completed at a depth of 6 feet. The test depth thereafter was adjusted to 5 feet because the water table at the site was around 9 feet, and so the deepest test needed to be raised to 7 feet. It was assumed that the small change in depth had minimal effect on test results. Tests conducted early in 2013 have stress-strain curves that indicate stiffer soil compared to tests conducted at later times. The majority of tests conducted after April of 2013 showed a similar grouping of tests results. The softest soil response occurred in August of 2014.

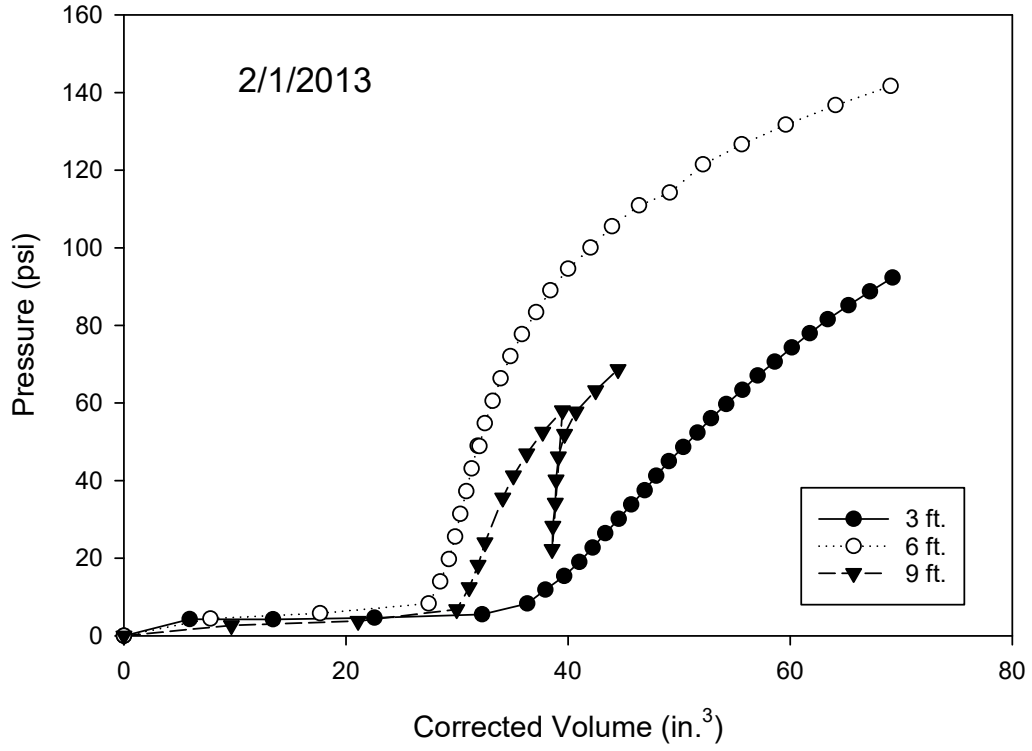

Figure A. 1: Corrected pressure-volume curve for Goldsby on 2/1/2013

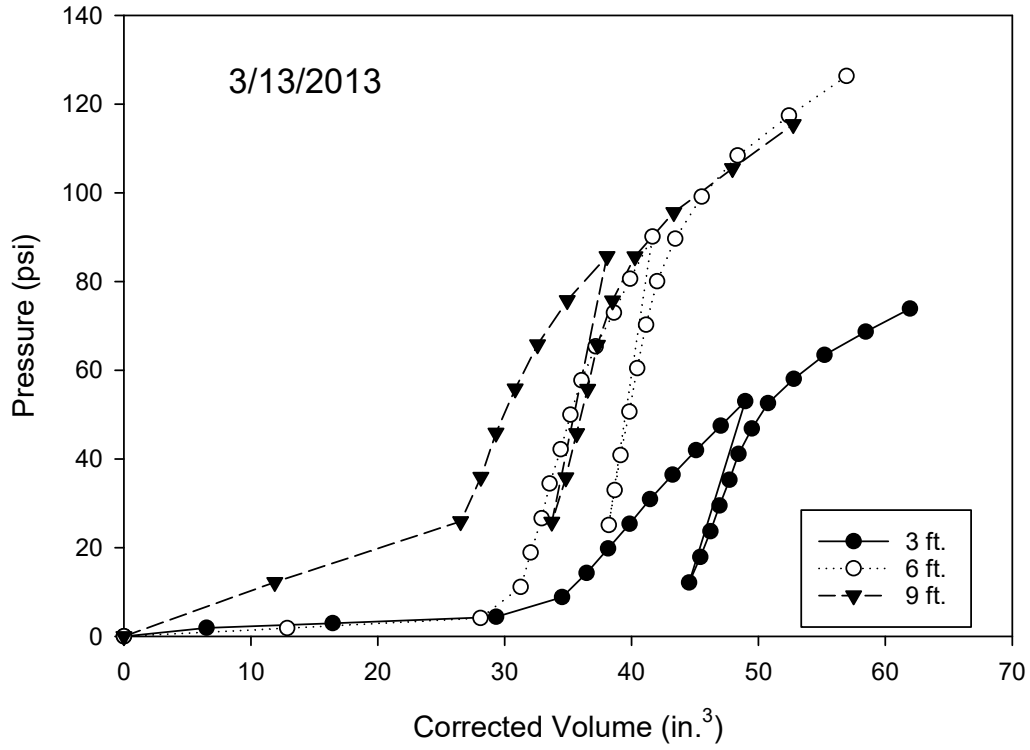

Figure A. 2: Corrected pressure-volume curve for Goldsby on 3/13/2013

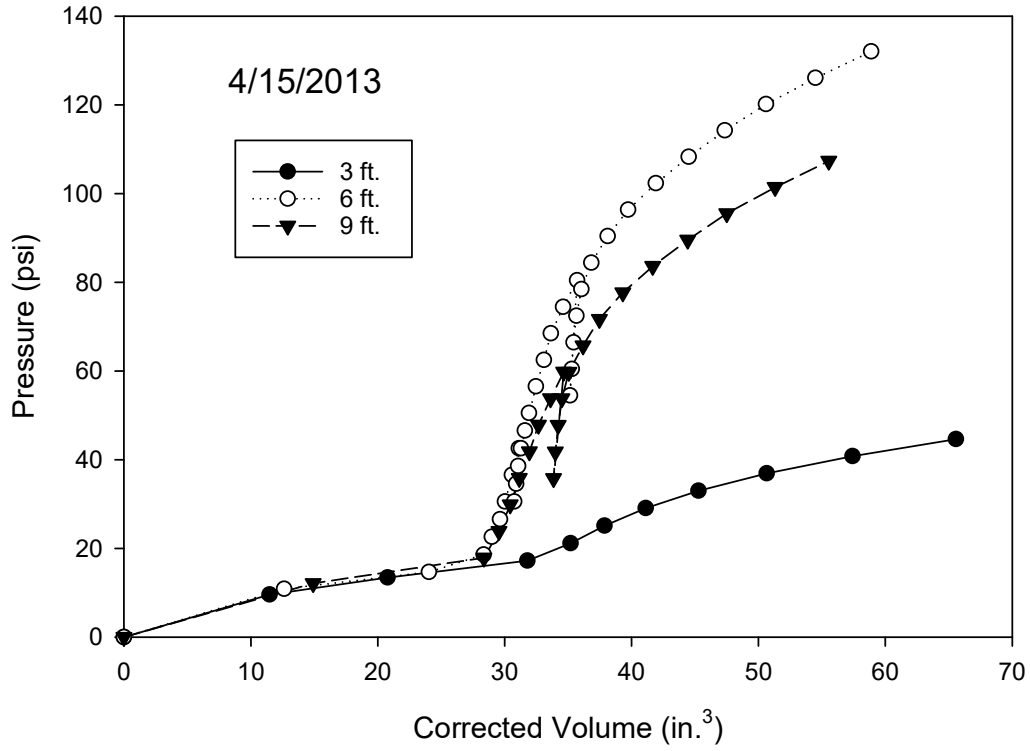

Figure A. 3: Corrected pressure-versus volume curve for Goldsby on 4/15/2013

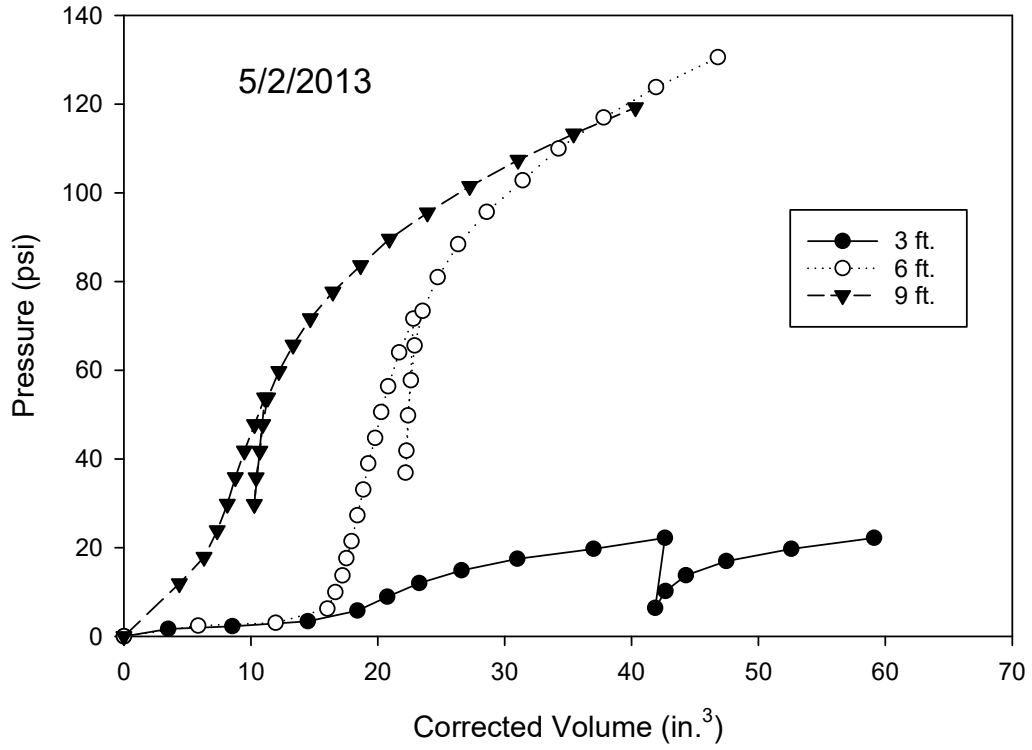

Figure A. 4: Corrected pressure-versus volume curve for Goldsby on 5/2/2013

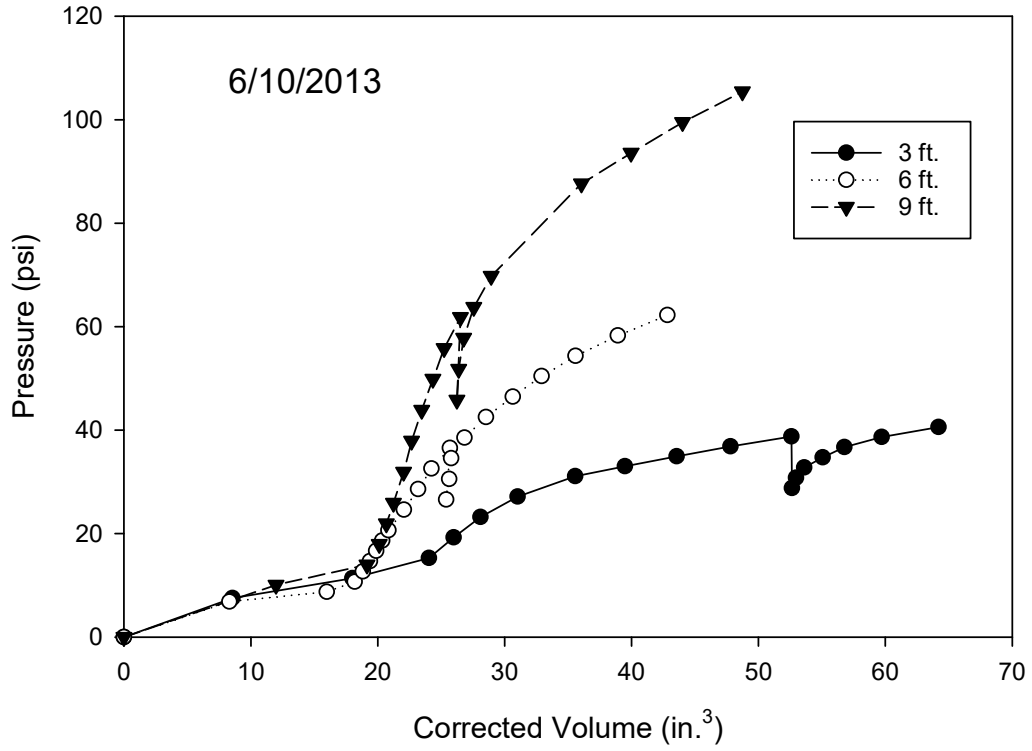

Figure A. 5: Corrected pressure-versus volume curve for Goldsby on 6/10/2013

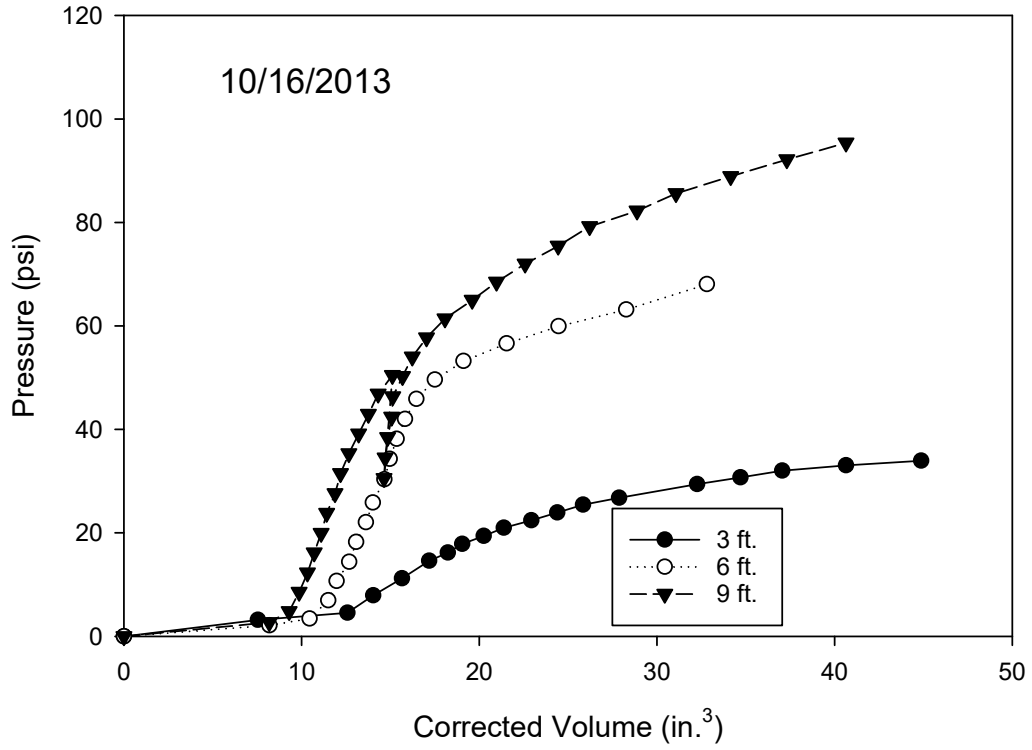

Figure A. 6: Corrected pressure-versus volume curve for Goldsby on 10/16/13

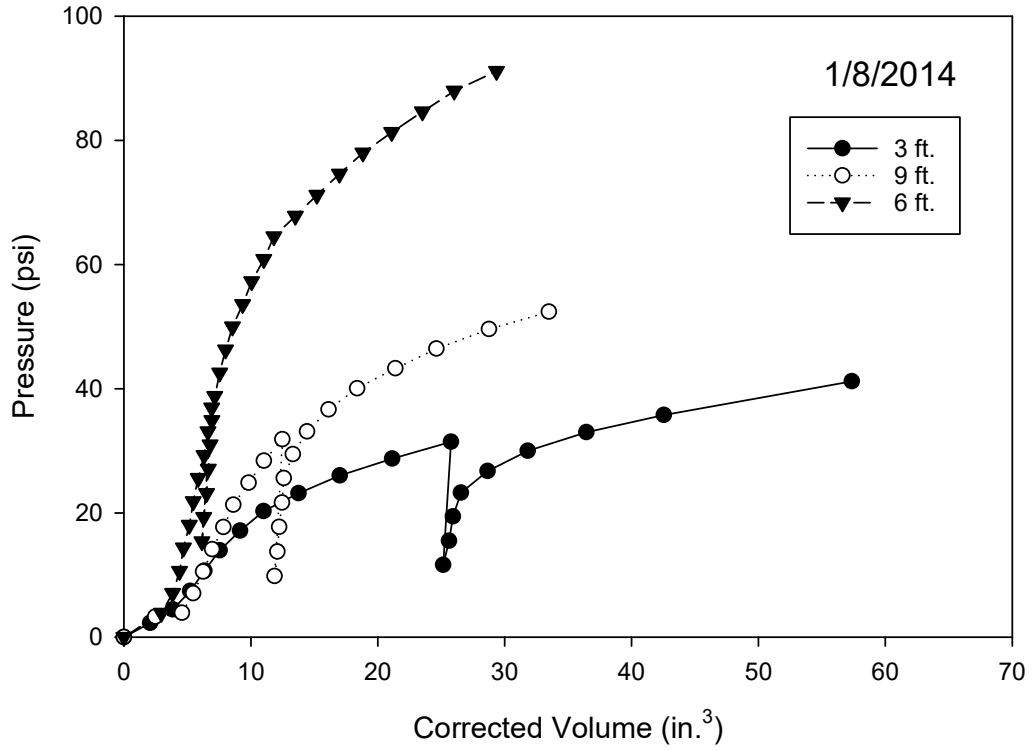

Figure A. 7 Corrected pressure-versus volume curve for Goldsby on 1/8/2014

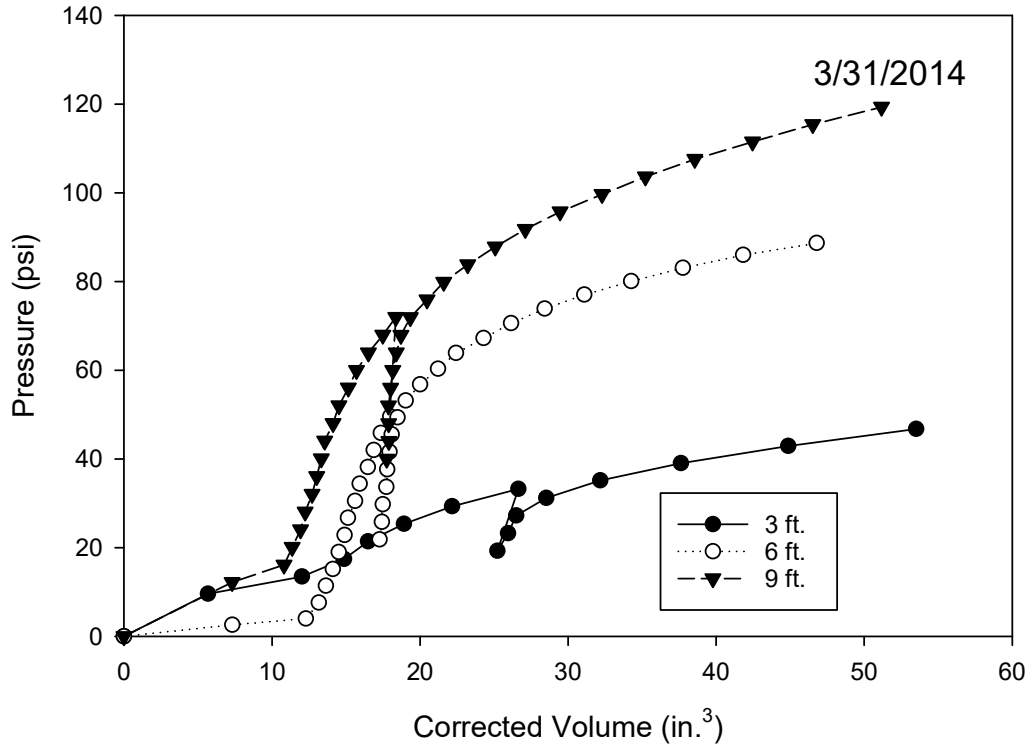

Figure A. 8: Corrected pressure-versus volume curve for Goldsby on 3/31/2014

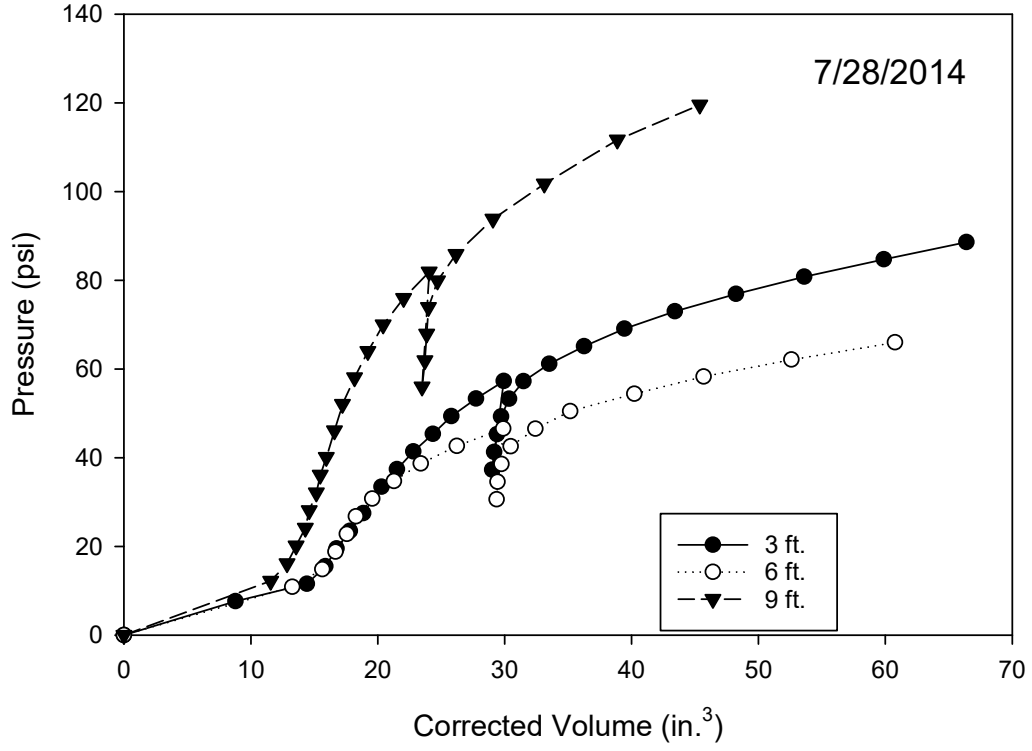

Figure A. 9: Corrected pressure-versus volume curve for Goldsby on 7/28/2014

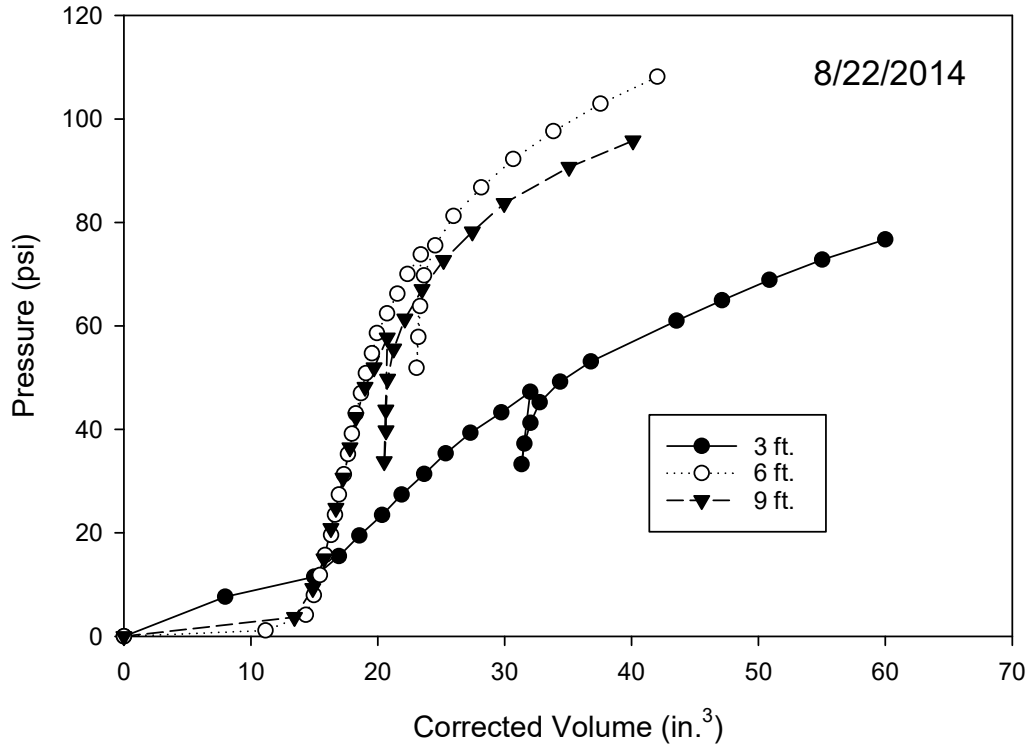

Figure A. 10: Corrected pressure-versus volume curve for Goldsby on 8/22/2014

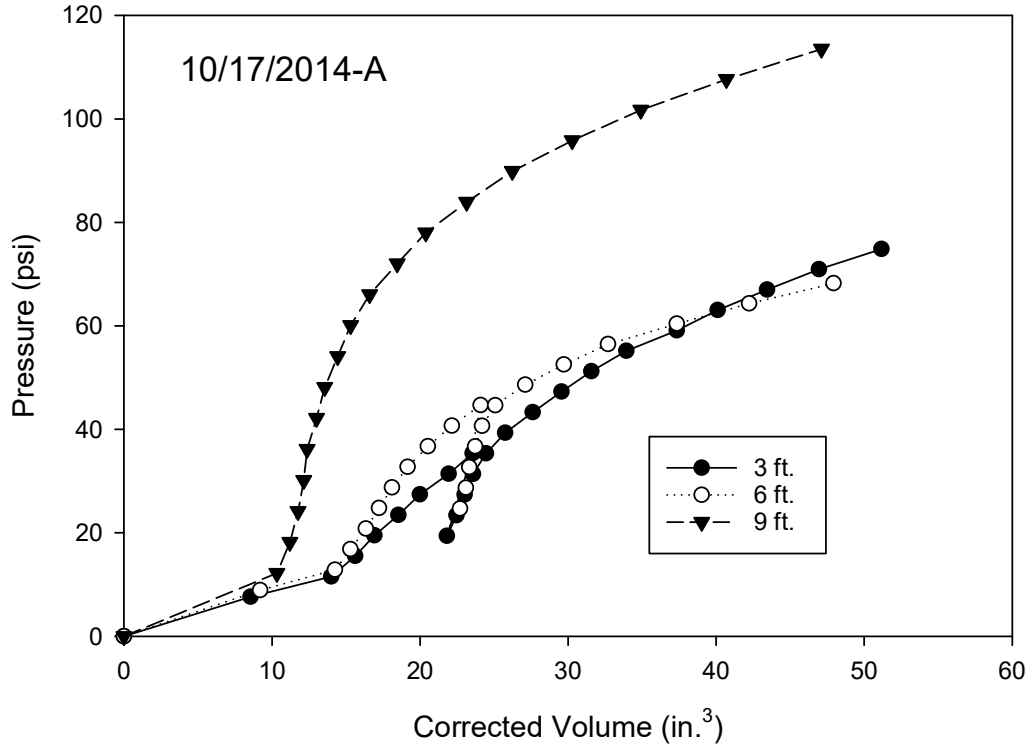

Figure A. 11: Corrected pressure-versus volume for Goldsby on 10/17/2014-A

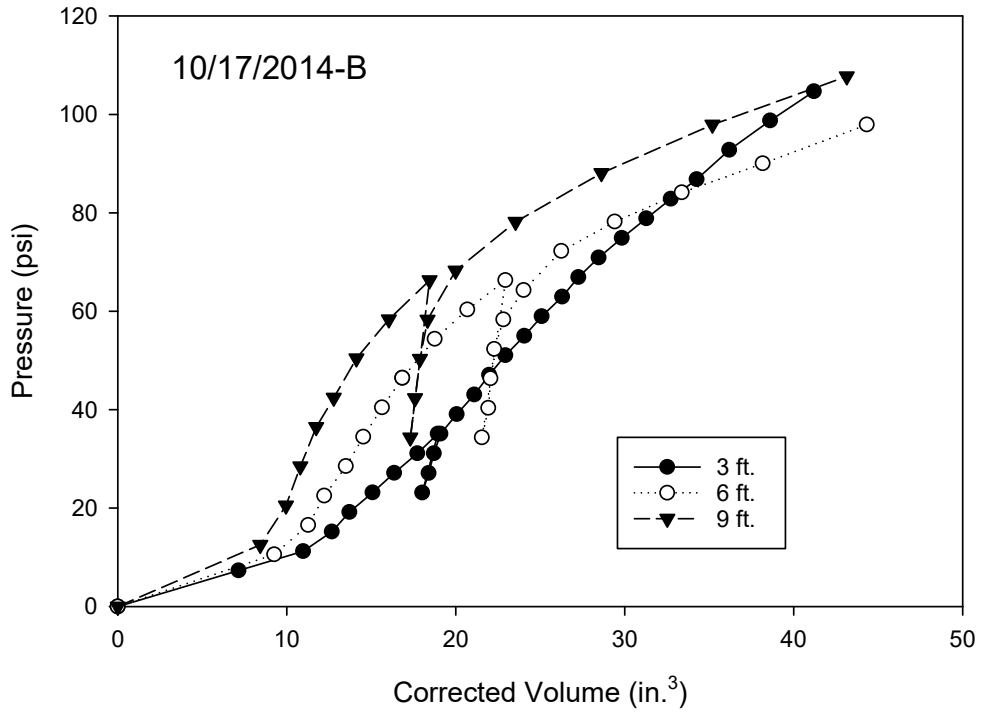

Figure A. 12: Corrected pressure-versus volume curve for Goldsby on 10/17/2014-B

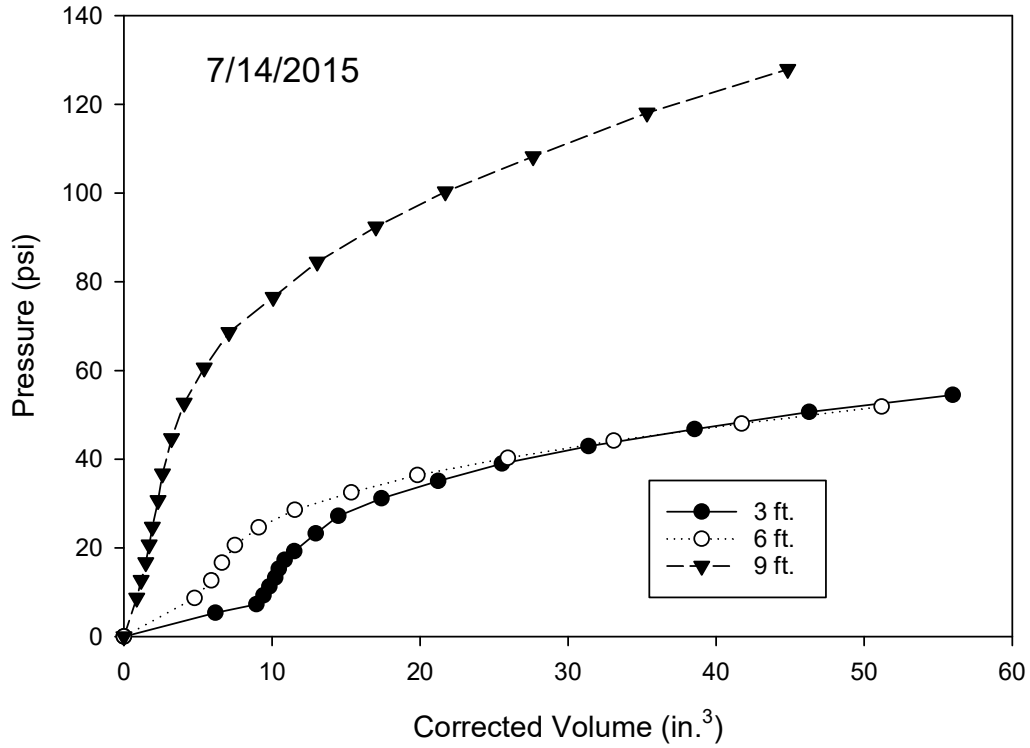

Figure A. 13: Corrected pressure-versus volume curve for Goldsby on 7/14/2015

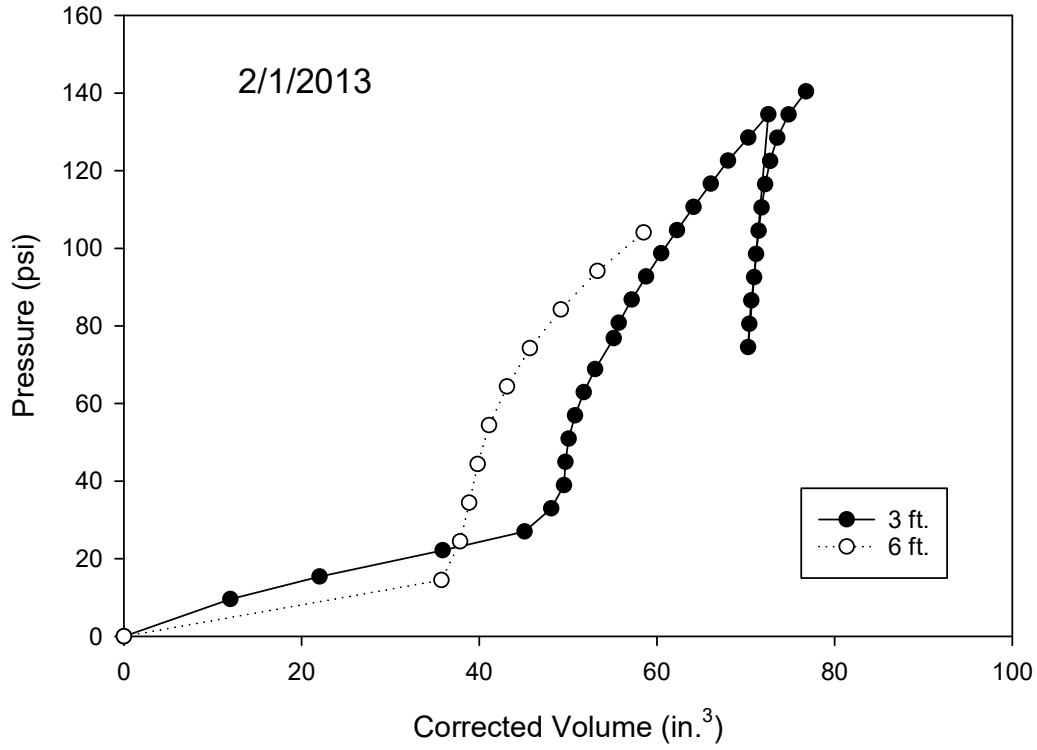

Figure A. 14: Corrected pressure- versus volume curve for North Base on 2/1/2013

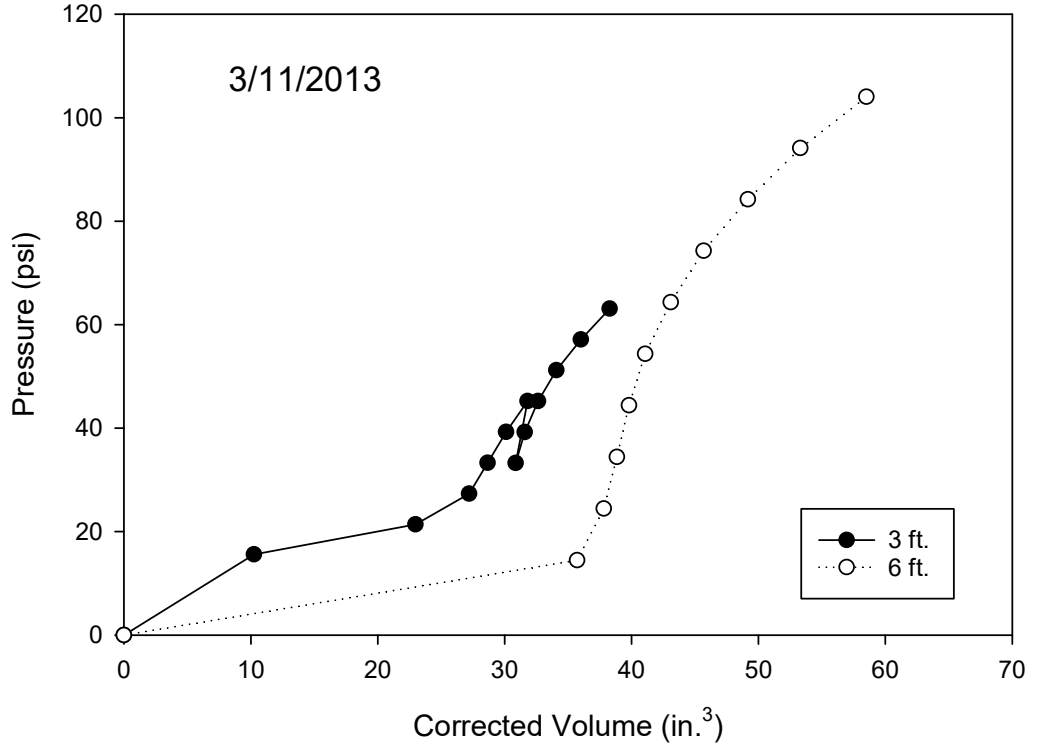

Figure A. 15: Corrected pressure-versus volume curve for North Base on 3/11/2013

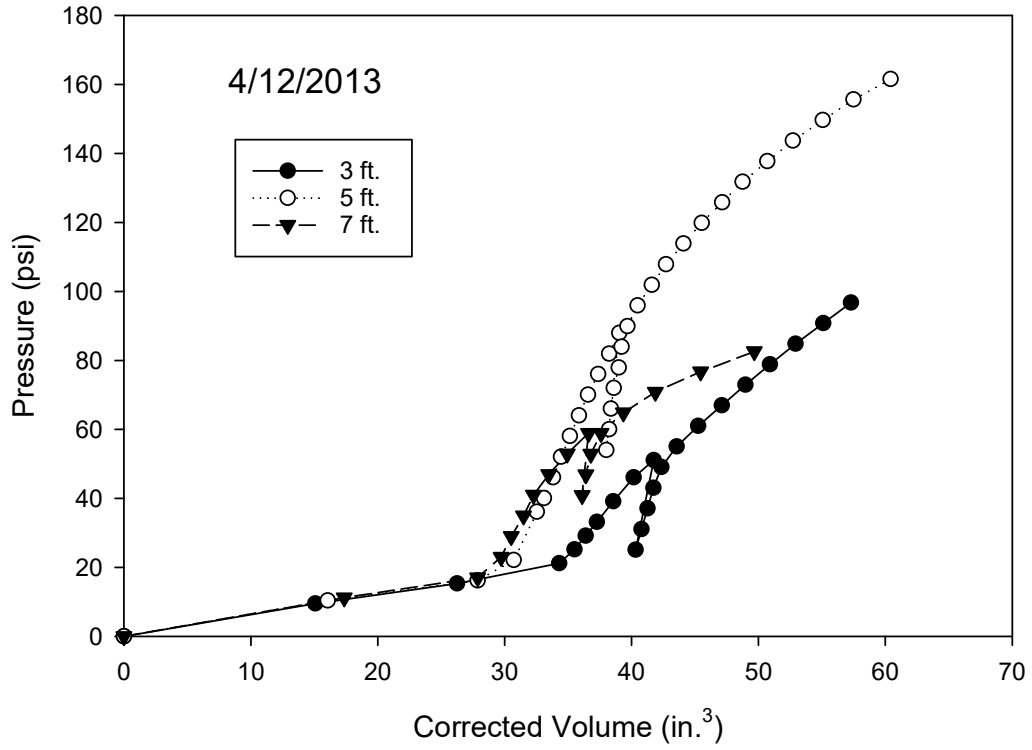

Figure A. 16: Corrected pressure-versus volume curve for North Base on 4/12/2013

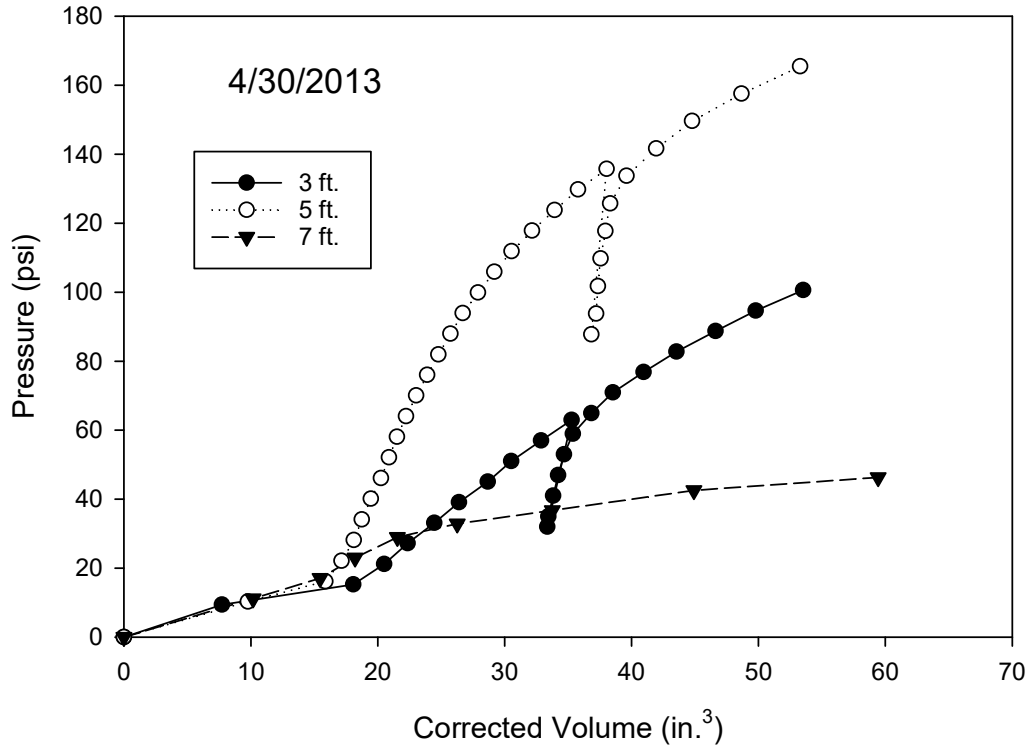

Figure A. 17: Corrected pressure-versus volume curve for North Base on 4/30/2013

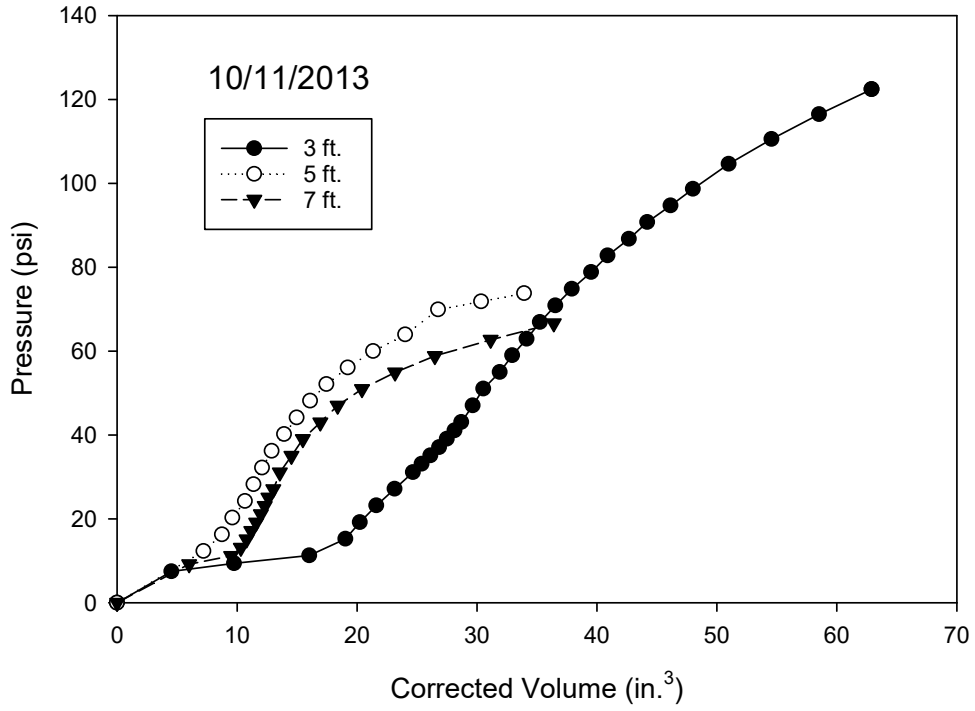

Figure A. 18: Corrected pressure-versus volume curves for North Base on 10/11/2013

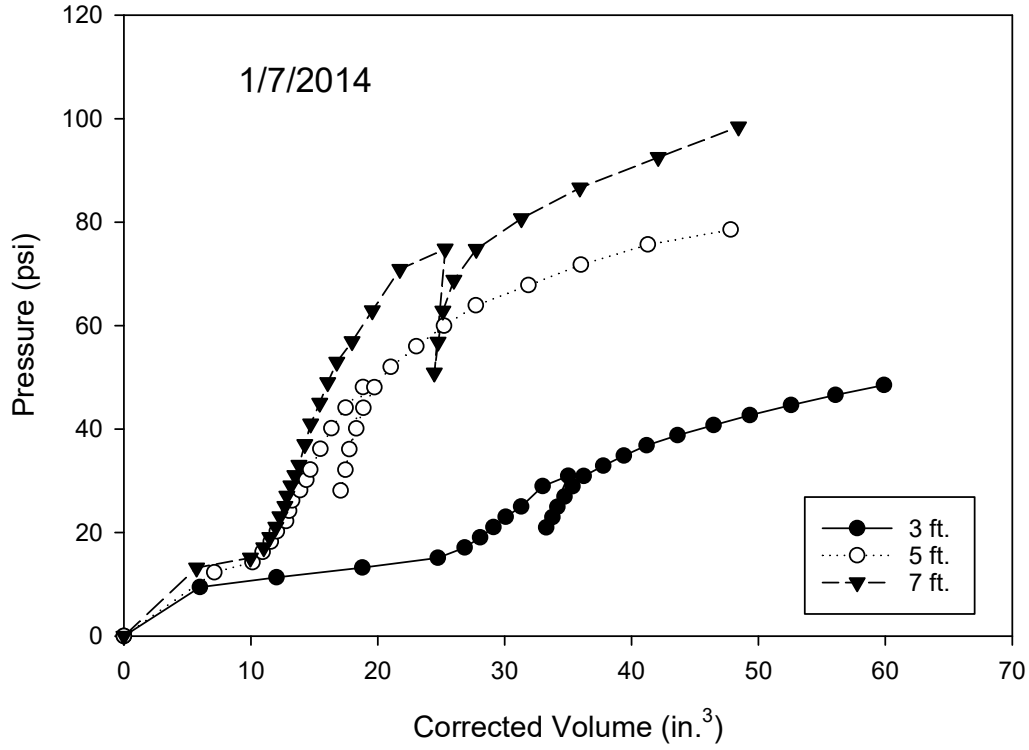

Figure A. 19: Corrected pressure-versus volume curves for North Base on 1/7/2014

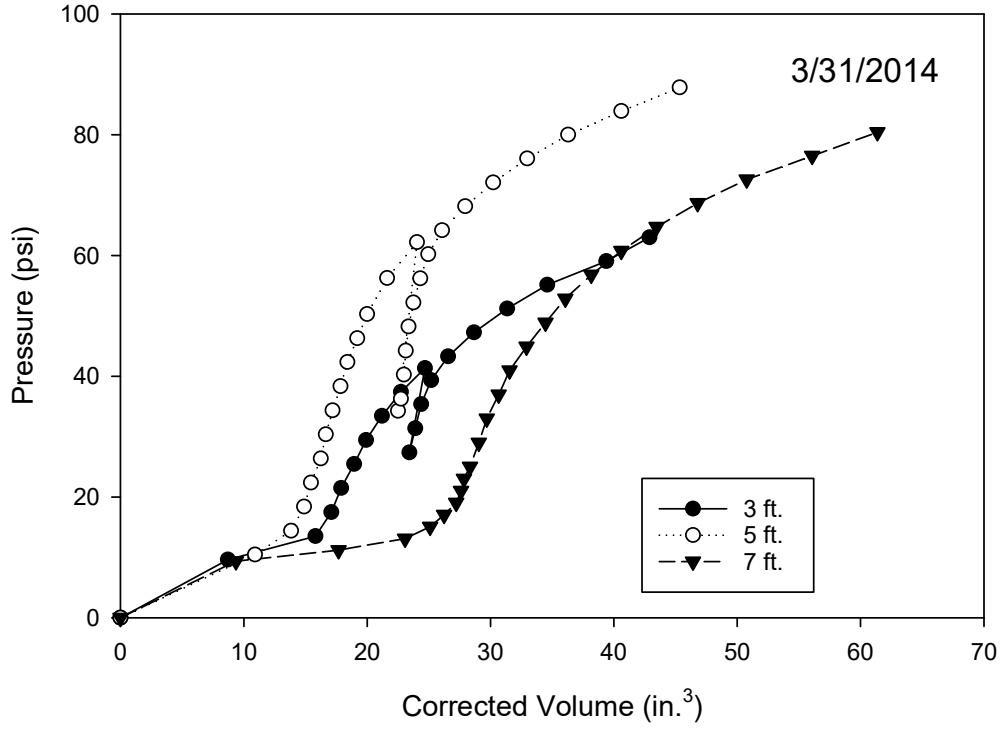

Figure A. 20: Corrected pressure-versus volume curves for North Base on 3/31/2014

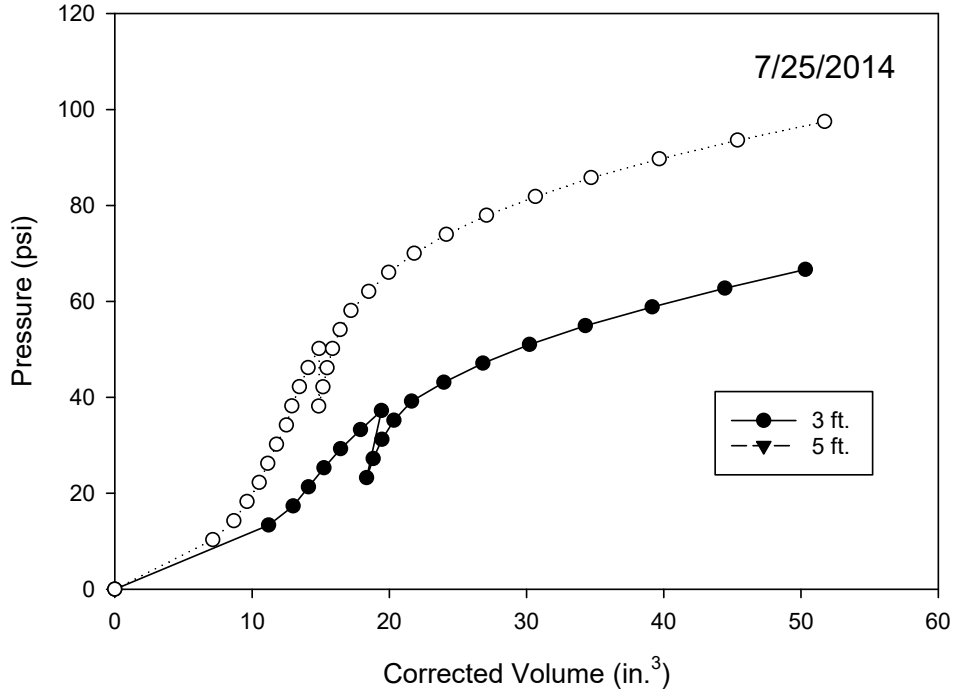

Figure A. 21: Corrected pressure-versus volume curves for North Base on 7/25/2014

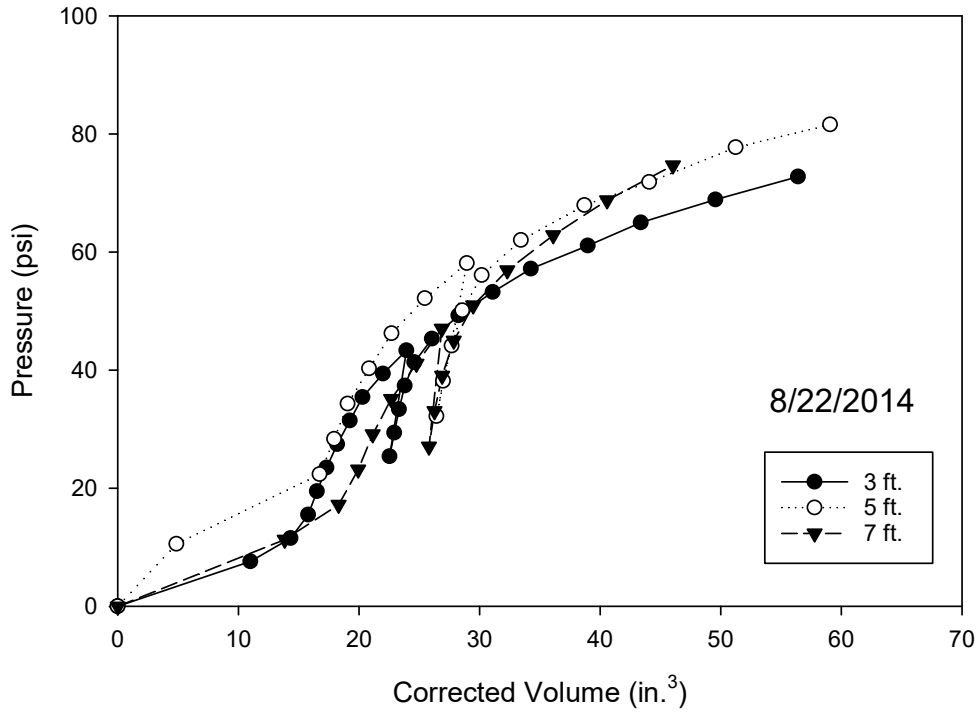

Figure A. 22: Corrected pressure-versus volume curves for North Base on 8/22/2014

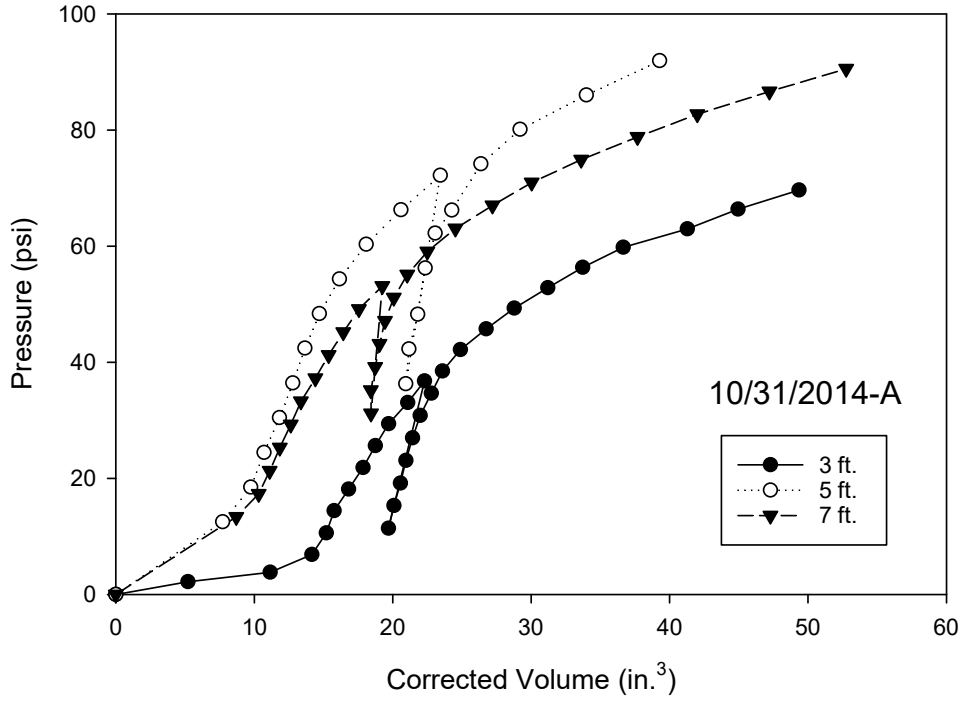

Figure A. 23: Corrected pressure-versus volume curves for North Base on 10/31/2014-A

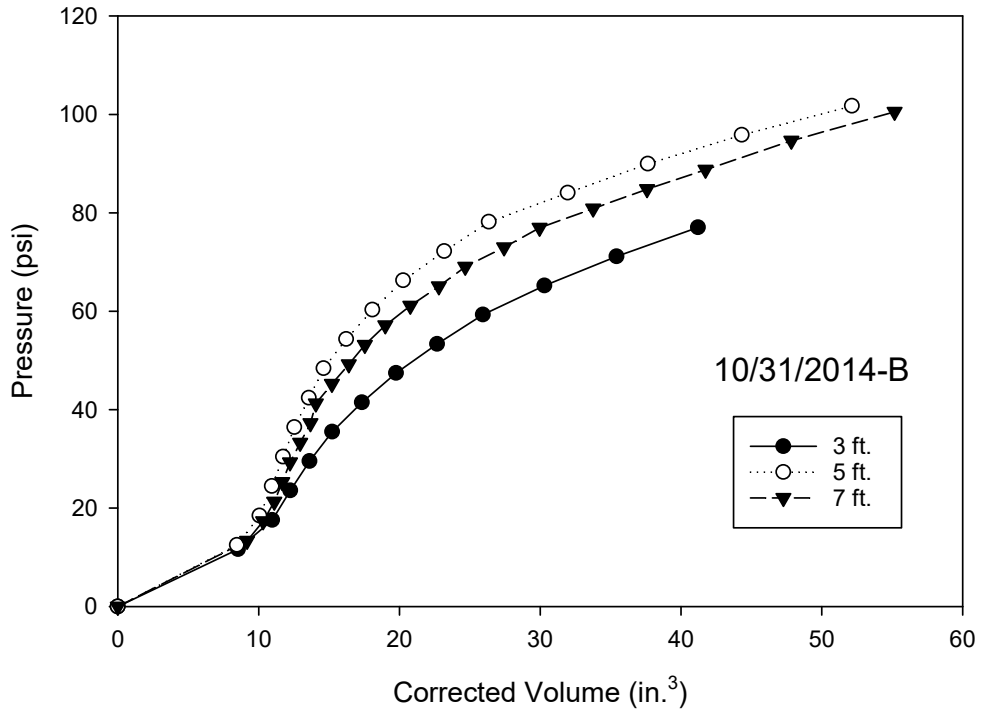

Figure A. 24: Corrected pressure-versus volume curves for North Base on 10/31/2014-B

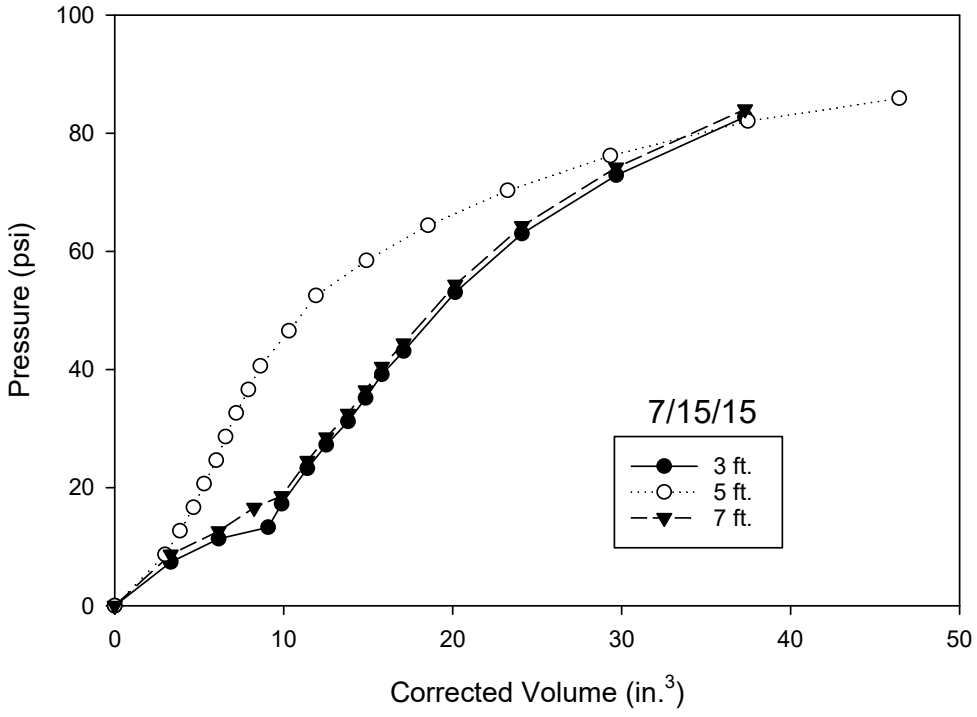

F

Figure A. 25: Corrected pressure-versus volume curves for North Base on 7/15/15

The plot for North Base for the test performed on 2/4/2013 is shown in Figure A.26. This test shows average tip resistance, and skin friction of 45 tsf, and 3.5 tsf, respectively. The average water content at the peak is nearly 16% while the matric suction is 55 psi.

The CPT data for North Base for the tests performed on 5/6/2013 is shown in Figure A.27. The average tip resistance for this date was 25 tsf; average sleeve friction is 2.0 tsf. The average moisture content is 25% and suction is 30 psi. CPT data for tests conducted at North Base on 9/3/2013 is presented in Figure A.28. This data has an average tip resistance of 50 tsf, with a corresponding skin friction value of 2.5 tsf. The average water content, and matric suction for these tests is 20% and 40 psi. Based on the data alone there is a noticeable trend between fluctuation in matric suction and its effect on tip resistance and sleeve friction. Similar trends are noticed in the normalized data.

The CPT data for North Base for tests conducted on 11/21/2013 is presented in Figure A.29. This data shows an average tip resistance of 15 tsf with an average sleeve friction of 1.0 tsf. The average moisture content for this date is 22%, with a corresponding average suction of 10 psi. Cone data for North Base on 2/18/2014 is presented in Figure A.30. The average tip resistance and sleeve friction for this date is 15, and 0.5 tsf, respectively. The average moisture content and matric suction for this test date is 24%, and 10 psi, respectively. The test data for these dates is very similar, which corresponds well with very similar soil moisture conditions.

Cone penetration test data for tests conducted on 9/10/2014 is presented in Figure A.31. The average tip resistance and skin friction for this test date is 60 tsf, and

2.5 tsf, respectively. The average soil moisture conditions for this date include 18% moisture content, and a matric suction of 35 psi. The test data for CPT tests conducted on 12/30/2014 is presented in Figure A.32. The average tip resistance for this date is 30 tsf, with a corresponding sleeve friction of two tsf. The average soil moisture conditions are 22% water content and a matric suction of 10 psi.

The data from CPT conducted at Goldsby is presented in Figures A.33-A.39. The data from tests performed at Goldsby on 2/1/2013 is shown in Figure A.33. The average tip resistance, and sleeve friction for Goldsby is 60 tsf, and 1.5 tsf, respectively. The soil moisture conditions for this test date are 16% water content, and a matric suction of 20 psi. Test data from Goldsby on 5/6/2013 is presented in Figure A.34. The average tip resistance and sleeve friction for this site is 50 tsf, and 1.75 tsf. Soil moisture conditions for Goldsby on this test date is 15% water content and 14-psi matric suction. The CPT data for Goldsby on 7/29/2013 is shown in Figure A.35. The average tip resistance, and sleeve friction for this test date is 30 tsf, and 1.0 tsf, respectively. The soil moisture conditions for this test date is 17% water content and 12-psi matric suction.

The CPT data from Goldsby on 11/21/2013 is presented in Figure A.36. The figure shows and average tip resistance, and sleeve friction for this date of 40 tsf, and 1 tsf, respectively. The average soil moisture conditions for this depth are 17%, and 14 psi, respectively. The CPT data from Goldsby on 2/18/2014 is presented in Figure A.37. The site on this date had an average tip resistance on 30 tsf, and an average skin friction of 1.0 tsf. The average soil moisture conditions for Goldsby are 17% moisture content, and a matric suction of 9.5 psi. The CPT data for Goldsby on 9/10/2014 are presented in

Figure A.38. This data shows an average tip resistance of 70 tsf, and an average sleeve friction of 3.0 tsf. The average soil moisture conditions for this test date include a moisture content of 19%, and a matric suction of 20 psi. Finally, the last test performed at Goldsby was on 2/25/2015. The test data for this date are presented in Figure A.39. The results show an average tip resistance equal to 40 tsf, and an average sleeve friction equal to 1.0 tsf. The average soil moisture conditions for this test date include a moisture content of 19%, and a matric suction of 20 psi.

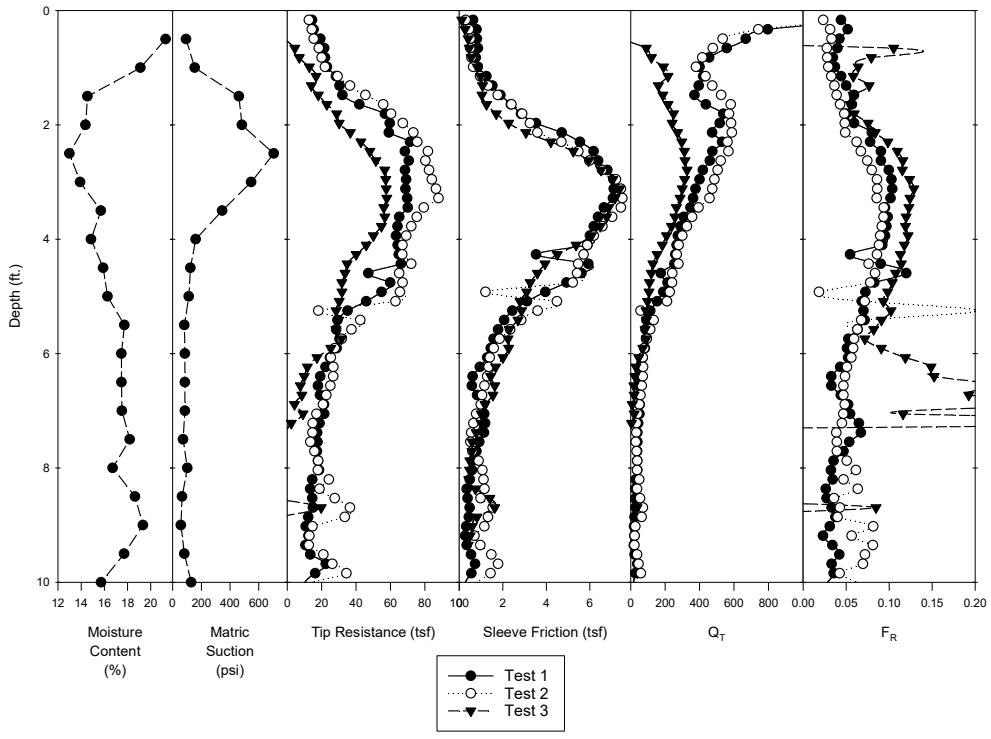

Figure A. 26: CPT data for tests performed at North Base on 2/4/2013

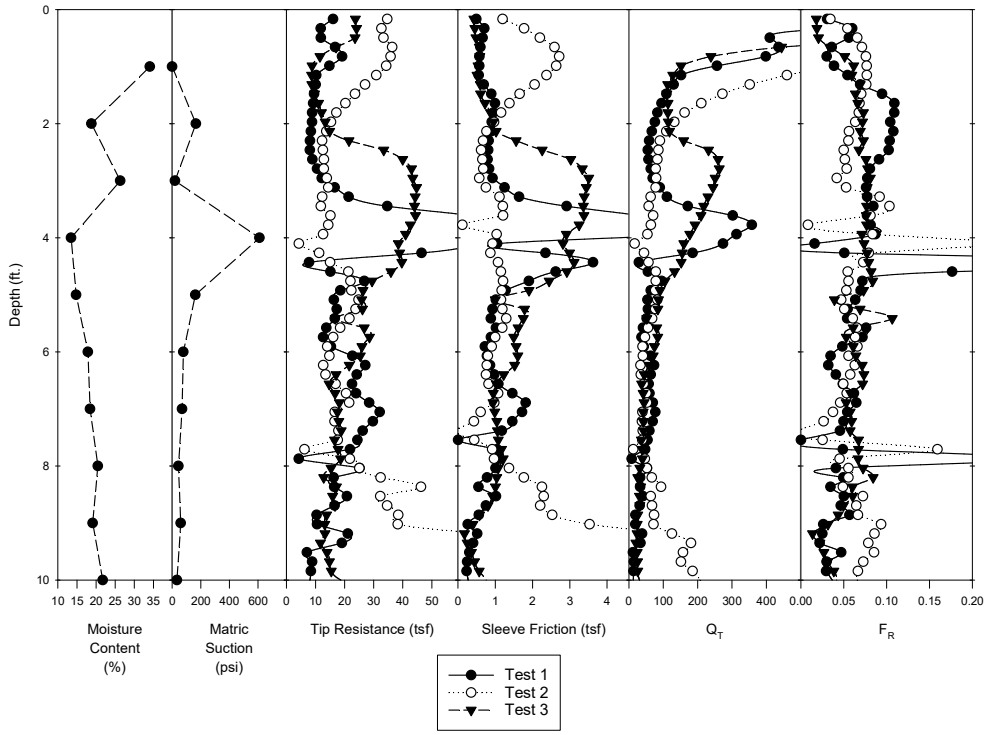

Figure A. 27: CPT data for tests performed at North Base on 5/6/2013

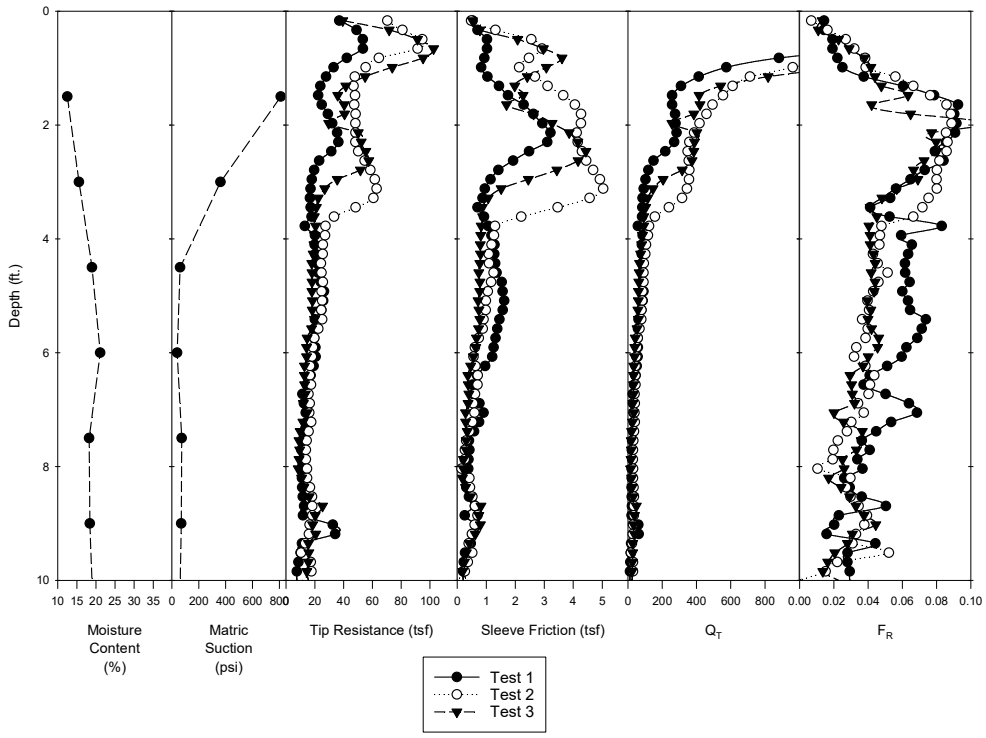

Figure A. 28: CPT data for tests conducted on 9/3/2013 at North Base

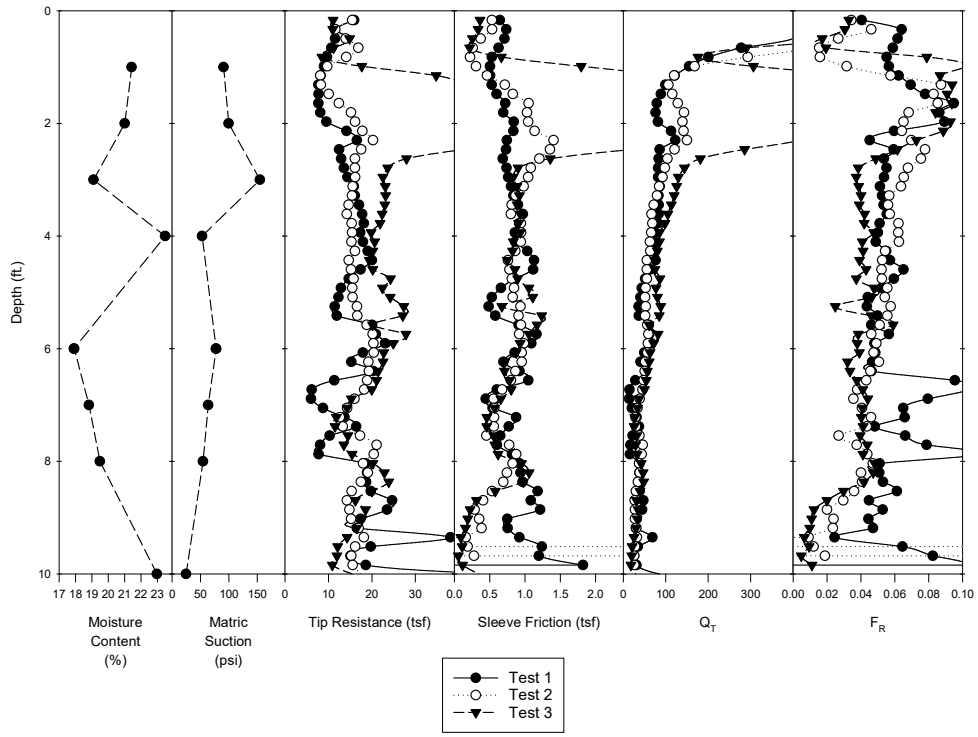

Figure A. 29: CPT data for tests conducted on 11/21/2013 at North Base

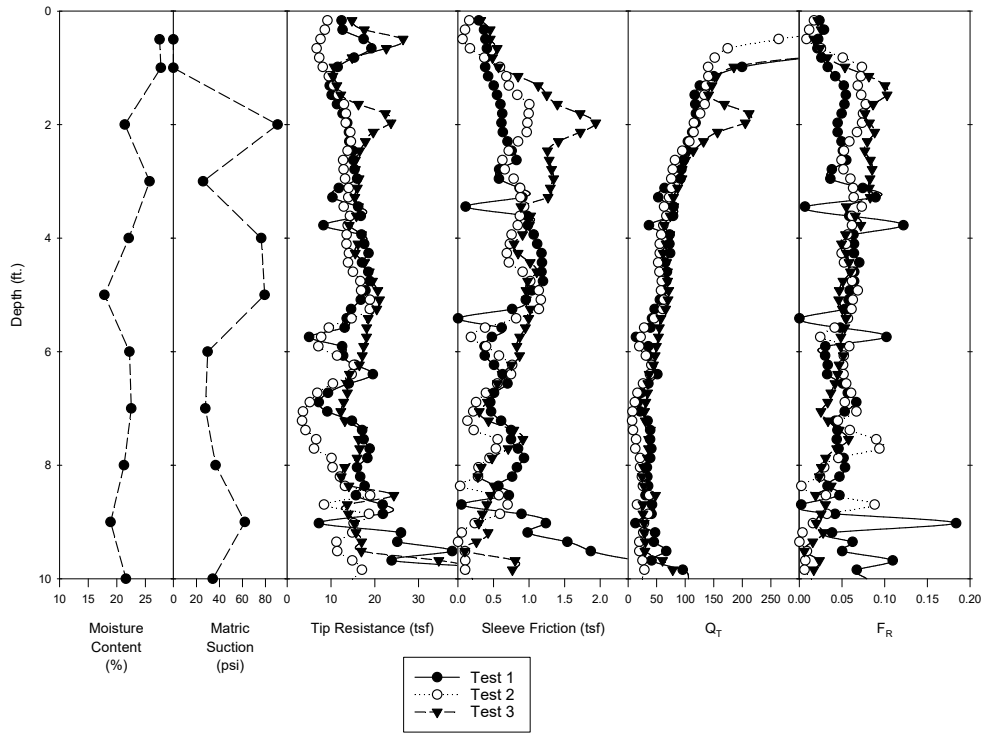

Figure A. 30: CPT data for tests conducted on 2/18/2014 at North Base

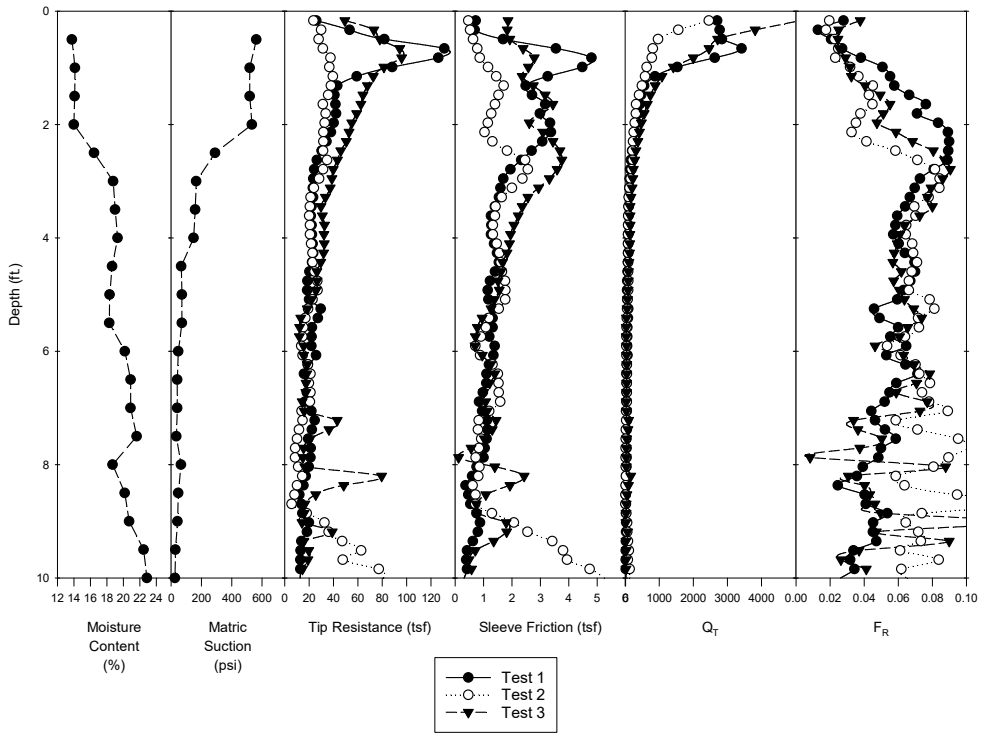

Figure A. 31: CPT data for tests conducted on 9/10/2014 at North Base

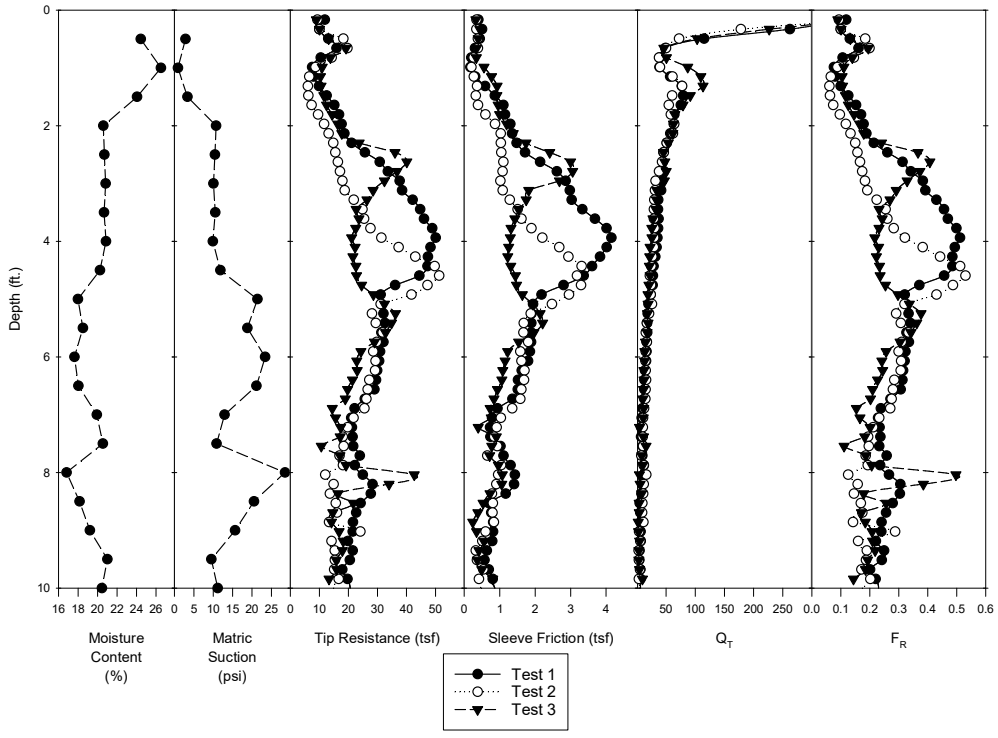

Figure A. 32: CPT data for tests conducted on 12/30/2014 at North Base

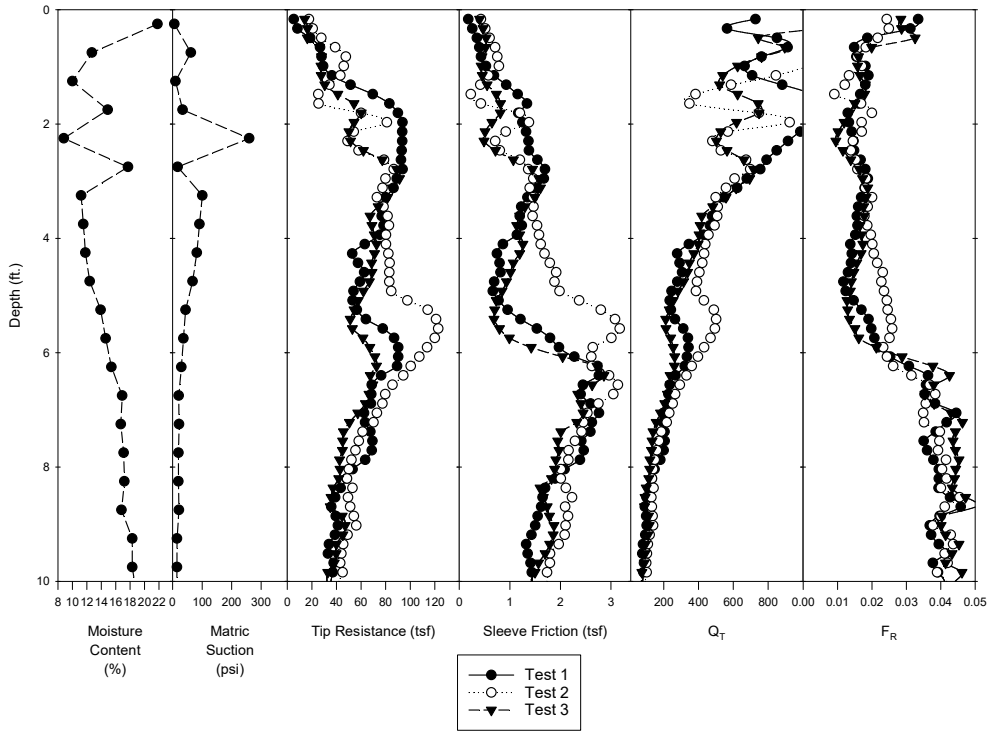

Figure A. 33: CPT data for tests conducted on 2/1/2013 at Goldsby

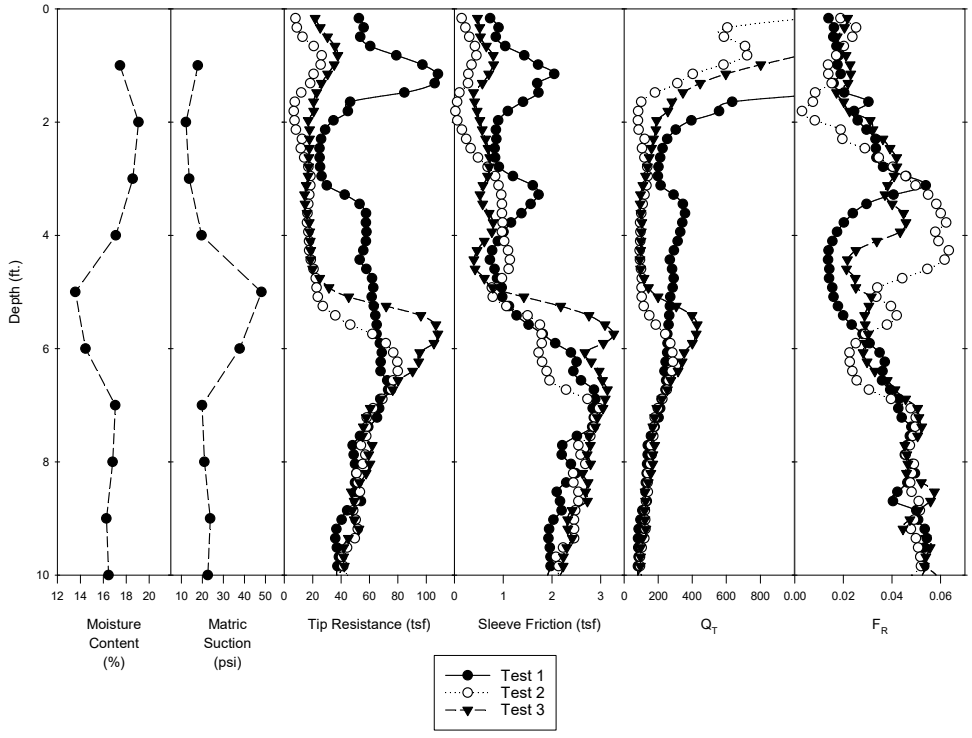

Figure A. 34: CPT data for tests conducted on 5/6/2013 at Goldsby

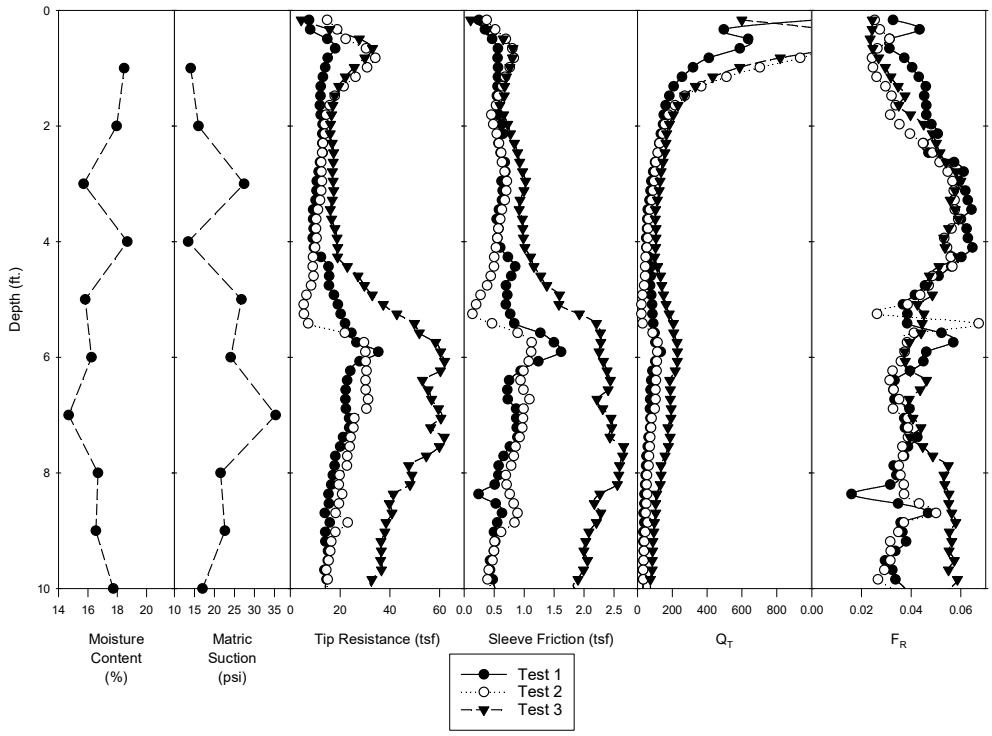

Figure A. 35: CPT data for tests conducted on 7/29/2013 at Goldsby

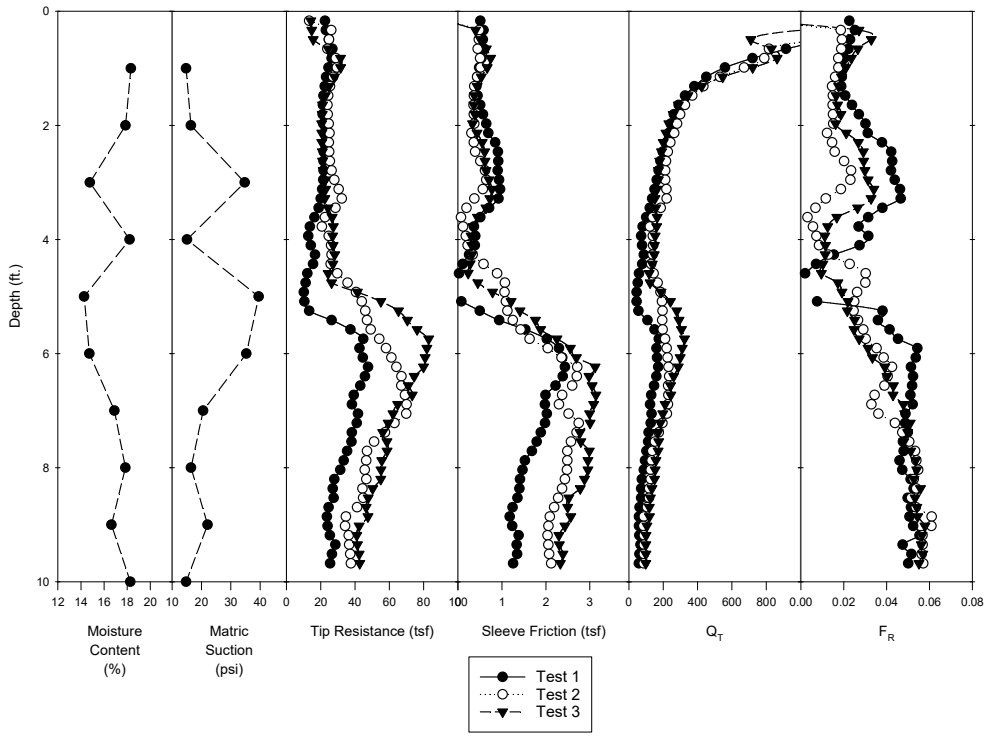

Figure A. 36: CPT data for tests conducted on 11/21/2013 at Goldsby

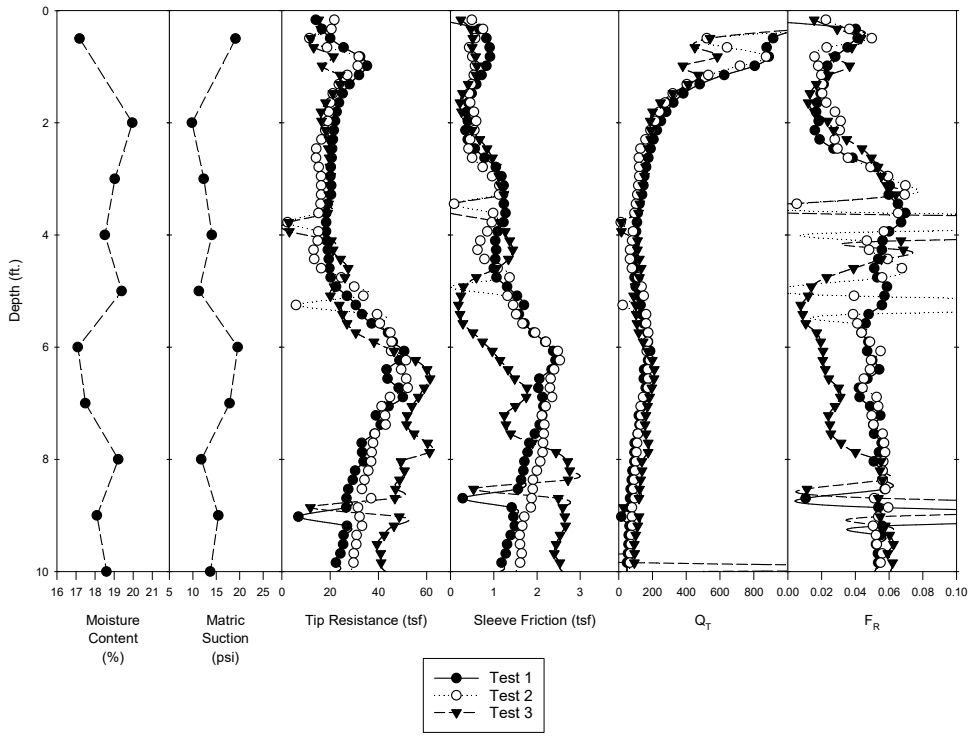

Figure A. 37: CPT data for tests conducted on 2/18/2014 at Goldsby

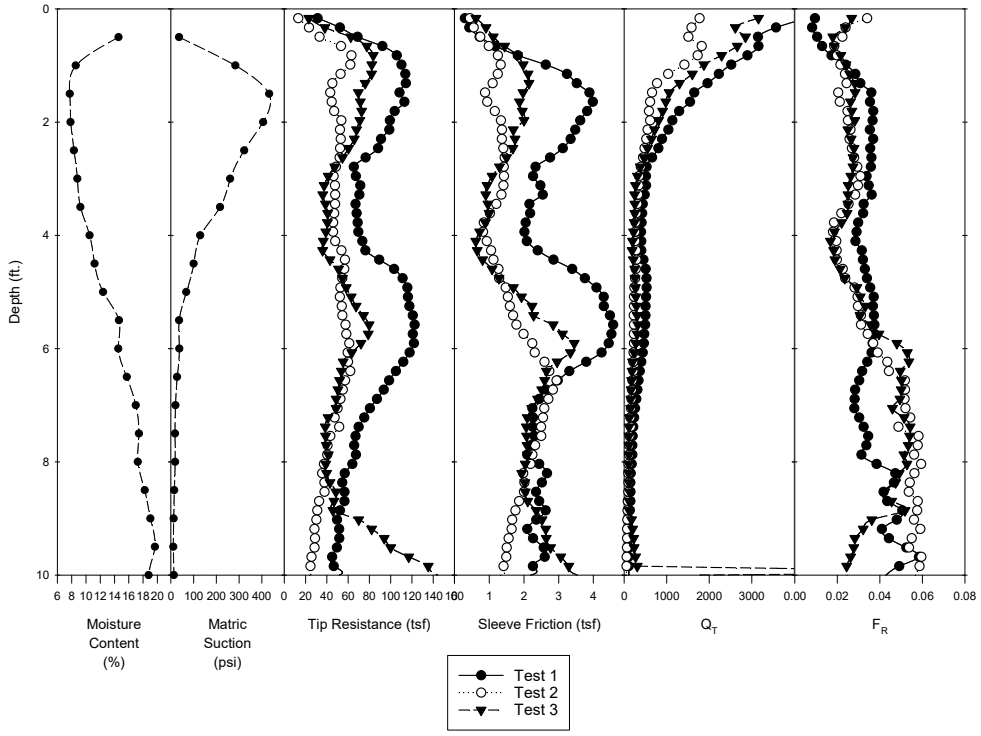

Figure A. 38: CPT data from tests conducted on 9/10/2014 at Goldsby

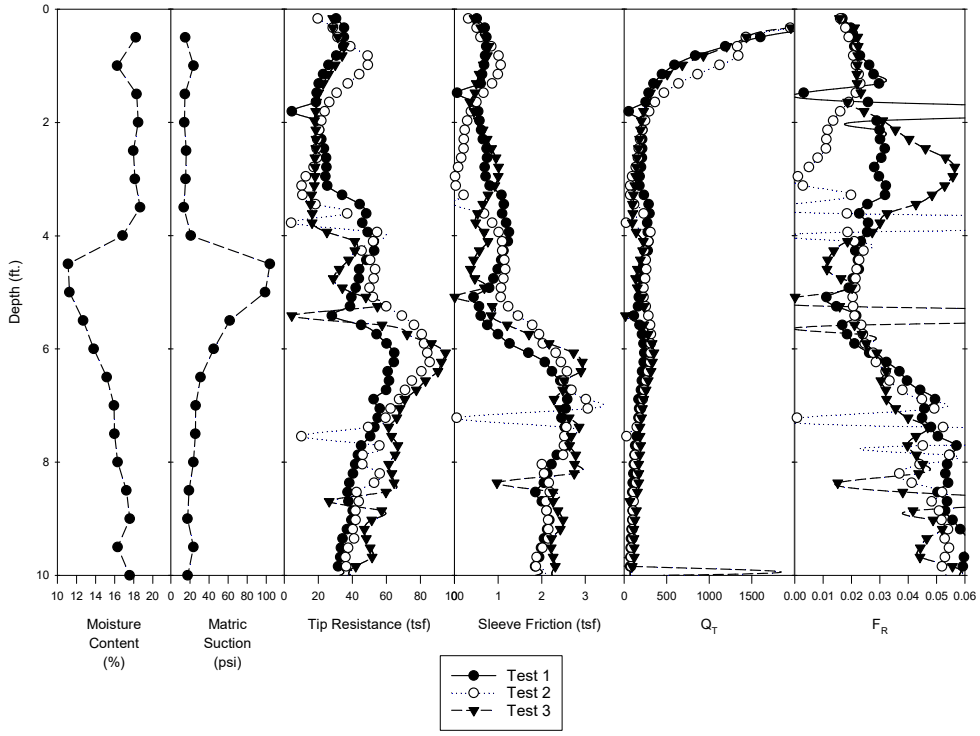

Figure A. 39: CPT data from tests conducted on 2/25/2015 at Goldsby

Figures A.40-A.44 present the corrected volume versus corrected pressure curves from miniature pressuremeter tests performed prior to model footing bearing capacity tests.

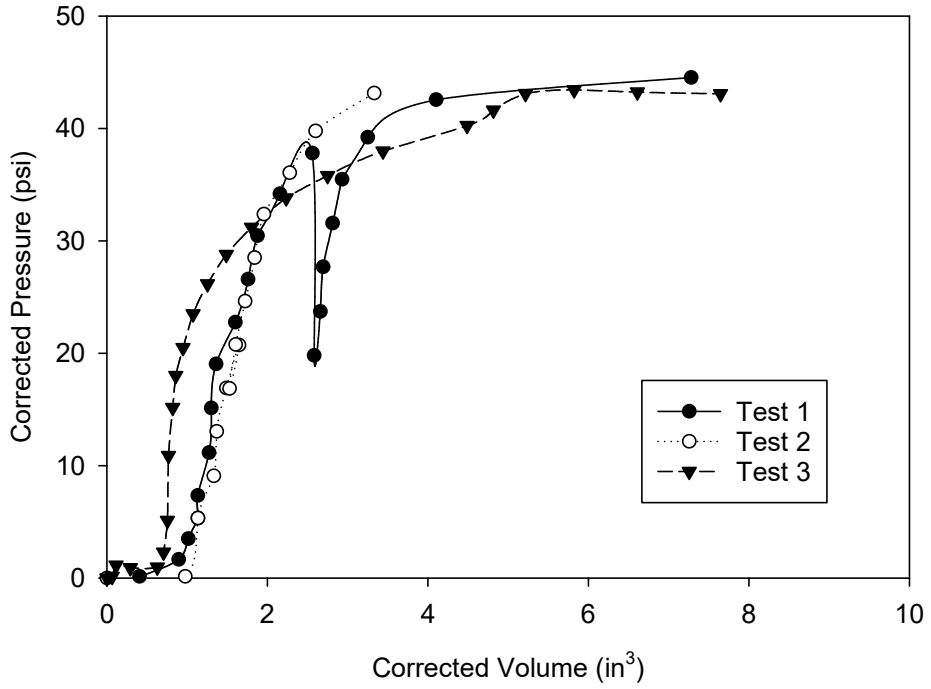

Figure A. 40: Corrected pressure-corrected volume curves for test on 2/29/2016

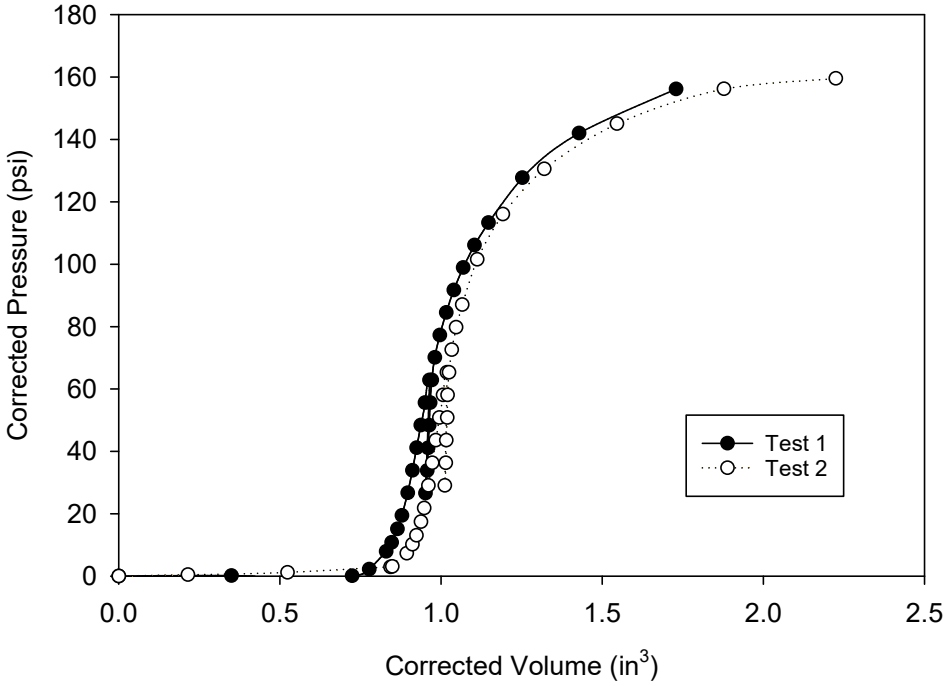

Figure A. 41: Corrected pressure-corrected volume curves for test on 3/14/2016

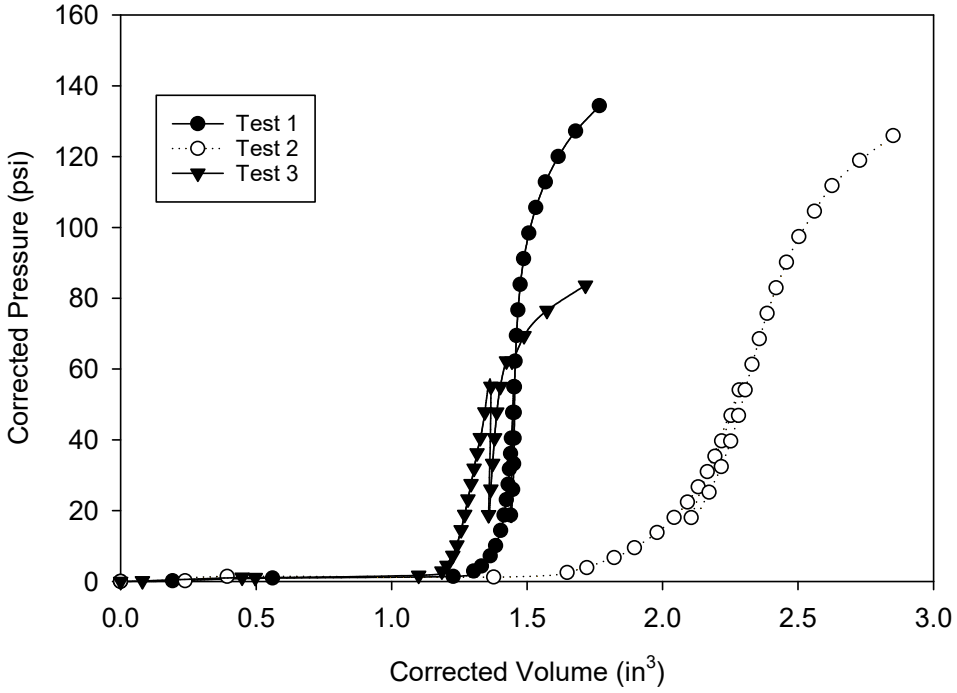

Figure A. 42: Corrected pressure-corrected volume curves for test on 3/28/2016

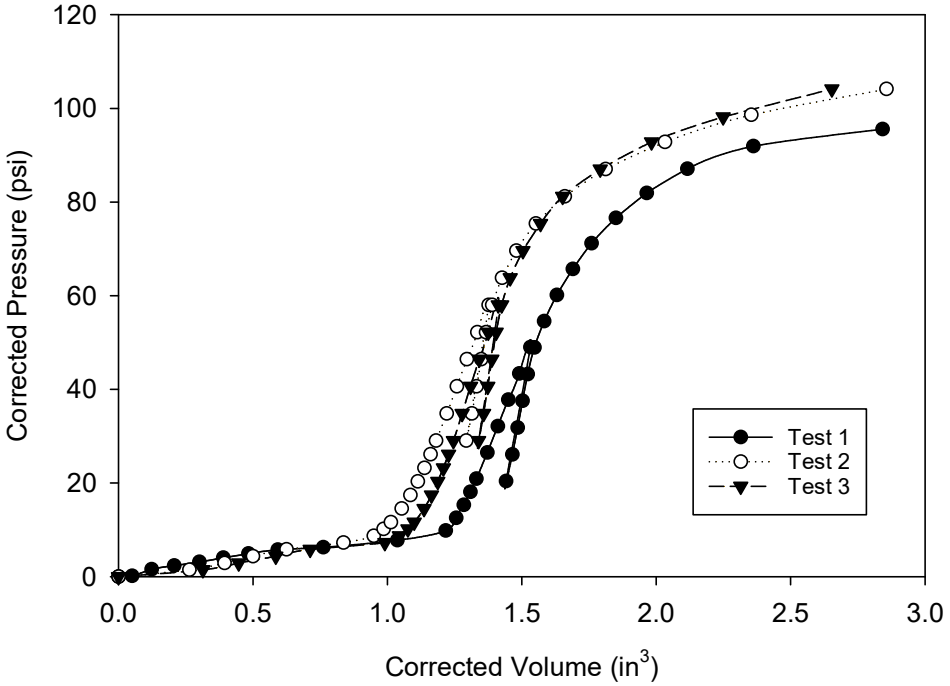

Figure A. 43: Corrected pressure-corrected volume curves for test on 5/5/2016

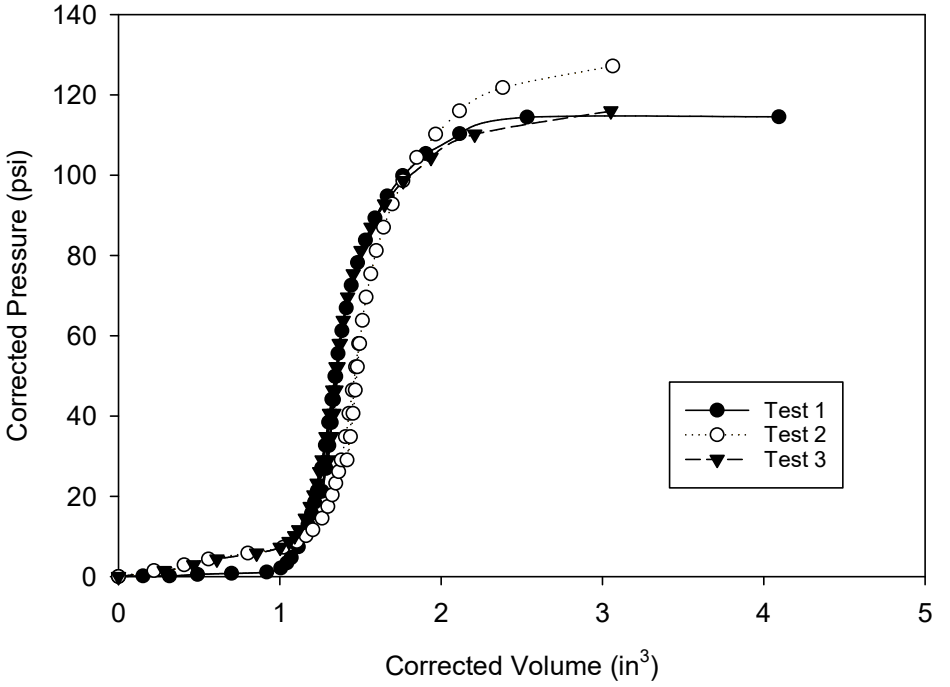

Figure A. 44: Corrected pressure-corrected volume curves for test on 5/27/2016